

**In compliance with the  
Canadian Privacy Legislation  
some supporting forms  
may have been removed from  
this dissertation.**

**While these forms may be included  
in the document page count,  
their removal does not represent  
any loss of content from the dissertation.**



University of Alberta

The Molecular Basis of Renal Senescence  
and its Disease Implications

by

Anette Melk



A thesis submitted to the Faculty of Graduate Studies and Research

in partial fulfillment of the requirements for the degree of

Doctor of Philosophy

in

Experimental Medicine

Department of Medicine

Edmonton, Alberta

Fall, 2003



National Library  
of Canada

Bibliothèque nationale  
du Canada

Acquisitions and  
Bibliographic Services

Acquisitons et  
services bibliographiques

395 Wellington Street  
Ottawa ON K1A 0N4  
Canada

395, rue Wellington  
Ottawa ON K1A 0N4  
Canada

*Your file* *Votre référence*

*ISBN: 0-612-88022-2*

*Our file* *Notre référence*

*ISBN: 0-612-88022-2*

The author has granted a non-exclusive licence allowing the National Library of Canada to reproduce, loan, distribute or sell copies of this thesis in microform, paper or electronic formats.

L'auteur a accordé une licence non exclusive permettant à la Bibliothèque nationale du Canada de reproduire, prêter, distribuer ou vendre des copies de cette thèse sous la forme de microfiche/film, de reproduction sur papier ou sur format électronique.

The author retains ownership of the copyright in this thesis. Neither the thesis nor substantial extracts from it may be printed or otherwise reproduced without the author's permission.

L'auteur conserve la propriété du droit d'auteur qui protège cette thèse. Ni la thèse ni des extraits substantiels de celle-ci ne doivent être imprimés ou autrement reproduits sans son autorisation.

# Canada

University of Alberta  
Library Release Form

Name of Author: Anette Melk

Title of Thesis: The Molecular Basis of Renal Senescence and its Disease  
Implications

Degree: Doctor of Philosophy

Year this Degree Granted: 2003

Permission is hereby granted to the University of Alberta Library to reproduce single copies of this thesis and to lend or sell such copies for private, scholarly or scientific research purposes only.

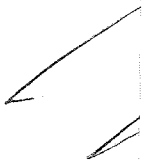
The author reserves all other publication and other rights in association with the copyright in the thesis, and except herein before provided, neither the thesis nor any substantial portion thereof may be printed or otherwise reproduced in any material form whatever without the author's prior written permission.

September 2, 2003

University of Alberta

Faculty of Graduate Studies and Research

The undersigned certify that they have read, and recommend to the Faculty of Graduate Studies and Research for acceptance, a thesis entitled "The Molecular Basis of Renal Senescence and its Disease Implications" submitted by Anette Melk in partial fulfillment of the requirements for the degree of Doctor of Philosophy in Experimental Medicine.



---

Dr. Gary E. Striker  
External Examiner  
University of Miami

June 26, 2003

Ignorance is the curse of God,

Knowledge the wing wherewith we fly to heaven.

William Shakespeare: *Henry IV*

To Bernhard,

for your unconditional, infinite love and belief in me.

In memory of Frau Bär.



## Abstract

Renal senescence has many implications for nephrology, including normal aging, increased incidence in end stage renal disease, poorer graft survival and increased cancer rates. The phenotype of renal senescence is characterized by the loss of function, cells, and nephron mass. I hypothesized that the loss of functioning cells and units in aging and diseased kidneys could follow molecular pathways described for cellular senescence. Cellular senescence had been studied extensively in human fibroblasts and mouse embryonic fibroblasts *in vitro*, but had not been studied in organs *in vivo*.

I studied whether molecular changes and pathways involved in cellular senescence *in vitro* occurred in aged kidneys *in vivo* and assessed their relative contribution in different species, in particular human and rodent (rat and mouse). I found that human kidney cortex displayed telomere shortening and increased p16<sup>INK4a</sup> expression with age. Rodent kidneys showed increases in p16<sup>INK4a</sup> expression without telomere shortening resembling the species differences described for fibroblasts in culture. Lipofuscin and senescence-associated  $\beta$ -galactosidase that are manifestations of age-induced cellular deterioration had their greatest relationship with age in rat kidneys.

Since p16<sup>INK4a</sup> was consistently associated with kidney aging in all

species, I investigated the importance of p16<sup>INK4a</sup> in transplantation, where aged kidneys are subjected to stresses such as ischemia-reperfusion and rejection. I found that acute injuries induced p16<sup>INK4a</sup> mRNA and protein expression in transplants from old mice. Transplantation also resulted in a faster development of features of tubular atrophy and deterioration. Human biopsies showing allograft nephropathy had increased p16<sup>INK4a</sup> expression when compared to biopsies at time of transplantation.

This data suggests that some changes that accompany cellular senescence *in vitro* occur in kidneys with age and could contribute to the phenotype of renal aging and perhaps certain disease states. My findings would indicate that cells in the kidney that show senescent features are not necessarily malfunctioning but might be harmful if the old kidney is exposed to certain injuries. In this case such cells might contribute to the decreased capability of organ repair leading to signs of deterioration and atrophy which will result in organ malfunction.

## Acknowledgements

Many people have contributed to the success of the work presented in this thesis. Their contributions range from scientific ideas to sincere friendship. I am very grateful to every one of them, even though I am unable to name them all here.

To Phil Halloran: You have played a key role in my development as a scientist and a human being. Thank you for the many possibilities that you have provided for me. I feel that I am ready now to take on any future challenges.

To Carol Cass, Kim Solez, Susan Andrew and Gary Striker: As my committee and examiners, you have created a most nurturing scientific environment. Even through my exams it has been a place for me to grow and learn. Thanks for helping me take on the challenge of exploring renal aging and for steering the project to make it a success.

To Joan Urmson and David Rayner: I greatly admire your modest and unassuming ways. Working with you and knowing you has not only contributed to the success of my scientific work but also made my life so much more enjoyable. Thank you.

To my friends and colleagues: Allan, Annette, Adis, Attapong, Brendan, Doreen, Enid, Gerry, Gian, Gunilla, Irwindeep, Jean, Jo, Kathleen, Kathryn, Kieran, Konrad, Lina, Lin Fu, Luis, Marjan, Maura, Oki, Randy, Robin, Ron, Sita, Srivila, Trish, Vido. Thank you for your friendship, support, and all the great memories.

To my “foster” family here in Canada: Lorraine, Tom, Jill, Ken, Patty, Allan, Susan, Joe, Pam, Matthew, Jackson, Ian, Daniel and Christopher. I consider myself very lucky that I had you. Thank you for your support and encouragement over the past years.

And most importantly, to my family: Bernhard, Ma, Pa, Barbara, Jan, Andreas, Heike, Kathrin, Goda and Bebi. You have made all the difference. You have laid the foundation for everything I have achieved. You have been with me every step of the way. Even when I doubted myself, you still believed in me. Without you I would not have been able to do this.

This thesis has been supported by the Roche Organ Transplantation  
Research Foundation and Hoffmann La-Roche Canada.

# Table of Contents

Chapter 1: Introduction	1
1.1 Introduction	2
1.2 Terms and definitions	2
1.3 Molecular events in replicative senescence <i>in vitro</i>	3
1.3.1 Telomere Shortening	4
1.3.2 Mechanisms of cell cycle arrest in senescent cells	7
1.3.3 Senescence may occur by fundamentally different mechanisms in man compared to mice	9
1.3.4 Molecular changes in cultured aged cells	10
1.4 The molecular basis of the senescence phenotype <i>in vivo</i>	10
1.4.1 Evidence concerning telomere shortening <i>in vivo</i>	13
1.4.2 Evidence for the importance of cell cycle regulators <i>in vivo</i>	13
1.4.3 Role of oxidant injury in the senescence phenotype <i>in vivo</i>	14
1.4.4 Accumulation of oxidative end products and advanced glycation end products (AGEs) <i>in vivo</i>	15
1.4.5 Do senescent cells exist <i>in vivo</i> ?	16
1.4.6 Relationship of cellular senescence to cancer and to tissue senescence	17
1.5 Does cellular senescence contribute to the phenotype of renal senescence?	18
1.6 Perspective	21
1.7 Figures	24
1.8 References	29

<b>Chapter 2: Telomere shortening in human kidneys with age</b>	<b>35</b>
2.1 Introduction	36
2.2 Materials and Methods	39
2.2.1 Terminal restriction fragments (TRF)	39
2.2.2 GFR	40
2.3 Results	40
2.3.1 Demographic data	40
2.3.2 Telomere length in kidney cortex and medulla	41
2.3.3 Comparing cortex versus medulla in paired samples	43
2.3.4 GFR versus telomere length	44
2.4 Discussion	44
2.5 Tables	50
2.6 Figures	53
2.7 References	67
<b>Chapter 3: Cell senescence in rat kidneys in vivo increases with growth and age despite lack of telomere shortening</b>	<b>71</b>
3.1 Introduction	72
3.2 Materials and Methods	74
3.2.1 Kidneys	74
3.2.2 Pathology and lipofuscin assessment	75
3.2.3 Sirius Red staining	75
3.2.4 Terminal restriction fragments (TRF)	76
3.2.5 Reverse transcription (RT) and real-time polymerase chain reaction (PCR)	77
3.2.6 Immunohistochemistry for p16 <sup>INK4a</sup>	79
3.2.7. Western blot analysis	79

3.2.8	Senescence associated (SA) $\beta$ -galactosidase ( $\beta$ -GAL) staining	80
3.2.9.	Terminal deoxynucleotidyl transferase mediated dUTP Nick End Labeling (TUNEL)	81
3.2.10	Statistical Analysis	82
3.3	Results	82
3.3.1	Renal changes with growth and aging	82
3.3.2	Mean TRF length in rat kidney samples	84
3.3.3	P16 <sup>INK4a</sup> mRNA expression in rat kidney, spleen, brain and heart samples	84
3.3.4	P16 <sup>INK4a</sup> protein expression in rat kidneys	85
3.3.5.	SA- $\beta$ -GAL	86
3.3.6	TUNEL	87
3.3.7.	Lipofuscin	87
3.4	Discussion	88
3.5	Tables	94
3.6	Figures	99
3.7	References	110

#### Chapter 4: The strong association of cell cycle regulator p16<sup>INK4a</sup> expression with renal senescence in mouse kidney 115

4.1	Introduction	116
4.2	Materials and Methods	118
4.2.1	Mice	118
4.2.2	Reverse transcription (RT) and real-time polymerase chain reaction (PCR)	119
4.2.3	Histopathology assessment	120

4.2.4	Senescence associated (SA) $\beta$ -galactosidase ( $\beta$ -GAL) staining	120
4.2.5	Immunohistochemistry for p16 <sup>INK4a</sup>	121
4.2.6	Terminal restriction fragments (TRF)	122
4.2.7	Statistical analysis	123
4.3	Results	123
4.3.1	Morphologic changes	123
4.3.2	Telomere length and expression of telomere regulating genes	124
4.3.3	P16 <sup>INK4a</sup> mRNA and protein expression	125
4.3.4	Expression of p19 <sup>ARF</sup> and other candidate senescence genes	126
4.3.5	Comparison of kidney with other organs	127
4.4	Discussion	128
4.5	Tables	134
4.6	Figures	148
4.7	References	170

Chapter 5: Expression of p16<sup>INK4a</sup> and other cell cycle regulator and senescence associated genes in aging human kidney 176

5.1	Introduction	177
5.2	Materials and Methods	179
5.2.1	Kidneys	179
5.2.2	Real-time RT-PCR	180
5.2.3	Senescence associated (SA) $\beta$ -galactosidase ( $\beta$ -GAL) staining	181
5.2.4	Immunoperoxidase staining for p16 <sup>INK4a</sup>	182
5.2.5	Statistical Analysis	183
5.3	Results	183
5.3.1	P16 <sup>INK4a</sup> mRNA expression in normal human kidney samples	183
5.3.2	P16 <sup>INK4a</sup> protein expression in normal human kidney sections	184



5.3.3	Expression of candidate senescence genes in human kidney cortex	185
5.3.4	COX1 and COX2 mRNA expression in normal human kidney	186
5.3.5	SA- $\beta$ -GAL and lipofuscin in human kidney samples	187
5.4	Discussion	188
5.5	Tables	194
5.6	Figures	199
5.7	References	213

Chapter 6:	Evidence that acute rejection induces epithelial cell senescence in mouse kidney	218
------------	--	-----

6.1	Introduction	219
6.2	Materials and Methods	221
6.2.1	Mice	221
6.2.2	Renal Transplantation	221
6.2.3	Histopathology	222
6.2.4	Antibodies	224
6.2.5	Immunohistochemistry	224
6.2.6	RNA isolation	226
6.2.7	Reverse transcription (RT) and real-time polymerase chain reaction (PCR)	226
6.2.8	Statistical analysis	227
6.3	Results	228
6.3.1	Histopathology	228
6.3.1.1	Normal CBA mice	228
6.3.1.2	CBA mice at day 7 after renal transplantation	229
6.3.1.2	CBA mice at day 21 after renal transplantation	230
6.3.2	RT-PCR for senescence-associated genes	231
6.3.2.1	Normal CBA mice	231

6.3.1.2 CBA mice at day 7 after renal transplantation	231
6.3.1.3 CBA mice at day 21 after renal transplantation	231
6.3.3 P16 <sup>INK4a</sup> staining	232
6.3.3.1 Normal CBA mice	232
6.3.3.2 CBA mice at day 7 after renal transplantation	232
6.3.3.3 CBA mice at day 21 after renal transplantation	233
6.3.4 MHC class I and II staining	233
6.3.4.1 Normal CBA mice	233
6.3.4.2 MHC expression in CBA mice at day 7 after renal transplantation	233
6.3.4.3 CBA mice at day 21 after renal transplantation	233
6.3.5 Cytology and number of infiltrating lymphocytes	234
6.3.5.1 Normal CBA mice	234
6.3.5.2 CBA mice at day 7 after renal transplantation	235
6.3.5.3 CBA mice at day 21 after renal transplantation	235
6.3.6 RT-PCR for Granzyme B, Perforin and IFN- $\gamma$	236
6.3.6.1 Normal CBA mice	236
6.3.6.2 CBA mice at day 7 after renal transplantation	236
6.3.6.3 CBA mice at day 21 after renal transplantation	236
6.4 Discussion	237
6.5 Tables	241
6.6 Figures	247
6.7 References	261
 Chapter 7: P16 <sup>INK4a</sup> expression increases in human allograft nephropathy biopsies	 264
7.1 Introduction	265
7.2 Material and Methods	267
7.2.1 Biopsies	267

7.2.2	Immunoperoxidase staining for p16 <sup>INK4a</sup>	267
7.2.3	Statistical analysis	268
7.3	Results	268
7.3.1	Demographic data	268
7.3.2	Histology	269
7.3.3.	P16 <sup>INK4a</sup> protein expression	269
7.4	Discussion	270
7.5	Tables	274
7.6	Figures	277
7.7	References	285
Chapter 8: General Discussion and Conclusions		289
8.1	Introduction	290
8.2	Objectives of the thesis	291
8.3	Evidence for cellular senescence in kidneys <i>in vivo</i>	291
8.3.1	Telomere Shortening	291
8.3.2	Cellular senescence reached by other mechanisms	292
8.3.3	<i>In vivo</i> senescence marker	294
8.4	Evidence for cellular senescence in transplantation	295
8.4.1	Acute rejection	295
8.4.2	Cellular senescence in allograft nephropathy	296
8.5	Summary of the findings	297
8.6	Implications for nephrology and transplantation	298
8.7	Future work	301
8.8	Figures	303
8.9	References	305

## List of Tables

### Chapter 2

Table 2.1:	Demographic data on the 24 individuals from whom the kidneys were derived.	51
Table 2.2:	Telomere length in paired cortical and medullary samples with age.	52

### Chapter 3

Table 3.1:	Kidney function and weight.	95
Table 3.2:	Pathology of rat kidneys.	96
Table 3.3:	Lipofuscin distribution [%] in tubular epithelium of rat kidney.	97
Table 3.4:	Association of lipofuscin with SA- $\beta$ -GAL staining in tubular epithelium.	98

### Chapter 4

Table 4.1:	Sequences for primers and probes used in Real-time PCR studies.	135
Table 4.2:	Kidney weight, body weight and kidney/body weight ratio.	136
Table 4.3:	P16 <sup>INK4a</sup> mRNA expression values for heart and brain in comparison to kidney.	137
Table 4.4:	P19 <sup>ARF</sup> mRNA expression values for heart and brain in comparison to kidney.	138
Table 4.5:	MT1 mRNA expression values for heart and brain in comparison to kidney.	139

Table 4.6:	MT3 mRNA expression values for heart and brain in comparison to kidney.	140
Table 4.7:	Hsp70 mRNA expression values for heart and brain in comparison to kidney.	141
Table 4.8:	TGF- $\beta$ mRNA expression values for heart and brain in comparison to kidney.	142
Table 4.9:	PCNA mRNA expression values for heart and brain in comparison to kidney.	143
Table 4.10:	HIC-5 mRNA expression values for heart and brain in comparison to kidney.	144
Table 4.11:	SMP30 mRNA expression values for heart and brain in comparison to kidney.	145
Table 4.12:	GADD45 mRNA expression values for heart and brain in comparison to kidney	146
Table 4.13:	Predicted and actual changes for the candidate senescence genes.	147

## Chapter 5

Table 5.1:	Demographic data and histological grading on the 42 individuals from whom normal kidneys were derived.	195
Table 5.2:	Sequences for primers and probes used in Real-time PCR studies	196
Table 5.3:	Linear regression analysis for kidney cortex.	197
Table 5.4:	Expression of candidate senescence genes ( $M \pm SD$ ) for kidney cortex in three different age groups.	198

## Chapter 6

Table 6.1:	Sequences for primers and probes used in Real-time PCR studies.	242
Table 6.2:	Histopathology for kidneys from CBA mice.	243
Table 6.3:	Basement membrane wrinkling, tubular diameter and cell number for kidneys from CBA mice.	244
Table 6.4:	Donor (CBA) and recipient (B6) MHC class I and class II expression.	245
Table 6.5:	Cytology and cell counts for infiltrating lymphocytes.	246

## Chapter 7

Table 7.1:	Demographic data for the 14 individuals from whom the biopsies were derived.	275
Table 7.2:	Banff scores for the 28 biopsies.	276

## List of Figures

### Chapter 1

Figure 1.1:	Telomere Hypothesis.	25
Figure 1.2:	The ARF/p53 and p16/retinoblastoma (Rb) pathways.	26
Figure 1.3:	Differences in cellular senescence between human and mouse fibroblasts.	27
Figure 1.4:	Histology of renal senescence.	28

### Chapter 2

Figure 2.1:	Telomere length in human renal cortex samples.	54
Figure 2.2:	Regression of telomere length measurements in renal cortex by Southern blotting against age.	55
Figure 2.3:	Regression of telomere length measurements in renal cortex by Southern blotting against age.	56
Figure 2.4:	Regression of telomere length measurements in renal cortex by Southern blotting against age.	57
Figure 2.5:	Regression of telomere length measurements in renal cortex by Southern blotting against age.	58
Figure 2.6:	Telomere length in human renal medulla samples.	59
Figure 2.7:	Regression of telomere length measurements in renal medulla by Southern blotting against age.	60
Figure 2.8:	Regression of telomere length measurements in renal medulla by Southern blotting against age.	61
Figure 2.9:	Regression of telomere length measurements in renal medulla by Southern blotting against age.	62
Figure 2.10:	Regression of telomere length measurements in renal medulla by Southern blotting against age.	63

Figure 2.11: Regression of the difference between cortical and medullary telomere lengths against age.	64
Figure 2.12: The regression between GRF and age.	65
Figure 2.13: The regression between GFR and telomere length by Southern blotting.	66

### Chapter 3

Figure 3.1: Fraction of cortical interstitial fibrosis in rat kidneys of three different age groups.	100
Figure 3.2: TGF- $\beta$ 1 mRNA in rat kidneys of three different age groups.	101
Figure 3.3: Representative TRF gel.	102
Figure 3.4: Mean telomere restriction fragment (TRF) length $\pm$ SD of mean TRF length in rat kidneys of three different age groups.	103
Figure 3.5: P16 <sup>INK4a</sup> mRNA expression in rat kidneys of three different age groups.	104
Figure 3.6: P16 <sup>INK4a</sup> mRNA expression in rat spleens of three different age groups.	105
Figure 3.7: P16 <sup>INK4a</sup> mRNA expression in rat brains of three different age groups.	106
Figure 3.8: P16 <sup>INK4a</sup> mRNA expression in rat hearts of three different age groups.	107
Figure 3.9: Representative p16 <sup>INK4a</sup> staining in rat kidney tubular sections from a 1 month and 24 months old rat.	108
Figure 3.10: Representative SA- $\beta$ -GAL staining in rat kidney tissue from a 1 month, 9 months and 24 months old rat.	109



## Chapter 4

Figure 4.1:	Representative kidney sections stained with PAS for 1 month, 3 months and 18 months old Balb/c mice.	149
Figure 4.2:	Representative TRF gel.	150
Figure 4.3:	Mean telomere restriction fragment (TRF) length $\pm$ SD of mean TRF length in mouse kidneys of three different age groups.	151
Figure 4.4:	Tert mRNA expression in mouse kidneys of four different age groups.	152
Figure 4.5:	TRF1 mRNA expression in mouse kidneys of four different age groups.	153
Figure 4.6:	TRF2 mRNA expression in mouse kidneys of four different age groups.	154
Figure 4.7:	P16 <sup>INK4a</sup> mRNA expression in mouse kidneys of four different age groups.	155
Figure 4.8:	Representative kidney sections stained for p16 <sup>INK4a</sup> and counterstained with hematoxylin for 1 month, 3 months and 18 months old Balb/c mice.	156
Figure 4.9:	P16 <sup>INK4a</sup> protein expression in tubular cells in mouse kidney.	157
Figure 4.10:	P16 <sup>INK4a</sup> protein expression in glomeruli of mouse kidney.	158
Figure 4.11:	P16 <sup>INK4a</sup> protein expression in interstitial cells of mouse kidney.	159
Figure 4.12:	P16 <sup>INK4a</sup> protein expression in arteries and arterioles in mouse kidney.	160
Figure 4.13:	P19 <sup>ARF</sup> mRNA expression in mouse kidneys of four different age groups.	161

Figure 4.14: MT1 mRNA expression in mouse kidneys of four different age groups.	162
Figure 4.15: MT3 mRNA expression in mouse kidneys of four different age groups.	163
Figure 4.16: Hsp70 mRNA expression in mouse kidneys of four different age groups.	164
Figure 4.17: TGF- $\beta$ mRNA expression in mouse kidneys of four different age groups.	165
Figure 4.18: PCNA mRNA expression in mouse kidneys of four different age groups.	166
Figure 4.19: HIC-5 mRNA expression in mouse kidneys of four different age groups.	167
Figure 4.20: SMP30 mRNA expression in mouse kidneys of four different age groups.	168
Figure 4.21: GADD45 mRNA expression in mouse kidneys of four different age groups.	169

## Chapter 5

Figure 5.1: Regression for p16 <sup>INK4a</sup> mRNA expression in renal cortex and renal medulla.	200
Figure 5.2: P16 <sup>INK4a</sup> mRNA expression in renal cortex and medulla.	201
Figure 5.3: Representative pictures of p16 <sup>INK4a</sup> staining in kidney.	202
Figure 5.4: P16 <sup>INK4a</sup> protein expression in tubular cells in renal cortex.	204
Figure 5.5: P16 <sup>INK4a</sup> protein expression in glomeruli.	205
Figure 5.6: P16 <sup>INK4a</sup> protein expression in interstitial cells in renal cortex.	206

Figure 5.7:	P16 <sup>INK4a</sup> protein expression in renal arteries.	207
Figure 5.8:	Regression for COX1 mRNA expression in renal cortex and renal medulla.	208
Figure 5.9:	COX1 mRNA expression in renal cortex and medulla.	209
Figure 5.10:	Regression for COX2 mRNA expression in renal cortex and renal medulla.	210
Figure 5.11:	COX2 mRNA expression in renal cortex and medulla.	211
Figure 5.12:	SA- $\beta$ -GAL expression in renal cortex and medulla.	212

## Chapter 6

Figure 6.1:	Tubular diameter for CBA kidneys.	248
Figure 6.2:	Number of cells per tubular cross-section for CBA kidneys.	249
Figure 6.3:	Tubular cross sections in normal CBA.	250
Figure 6.4:	Tubular cross sections in CBA donors 7 days after transplantation.	251
Figure 6.5:	Tubular cross sections in CBA donors 21 days after transplantation.	252
Figure 6.6:	P16 <sup>INK4a</sup> mRNA expression for CBA kidneys.	253
Figure 6.7:	P19 <sup>ARF</sup> mRNA expression for CBA kidneys.	254
Figure 6.8:	P16 <sup>INK4a</sup> protein expression in tubular cells in renal cortex of CBA kidneys.	255
Figure 6.9:	P16 <sup>INK4a</sup> protein expression in glomeruli of CBA kidneys.	256
Figure 6.10:	P16 <sup>INK4a</sup> protein expression in interstitial cells in renal cortex of CBA kidneys.	257
Figure 6.11:	Granzyme B mRNA expression for CBA kidneys.	258
Figure 6.12:	Perforin mRNA expression for CBA kidneys.	259
Figure 6.13:	IFN- $\gamma$ mRNA expression for CBA kidneys.	260

## Chapter 7

- Figure 7.1: Kidney biopsies showing p16<sup>INK4a</sup> staining prior to and after transplantation. 278
- Figure 7.2: Kidney biopsy showing p16<sup>INK4a</sup> staining affecting one nephron. 279
- Figure 7.3: P16<sup>INK4a</sup> protein expression in tubular cells in 14 human kidney biopsies. 280
- Figure 7.4: P16<sup>INK4a</sup> protein expression in glomeruli in 14 human kidney biopsies. 281
- Figure 7.5: P16<sup>INK4a</sup> protein expression in interstitial cells in 14 human kidney biopsies. 282
- Figure 7.6: P16<sup>INK4a</sup> protein expression in arteries in 14 human kidney biopsies. 283
- Figure 7.7: P16<sup>INK4a</sup> protein expression measured as cytoplasmic staining of tubular cross sections in 14 human kidney biopsies. 284

## Chapter 8

- Figure 8.1: Cellular senescence in renal cells *in vivo*. 304

## List of Abbreviations

aka	also known as
AN	Allograft nephropathy
ANOVA	Analysis of variance
APCKD	Adult type polycystic kidney disease
AGE	Advanced glycation end product
ARF	Alternate reading frame
bp	base pairs
BSA	Bovine serum albumine
Bx	Biopsy
CAN	Chronic allograft nephropathy
cDNA	complementary deoxyribonucleic acid
CDK	Cyclin dependent kinase
CIP	CDK interacting protein
CKI	Cyclin dependent kinase inhibitor
CLL	Chronic lymphocytic leukemia
COX1	Cyclooxygenase 1
COX2	Cyclooxygenase 1
Ct	Threshold cycle
D	Day
DAB	(3'3) diaminobenzidine tetrahydrochloride
DGF	Delayed graft function
DNA	Deoxyribonucleic acid

EM	Extraglomerular mesangium
ERA-EDTA	European Renal Association-European Dialysis and Transplantation Association
ESRD	End stage renal disease
Ets1	E26 avian leukemia oncogene 1
Ets2	E26 avian leukemia oncogene 2
FIT	Fibrous intimal thickening
GADD45	Growth arrest- and DNA damage-inducible gene 45
GADD153	Growth arrest- and DNA damage-inducible gene 153
GFR	Glomerular filtration rate
GM	Glomerulus
GRP78	Glucose Regulated Protein 78
HDM <sub>2</sub>	Human Double Minute 2
H&E	Hematoxylin and eosin
HIC-5	Hydrogen peroxide inducible clone 5 (=TGF- $\beta$ 1 induced transcript 1)
HPF	High power field
HPRT	Hypoxanthine phosphoribosyl-transferase
Hsp	Heat shock protein
Id	Inhibitor of DNA binding or Inhibitor of differentiation
IF	Interstitial fibrosis
IFN- $\gamma$	Interferon $\gamma$
IgG	Immunoglobulin G
INK4	Inhibitor of CDK4

kbp	kilo base pairs
KIP	Kinase inhibitory protein
mAb	monoclonal antibody
MAPK	Mitogen activated protein kinase
MD	Macula densa
MDM <sub>2</sub>	Mouse double minute 2
MDRD	Modification of diet in renal disease
MEF	Mouse embryonic fibroblast
MEK	Mitogen activated protein kinase kinase
MHC	Major histocompatibility complex
MMP1	Matrix metalloproteinase 1
MMLV	Moloney murine leukemia virus
mRNA	messenger ribonucleic acid
MT	Metallothionein
NCBA	Normal CBA mice
NIH	National Institute of Health
N.S.	Not significant
MW	Molecular weight
OCT	22-oxacalcitriol
OD	Optical density
PAI1	Plasminogen activator inhibitor type 1
PAS	Periodic Acid Schiff
PBS	Phosphate buffered saline
PCNA	Proliferating cell nuclear antigen

PCR	Polymerase chain reaction
PN	Pyelonephritis
PTC	peritubular capillary congestion
Rb	Retinoblastoma-susceptibility tumor suppressor protein
RCC	Renal cell carcinoma
RIPA buffer	Radioimmunoprecipitation assay buffer
RNA	Ribonucleic acid
ROS	Reactive oxygen species
RT	Room temperature
RT-PCR	Reverse transcription-polymerase chain reaction
SA- $\beta$ -GAL	Senescence-associated $\beta$ -galactosidase
SD	Standard deviation
SDS	Sodium dodecyl sulfate
SDS-PAGE	Sodium dodecyl sulfate polyacrylamide gel electrophoresis
SMP30	Senescence marker protein 30
SPSS	Statistical package for the social sciences
SSC	Standard sodium citrate
SSPE	Saline-sodium phosphate ethylenediamine tetraacetic acid
STASIS	Stimulation and stress-induced senescent-like arrest or Stress or aberrant signal induced senescence
TA	Tubular atrophy
TBM	Tubular basement membrane
TCC	Transitional cell carcinoma
TDT	Terminal deoxynucleotidyl transferase



TE buffer	Tris and ethylenediamine tetraacetic acid buffer
Tert	Telomerase reverse transcriptase
TGF- $\beta$ 1	Transforming growth factor $\beta$ 1
TIFF	Tagged-image file format
TRF	Terminal restriction fragments
TRF1	Telomeric repeat binding factor 1
TRF2	Telomeric repeat binding factor 2
TUNEL	Terminal deoxynucleotidyl transferase mediated dUTP nick end labeling
USRDS	United states renal data system
UV	Ultra violet rays
$V_{\text{IntFib}}$	Cortical fractional interstitial fibrosis volume
WAF1	Wild type p53 activated protein 1
X-gal	5-bromo-4-chloro-3-indolyl-beta-D-galactopyranoside

# Chapter 1

## Introduction

Portions of this chapter have been published.

Anette Melk, and Philip F. Halloran: Cell senescence and its implications for nephrology. *Journal of the American Society of Nephrology* 2001; 12: 385-393. Used with permission of Lippincott Williams & Wilkins.

## 1.1 Introduction

Age-associated changes of the kidney are important not only because normal aging alters renal function but also because of the high frequency of end stage renal disease (ESRD) in the elderly (USRDS and ERA-EDTA Registry Reports 2000). Old kidneys perform poorly when transplanted, and donor age is a major determinant of graft survival (1). It has been proposed that interactions between aging and diseases may contribute to these problems. Understanding the mechanisms of declining organ function with age may be instructive concerning the mechanisms of decline in disease states, since stress might accelerate aging changes. Kidney aging is also of interest as a general model for organ aging because renal function can be assessed with relative ease in clinical practice, and has been quantified in longitudinal studies (2). The molecular basis of aging changes in organs is not known but organ aging may reflect aspects of cellular senescence which we understand better now than a few years ago.

## 1.2 Terms and definitions

The term “age” reflects the time that has elapsed since birth. The term “renal senescence” is used to describe the structural and functional phenotype associated with aged kidneys. “Cellular senescence” describes a phenotype of permanent and irreversible growth arrest shown by mammalian cells in culture. Originally described in human fibroblasts by

Hayflick (3), this term was synonymously used with “replicative senescence”. However in recent years, the concept of cellular senescence has been expanded to include other forms of permanent, irreversible cell cycle arrest. The reason for this extension partly comes from the observation that mouse embryonic fibroblasts in culture do not use replicative senescence to cease replication, but share other senescence features with human fibroblasts such as altered morphology, greater heterogeneity, expression of senescence associated  $\beta$ -galactosidase (SA- $\beta$ -GAL) and accumulation of lipofuscin granules. This had been referred to as “premature senescence” or “stress induced senescence” and most recently as “stimulation and stress-induced senescent-like” arrest (STASIS) (4).

It is important to realize that “cellular senescence” or “replicative senescence” refers to an *in vitro* phenotype of cultured somatic cells that have reached their finite limit for growth or replication. This state may or may not exist for similar cells *in vivo*. Also, *in vitro* studies of aged cells (i.e. derived from an old donor) should be distinguished from senescent cells (i.e. cells that have developed the *in vitro* senescence phenotype).

### 1.3 Molecular events in replicative senescence *in vitro*

The molecular basis of the *in vitro* cellular senescence phenotype probably differs between cell types and between species e.g. humans

versus mice (5). Hayflick and Moorhead recognized that cultured human somatic cells *in vitro* displayed a limitation in their number of cycles (3). This number of cycles was called their Hayflick number. It is lower in cells from older donors and unaffected by pausing. Thus human somatic cells have a mechanism for counting the number of times that they have divided, a “mitotic clock”. They stop irreversibly when this cycle number is reached, and manifest the state of replicative senescence.

### 1.3.1 Telomere Shortening

In human cells, shortening of telomeres is critical to replicative senescence (6). Telomeres are DNA repeats (TTAGGG) at the ends of chromosomes that shorten in dividing normal cells. Telomeres prevent chromosome ends from being confused with DNA breaks and probably have other functions in tethering and sorting chromosomes. The ends of telomeres must be replicated by the enzyme telomerase, a ribonucleoprotein expressed in germline and in immortal cell populations that maintains telomere length constant (7;8). In 1973, Olovnikov proposed the telomere theory: namely that somatic cells were limited because they cannot fully replicate their telomeres (9) (Figure 1.1). The Hayflick limit was validated by the demonstration that human fibroblasts in culture lack telomerase, shorten their telomeres with each cycle, and develop replicative senescence when telomere length becomes critical (6). The critical

experiment was the demonstration that transfection of telomerase into cultured human cells extends their life span and replication remarkably (10), thus bypassing the Hayflick limit.

Telomeric DNA diminishes by about 50 to 100 bp in dividing normal somatic cells at each cell doubling. The loss of telomeres can trigger the response to DNA breaks, which results in an organised cellular state, the senescence phenotype (M1 in figure 1.1). Cells driven to continue dividing by abnormal stimuli develop massive genomic instability or crisis (M2). Germline cells and immortal cell populations like most cancer cell lines possess mechanisms, which are either telomerase activation or an alternative mechanism, to preserve their telomere length indefinitely despite cell division thus protecting their genome.

The problem with short telomeres may be that they are not “capped” i.e. their ends are not protected in a specialized complex of proteins, which prevent the ends from being recognized as DNA breaks. A “two-state model” of telomere capping has been described (11;12). The model suggests that telomeres in cells in early culture are functionally capped and cycle. With increasing cycle number a fraction of cells becomes uncapped, releasing a signal to activate the DNA damage response. The fraction of uncapped telomeres increases as telomeres shorten, which results in cell cycle arrest. Telomere capping is probably achieved by a combination of mutually reinforcing factors, such as DNA-protein complex on terminal

repeats (telomere binding proteins) and active telomerase.

The state of replicative senescence in human skin fibroblasts includes cessation in replication, altered patterns of gene expression, and resistance to apoptosis. Senescent fibroblasts remain viable with ongoing RNA and protein synthesis. However, senescent cells cannot be stimulated to enter the S phase of the cell cycle by any combination of growth factors or physiological mitogens. Senescent human fibroblasts show an enlarged and flat morphology, and accumulate lipofuscin pigment and senescence associated SA- $\beta$ -GAL activity.

The important alterations in gene expression are probably in the genes controlling the cell cycle (see below). Other changes in gene expression include increased expression of the genes encoding Alzheimer's beta-amyloid precursor protein, certain metalloproteinases, such as MMP1, and genes whose products contribute to the extracellular matrix, interferon responses, and inflammation. If tissue senescence *in vivo* is associated with similar changes, it is conceivable that the products of senescent cells could influence not only the cell loss but also the matrix changes and focal inflammation in aged tissues.

The key feature of the senescence phenotype *in vitro* is irreversible cessation of cell cycling. In human cells, telomere shortening is the crucial event triggering cell cycle arrest. Telomere length for human cells has been compared to the gasoline supply of car: it is definitely limiting, but is

certainly not the only mechanism for stopping (13). Other stresses may also induce some aspects of senescence in human cells, and even more so in mouse cells as discussed below. Nevertheless in human somatic cells *in vitro* critical telomere shortening is the trigger for senescence and is responsible for the Hayflick limit.

### 1.3.2 Mechanisms of cell cycle arrest in senescent cells

Senescence-associated growth arrest is mediated by expression of cell cycle inhibitory genes and by downregulation of positive acting cell cycle regulators. At the center of the machinery for cell cycling are the cyclin dependent kinases (CDKs), which receive and integrate regulatory signals. CDKs are activated in a two step manner. Step 1 is engagement of the regulators, the cyclins, which cause conformational changes that partially activate the kinase activity. Step 2 is the phosphorylation of a key threonine, leading to full activation. CDK inhibitors (CKIs) prevent or reverse activation of CDKs (Figure 1.2). There are two main families of CKIs: the INK4 (INK4a for 'inhibitor of CDK4') CKIs (e.g. p16<sup>INK4a</sup>) and the CIP/KIP CKIs (e.g. p21<sup>WAF1/CIP1</sup>).

The protector of the genome, p53, responds to telomere shortening and controls the G1 arrest checkpoint. In response to DNA injury, p53 levels increase by a post-transcriptional mechanism. This results in the transcriptional activation of p21<sup>WAF1/CIP1</sup>, a Cip1 CKI, which can mediate G1



arrest (14). Inactivation of p53 is the most common genetic event in human cancer and p53 deficiency prevents telomere loss from inducing cell cycle arrest (15).

The retinoblastoma-susceptibility tumor suppressor protein (Rb) is a major regulator of cell cycling and the critical substrate of the CDK4 and CDK6. Rb negatively controls passage from G1 into S phase by sequestering transcription factors, such as E2F, that are required for the G1/S transition. The ability of Rb to bind transcription factors is abolished by phosphorylation (16). CDK 4 and CDK6 phosphorylate Rb and thus activate E2F and the cell cycle. Extension of lifespan beyond the Hayflick Limit can be achieved by viral oncoprotein-induced inactivation of p53 and Rb, indicating that these tumor suppressor pathways are critical mediators of the telomere shortening checkpoint response.

P16<sup>INK4a</sup> causes G1 cell cycle arrest by specific inhibition of CDK4 and CDK6, preventing Rb hyperphosphorylation and S phase entry (17;18). P16<sup>INK4a</sup> is strongly associated with senescence: as mouse or human cells *in vitro* approach senescence they express p16<sup>INK4a</sup>. The gene for p16<sup>INK4a</sup> is unusual in that it contains an alternative reading frame that allows it to encode both p16<sup>INK4a</sup> and another factor, p19<sup>ARF</sup> (or its human equivalent p14<sup>ARF</sup>) (19-22). Telomerase activity alone is insufficient to immortalize some human epithelial cells, inactivation of Rb and p16<sup>INK4a</sup> is the second crucial step (23). Some oncogenes induce senescence in non-transformed

human cells via p16<sup>INK4a</sup>. For example, Ras-induced senescence depends on the expression of p16<sup>INK4a</sup> and p53 (24), and Raf can induce senescence in cells that lack p53 function, probably via p16<sup>INK4a</sup> alone.

### 1.3.3 Senescence may occur by fundamentally different mechanisms in man compared to mice

Both human fibroblasts and mouse embryonic fibroblasts can manifest a senescence phenotype after cycling *in vitro*. However, the senescence state is mediated by telomere shortening in human cells but not in mouse cells (5;25) (Figure 1.3). The senescent state in mouse cells resembles that in human cells at the Hayflick limit, including expression of p16<sup>INK4a</sup>. But growth arrest in mouse embryo fibroblasts occurs after fewer cycles and without appreciable telomere attrition, probably because accumulated damage from culture conditions ("culture shock") triggers the p53 response. Thus "senescence of cultured cells results from two sources of signals, either of which can induce the expression of a common set of inhibitors of the cell division cycle" (25). One set of triggers is extrinsic and stems from stresses from the environment. Culture stresses such as oxidant injury may simulate the stresses of life *in vivo* over a longer time frame. The second set of triggers is intrinsic and depends upon the machinery that monitors the integrity of telomeres (a "mitotic clock"). Humans have a mitotic clock, and mice do not. Differences in the

proliferative capacity of cultured mouse and human cells reflect the extent to which they respond to these signaling pathways. Rat cells may be like mouse cells, since they also have very long telomeres.

#### 1.3.4 Molecular changes in cultured aged cells

Recent studies demonstrated that fibroblast lines from older humans (aged fibroblasts) displayed mitotic misregulation (26). The investigators took dermal fibroblast cell lines from young, middle-age and old individuals, and from people with Hutchinson-Gilford progeria. Using DNA microarrays of 6,000 genes, they identified 61 transcripts that were upregulated or downregulated at least twofold in old, middle-aged versus young. Surprisingly, many transcripts regulate the G2/M stage of the cell cycle, suggesting that aging alters expression of genes involved in cell division. The authors suggest that aging "may occur gradually and in mosaic patterns" (26). Such observations have limitations in sampling, and by definition select only replicating cells, thus limiting the conclusions (27).

#### 1.4 The molecular basis of the senescence phenotype *in vivo*

The theories of aging emphasize cumulative damage in post-mitotic cells and exhaustion of the finite capacity for replication in cells with mitotic potential. Reactive oxygen species (ROS) that are generated by cellular respiration cause cumulative damage to lipids, proteins and DNA (28).

Genomic instability can result in changes in mitochondrial DNA and in loss of telomeric DNA. Some have postulated that the aging phenotype reflects an underlying genetic program like development, but this seems less likely than the role of cumulative damage and finite repair. Studies of the genetics of aging suggest that most of aging is driven by environmental factors (29). Because aging is accompanied by a loss of cells, dysregulation of programmed cell death could play a role in aging. Alternatively, net loss of cells could reflect finite ability to replace cells rather than excess loss. Moreover, in some cell types senescence *in vitro* causes loss of their ability to undergo apoptosis as well as other abnormal features, suggesting that accumulation of senescent cells could contribute to aging and age related diseases. Interdependence of organs through humoral factors could contribute to aging: for example, through loss of hormone functions.

Several biomarkers of aging can be found *in vivo*. These include the accumulation of lipofuscin, advanced glycation end products (AGEs), and SA- $\beta$ -GAL. Lipofuscin, a yellow brown pigment, probably reflects accumulation of damaged organelles, and also occurs in senescent cells *in vitro* (30). Some of these features also occur in premature aging phenotypes, called segmental progerias. The molecular basis of the progerias is becoming more evident, but it is not clear whether the mechanisms mutated in progerias are critical in normal aging.

The hypotheses proposed for cellular and organism senescence

include either damage to intra- or extracellular molecules or programmed or epigenetic changes in gene expression. The tissue function and phenotype will reflect accumulation of damaged and/or senescent cells, loss of cells, loss of ability to respond by replication due to senescence in mitotic or stem cells, by changes in matrix, or disordered function of blood supply, inflammation, immunity and endocrine control. Post-mitotic (permanently non-dividing) and mitotic (proliferation-competent) cells age by different mechanisms. Post-mitotic cells that have ceased to replicate cannot undergo replicative senescence. Aging could be caused by changes in gene expression in mitotic cells, whereas in post-mitotic cells damage might play a more important role. Cells in the kidney replicate at a slow rate: Studies of the expression of cycle associated markers suggest that the tubular epithelial cells had a higher proliferation index than the glomerular cells, with the highest proliferation rate being in capillary endothelial cells (31). Nevertheless old kidneys retain considerable replicative potential, and can recover from acute injury such as acute tubular necrosis.

Because “most if not all epithelia contain stem cells” (32), stem cells may exist in kidney epithelium. The key senescence changes that limit replication may occur in the stem cells. Then the somatic cells, which would undergo turnover, may persist and manifest abnormalities, which accumulates because these cells cannot be replaced. The tissue phenotype would include the lack of replacement of damaged cells due to senescence

in the stem cells or at least in proliferation-competent cells, and the changes in matrix and blood vessels.

#### 1.4.1 Evidence concerning telomere shortening *in vivo*

A recent study (33) has associated shorter telomere length in blood cells with poorer survival. It has been shown that bone marrow transplantation accelerates telomere attrition probably due to increasing replication (34;35). And that this can be prevented by expression of telomerase (36). Telomere length has also been studied in solid organs and telomere shortening has been associated with aging (37-41). Differences were found in the shortest telomeres and in the variation of telomere length between the fetal tissue and tissues derived from older individuals (37;39-41). Telomere length was shorter and more variable for old tissues studied, with the greatest differences observed in blood cells.

#### 1.4.2 Evidence for the importance of cell cycle regulators *in vivo*

Studies on cell cycle regulatory proteins in renal glomerular disease suggest not only a role in proliferation but also in hypertrophy and differentiation of rodent renal cells. P21<sup>WAF1/CIP1</sup> induction could be shown after experimental glomerulonephritis and after DNA damage in cisplatin-induced acute renal injury, transient ischemic injury, or ureteral obstruction (42;43). P21<sup>WAF1/CIP1</sup> protects by preventing DNA-damaged cells to enter

the cell cycle. However, a more recent study found that in p21<sup>WAF1/CIP1</sup> knockout mice do not develop glomerular sclerosis and chronic renal failure after partial renal ablation (44). Thus in the absence of p21<sup>WAF1/CIP1</sup> repair leads to hyperplasia instead of hypertrophy.

#### 1.4.3 Role of oxidant injury in the senescence phenotype *in vivo*

The oxidative stress hypothesis proposes that changes associated with aging are a consequence of random oxidative damage to biomolecules: nucleic acids, membranes, and proteins. *Caenorhabditis elegans* and *Drosophila* transgenic for genes encoding antioxidants have an extended lifespan (45;46). Oxidative damage to the mitochondria increased the rate of deleterious ROS and modifications of nucleosides, mutations and deletions. Thus oxidant injury may promote oxidant injury: damage to mitochondrial DNA may lead to a derangement of mitochondrial respiratory activity leading to ROS. The majority of comparative studies have detected the highest mitochondrial DNA deletion levels in nonreplicating, high energy demanding tissues, such as skeletal and cardiac muscle and brain (47). The number of cells affected is usually much lower (less than 1% of total mitochondrial DNA) than in studies of hereditary diseases in which more than 50-80% of the genome is mutated (48). In addition, the extent to which mitochondrial DNA deletions contribute to age-associated declines in the activities of the electron transport system

complexes I to IV remains unclear.

#### 1.4.4 Accumulation of oxidative end products and advanced glycation end products (AGEs) *in vivo*

Lipofuscin accumulates in postmitotic cells, located in small granules in secondary lysosomes and consists mostly of cross-linked lipid and protein residues formed during lipid peroxidation (49). Lipofuscin accumulates in cultured human and rat cells and accumulation is enhanced under increasing oxygen pressure (30;50). Antioxidants inhibit lipofuscin formation (51). Although oxidative damage to organelles seems responsible for depositing lipofuscin in lysosomes of senescent mammals, it is not clear whether it is a biomarker or a mechanism of aging. Two explanations for the increase of lipofuscin with age have been suggested. The first theory is based on the fact that lipofuscin is not totally eliminated and accumulates in postmitotic cells over time. The second suggests that lipofuscin accumulation reflects a derangement of autophagocytosis associated with decline in intralysosomal degradation, as more lysosomal volume is occupied by indigestible material (52).

Some extracellular proteins undergo oxidative modification and have a long half-life since they are rarely recycled. The modifications are initiated by the reaction of reducing sugars with free amino groups (glycation). Further nonoxidative and oxidative processes result in stable, cross-linked



AGEs. The abundance of AGEs is an excellent biomarker of age. Pentosidine, one such 'glycooxidation product' accumulates as a function of age and is much higher in long-lived than in short-lived species (53). Humans suffering from Werner's syndrome, a disease characterized by premature senescence, have more extensive protein oxidation. Fibroblasts from Werner's patients of all ages have levels of protein carbonyls equivalent to that in 80-year-old control individuals (54).

Patients with chronic renal failure, diabetes or in advancing age show a progressive accumulation of AGEs. The development of AGEs is proportional to long-term blood glucose levels in diabetic patients. However, glomerular changes occur with the exposure to AGEs even in the absence of coexisting hyperglycemia. The aging changes in the kidney reflect accumulation of AGEs in renal tissues resulting in altered release of growth factors and cytokines and accumulation of oxidants and lipids (55). Although the accumulation of AGEs may contribute to deterioration in renal function with age, it is not a sufficient explanation for the reduced capacity to respond to stress in the elderly. Moreover, there is little in common between the renal phenotypes of diabetes and aging.

#### 1.4.5 Do senescent cells exist *in vivo*?

Attempts have been made to show that the senescent cells occur *in vivo*.  $\beta$ -GAL activity in senescent cells has been shown by enzyme

histochemical staining at a pH optimum of 6.0. SA- $\beta$ -GAL activity was increases in human skin with replicative and physiological age, reflecting an accumulation of senescent fibroblasts and keratinocytes *in vivo* (56). SA- $\beta$ -GAL activity has been widely used as an *in vivo* senescence marker. SA- $\beta$ -GAL activity was shown in retinal pigment epithelium and hepatocytes *in vivo*.

#### 1.4.6 Relationship of cellular senescence to cancer and to tissue senescence

The cellular senescence mechanism may be a fundamental protection against cancer but could also contribute to cancer formation. Telomere shortening and senescence prevent unlimited growth and thus arrest most mutated cells that have begun to proliferate abnormally. On the other hand, the genomic instability of senescent cells with telomere shortening could promote malignant transformation (57). In aging, some cells persist in damaged form, some drop out completely, and others may remain as senescent cells. Senescent cells could also contribute to the rise in cancer by altering the tissue microenvironment.

The potential importance of the persistence of senescent cells *in vivo* might be that they compromise the function and integrity of the tissue. Ordinarily, the organized tissue is the unit of function, not the cell. By disrupting the tissue organization, replicative senescence might disrupt

function. For example, in the case of dermal fibroblasts there is a switch from a matrix-producing to a matrix-degrading phenotype (58). Thus senescent cells could contribute to the matrix changes of aging.

#### 1.5 Does cellular senescence contribute to the phenotype of renal senescence?

The aging human kidney has four features that require explanation: the phenotype of “normal” renal senescence, the high incidence of ESRD, a high frequency of cancer, and poor performance after renal transplantation, particularly cadaveric transplantation.

It is important to specify species when discussing kidney aging. The aging changes of the rat and other laboratory animals (59) differ from those of long-lived species including humans. For example, the characteristic arterial changes of senescence do not develop in species that live less than 12 years (60). A rigorous distinction between observations in humans and experimental animals is particularly important given the recent evidence that the cellular senescence mechanisms of mice and humans are fundamentally different.

The phenotype of renal senescence in humans is associated with loss of mass, particularly in the cortex, and cellular loss (61), an increase in heterogeneity, and the appearance of focal abnormalities. Cellular loss leads to an underestimate of potential role of senescence mechanisms

because the affected cells disappear. The principal histologic features of renal senescence are deterioration of the arteries (hyalinosis and fibrous intimal thickening of arteries and hyalinosis of arterioles), global sclerosis of glomeruli (not focal sclerosis) with reduplication of Bowman's capsule, focal tubular atrophy with lipofuscin pigment, interstitial fibrosis, and patchy inflammation (Figure 1.4). The functional phenotype includes a rise in renal vascular resistance, a decline in glomerular filtration rate (GFR), and a rise in filtration fraction. It is not clear how these changes are related i.e. whether glomerular sclerosis, tubular atrophy, and interstitial fibrosis are primary or secondary events. Features not found in human renal senescence include heavy proteinuria, hematuria, development of ESRD, focal sclerosis, and infarction due to arterial occlusion.

The effect of aging of kidney in an unselected human population can be described by a variety of equations such as the Cockcroft-Gault equation (62) and the MDRD equation (63). These equations describe an unselected functional phenotype of renal senescence, which reflects the normal changes with loss of mass and function and those changes driven by age-related diseases, such as hypertension and heart failure. Although studies in selected populations ((64) and Baltimore Longitudinal Study of Aging (2)), excluding all renal diseases, hypertension and heart failure, demonstrated a mean loss of GFR of 0.75 ml/min per year (2), they also found that one (2) to two (64) third of the elderly had perfectly normal glomerular filtration

rates.

The senescence phenotype in an unselected population reflects the effect of aging and age-related diseases. Renal aging is regulated by genetic factors, intrinsic stresses, and extrinsic environmental factors. Hypertension and heart failure accelerate renal senescence (64). Thus a general model of renal senescence must include the potential for acceleration by abnormal stresses. Thus, at some point a senescent nephron is irreversibly shut down, but what abnormality triggers this event is not clear: vascular, glomerular, tubular or other changes. It seems possible that a physiologic shutdown mechanism is triggered, directly or indirectly, by molecular changes of senescence in the limiting cell type, as sensed by a regulatory mechanism in the nephron.

The incidence of ESRD is 50 to 100 fold higher in those above age 65 compared to people less than 20 (USRDS and ERA-EDTA Registry Reports 2000). This propensity can be attributed in part by the high incidence of diseases causing ESRD in the elderly and the time dependency of their effects. It is also possible that the processes of renal senescence include a decreased ability of the aged nephrons to cope with disease stress, i.e. an interaction between disease stress and intrinsic senescence processes.

The poor performance of transplant kidneys from older donors, particularly cadaveric donors, may be a special case of this. Terasaki and

colleagues emphasize “the greatest adverse impact on function in cadaver kidney transplants is donor age”. The older kidney displays increased probability of delayed graft function, acute rejection, chronic allograft nephropathy (also known as “chronic rejection”), strikingly impaired GFR, and an increased probability of early and late failure. Some of these features are attributable to the features of the older cadaver donors, which include an increased frequency of intracerebral hemorrhage and hypertension. There is much less effect of donor age in live donor transplantation, which may reflect selection plus the lack of the special stresses of cadaver donation (65). Cellular senescence may contribute to the diminished ability of aged nephrons to cope with the stresses of the brain death, preservation, and inflammation after cadaver transplantation. As a result the limiting cells in many aged nephrons reach senescence limits and the nephron irreversibly shuts down.

## 1.6 Perspective

In summary, the phenotype of renal senescence is attributable to both a decline in the number of functioning nephrons, and inherent limitations of age on the residual nephrons as revealed by a disease stress. This does not violate the intact nephron principle: it only states that an aged nephron has an inherent limitation due to the finite characteristics of its limiting cells. Many clinical nephrology problems in the elderly (and perhaps

in diseases with high proliferative requirements) could involve an interaction between cellular senescence and disease stresses. This may contribute to the normal renal senescence phenotype, the acceleration of this phenotype by hypertension and heart failure, the high frequency of ESRD in the elderly, and the massive nephron dropout after the stresses of cadaver donation. The relationship between cellular senescence and cancer is already well established e.g. by virtue of the very high frequency of abnormalities of p53, p16<sup>INK4a</sup>, and Rb and the universal re-expression of telomere replication mechanisms in cancer.

Are cellular senescence mechanisms good or bad? Cellular senescence is a protection against cancer, but it can also lead to genomic instability. Thus some cancers may arise in senescent cells. Perhaps the nephron shutdown mechanism in the normal elderly is fundamentally good, abrogating the possibility of serious malfunction by nephrons whose cells have passed certain limits. However, senescent cells may accumulate and potentially disrupt the functioning parenchyma or extracellular matrix, and evoke inflammation.

One of the appeals of studying mechanisms of cellular senescence in nephrology is the potential for predicting or intervening. Identifying those at risk of ESRD could be followed by strategies to reduce the stresses. It is possible that bypassing of cell senescence mechanisms by drugs or gene therapy could extend the life of old kidneys faced with abnormal stresses

such as cadaveric donation or renal disease. This may have to be balanced against the potential to increase renal cancer. The role of cell cycle regulatory proteins and senescence mechanisms in chronic stresses such as glomerular diseases, proteinuria, hypertension, and polycystic disease should be explored, even independent of the problem of aging.



## 1.7 Figures

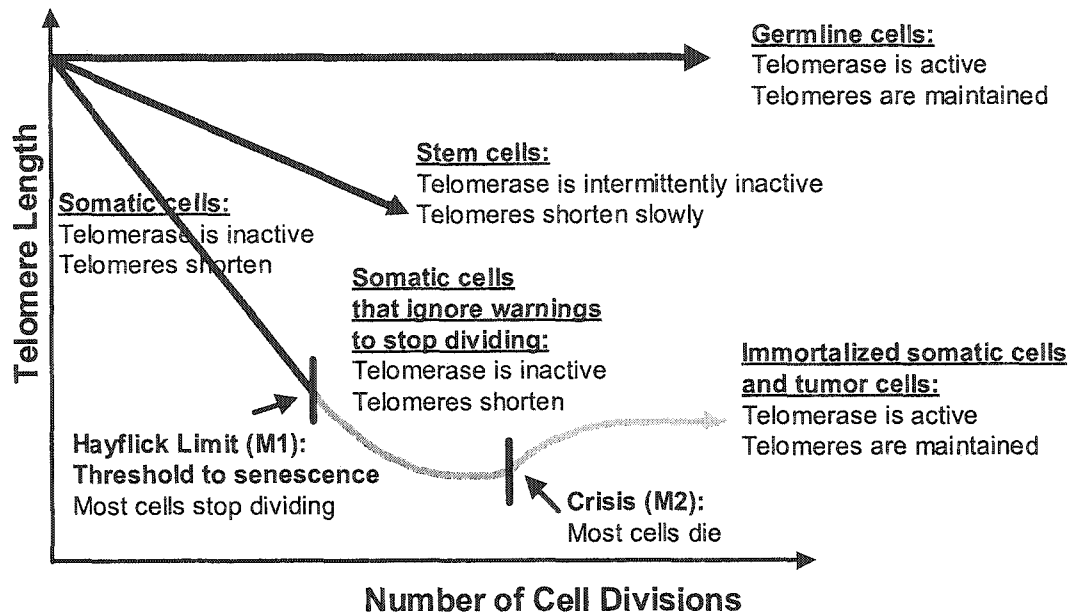


**Figure 1.1:** Telomere Hypothesis. Telomerase is active in germ line cells, maintaining long stable telomeres, but is repressed in most normal somatic cells, resulting in telomere loss in dividing cells. At M1, the Hayflick limit, there is a presumed critical telomere loss in one or perhaps a few chromosomes signaling irreversible cell cycle arrest. This would correspond to the phenotype of replicative senescence. Transformation events may allow somatic cells to bypass M1 without activating telomerase. When chromosomes become critically short on a large number of telomeres, cells are genomic unstable and enter crisis (M2). Rare clones that activate telomerase escape M2, stabilize their genome, and acquire indefinite growth capacity.

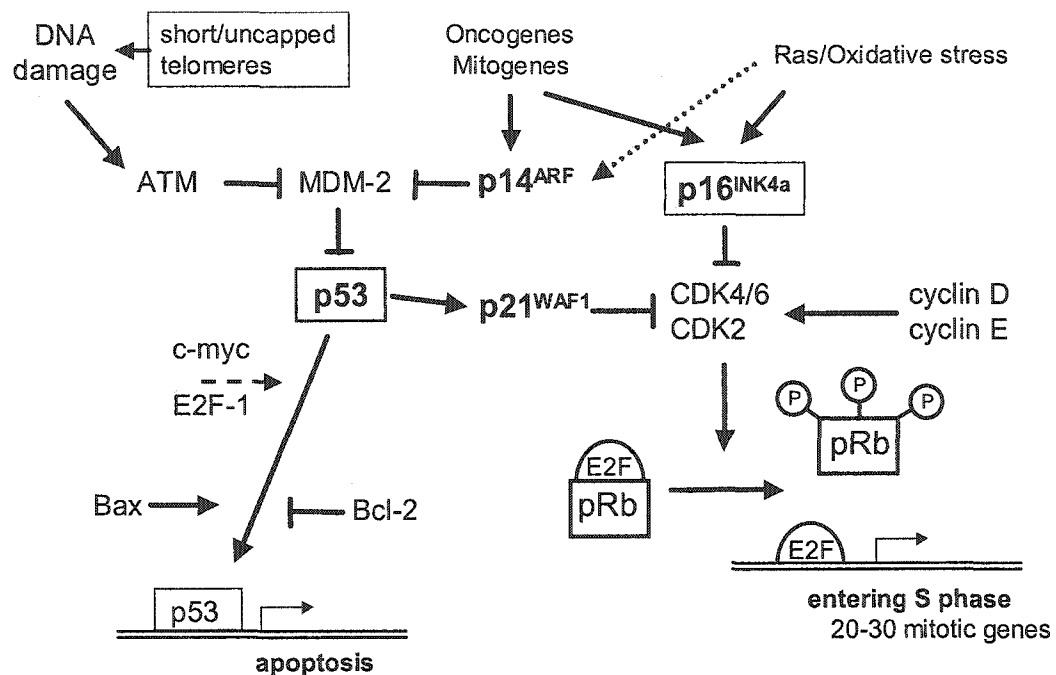


**Figure 1.2:** The ARF/p53 and p16/retinoblastoma (Rb) pathways. P53 is upregulated by DNA damage, telomere shortening and/or telomere uncapping. P53 is targeted by MDM2 (or the human equivalent HDM2) for ubiquination and degradation. P19<sup>ARF</sup> (or the human equivalent p14ARF) binds to MDM2 (or HDM2) and prevents ubiquination of p53, thereby stabilizing p53. The stabilization of p53 allows either induction of genes important for apoptosis (e.g. Bax) or can result in growth arrest mediated through its main transactivational target p21<sup>WAF1/CIP1</sup>. Increases in p16<sup>INK4a</sup> caused by environmental stresses (possible oxidative stress) will lead to the activation of the p16/RB pathway. P16<sup>INK4a</sup> interferes with D-type cyclins binding to the kinases CDK4 and 6 decreasing their activity. This results in less hyperphosphorylated retinoblastoma protein and thus interferes with the progression through the G1/S checkpoint. Hypophosphorylated Rb binds to and represses transcription factor E2F. E2F is important for transactivation of many genes important for mitosis and thereby G1/S progression.

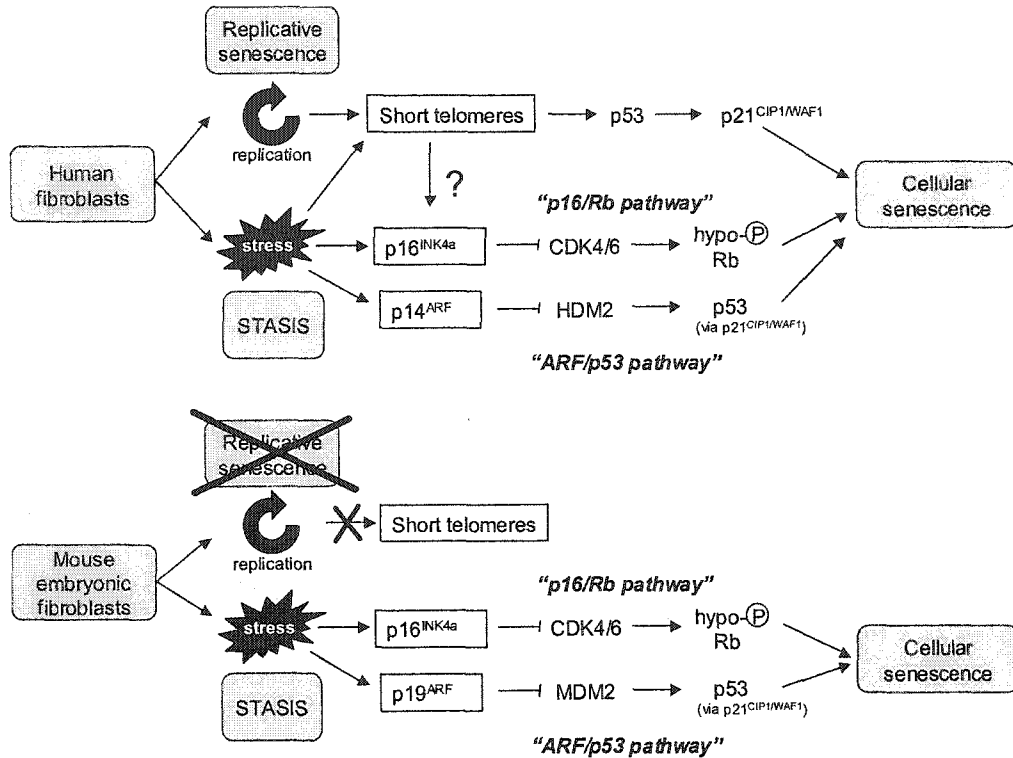


**Figure 1.3:** Differences in cellular senescence between human and mouse fibroblasts. The cartoon indicates the differences between the two forms of cellular senescence: “replicative senescence” and “STASIS”. In human fibroblasts, short, dysfunctional telomeres will trigger a DNA damage response by activation of p53 and possible p16<sup>INK4a</sup> (also p16<sup>INK4a</sup> does not seem to be essential for “replicative senescence” based on *in vitro* data). P53 leads to cell cycle arrest via its main transactivational target p21<sup>CIP1/WAF1</sup>. The increases seen in p16<sup>INK4a</sup> could be caused by environmental stresses (possibly oxidative stress) leading to the activation of the “p16/Rb pathway”. In mouse fibroblasts, replication in the presence of continuous telomerase expression does not result in short telomeres. Increases in p16<sup>INK4a</sup> or p19<sup>ARF</sup> result in activation of the “p16/Rb pathway” or the “ARF/p53 pathway”, respectively. Based on data from knockout experiments, it seems that mouse embryonic fibroblasts rely more on the ARF/p53 than on the p16/Rb pathway. The discussion whether stress can lead to telomere shortening reflecting STASIS rather than replicative senescence remains controversial. However, the data on this seems to be more substantiated for human fibroblasts.

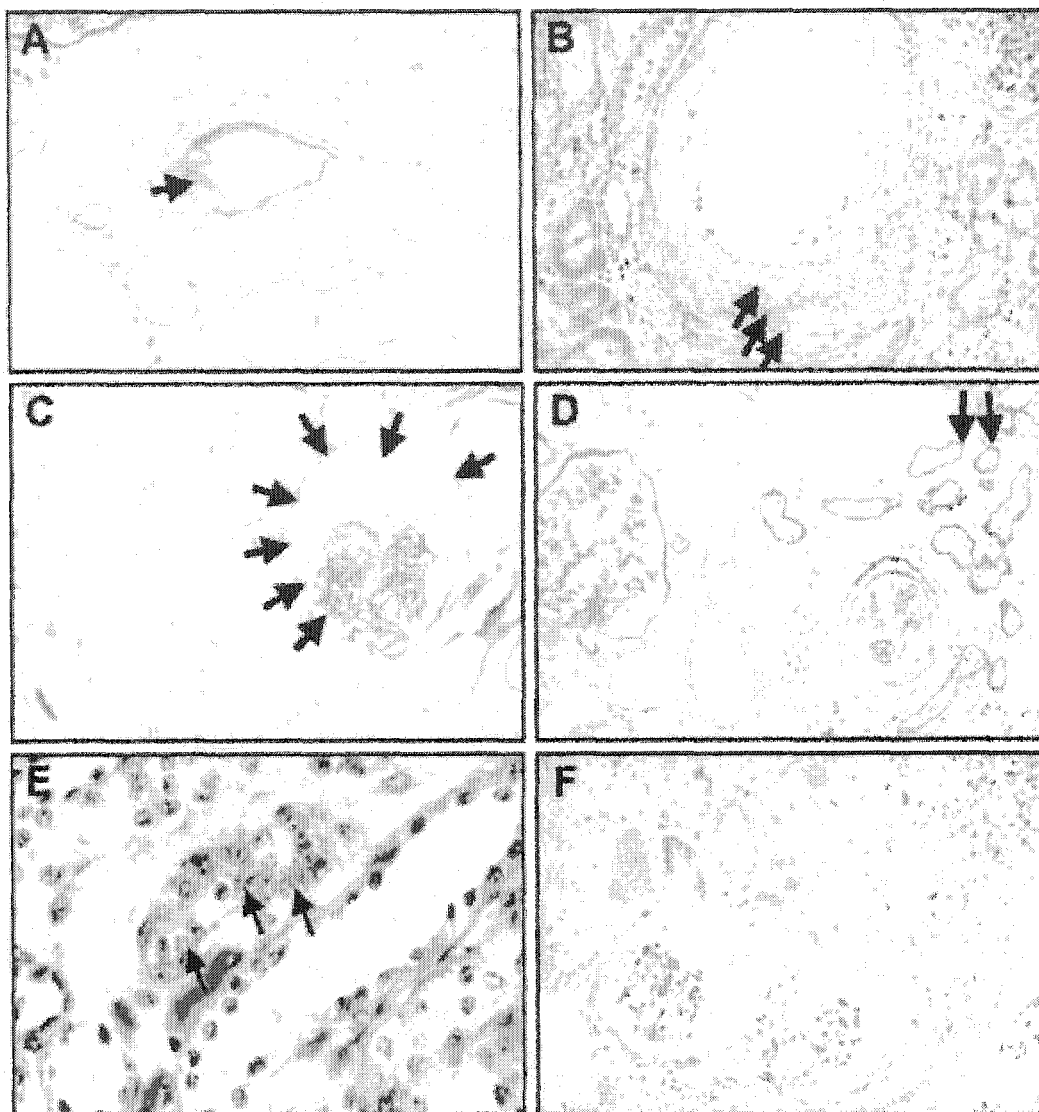


**Figure 1.4:** Histology of renal senescence. (A) Arteriohyalinosis; (B) Fibrous intimal thickening; (C) Glomerulosclerosis; (D) Tubular atrophy; (E) Lipofuscin pigment; (F) Interstitial fibrosis. (All pictures are a courtesy of Marjan Afrouzian).

## 1.8 References

1. Terasaki PI, Cecka JM, and Gjertson D.W.: Impact analysis: a method for evaluating the impact of factors in clinical renal transplantation. *Clinical Transplants*. Edited by Cecka JM and Terasaki PI. Los Angeles, CA, UCLA Tissue Typing Laboratory, 1998, pp. 437-441
2. Lindeman RD, Tobin J, and Shock NW: Longitudinal studies on the rate of decline in renal function with age. *J Amer Ger Soc* 1985, 33: 278-285
3. Hayflick L and Moorhead PS: The serial cultivation of human diploid cell strains. *Exp Cell Res* 1961, 25: 585-621
4. Wright WE and Shay JW: Historical claims and current interpretations of replicative aging. *Nature Biotechnology* 2002, 20: 682-688
5. Wright WE and Shay JW: Telomere dynamics in cancer progression and prevention: fundamental differences in human and mouse telomere biology. *Nature Medicine* 2000, 6: 849-851
6. Harley CB, Futcher AB, and Greider CW: Telomeres shorten during ageing of human fibroblasts. *Nature* 1990, 345: 458-460
7. Lee H-W, Blasco MA, Gottlieb GJ, Horner JWII, Greider CW, and DePinho RA: Essential role of mouse telomerase in highly proliferative organs. *Nature* 1998, 392: 569-574
8. Blasco MA, Lee H-W, Hande MP, Samper E, Lansdorp PM, DePinho RA, and Greider CW: Telomere shortening and tumor formation by mouse cells lacking telomerase RNA. *Cell* 1997, 91: 25-34
9. Olovnikov AM: A theory of marginotomy. The incomplete copying of template margin in enzymatic synthesis of polynucleotides and biological significance of the phenomenon. *J Theoret Biol* 1973, 41: 181-190
10. Bodnar AG, Ouellette M, Frolkis M, Holt SE, Chiu C-P, Morin GB, Harley CB, Shay JW, Lichtsteiner S, and Wright WE: Extension of life-span by introduction of telomerase into normal human cells. *Science* 1998, 279: 349-352
11. Blackburn EH: Switching and signaling at the telomere. *Cell* 2001, 106: 661-673
12. Blackburn EH: Telomere states and cell fates. *Nature* 2000, 408: 53-56
13. de Lange T and DePinho RA: Unlimited mileage for telomerase? *Science* 1999, 283: 947-949

14. Harper JW, Adami GR, Wei N, Keyomarsi K, and Elledge SJ: The p21 cdk-interacting protein cip1 is a potent inhibitor of G1 cyclin-dependent kinases. *Cell* 1993, 75: 805-816
15. Chin L, Artandi SE, Shen Q, Tam A, Less S-L, Gottlieb GJ, Greider CW, and DePinho RA: p53 deficiency rescues the adverse effects of telomere loss and cooperates with telomere dysfunction to accelerate carcinogenesis. *Cell* 1999, 97: 527-538
16. Weinberg RA: The retinoblastoma protein and cell cycle control. *Cell* 1995, 81: 323-330
17. Serrano M, Hannon GJ, and Beach D: A new regulatory motif in cell-cycle control causing specific inhibition of cyclin D/CDK4. *Nature* 1993, 366: 704-707
18. Zhang HS, Postigo AA, and Dean DC: Active transcriptional repression by the Rb-E2F complex mediates G1 arrest triggered by p16INK4a, TGFbeta, and contact inhibition. *Cell* 1999, 97: 53-61
19. Haber DA: Splicing into senescence: the curious case of p16 and p19<sup>ARF</sup>. *Cell* 1997, 91: 555-558
20. Kamijo T, Zindy F, Roussel MF, Quelle DE, Downing JR, Ashmun RA, Grosveld G, and Sherr CJ: Tumor suppression at the mouse *INK4a* locus mediated by the alternative reading frame product p19<sup>ARF</sup>. *Cell* 1997, 91: 649-659
21. Quelle DE, Zindy F, Ashmun RA, and Sherr CJ: Alternative reading frames of the INK4a tumor suppressor gene encode two unrelated proteins capable of inducing cell cycle arrest. *Cell* 1995, 83: 993-1000
22. Serrano M, Lee H-W, Chin L, Cordon-Cardo C, Beach D, and DePinho RA: Role of the INK4a locus in tumor suppressor and cell mortality. *Cell* 1996, 85: 27-37
23. Kiyono T, Foster SA, Koop JI, McDougall JK, Galloway DA, and Klingelhutz AJ: Both Rb/p16<sup>INK4a</sup> inactivation and telomerase activity are required to immortalize human epithelial cells. *Nature* 1998, 396: 84-88
24. Serrano M, Lin AW, McCurrach ME, Beach D, and Lowe SW: Oncogenic ras provokes premature cell senescence associated with accumulation of p53 and p16(INK4a). *Cell* 1997, 88: 593-602
25. Sherr CJ and DePinho RA: Cellular senescence: mitotic clock or culture shock? *Cell* 2000, 102: 407-410
26. Ly DH, Lockhardt DJ, Lerner RA, and Schultz PG: Mitotic misregulation and human aging. *Science* 2000, 287: 2486-2492

27. Cristofalo VJ: A DNA chip off the aging block. *Nature Medicine* 2000, 6: 507
28. Johnson FB, Sinclair DA, and Guarente L: Molecular biology of aging. *Cell* 1999, 96: 291-302
29. Finch CE and Tanzi RE: Genetics of aging. *Science* 1997, 278: 407-411
30. Sitte N, Merker K, Grune T, and von Zglinicki T: Lipofuscin accumulation in proliferating fibroblasts in vitro: an indicator of oxidative stress. *Exp Gerontol* 2001, 36: 475-486
31. Nadasdy T, Laszik Z, Blick KE, Johnson LD, and Silva FG: Proliferative activity of intrinsic cell populations in the normal human kidney. *J Am Soc Nephrol* 1994, 4: 2032-2039
32. Slack JMW: Stem cells in epithelial tissues. *Science* 2000, 287: 1431-1433
33. Cawthon RM, Smith KR, O'Brien E, Sivatchenko A, and Kerber RA: Association between telomere length in blood and mortality in people aged 60 years or older. *Lancet* 2003, 361: 393-395
34. Wynn RF, Cross MA, Hatton C, Will AM, Lashford LS, Dexter TM, and Testa NG: Accelerated telomere shortening in young recipients of allogeneic bone-marrow transplants. *Lancet* 1998, 351: 178-181
35. Allsopp RC, Cheshier S, and Weissman IL: Telomere shortening accompanies increased cell cycle activity during serial transplantation of hematopoietic stem cells. *J Exp Med* 2001, 193: 917-924
36. Allsopp RC, Morin GB, DePinho R, Harley CB, and Weissman IL: Telomerase is required to slow telomere shortening and extend replicative lifespan of HSC during serial transplantation. *Blood* 2003, 102: 517-520
37. Butler MG, Tilburt J, DeVries A, Muralidhar B, Aue G, Hedges L, Atkinson J, and Schwartz H: Comparison of chromosome telomere integrity in multiple tissues from subjects at different ages. *Cancer Genetics & Cytogenetics* 1998, 105: 138-144
38. Takubo K, Nakamura K, Izumiyama N, Furugori E, Sawabe M, Arai T, Esaki Y, Mafune K, Kammori M, Fujiwara M, Kato M, Oshimura M, and Sasajima K: Telomere shortening with aging in human liver. *J Gerontol A Biol Sci Med Sci* 2000, 55: B533-B536
39. Friedrich U, Griese E, Schwab M, Fritz P, Thon K, and Klotz U: Telomere length in different tissues of elderly patients. *Mech Ageing Dev* 2000, 119: 89-99



40. Friedrich U, Schwab M, Griese EU, Fritz P, and Klotz U: Telomeres in neonates: new insights in fetal hematopoiesis. *Pediatr Res* 2001, 49: 252-256
41. Youngren K, Jeanclos E, Aviv H, Kimura M, Stock J, Hanna M, Skurnick J, Bardeguet A, and Aviv A: Synchrony in telomere length of the human fetus. *Hum Genet* 1998, 102: 640-643
42. Megyesi J, Safirstein RL, and Price PM: Induction of p21<sup>WAF/CIP1/SDI1</sup> in kidney tubule cells affects the course of cisplatin-induced acute renal failure. *J Clin Invest* 1998, 101: 777-782
43. Kim Y-G, Alpers CE, Brugarolas J, Johnson RJ, Couser WG, and Shankland SJ: The cyclin kinase inhibitor p21<sup>CIP1/WAF1</sup> limits glomerular cell proliferation in experimental glomerulonephritis. *Kidney Int* 1999, 55: 2349-2361
44. Megyesi J, Price PM, Tamayo E, and Safirstein RL: The lack of functional p21<sup>WAF1/CIP1</sup> gene ameliorates progression to chronic renal failure. *Proc Natl Acad Sci USA* 1999, 96: 10830-10835
45. Orr WC and Sohal RS: Extension of life-span by overexpression of superoxide dismutase and catalase in *Drosophila melanogaster*. *Science* 1994, 263: 1128-1130
46. Larsen PL: Aging and resistance to oxidative damage in *Caenorhabditis elegans*. *Proc Natl Acad Sci USA* 1993, 90: 8905-8909
47. Lee CM, Weindruch R, and Aiken JM: Age-associated alterations of the mitochondrial genome. *Free Radic Biol Med* 1997, 22: 1259-1269
48. Sciacco M, Bonilla E, Schon EA, DiMauro S, and Moraes CT: Distribution of wild-type and common deletion forms mtDNA normal and respiration-deficient muscle fibers from patients with mitochondrial myopathy. *Hum Mol Genet* 1994, 3: 13-19
49. Tsuchida M, Miura T, and Aibara K: Lipofuscin and lipofuscin-like substances. *Chem Phys Lipids* 1987, 44: 297-325
50. Sohal RS, Marzabadi MR, Galaris D, and Brunk UT: Effect of ambient oxygen concentration on lipofuscin accumulation in cultured rat heart myocytes - a novel in vitro model of lipofuscinogenesis. *Free Radic Biol Med* 1989, 6: 23-30
51. Marzabadi MR, Jones C, and Rydstrom J: Indenoindole depresses lipofuscin formation in cultured neonatal rat myocardial cells. *Mech Ageing & Dev* 1995, 80: 189-197

52. Terman A and Brunk UT: Lipofuscin: mechanisms of formation and increase with age. *APMIS* 1998, 106: 265-276
53. Sell DR, Lane MA, Johnson WA, Masoro EJ, Mock OB, Reiser KM, Fogarty JF, Cutler RG, Ingram DK, Roth GS, and Monnier VM: Longevity and the genetic determination of collagen glycoxidation kinetics in mammalian senescence. *Proc Natl Acad Sci* 1996, 93: 485-490
54. Oliver CN, Ahn BW, Moerman EJ, Goldstein S, and Stadtman ER: Age-related changes in oxidized proteins. *J Biol Chem* 1987, 262: 5488-5491
55. Raj DSC, Choudhury D, Welbourne TC, and Levi M: Advanced glycation end products: a nephrologist's perspective. *Am J Kidney Dis* 2000, 35: 365-380
56. Dimri GP, Lee X, Basile G, Acosta M, Scott G, Roskelley C, Medrano EE, Linskens M, Rubelj I, Pereira-Smith O, Peacocke M, and Campisi J: A biomarker that identifies senescent human cells in culture and in aging skin *in vivo*. *Proc Natl Acad Sci USA* 1995, 92: 9363-9367
57. Artandi SE, Chang S, Lee SL, Alson S, Gottfried GJ, Chin L, and DePinho RA: Telomere dysfunction promotes non-reciprocal translocations and epithelial cancers in mice. *Nature* 2000, 406: 641-645
58. Campisi J: The role of cellular senescence in skin aging. *J Investig Dermatol Symp Proc* 1998, 3: 1-5
59. Baylis C and Corman B: The aging kidney: insights from experimental studies. *J Am Soc Nephrol* 1998, 9: 699-709
60. Tracy RE and Johnson LK: Aging of a class of arteries in various mammalian species in relation to the life span. *Gerontology* 1994, 40: 291-297
61. Gourtsoyiannis N, Prassopoulos P, Cavouras D, and Pantelidis N: The thickness of the renal parenchyma decreases with age. A CT study of 360 patients. *Am J Roentgenol* 1990, 155: 541-544
62. Cockcroft DW and Gault MH: Prediction of creatinine clearance from serum creatinine. *Nephron* 1976, 16: 31-41
63. Levey AS, Bosch JP, Lewis JB, Greene T, Rogers N, and Roth D: A more accurate method to estimate glomerular filtration rate from serum creatinine: a new prediction equation. Modification of Diet in Renal Disease Study Group. *Ann Intern Med* 1999, 130: 461-470
64. Fliser D, Franek E, Joest M, Block S, Mutschler E, and Ritz E: Renal function in the elderly: impact of hypertension and cardiac function. *Kidney Int* 1997, 51: 1196-1204

65. Cecka JM: The UNOS scientific renal transplant registry. Clinical Transplants. Edited by Cecka JM and Terasaki PI. Los Angeles, CA, UCLA Tissue Typing Laboratory, 1999, pp. 1-21

## Chapter 2

### Telomere Shortening in Human Kidneys with Age

A version of this chapter has been published.

Anette Melk, Vido Ramassar, Lisa M.H. Helms, Ron Moore, David Rayner, Kim Solez, and Philip F. Halloran: Telomere shortening in kidneys with age. *Journal of the American Society of Nephrology* 2000; 11: 444-453.

Portions of this publication that were contributed by co-authors are not included unless noted. Used with permission of Lippincott Williams & Wilkins.

## 2.1 Introduction

The kidney develops characteristic physiologic and pathologic changes with age termed "senescence" (1-3). Glomerular filtration rate (GFR) declines by about 0.75 ml/min per year over age 40 (2), whereas renal vascular resistance rises and the filtration fraction increases. The decline in function is variable and some healthy individuals preserve their GFR indefinitely (4) while hypertension and heart failure accelerate senescent changes (2). Pathologic changes include a 20-25% loss of volume, particularly in cortex, fibrous intimal thickening (FIT) of arteries, loss of glomeruli due to global sclerosis, (perhaps reflecting occlusion of the afferent arteriole) and patchy tubular atrophy and interstitial fibrosis. Histologic studies on autopsy kidneys indicate that aging is associated with a loss of cells and an increase in the size of the nuclei (5).

Renal senescence has many implications for nephrology, including normal aging, excess acute renal injury, increased end stage renal disease, decreased transplant survival, and increased cancer. The usual changes of normal aging are relevant to drug dosing and render individuals more susceptible to dehydration. The older population has a high frequency of acute renal failure, reflecting reduced renal reserve, increased comorbidities, and possibly increased susceptibility to acute insults. The elderly are also up to 100 times more likely to develop end stage renal failure than the young (6). As recently reviewed (7), donor age has become

the main identifiable influence on long term graft survival (8-11), and the pathology of chronic allograft nephropathy (CAN) overlaps the changes of aging (12;13). Kidney transplants from older donors have higher baseline serum creatinine, more delayed graft function, and reduced long-term survival. The effect of donor age in renal transplantation may be an example of the reduced ability of aged kidneys to tolerate and recover from injuries and stress. Hypertension and heart failure accelerate the changes of renal senescence (1;14). Renal cancer is age related, and the problem of malignant transformation is intimately related to cell senescence mechanisms (15).

In 1985 Kaysen and Myers pointed out that "the mechanisms and the full biochemical and physiologic consequences of renal senescence remain to be fully elucidated" (16), a statement that remains true. The molecular basis of senescent changes *in vivo* is not known, and many theories of aging have been proposed, including oxidative damage, genomic instability (including telomere loss), genetic programming, and cell death (17). However, considerable progress has been made in determining the mechanisms of senescence *in vitro*. Primary cultures of somatic cells complete a finite number of cycles (the "Hayflick limit" (18)), which reflects the age of the cell donor and their proliferative history. As they approach this limit, they cease to replicate and enter a state of replicative senescence. Replicative senescence *in vitro* is due at least in part to

telomere shortening because it can be bypassed by transfection with the enzyme telomerase (19). Telomeres are DNA repeats of the sequence (TTAGGG)<sub>n</sub> which protect the ends of chromosomes, and are generated mainly by the enzyme telomerase. Because telomerase is not expressed in most somatic cells, telomeres shorten with increasing age, reflecting the number of cycles that the cell has completed. The telomere hypothesis of cell aging suggests that telomere shortening in the absence of telomerase is the mitotic clock for replicative senescence in normal somatic cells (20;21). As shortening becomes critical for a telomere on a particular chromosome, that chromosome becomes unstable and the cell stops dividing. Studies on human blood cells and blood vessels suggest that chronic stresses requiring a higher replication rate increase telomere shortening in vivo in humans (22;23). Studies of expression of markers for mitosis suggest that the kidney is subjected to ongoing replicative stress, e.g. in endothelial cells (24).

I investigated telomere length in kidneys derived from nephrectomies and autopsy specimens from individuals of different ages. I found that telomeres in human kidney cortex shorten with age, and that the shortening is faster in cortex than in medulla. These observations suggest that telomere length may reflect either developmental changes or aging. While the causes and significance of telomere shortening in various renal cell populations will likely prove to be complex, these data are compatible

with a role for telomere shortening and replicative senescence in some of the phenomena that characterize renal aging.

## 2.2 Materials and Methods

### 2.2.1 Terminal restriction fragments (TRF)

Samples were taken of kidney tissues derived from total nephrectomies or from autopsies. Whenever possible I collected cortex and medulla separately. All samples were snap frozen in liquid nitrogen and were stored at -80° C. To obtain high molecular weight DNA without degradation, I disrupted the tissue by freeze grinding. DNA was then isolated by proteinase K digestion and phenol/chloroform extraction. DNA samples were digested with the restriction enzymes Hinf I and Rsa I (Boehringer Mannheim, Germany) to produce TRFs. Aliquots of undigested and digested DNA were resolved by 0.5% agarose gel electrophoresis (70V, 2h) and examined by ethidium bromide staining for the absence of unspecific degradation and complete digestion, respectively. 1.5 µg of each digested sample was resolved by 0.7% agarose gel electrophoresis (40V, 40h). DNA was Southern blotted onto a nitrocellulose membrane (Hybond-C Extra, Amersham) and probed as described previously (20;25) with minor modifications. The membranes were hybridized at 42° C overnight with a 5'-end-labelled <sup>32</sup>P-(TTAGGG)<sub>5</sub> oligonucleotide telomere probe in a buffer containing 25% formamide, 5X Denhardt's solution, 5X SSPE, 0.1% SDS



and 100 µg/ml denatured salmon sperm DNA. Following a 15 min stringency wash at 42° C in 0.2X SSC, 0.1% SDS, the autoradiography signal was digitized in a phosphoimage scanner (Fuji) using ImageGauge Software. All lanes were subdivided into intervals of approximately 1-2 mm. The mean size of the TRFs was estimated using the formula  $\Sigma(\text{OD}_i \times L_i) / \Sigma(\text{OD}_i)$ , where  $\text{OD}_i$  is the density reading from interval  $i$  and  $L_i$  is the size in kbp of the interval relative to the markers (20). Mean TRF length was determined over the range of 2.3 to 23.1 kbp markers (broad range) and also on the basis of the intensity of the signal (narrow range), where the intervals averaged were those intervals that were higher than 1% of the total signal in that lane. The median and mode values were also derived on the basis of the narrow range determination.

### 2.2.2 GFR

Creatinine clearance ( $\text{Cl}_{\text{Crea}}$ ) was predicted from serum creatinine ( $\text{S}_{\text{Crea}}$ ) in adult males where  $\text{Cl}_{\text{Crea}} = (140 - \text{age [years]}) * (\text{wt kg}) / (72 * \text{S}_{\text{Crea}} [\text{mg}/100 \text{ ml}])$  and in adult females with a correction factor of -15% (26).

## 2.3 Results

### 2.3.1 Demographic data

Table 2.1 lists the clinical data of the individuals from whom the kidneys were derived. 17 normal samples were derived from autopsies

(N=1) or nephrectomies from patients with either renal cell carcinoma (N=11), oncocytoma (N=2), Wilms tumor (N=1), transitional cell carcinoma (N=1), or severe renal artery atherosclerosis (N=1). Normal renal tissue remote from the tumor was chosen for analysis. I will refer to these samples as 'normal' kidneys when the histology was within the limits of changes expected for age. Three samples from the nephrectomies for renal tumors showed a small number of tumor cells representing a small minority of the cells present. Seven samples were derived from nephrectomies with histologic abnormalities such as pyelonephritis, hydronephrosis, atherosclerosis, and nephrosclerosis. I will refer to those kidneys as 'abnormal' kidneys. However, patients generally did not have marked renal insufficiency, as shown in table 2.1, and the serum creatinine values were markedly abnormal only in the one month old infant with acute renal failure, the 9 year old with adult type polycystic kidney disease (APCKD) and the 74 year old with chronic interstitial nephritis.

### 2.3.2 Telomere length in kidney cortex and medulla

TRFs in renal cortex shortened with age (Figure 2.1). From these blots I plotted regression relationships of various measurements of the TRF distribution against age (Figures 2.2-2.4). I analyzed the mean (Figure 2.2), median (Figure 2.3), and mode (Figure 2.3) of a narrowly defined TRF distribution ("narrow range"), and the mean of a more broadly defined

distribution ("broad range"; Figure 2.4). All of these measurements showed a significant TRF shortening with increasing age in renal cortex. Based on the mean (narrow range; Figure 2.2), the slope of the regression is 0.0293 kbp per year, i.e. 29 bp per year (0.24%). Nevertheless the outliers argue against a simple predictable annual loss. This regression analysis was not significantly altered if samples with histologic abnormalities were excluded: the regression was still significant (data not shown). To avoid selection bias all samples were included in the subsequent analyses. The Y intercept of these regression relationships provides an estimate of the TRF length at birth:  $12.4 \pm 0.64$  kbp by the narrow range, and  $11.2 \pm 0.34$  kbp by the broad range.

I grouped the mean cortex TRF lengths for kidneys of different ages to see if loss was accelerated in some age ranges. For this purpose the 29-year kidney with pyelonephritis and short TRF of 8.8 kbp was isolated as it was the only observation between 10 and 40. The groups showed mean TRF lengths as follows: age 0.1 to 9 years, 12.2 kbp; age 42-50 years, 11.5 kbp; age 51-58 years, 11.5 kbp; age 62-68 years, 10.6 kbp; age >71 years, 10.1 kbp. These data do not suggest acceleration in one age group. However, when the 17 kidneys older than 40 years were examined by regression the slope suggests TRF shortening of 82 bp per year ( $R^2=0.3985$ ;  $p=0.0066$ ), indicating that there is telomere shortening in cortex in the age range where senescence develops.

Medulla samples available on 20 specimens showed slightly shorter mean TRF length in young children (Figures 2.6-2.10). The estimated TRF lengths in medulla at birth (Y intercepts) were  $10.7 \pm 0.61$  kbp (narrow range) and  $10.1 \pm 0.32$  kbp (broad range), both significantly less than in cortex ( $p < 0.05$ ). However, the medulla showed less of a tendency to TRF shortening with age. The estimates of the slopes of the mean (Figure 2.7), median (Figure 2.8), and mode (Figure 2.9) of the narrow range and of the mean of the broad molecular weight range (Figure 2.10) are shown. Mean TRF length in medulla declined slightly as a function of age by 0.0129 kbp (narrow range) and 0.0091 kbp (broad range) per year (not significant). Hereafter, the "narrow range" mean is used.

### 2.3.3 Comparing cortex versus medulla in paired samples

I compared the TRF length in cortex versus medulla for paired samples (N=20) on which clear cortex-medulla distinctions could be made (Table 2.2). The mean TRF length in the cortex was longer ( $10.8 \pm 1.6$  kbp) than in medulla ( $10.1 \pm 1.2$  kbp) ( $p < 0.001$ ). In kidneys under age 10 (N=3) the TRF length in the cortex ( $12.2 \pm 1.2$  kbp) was about 1.7 kbp longer than in medulla ( $10.5 \pm 0.74$  kbp) ( $p = 0.012$ ). In kidneys age 50 and below (N=8) the TRF length in cortex was  $11.4 \pm 1.5$  kbp versus  $10.4 \pm 0.91$  kbp in medulla ( $p = 0.007$ ). For kidneys above age 50 (N=12) the mean TRF length in cortex was  $10.3 \pm 1.5$  kbp versus  $9.9 \pm 1.2$  kbp in medulla ( $p = 0.014$ ).

Above age 60 (N=8) the mean TRF length was  $9.9 \pm 1.5$  kbp for cortex versus  $9.7 \pm 1.4$  kbp for medulla ( $p=0.11$ ), only about 0.2 kbp difference. Thus increasing age was associated with more TRF shortening in cortex than medulla, tending to eliminate the differences between cortex and medulla (Figure 2.11).

#### 2.3.4 GFR versus telomere length

The relationship of TRF length to GFR was assessed because both of these measurements decline with age. The calculated GFR declined with age (Figure 2.12) as expected, by about 1.3% per year from the third decade. This is a higher rate than in a normal population and presumably reflects the selection for renal diseases. There was a weak positive relationship between calculated GFR and TRF length in cortex, which was not significant (Figure 2.13).

## 2.4 Discussion

This report documents that telomere DNA is lost with age in kidney, and that rate of loss in cortex is greater than in medulla. The TRFs were longer in cortex than medulla in young kidneys but the difference lessened with age due to greater telomere loss in cortex. Thus the present data suggest that telomere shortening may be a phenomenon of both development and aging. Whether the extent of telomere loss in older

kidneys would affect the ability of the kidney to sustain function against normal wear and tear or abnormal stresses is not known. However, given the heterogeneity of renal cell populations, and of telomere length on individual chromosomes, the present results raise the possibility that critical telomere shortening could become a limiting factor in some renal cell populations and could contribute to some of the features of the senescent kidney.

Certain caveats surround studies of telomere length. First, most studies (like these) are conducted on surgical specimens and must be confirmed on unselected normal tissues when the availability of tissue permits. Second, the critical measurements of telomere changes should be made in the population of renal cells that are likely to be limiting such as intimal cells in small arteries (22). Third, in presenting the regression between TRFs and age one cannot imply that these are truly linear. In 24 samples I cannot determine the shape of this relationship accurately (e.g. accelerated early or late telomere loss.) Fourth, population changes could be mistaken for telomere shortening if a cell population with longer TRFs was being replaced or infiltrated with a population with shorter TRFs. On the other hand if cells with short telomeres disappeared then telomere shortening would be underestimated. Finally, the TRF determination is the gold standard method but has limitations. Specifically, because TRFs are composed of telomeres plus 4-5 kbp of subtelomeric repeats (27), it is

conceivable that differences in the subtelomeric repeats between cell populations could contribute to differences in TRF length e.g. between cortex and medulla.

While telomere shortening with age has not previously been studied in kidney, it is known in other tissues, e.g. blood cells. The rate of loss of telomere DNA in cortex is less than that reported for human lymphocytes, where the rate of telomere loss is about 41 bp per year (28). Thus in renal cortex telomere DNA declines at a rate intermediate between highly proliferative cells as lymphocytes and less proliferative tissues such as brain or muscle, in which TRF shortening is not detected (29;30). A recent study (31) assessed TRF length in blood and skin cells from humans of different ages, and from 15 other tissues from the fetus and 8 other tissues from the 72-year-old male. Significant differences ( $p < 0.001$ ) were found in the shortest TRF size and in the variation of TRF length between the 20-week fetus and the 72-year-old male. The 72-year-old male showed the shorter and more variable TRFs for all tissues studied, but the greatest differences were observed in blood cells (e.g. average TRF length was 12.2 kbp in the fetus and 7.2 kbp in the 72-year-old male).

Although telomere regulation is complex, the principal cause of telomere loss is likely to be replication. Cell division in fibroblasts lacking telomerase shortens TRFs by about 75 bp *in vivo* and 48 bp *in vitro* per population doubling (27). The observed telomere shortening in cortex with

age may reflect the generation of renal cells through development and the replacement of cells lost through normal wear and tear or injury. Thus telomere shortening reflects the replicative history of the tissue. There are also mechanisms of telomere shortening independent of proliferation. Fibroblasts *in vitro* show telomere shortening when exposed to high oxygen concentrations, even when their proliferation is inhibited, suggesting that free radical-mediated damage may shorten telomeres independent of replication (32) and may be prevented by anti oxidant strategies (33). Hemodynamic stress may cause telomere shortening in arteries, but whether the mechanism is dependent on proliferation is not known (22).

Telomere shortening may be accelerated by disease stresses, either by proliferative or other mechanisms, and could represent a mechanism of disease progression. For example, in active ulcerative colitis, mucosal cells of the affected colon show rapid turnover, and TRF length of the colonic mucosa of patients with colitis was shorter than that of the controls and of uninvolved mucosa (34). Thus telomere shortening in the colonic mucosa may contribute to the chronic pathology of ulcerative colitis. Similarly the stem cells of bone marrow transplant recipients show accelerated telomere shortening in the recipient compared to the donors (23). Thus cycles of injury and repair in disease states may cause critical telomere shortening and eventually establish limits to tissue survival. In the present study we did not find differences between tissues with histologic abnormalities and



normal tissues. However, we have not sampled progressive and end stage renal diseases adequately to answer this question.

The significance of telomere shortening in kidney over the range described is not clear. *In vitro*, telomere length predicts replicative capacity and the propensity to develop replicative senescence (27). Telomere shortening for a cell becomes critical when even one telomere reaches its threshold, because the effects of telomere shortening are dominant. Cell replication ceases and the cell expresses a new pattern of gene expression characteristic of replicative senescence (35). The mean TRF length in senescent fibroblasts is about 7 to 8 kbp but shows variation between clones. It is difficult to extrapolate from cultured fibroblasts to whole organs *in vivo*. In order to determine whether critical telomere shortening in the kidney contributes to renal senescence, more information would be needed. First, one should establish the rate of replication in renal cells at different ages and in disease states. Second, one should get estimates of telomere shortening in individual cell types e.g. intimal cells in arteries, mesangial cells. Third, one should determine whether lesser degrees of telomere shortening can induce functional changes without replicative senescence. Finally one needs to rule out the possibility that cells with short telomeres rapidly disappear, underestimating telomere shortening.

It is probable that molecular explanations will be found for normal renal aging, for the excess of end stage disease in the elderly, for the poor

performance of kidney transplants from old donors, and for the sensitivity of older kidneys to acute injuries. The development of new animal models and new technologies for studying human biopsy material would aid the identification of these mechanisms. Most common rat and mouse strains have very long telomeres, limiting their value in addressing the telomere regulation (36). Moreover the changes in rat and mouse kidneys with age (37) differ from those in long-lived species such as the human. For example spontaneous fibrous intimal thickening in arteries is characteristic of long lived but not short-lived mammals (38;39). New mouse models such as the telomerase knockout mouse (40), or *Mus spretus* (36) which has telomeres resembling humans in length, should establish the significance of telomere shortening. Ultimately we must study human kidneys to determine the mechanisms and significance of telomere shortening and other candidate molecular changes of senescence. The TRF method requires more DNA than is available from needle biopsy specimens, hampering our ability to answer such questions directly. We need methods to measure telomere changes and other candidate mechanisms of senescence in microscopic renal components (e.g. arteries, glomeruli) and individual cells (e.g. endothelial cells) likely to be limiting in aging, in diseases, and in transplants.

## 2.5 Tables

**Table 2.1:** Demographic data on the 24 individuals from whom the kidneys were derived.

Age (years)	Gender	History of DM	History of HTN	BP	Crea (μmol/L)	Urea	Clinical diagnosis	Histology of renal parenchyma
0.1	M	No	No	58/30	143	20.7	Multiorgan failure	Normal
0.8	M	No	Yes	119/84	48	4.4	Renal dysplasia, secondary inflammation	Renal dysplasia, interstitial nephritis*
4	F	No	No	99/57	56	3.7	Chronic PN, reflux	Acute on chronic PN*
4	F	No	No	80/50	50	3.1	Wilms tumor	Normal
5	M	No	No	114/66	85	N/A	HN secondary to obstruction at ureteropelvic junction	HN*
9	F	No	No	105/70	682	33.8	APCKD	Multiple cysts*
29	F	No	No	128/80	81	N/A	Acute PN	Infiltrate, TA*
42	M	No	Yes	132/80	165	N/A	RCC II, Oncocytoma I	Normal
47	M	No	No	112/66	123	8.8	RCC III	Normal
50	M	No	No	150/96	114	N/A	RCC II	Normal
50	M	No	No	118/70	123	N/A	RCC III	Normal
51	F	No	No	118/70	82	3.4	HN	HN*
55	M	No	Yes	150/80	108	5	Oncocytoma II	Normal
57	M	No	No	120/70	109	4.3	RCC II	Normal
57	F	No	No	170/90	83	N/A	RCC III	Normal
58	M	No	No	120/70	117	5.8	RCC	Mild age changes IF, TA
62	M	No	Yes	122/62	136	N/A	RCC III	Mild age changes IF, TA
67	M	No	No	120/68	99	7.6	RCC II, CLL	Lymphoma infiltrate
68	F	No	Yes	140/84	137	5.5	Severe renal artery atherosclerosis	Age changes IF, TA, FIT
71	M	No	No	120/80	126	N/A	RCC III	Normal
74	F	No	No	135/105	113	4.4	Papillary TCC	IF, TA, FIT; compatible with age
74	F	No	Yes	150/80	189	N/A	HN, PN	Chronic interstitial nephritis*
79	F	no	No	140/84	112	N/A	RCC I	Moderate TA, IF, FIT
88	F	no	Yes	180/88	96	N/A	RCC II	Focal inflammation, IF

DM, diabetes mellitus; HTN, hypertension; BP, blood pressure; Crea, Creatinine; N/A, not assessed; RCC, renal cell carcinoma; TCC, transitional cell carcinoma; HN, hydronephrosis; PN, pyelonephritis; APCKD, adult type polycystic kidney disease; CLL, chronic lymphocytic leukemia; IF, interstitial fibrosis; TA, tubular atrophy; FIT, fibrous intimal thickening.

\*"Abnormal" with histology outside the limits of changes expected for age.

**Table 2.2:** Telomere length in paired cortical and medullary samples with age.

Age	Telomere Length (kbp)		P value
	Cortex	Medulla	
All paired samples (N=20)	10.77 ± 1.62	10.06 ± 1.16	0.0004
Under age 10 (N=3)	12.16 ± 1.16	10.47 ± 0.47	0.0120
Under 50 years (N=8)	11.43 ± 1.50	10.38 ± 0.91	0.0070
50 years and over (N=12)	10.33 ± 1.53	9.85 ± 1.23	0.0144
Over 60 years (N=8)	9.93 ± 1.46	9.65 ± 1.38	0.1144

## 2.6 Figures

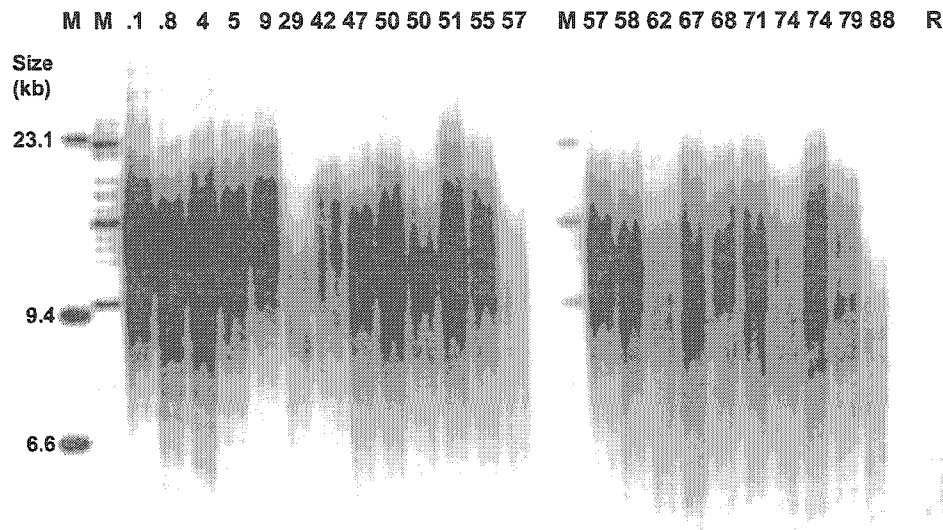


**Figure 2.1:** Telomere length in human renal cortex samples. Genomic DNA from cortex samples derived from different donors of indicated ages was prepared as described and resolved by agarose gel electrophoresis. Telomere restriction fragments were detected with a  $^{32}\text{P}$ -labelled telomeric oligonucleotide. Size [kbp] is indicated. M=molecular weight marker, R=Raji cells.

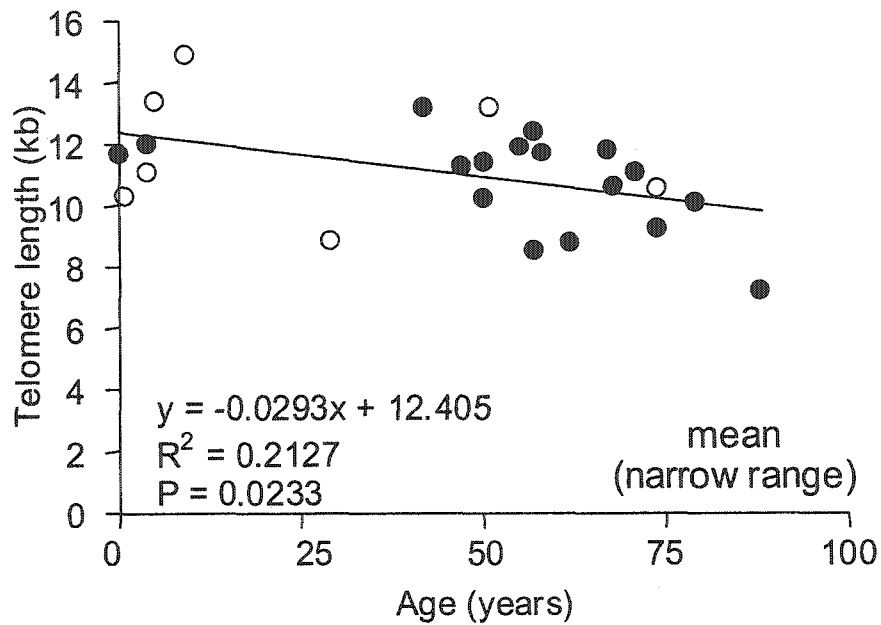


**Figure 2.2:** Regression of telomere length measurements in renal cortex by Southern blotting against age. Panels represent the mean of a narrowly defined telomere distribution (“narrow range”). Unfilled symbols represent “abnormal” kidney samples with histological changes outside the limits of changes expected for age.



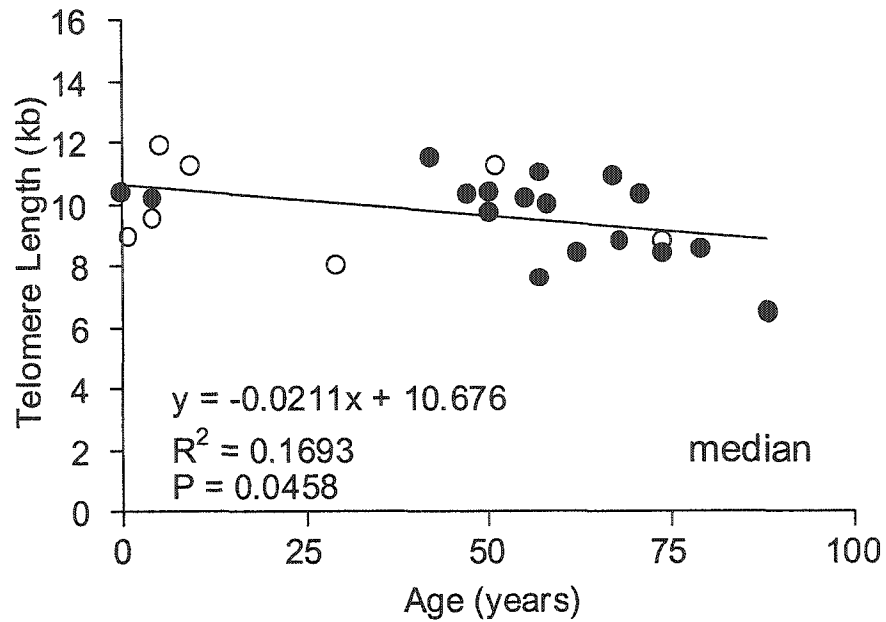


**Figure 2.3:** Regression of telomere length measurements in renal cortex by Southern blotting against age. Panels represent the median of a narrowly defined telomere distribution ("narrow range"). Unfilled symbols represent "abnormal" kidney samples with histological changes outside the limits of changes expected for age.

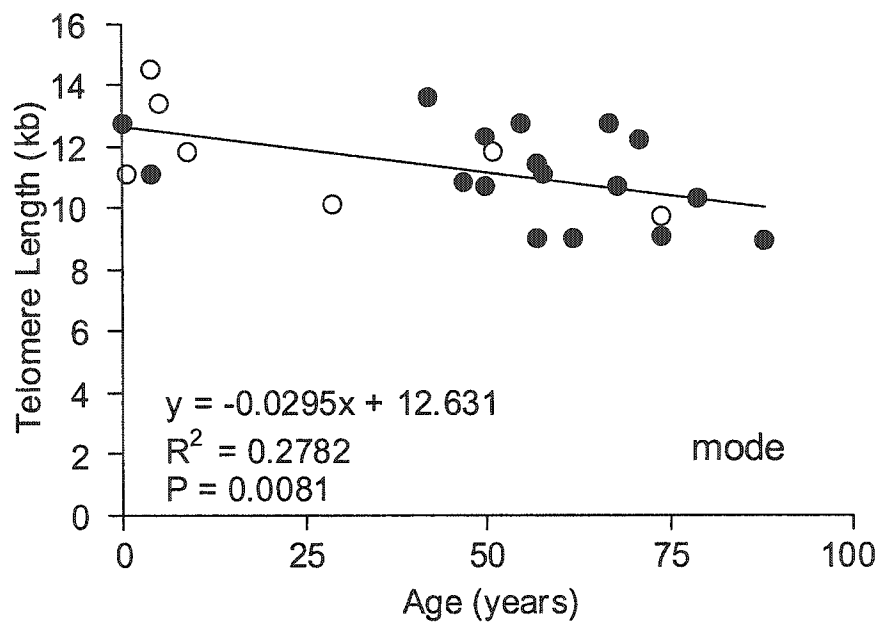


**Figure 2.4:** Regression of telomere length measurements in renal cortex by Southern blotting against age. Panels represent the mode of a narrowly defined telomere distribution ("narrow range"). Unfilled symbols represent "abnormal" kidney samples with histological changes outside the limits of changes expected for age.

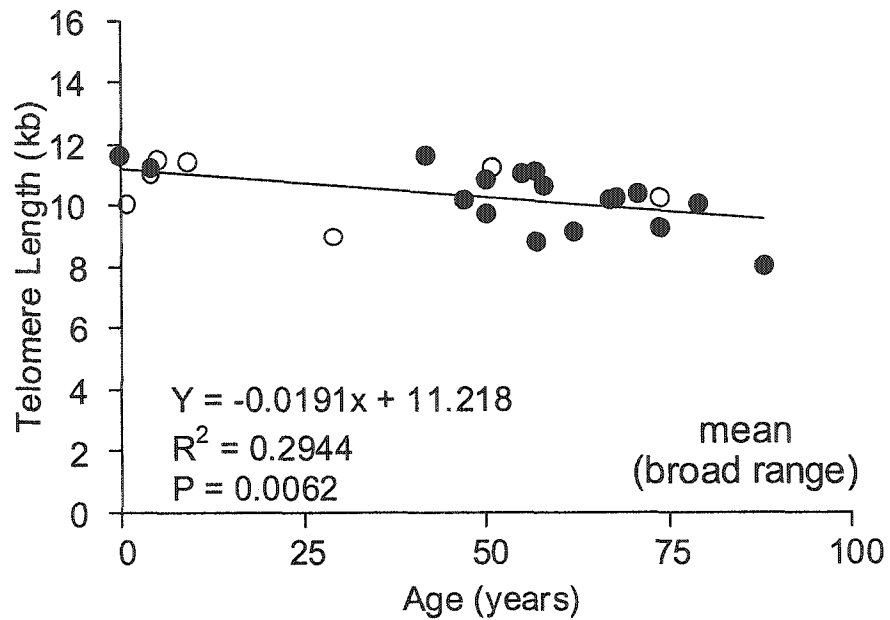


**Figure 2.5:** Regression of telomere length measurements in renal cortex by Southern blotting against age. Panels represent the median of a more broadly defined telomere distribution ("broad range"). Unfilled symbols represent "abnormal" kidney samples with histological changes outside the limits of changes expected for age.

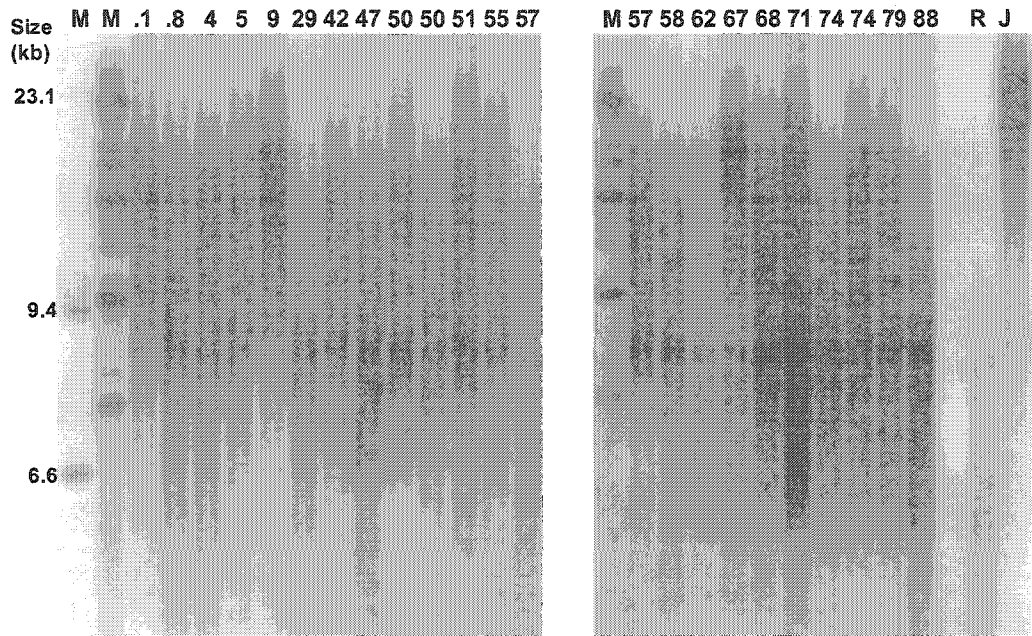


**Figure 2.6:** Telomere length in human renal medulla samples. Genomic DNA from medulla samples derived from different donors of indicated ages was prepared as described and resolved by agarose gel electrophoresis. Telomere restriction fragments were detected with a  $^{32}\text{P}$ -labelled telomeric oligonucleotide. Size [kbp] is indicated. M=molecular weight markers, R=Raji cells, J=Jurkat cells.

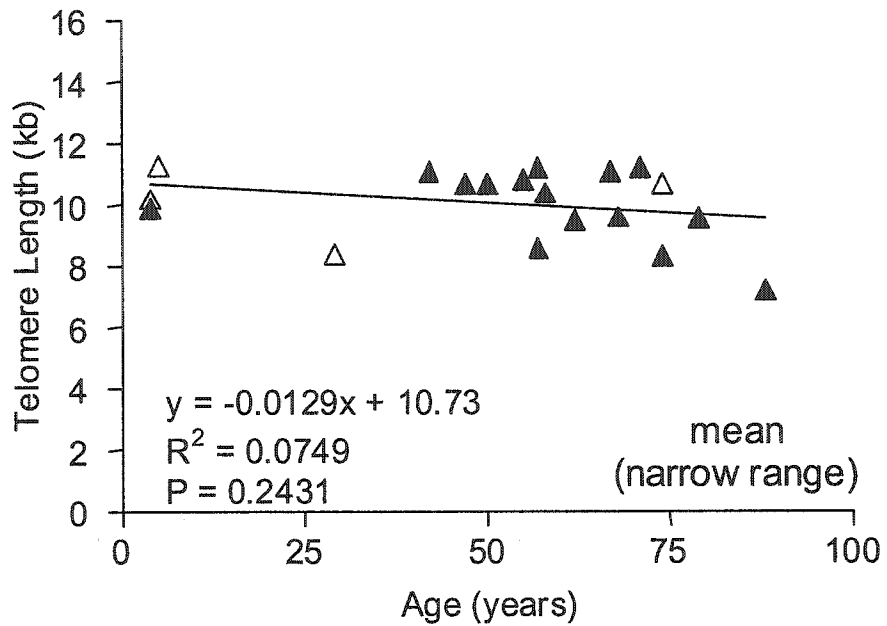


**Figure 2.7:** Regression of telomere length measurements in renal medulla by Southern blotting against age. Panels represent the mean of a narrowly defined telomere distribution (“narrow range”). Unfilled symbols represent “abnormal” kidney samples with histological changes outside the limits of changes expected for age.

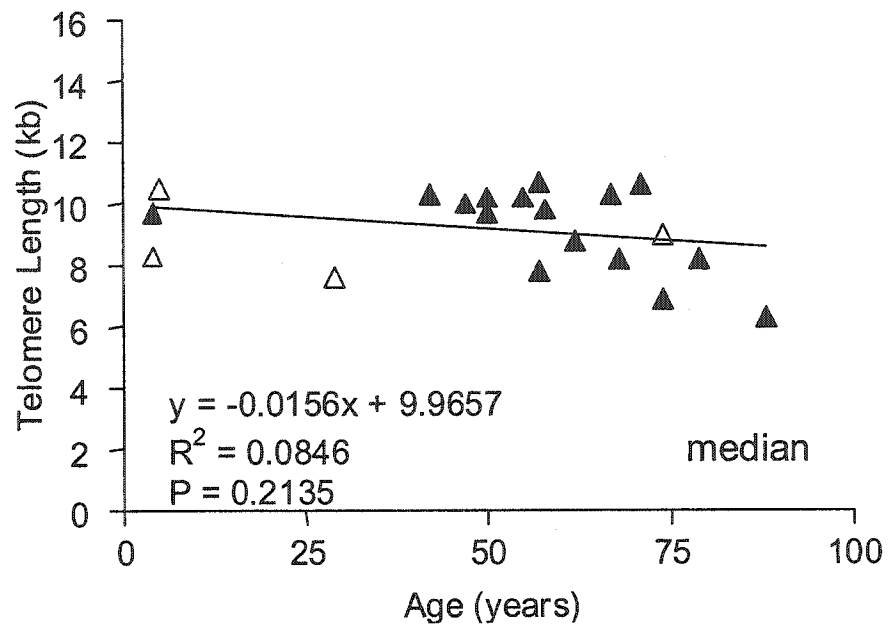


**Figure 2.8:** Regression of telomere length measurements in renal medulla by Southern blotting against age. Panels represent the median of a narrowly defined telomere distribution (“narrow range”). Unfilled symbols represent “abnormal” kidney samples with histological changes outside the limits of changes expected for age.

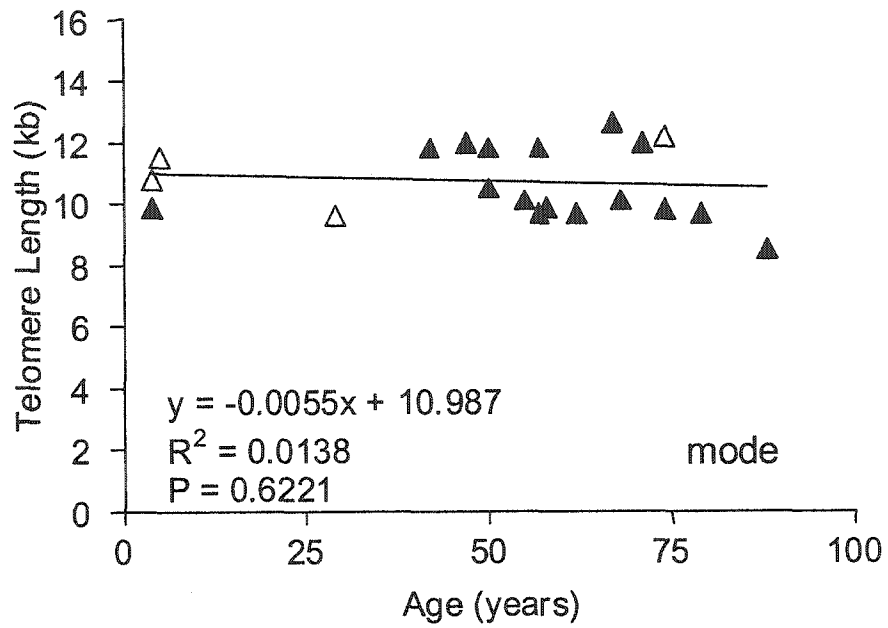


**Figure 2.9:** Regression of telomere length measurements in renal medulla by Southern blotting against age. Panels represent the mode of a narrowly defined telomere distribution (“narrow range”). Unfilled symbols represent “abnormal” kidney samples with histological changes outside the limits of changes expected for age.

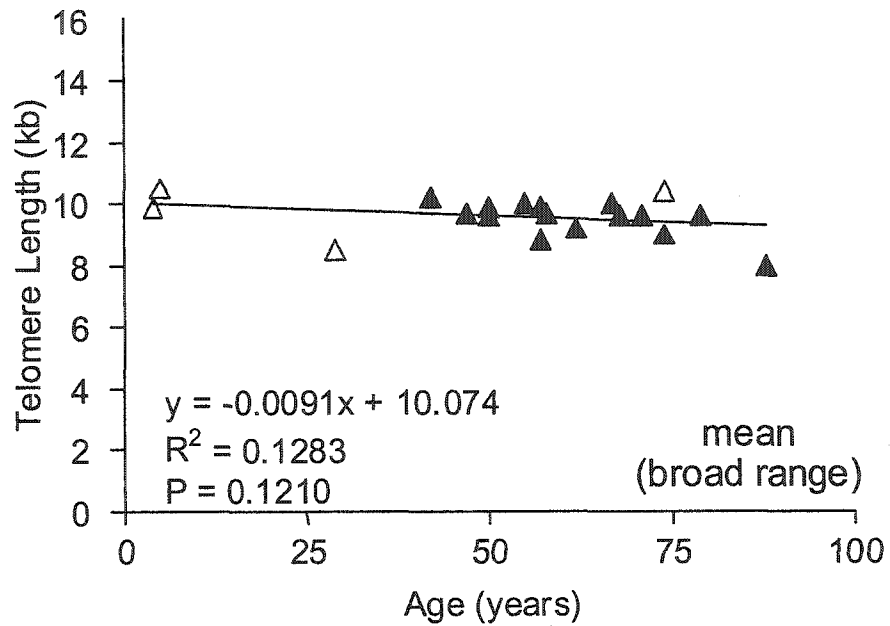


**Figure 2.10:** Regression of telomere length measurements in renal medulla by Southern blotting against age. Panels represent the median of a more broadly defined telomere distribution ("broad range"). Unfilled symbols represent "abnormal" kidney samples with histological changes outside the limits of changes expected for age.



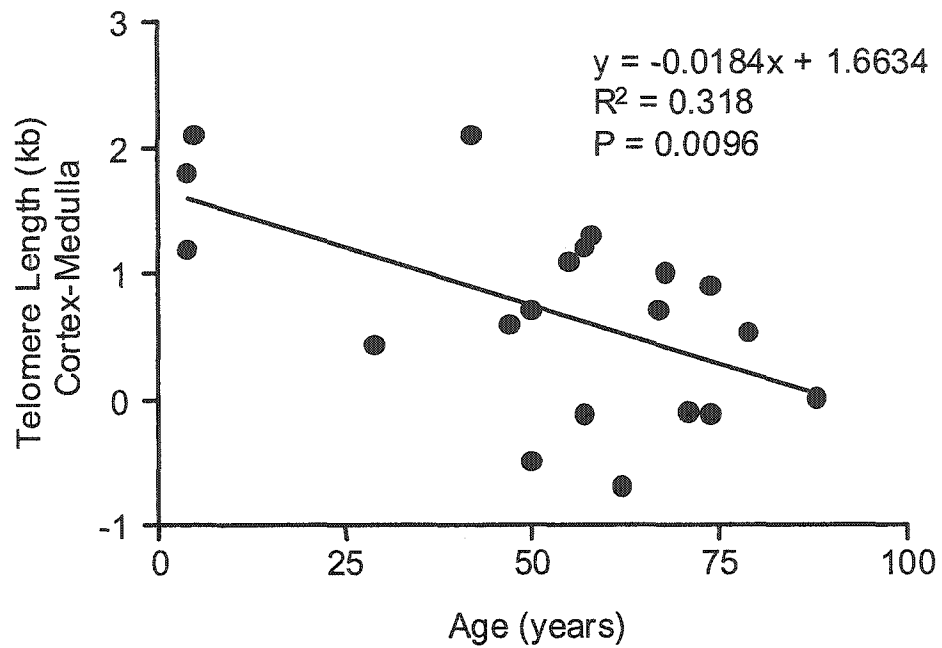


**Figure 2.11:** Regression of the difference between cortical and medullary telomere lengths against age. Telomere length in paired renal cortex and medulla samples were determined by Southern blotting as described. The difference between cortex and medulla telomere lengths from 20 different donors is plotted against age.

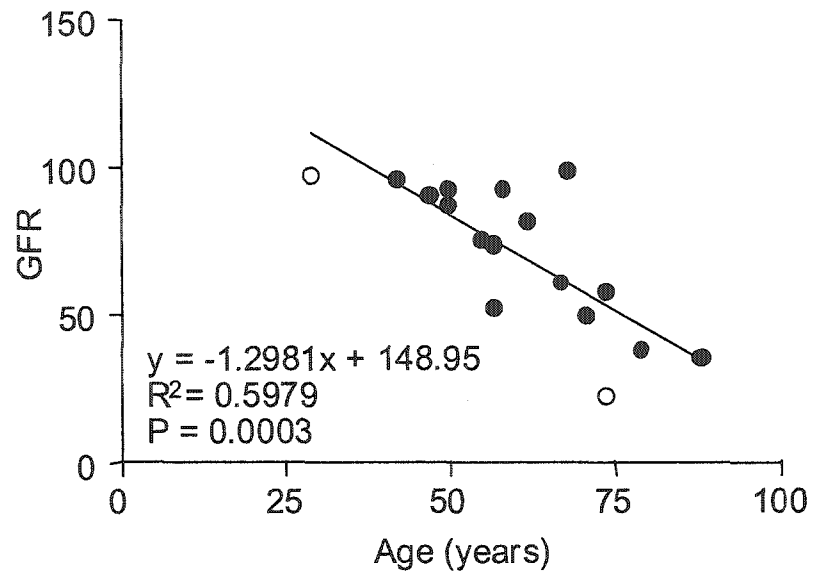


**Figure 2.12:** The regression between GRF and age. GFR was calculated using the Cockcroft-Gault equation in those patients over the age of 20 from whom kidney biopsies were taken. Unfilled symbols represent “abnormal” kidney samples with histological changes outside the limits of changes expected for age.

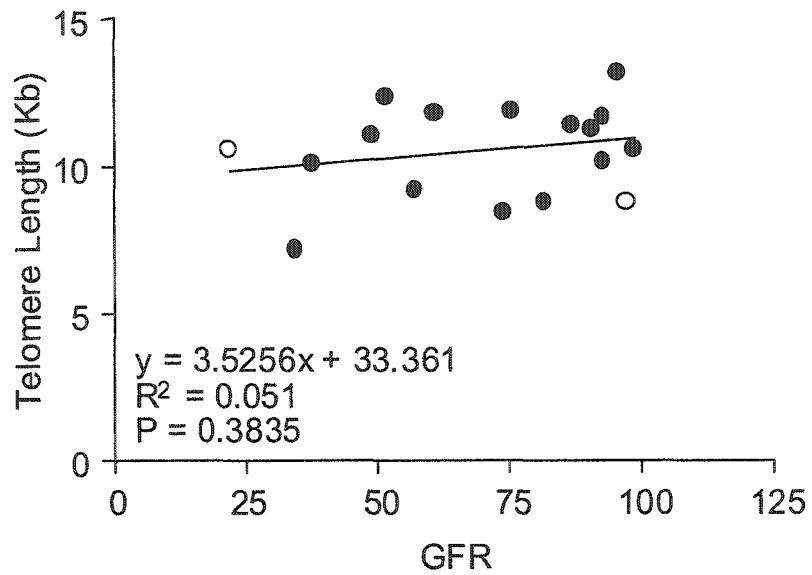


**Figure 2.13:** The regression between GFR and telomere length by Southern blotting. GFR was calculated using the Cockcroft-Gault equation in those patients over the age of 20 from whom kidney biopsies were taken. Unfilled symbols represent “abnormal” kidney samples with histological changes outside the limits of changes expected for age.

## 2.7 References

1. Fliser D and Ritz E: Relationship between hypertension and renal function and its therapeutic implications in the elderly [review]. *Gerontology* 1998, 44: 123-131
2. Fliser D, Franek E, Joest M, Block S, Mutschler E, and Ritz E: Renal function in the elderly: impact of hypertension and cardiac function. *Kidney Int* 1997, 51: 1196-1204
3. Levi M and Rowe JW: Aging and the kidney. *Diseases of the Kidney*. Edited by Schrier RW and Gottschalk CW. Boston, MA, Little, Brown, and Company, 1993, pp. 2405-2432
4. Lindeman RD, Tobin J, and Shock NW: Longitudinal studies on the rate of decline in renal function with age. *J Amer Ger Soc* 1985, 33: 278-285
5. Goyal VK: Changes with age in the human kidney. *Exp Geront* 1982, 17: 321-331
6. USRDS 1996 annual data report. Renal data system. 1996.
7. Halloran PF, Melk A, and Barth C: Rethinking chronic allograft nephropathy: the concept of accelerated senescence. *J Am Soc Nephrol* 1999, 10: 167-181
8. Walker SR, Parsons DA, Coplestons P, Fenton SSA, and Greig PD: The Canadian organ replacement register. *Clinical Transplants 1996*. Edited by Cecka JM and Terasaki PI. Los Angeles, CA, UCLA Tissue Typing Laboratory, 1997, pp. 91-107
9. Strandgaard S and Hansen U: Hypertension in renal allograft recipients may be conveyed by cadaveric kidneys from donors with subarachnoid hemorrhage. *Br J Med* 1986, 292: 1041-1044
10. Smits JMA, De Meester J, Persijn GG, Claas FHJ, and Vanrenterghem Y: Long-term results of solid organ transplantation. Report from the Eurotransplant International Foundation. *Clinical Transplants 1996*. Edited by Cecka JM and Terasaki PI. Los Angeles, CA, UCLA Tissue Typing Laboratory, 1997, pp. 109-127
11. Gjertson DW: A multi-factor analysis of kidney graft outcomes at one and five years posttransplantation: 1996 UNOS update. *Clinical Transplants 1996*. Edited by Cecka JM and Terasaki PI. Los Angeles, CA, UCLA Tissue Typing Laboratory, 1997, pp. 343-360
12. Kasiske BL, Kalil RSN, Lee HS, and Rao V: Histopathologic findings associated with a chronic, progressive decline in renal allograft function. *Kidney Int* 1991, 40: 514-524

13. Nickerson P, Jeffery J, Gough J, McKenna R, Grimm P, Cheang M, and Rush D: Identification of clinical and histopathologic risk factors for diminished renal function 2 years posttransplant. *J Am Soc Nephrol* 1998, 9: 482-487
14. Epstein M: Aging and the kidney. *J Am Soc Nephrol* 1996, 7: 1106-1122
15. Kim NW, Piatyszek MA, Prowse KR, Harley CB, West MD, Ho PLC, Coviello GM, Wright WE, Weinrich SL, and Shay JW: Specific association of human telomerase activity with immortal cells and cancer. *Science* 1994, 266: 2011-2015
16. Kaysen GA and Myers BD: The aging kidney [review]. *Clinics in Geriatric Medicine* 1985, 1: 207-222
17. Johnson FB, Sinclair DA, and Guarente L: Molecular biology of aging. *Cell* 1999, 96: 291-302
18. Hayflick L: Mortality and immortality at the cellular level. A review. *Biochemistry* 1997, 62: 1180-1190
19. Bodnar AG, Ouellette M, Frolkis M, Holt SE, Chiu C-P, Morin GB, Harley CB, Shay JW, Lichtsteiner S, and Wright WE: Extension of life-span by introduction of telomerase into normal human cells. *Science* 1998, 279: 349-352
20. Harley CB, Futcher AB, and Greider CW: Telomeres shorten during ageing of human fibroblasts. *Nature* 1990, 345: 458-460
21. Harley CB, Vaziri H, Counter CM, and Allsopp RC: The telomere hypothesis of cellular aging. *Exp Gerontol* 1992, 27: 375-382
22. Chang E and Harley CB: Telomere length and replicative aging in human vascular tissues. *Proc Natl Acad Sci USA* 1995, 92: 11190-11194
23. Wynn RF, Cross MA, Hatton C, Will AM, Lashford LS, Dexter TM, and Testa NG: Accelerated telomere shortening in young recipients of allogeneic bone-marrow transplants. *Lancet* 1998, 351: 178-181
24. Nadasdy T, Laszik Z, Blick KE, Johnson LD, and Silva FG: Proliferative activity of intrinsic cell populations in the normal human kidney. *J Am Soc Nephrol* 1994, 4: 2032-2039
25. Bich-Thuy L and Fauci AS: Recombinant interleukin-2 and gamma-interferon (IFN- $\gamma$ ) act synergistically on distinct steps of *in vitro* terminal human B cell maturation. *J Clin Invest* 1986, 77: 1173-1179
26. Cockcroft DW and Gault MH: Prediction of creatinine clearance from serum creatinine. *Nephron* 1976, 16: 31-41

27. Allsopp RC, Vaziri H, Patterson C, Goldstein S, Younglai EV, Futcher AB, Greider CW, and Harley CB: Telomere length predicts replicative capacity of human fibroblasts. *Proc Natl Acad Sci USA* 1992, 89: 10114-10118
28. Vaziri H, Schächter F, Uchida I, Wei L, Zhu X, Effros R, Cohen D, and Harley CB: Loss of telomeric DNA during aging of normal and trisomy 21 human lymphocytes. *Am J Hum Genet* 1993, 52: 661-667
29. Allsopp RC, Chang E, Kashefi-Azham M, Rogaev EI, Piatyszek MA, Shay JW, and Harley CB: Telomere shortening is associated with cell division *in vitro* and *in vivo*. *Exp Cell Res* 1995, 220: 194-200
30. Oexle K, Zwirner A, Freudenberg K, Kohlschütter A, and Speer A: Examination of telomere lengths in muscle tissue casts doubt on replicative aging as cause of progression in Duchenne muscular dystrophy. *Pediatr Res* 1997, 42: 226-231
31. Butler MG, Tilburt J, DeVries A, Muralidhar B, Aue G, Hedges L, Atkinson J, and Schwartz H: Comparison of chromosome telomere integrity in multiple tissues from subjects at different ages. *Cancer Genetics & Cytogenetics* 1998, 105: 138-144
32. von Zglinicki T, Saretzki G, Döcke W, and Lotze C: Mild hyperoxia shortens telomeres and inhibits proliferation of fibroblasts: a model for senescence? *Exp Cell Res* 1995, 220: 186-193
33. Furumoto K, Inoue E, Nagao N, Hiyama E, and Miwa N: Age-dependent telomere shortening is slowed down by enrichment of intracellular vitamin C via suppression of oxidative stress. *Life Sci* 1998, 63: 935-948
34. Kinouchi Y, Hiwatashi N, Chida M, Nagashima F, Takagi S, Maekawa H, and Toyota T: Telomere shortening in the colonic mucosa of patients with ulcerative colitis. *J Gastroenterol* 1998, 33: 343-348
35. Linskens MH, Feng J, Andrews WH, Enlow BE, Saati SM, Tonkin LA, Funk WD, and Villeponteau B: Cataloging altered gene expression in young and senescent cells using enhanced differential display. *Nucleic Acids Res* 1995, 23: 3244-3251
36. Coviello-McLaughlin GM and Prowse KR: Telomere length regulation during postnatal development and ageing in *Mus spretus*. *Nucleic Acids Res* 1997, 25: 3051-3058
37. Baylis C and Corman B: The aging kidney: insights from experimental studies. *J Am Soc Nephrol* 1998, 9: 699-709
38. Tracy RE and Johnson LK: Aging of a class of arteries in various mammalian species in relation to the life span. *Gerontology* 1994, 40: 291-297

39. Takeda T, Imada A, Horiuchi A, Kimura M, Maekura S, and Hashimoto S: Age-related changes in morphological studies in rat and human kidney {Japanese}. *Japanese J Nephrol* 1996, 38: 555-562
40. Lee H-W, Blasco MA, Gottlieb GJ, Horner JWII, Greider CW, and DePinho RA: Essential role of mouse telomerase in highly proliferative organs. *Nature* 1998, 392: 569-574

Chapter 3

Cell Senescence in Rat Kidneys *in vivo* Increases  
with Growth and Age  
Despite Lack of Telomere Shortening

A version of this chapter has been published.

Anette Melk, Wipawee Kittikowit, Irwindeep Sandhu, Kieran M. Halloran, Paul Grimm, Bernhard M.W. Schmidt, and Philip F. Halloran: Cell senescence in rat kidneys *in vivo* increases with growth and age despite lack of telomere shortening. *Kidney International* 2003; 63: 2134-2143.

Portions of this publication that were contributed by co-authors are not included unless noted. Used with permission of Blackwell Publishing.



### 3.1 Introduction

Renal aging and the phenotype of age, which is termed renal senescence, are important clinical issues (1;2). Renal senescence is associated with many health problems: increased renal cancer, a high incidence of end stage renal disease, and poor performance of renal transplants from the elderly. Kidney aging is associated with functional and anatomical changes (3-7). The cellular and molecular basis of renal aging remains largely unknown, but environmental stress and genomic changes such as loss of telomeres are believed to contribute (8;9). One possible explanation of the phenotypic changes of renal aging is that critical cells reach their finite limits and develop changes analogous to the limits reached by somatic cells in culture. Cultured mammalian somatic cells such as fibroblasts, after a finite number of population doublings, eventually reach a state in which they irreversibly cease replication and manifest abnormalities (10). This state has been called replicative senescence for human cells and STASIS for murine cells (11), but here will be referred to as cell senescence. Mouse and human fibroblasts *in vitro* show major differences in how the state of senescence is reached (11). Human cells manifest loss of telomeres, and their state of senescence can be bypassed by transfection of telomerase, which greatly extends their replicative capacity. In contrast, mouse fibroblasts show even more limited proliferative capacity *in vitro*, but their long telomeres are not limiting and the senescent state is

produced by environmental stress ("culture shock") (11-15). However, mouse and human cells at arrest manifest similar changes, including expression of a cell cycle regulator p16<sup>INK4a</sup> and organelle changes such as senescence associated  $\beta$ -galactosidase (SA- $\beta$ -GAL) and lipofuscin (16-19). Cell senescence could also occur during renal development and growth as well as during aging.

Aging events in rat kidneys are of interest in themselves and for comparison to the processes of human kidney senescence. There is a wide variability in the effects of aging on the rat kidney. In particular, strains differ in the development of proteinuria that is associated with glomerular changes, typically focal and segmental sclerosis (20), and the environment influences the phenotype within strains. Rat kidneys, unlike human kidneys, manifest no loss of renal mass and little or no loss of function with age unless they have concomitant kidney disease (21;22).

In this study I explored whether characteristic features of senescence in cultured cells develop in the rat kidney with development and aging. Senescent cells *in vitro* are resistant to apoptosis, and could persist in their abnormal state and thus contribute to pathology in complex tissues and organs, interfering with organ homeostasis. My purpose was to seek evidence for or against the concept that cell senescence as defined in culture is actually a phenomenon *in vivo*, and that it may contribute to the phenotype of renal aging. This in turn would assist in generating testable

models of renal aging.

## 3.2 Materials and Methods

### 3.2.1 Kidneys

Rat samples were derived from 32 Fischer 344 rats of three age groups (1 month, n=11, 9 months, n=10 and 24 months, n=11). One-month old rats were derived from the University of Alberta animal colony and 9- and 24-month old rats from the NIA colony were purchased from Harlan (Indianapolis, IN) (9- and 24-month group). All animals were housed barrier maintained and specific pathogen free. The animals were killed within one week after arrival in our colony.

Rats were anesthetized and blood was drawn for measurement of serum creatinine, urea, and electrolytes. Then a midline incision was performed and kidneys, spleen, and heart were quickly removed. Brains were harvested last. All tissue samples were immediately snap-frozen in liquid nitrogen and stored at  $-70^{\circ}\text{C}$ . In addition, tissue was embedded in OCT for frozen sections and fixed with paraformaldehyde for paraffin embedded sections. All experiments were performed according to the University of Alberta Animal Policy and Welfare Committee's animal care protocols.

### 3.2.2 Pathology and lipofuscin assessment

Paraffin wax sections were cut at 2  $\mu\text{m}$  and stained with hematoxylin and eosin, Periodic Acid Schiff (PAS) and Mason-Trichrome for histopathological assessment by a renal pathologist (Wipawee Kittikowit). Lipofuscin counts were performed in high power fields (HPFs) by Wipawee Kittikowit and myself.

### 3.2.3 Sirius Red staining

Unstained paraffin embedded sections were baked at 60°C for one hour. Slides were soaked in xylene for 24 hrs followed by acetone for 24 hrs to reduce paraffin contamination. Then slides were taken through xylene and graded ethanols into distilled water and stained overnight in saturated picric acid with 0.1% Sirius Red F3BA (Aldrich Chemicals). Slides were washed in hydrochloric acid (0.01N) and rapidly dehydrated and mounted. Sirius Red staining was only performed on a subgroup of 12 rats (1 month: n=5, 9 months: n=2, 24 months: n=5).

Image analysis was performed by a technician blinded to the source of the sample. The slides were examined with a Nikon E600 microscope, and a Hitachi analog 3 CCD camera was used to capture gray scale 256 bit images that were archived as TIFF files. A background image was initially obtained and background correction was performed in real time while the images were being acquired using the 40X objective. Images of the kidney

cortex were obtained in a serpentine fashion starting at one end of the tissue and working toward the other. Large glomeruli, vessels larger than the size of adjacent tubules and the medulla were not included in the image acquisition. Image analysis was performed using an automated macro specially written for the software package NIH Image. Automated analysis of the images was performed with operator supervision. Data is expressed as Cortical Fractional Interstitial Fibrosis Volume ( $V_{\text{IntFib}}$ ), a value of 1 would reflect 100% fibrosis. (Sirius Red staining and analysis was done by Paul Grimm.)

#### 3.2.4 Terminal restriction fragments (TRF)

To obtain high molecular weight DNA without degradation, the tissue was disrupted by freeze grinding. DNA was then isolated by proteinase K digestion and phenol/chloroform extraction. Concentration was measured at  $OD_{260}$ . DNA samples were digested with the restriction enzymes Hinf I and Rsa I (Boehringer Mannheim, Germany) to produce TRFs. 1.5  $\mu\text{g}$  of each digested sample was resolved on a 1.0 % agarose gel by pulse field gel electrophoresis (buffer temperature 14°C, voltage gradient 6.0 V/cm, switching interval 1-30 sec., 12h). Gel was probed directly as described previously (23) with minor modifications (24). Hybridization was done at 42° C overnight with a 5'-end-labelled  $^{32}\text{P}$ -(TTAGGG)<sub>5</sub> oligonucleotide telomere probe in a buffer containing 6x SSC, 5x

Denhardt's solution, 50mM NaH<sub>2</sub>PO<sub>4</sub> (pH 7.4), 0.1 mg/ml salmon sperm DNA, 0.1 % SDS. Following stringency washes at RT in 0.2X SSC, 0.1% SDS, the autoradiography signal was digitized in a phosphoimage scanner (Fuji) using ImageGauge Software. All lanes were subdivided into intervals of 1 mm. The mean size of the TRFs was estimated using the formula  $\Sigma(\text{OD}_i \times L_i) / \Sigma(\text{OD}_i)$ , where OD<sub>i</sub> is the density reading from interval i and L<sub>i</sub> is the size in kbp of the interval relative to the markers (25). Mean TRF length was determined on the basis of the intensity of the signal, where the intervals averaged were those intervals, which were higher than 1% of the total signal in that lane. (Irwindeep Sandhu did some TRF gels as part of his summer student project).

### 3.2.5 Reverse transcription (RT) and real-time polymerase chain reaction (PCR)

Total RNA was extracted from tissue samples according to a modification of the method described by Chirgwin et al. (26). Tissues were homogenized with a polytron in 4 M guanidinium isothiocyanate, and the RNA was pelleted through a 5.7M CsCl<sub>2</sub> cushion. RNA was isolated by phenol/chloroform extraction. Concentrations were determined by absorbance at 260 nm. Transcription into cDNA was done using MMLV reverse transcriptase and random primers (Life Technologies, Burlington, Ontario). The principle of real-time quantitative PCR has been described by

Heid et al. (27). cDNA (0.75  $\mu$ l) was amplified in an ABI PRISM 7700 Sequence Detector (Applied Biosystems, Foster City, CA). All samples were done in duplicates. Sequence specific primers and probe for p16<sup>INK4a</sup> (forward primer: 5'-ACG AGG TGC GGG CAC TG-3'; reverse primer: 5'-TTG ACG TTG CCC ATC ATC ATC-3'; probe: 5'-FAM-CCG AAC ACT TTC GGT CGT ACC CCG ATA-TAMRA-3') and TGF- $\beta$ 1 (forward primer: 5'-GGC TAC CAT GCC AAC TTC TGT CT-3'; reverse primer: 5'-CCG GGT TGT GTT GGT TGT AGA-3'; probe: 5'-FAM-CAC ACA GTA CAG CAA GGT CCT TGC CCT-TAMRA-3') were designed using Primer Express Software (Applied Biosystems, Foster City, CA). Pre-developed assay reagents for 18S ribosomal RNA (18S RNA) were purchased (Applied Biosystems, Foster City, CA). The number of PCR cycles that are needed to reach the fluorescence threshold is called threshold cycle (Ct). The Ct value for each sample is proportional to the log of the initial amount of input cDNA. After calculation of the mean Ct value for the duplicates, the Ct values for all samples were normalized to 18S RNA by subtraction (Ct for p16<sup>INK4a</sup> minus Ct for 18S RNA), called  $\Delta$ Ct. Relative quantification of gene expression was calculated as  $2^{-\Delta Ct}$ . A mixture of equal amounts of different rat spleen cDNA was used as an internal control and was run with each experiment. The mean  $\Delta$ Ct value for this sample was 21.7 and the variation coefficient for all experiments was 2.01%.

### 3.2.6 Immunohistochemistry for p16<sup>INK4a</sup>

Immunoperoxidase staining for p16<sup>INK4a</sup> was performed using 2  $\mu$ m sections of paraffin embedded tissue. Briefly, sections were deparaffinized and hydrated. The sections were immersed in 3% H<sub>2</sub>O<sub>2</sub> methanol to inactivate endogenous peroxidase. Slides were blocked with 20% normal goat serum. Tissue sections were then incubated for 1 hr at RT with the primary antibody (mouse monoclonal antibody, Clone F-12, Santa Cruz, CA) and rinsed with PBS. Following 30 minutes of incubation with the Envision monoclonal system (Dako, Ontario), sections were washed again in PBS. Visualization was performed using the DAB substrate kit (Dako, Ontario). The slides were counterstained with hematoxylin and mounted. Analysis was done by counting 5 HPF. Percentage of positive nuclei was assessed for tubules, glomeruli and interstitium.

### 3.2.7. Western blot analysis

Tissue was homogenized in RIPA buffer containing the protease inhibitors phenylmethylsulfonylfluoride (100 $\mu$ g/ml), aprotinin (100 $\mu$ g/ml) and sodium orthovanadate (1mM). Homogenates were centrifuged and supernatants were snap frozen and stored at -80 °C. Protein concentrations were determined using the BioRad Lowry protein assay (BioRad Labs, Hercules, CA). 50  $\mu$ g per sample were loaded and proteins were separated by 11.5% sodium dodecyl sulfate polyacrylamide gel



electrophoresis (SDS-PAGE) followed by electrophoretic transfer to a nitrocellulose membrane. Retinoblastoma protein was detected using a rabbit polyclonal antibody against total retinoblastoma protein (C-15, Santa Cruz Biotechnology, Santa Cruz, CA) that showed two separate bands for phosphorylated and hypophosphorylated retinoblastoma. This was followed by peroxidase-conjugated goat anti rabbit IgG (Jackson Immuno Research Laboratories, West Grove, PA) and enhanced chemiluminescence (SuperSignal®, Pierce, IL).

### 3.2.8 Senescence associated (SA) $\beta$ -galactosidase ( $\beta$ -GAL) staining

Frozen sections were cut at 4  $\mu$ m and kept at -20°C until further processed. Staining was done according to Dimri et al. (28) including modifications by Chkhotua et al. (29). Briefly, slides were brought to RT and fixed with 2% formaldehyde/0.2% glutaraldehyde in PBS. Slides were then incubated for 14 hours at 37°C in a humidified chamber with SA- $\beta$ -GAL staining solution (2mg/ml X-gal in dimethylformamide, 40mM citric acid/sodium phosphate (dibasic), pH 6, 5mM potassium ferrocyanide, 5mM potassium ferricyanide, 150mM sodium chloride, 20mM magnesium chloride). Controls were stained for lysosomal  $\beta$ -GAL using the same SA- $\beta$ -GAL staining solution adjusted to pH 4. Following staining, slides were counterstained with eosin, dehydrated and mounted.

Quantification of the SA- $\beta$ -GAL staining was accomplished by

Image-Pro Plus Software. A set of slides without counterstain was produced and photographed. The image was opened in Image-Pro Plus and staining density for the whole section was calculated. The mean staining density of two independent experiments was taken for further calculations and statistical analysis.

### 3.2.9. Terminal deoxynucleotidyl transferase mediated dUTP Nick End Labeling (TUNEL)

Paraffin embedded sections were deparaffinized and hydrated. The sections were immersed in 1% H<sub>2</sub>O<sub>2</sub> to inactivate endogenous peroxidase. The sections were treated with proteinase K (20µg/ml in PBS) for 10 min at RT and rinsed in PBS. Sections were incubated with terminal deoxynucleotidyl transferase (TDT) buffer (30 mM Tris-HCl, pH 7.2, 1 mM CoCl<sub>2</sub>, 140 mM sodium cacodylate) for 30 min at RT. Then the TDT buffer was replaced with TDT buffer containing 0.025 nmoles/µl biotin-16-dUTP (Roche, Laval, Quebec) and 0.25U/µl TDT (Roche, Laval, Quebec) and incubated for 1 hr at 37 °C in a humidified chamber. Slides were rinsed in PBS. Non-specific staining was blocked by immersing the slides in 2% BSA in PBS. The slides were then incubated with the avidin-biotin complex (Vector Laboratories, Burlingame, CA) for 30 minutes. The reaction was visualized using the DAB substrate kit (Vector Laboratories, Burlingame, CA). The slides were counterstained with alcian blue, dehydrated and

mounted. For negative controls TDT was omitted. Kidney sections treated with 1000 ng/ml DNAase I (Sigma Chemical Co, St. Louis, MO) were used as positive controls. Analysis was done by counting all positive nuclei per kidney section.

### 3.2.10 Statistical Analysis

Data analyses were performed using SPSS. Means among three groups of rats were compared using Kruskal-Wallis nonparametric tests, and Mann-Whitney tests with Bonferroni correction were used for multiple pair-wise comparisons. The Fisher-Exact test was used to test for differences in proportions, 1-month with 9-months, 9-month with 24-months old rats.

## 3.3 Results

### 3.3.1 Renal changes with growth and aging

Because environment, subline genetic differences (30;31), and specific renal diseases can alter the phenotype of growth and aging in kidney (20), it was essential that to characterize the extent of the previously reported changes (20;30-33) at each age in the rats, to permit correlation with the indicators of cellular senescence. I arbitrarily termed the 1 to 9 months interval 'growth' and the 9 to 24 months interval 'aging'. Creatinine increased significantly during growth (9 months versus 1 month) but not

during aging (24 months versus 9 months); urea and electrolytes showed no changes (table 3.1). I confirmed that my rats displayed this pattern: both kidney and body weight from age 1 month to age 9 months increased, by 60 % and 169%, respectively. Kidney weight increased by a further 21% from 9 months to 24 months old rats, but body weight did not change. The kidney-to-body-weight ratio decreased during growth and increased during aging. The protein/DNA ratio was stable for all three ages ( $15.2 \pm 2.0$  in 1 month vs.  $15.3 \pm 1.5$  in 24 months old rats).

The histologic changes of growth and aging were evaluated using a pathology scoring system incorporating features of the Banff classification for transplant pathology (34) and previous reports (20) (table 3.2). None of the 1 month old rats had features suggesting renal diseases beyond the changes of aging. By 9 months the percentage of glomeruli with widened Bowman's space and the number of casts in cortex and medulla increased, and occasional foci of mononuclear infiltrate appeared. Some rats at 9 months manifest occasional totally sclerotic (2 of 6) or partially (segmental) sclerotic glomeruli (1 of 6), tubular atrophy (3 of 6) and dilated tubules (1 of 6). By 24 months all kidneys showed histologic features of aging, including total and partial (segmental) sclerosis (although only 4.4% of glomeruli were affected), hyaline droplets, tubular atrophy, interstitial fibrosis, and arteriolar hyalinosis. No rats showed arterial fibrous intimal thickening. The number of cells per tubular cross-section did not change with age.

Cortical fibrosis was quantitated by Sirius Red staining (figure 3.1) and increased significantly with growth ( $V_{\text{intFib}}$   $0.01 \pm 0.005$  at 1 month vs.  $0.024 \pm 0.003$  at 9 months;  $p < 0.05$ ). The further increase with aging ( $V_{\text{intFib}}$   $0.033 \pm 0.010$  at 24 months) did not reach statistical significance. Because of the increase in fibrosis, we measured the amount of TGF- $\beta$ 1 mRNA (figure 3.2). TGF- $\beta$ 1 expression was highest in the 24-months old rats ( $13 \pm 16.1$ ) but the differences between age groups were not statistically significant.

### 3.3.2 Mean TRF length in rat kidney samples

Figure 3.3 shows a typical TRF length gel obtained by pulse field gel electrophoresis. The mean  $\pm$  SD for mean TRF length (kb) was  $38.5 \pm 1.0$  for 1 month,  $40.6 \pm 4.8$  for 9 months and  $35.1 \pm 6.0$  for 24 months old rat kidneys (figure 3.4). There was no significant change in TRF length with growth or aging ( $p = 0.49$ ). The mean TRF length in rat samples was above 30 kb, similar to what has been shown for *M. musculus* strains (35) and much longer than in human kidney (about 12Kb) (36).

### 3.3.3 P16<sup>INK4a</sup> mRNA expression in rat kidney, spleen, brain and heart samples

P16<sup>INK4a</sup> mRNA was absent in most 1 month old kidneys but increased 27 fold with growth and a further 72 fold with aging (figure 3.5). The p16<sup>INK4a</sup> mRNA levels were undetectable in 10 out of 11 samples in 1

month old rats and very low ( $1.75 \times 10^{-9}$ ) in the remaining one rat. Nine months old rats had detectable levels in all 10 animals. Highest levels were found in the group of 24 months old rats. Mean values ( $\pm$ SD) for p16<sup>INK4a</sup> expression normalized to 18S RNA in kidney were  $1.6 \times 10^{-10}$  ( $\pm 5.29 \times 10^{-10}$ ) for 1 month,  $43.8 \times 10^{-10}$  ( $\pm 29.2 \times 10^{-10}$ ) for 9 month, and  $3160 \times 10^{-10}$  ( $\pm 8850 \times 10^{-10}$ ) for 24 months old rats. The latter group showed considerable variability in p16<sup>INK4a</sup> levels.

Increases in p16<sup>INK4a</sup> were seen for three other tissues investigated (spleen  $p < 0.001$ , figure 3.6; brain  $p < 0.05$ , figure 3.7; heart  $p < 0.05$ , figure 3.8). Interestingly, p16<sup>INK4a</sup> was expressed in both spleen and heart even in the 1 month old group, whereas p16<sup>INK4a</sup> was not detected in any of the brain tissues for the 1 month old rats. This was the case for most of the kidneys, but the brain showed no significant increase between 9 and 24 months old rats.

#### 3.3.4 P16<sup>INK4a</sup> protein expression in rat kidneys

I was able to corroborate the mRNA results by immunoperoxidase staining for p16<sup>INK4a</sup>. Representative tubular sections are shown in figure 3.9. Young rat kidneys, which lacked or had very low p16<sup>INK4a</sup> levels showed no or occasional staining of single nuclei (mean of positive nuclei in tubules 4%; in glomeruli 4%; in interstitium 1%). The increase with aging was highly significant for all investigated compartments. The mean of

positive nuclei in 9 months versus 24 months old rats was 5% versus 46% in tubules ( $p < 0.001$ ), 6% versus 38% in glomeruli ( $p < 0.001$ ) and 1% versus 18% in interstitium ( $p < 0.0001$ ). Very rarely single lymphocytes within a mononuclear infiltration stained.

By Western blot, we did not find any differences in the amount of retinoblastoma, a downstream target of p16<sup>INK4a</sup>, between young and old rats.

### 3.3.5. SA- $\beta$ -GAL

SA- $\beta$ -GAL was described in senescent human fibroblast cultures (28), but not in quiescent or terminally differentiated cells, and *in vivo* in skin cells from old humans. SA- $\beta$ -GAL has been recommended as an indicator of cell senescence *in vitro* (37) and *in vivo* (38;39). I assessed SA- $\beta$ -GAL staining for rat specimens of different ages (for representative pictures see figure 3.10). SA- $\beta$ -GAL staining was found only in tubular cells, not in glomeruli or vessels. As can be seen in figure 3.11, a patchy pattern was observed in 24 months old rats, suggesting those SA- $\beta$ -GAL stained tubules belonged to the same nephron. SA- $\beta$ -GAL staining was quantitated by a photo-imaging technique for which a whole cross-section of the kidney was photographed. Mean staining densities (arbitrary units) were 0.003 ( $\pm 0.002$ ) for 1 month old, 0.008 ( $\pm 0.003$ ) for 9 months old and 0.020 ( $\pm 0.007$ )

for 24 months old rats ( $p < 0.005$ ). Thus SA- $\beta$ -GAL increased during growth but further increased during aging.

### 3.3.6 TUNEL

To assess the amount of apoptotic cells TUNEL staining was performed. Apoptotic cells were overall rare, but increased continuously with age. Young rats had an average of 1 positive nucleus per kidney cross section, 9 months old rats had 6 positive nuclei and in 24 months old rats we found 12 positive nuclei. Positive nuclei were almost always found in tubules, interstitial cells showed some positive nuclei, and only one old rat had a positive nucleus in its glomerulus.

### 3.3.7. Lipofuscin

Lipofuscin is an intracellular, age-related, fluorescent, cytoplasmic, granular pigment found mainly in secondary lysosomes of post-mitotic cells (40). We assessed lipofuscin in proximal, non-proximal and atrophic tubules for four different areas in the kidney: superficial cortex, mid cortex, juxtamedullary cortex and medulla. Lipofuscin was usually absent at 1 month: only one of the six 1 month old rats displayed any lipofuscin, confined to occasional tubules of the juxtamedullary cortex and medulla. Lipofuscin was present in every kidney of the 9 and 24 months old animals (table 3.3), confined to tubular cells, mainly proximal tubules. Highest



amounts were found in atrophic tubular cells. Thus like SA- $\beta$ -GAL lipofuscin increased in growth and in aging.

Lipofuscin appeared in proximal tubules in all four areas of the 9 months group, whereas non-proximal tubules were only affected in one out of six rats. The 24 months old kidneys displayed a further increase in lipofuscin in proximal tubules in all areas and in non-proximal tubules in superficial and mid cortex. Lipofuscin was present in up to 50% of atrophic tubules in the 24 months kidneys.

In both the 9 months old and the 24 months old kidneys lipofuscin was significantly associated with SA- $\beta$ -GAL staining (table 3.4).

### 3.4 Discussion

To explore the relationship between cellular senescence and the phenotypic changes of aging, I studied whether features that characterize senescent cells *in vitro* can be detected *in vivo* in a well-studied model of renal aging, the Fischer 344 rat kidney. I found that rat kidneys had long telomeres that did not shorten with age, unlike telomeres in human renal cortex, which were much shorter and shortened further with age (36). The cyclin-dependent kinase inhibitor p16<sup>INK4a</sup>, a marker of senescence for murine and human cells in culture (16;17;41) increased strikingly both with growth and aging and emerges as a unique marker for somatic cell senescence in growth and aging in the kidney. Lipofuscin and SA- $\beta$ -GAL

staining, markers of senescence *in vitro*, increased in tubular epithelium with age, with lipofuscin appearing first in the medulla and juxtamedullary cortex. Thus in rat kidney, the epithelial cells manifest cell senescence changes independent of telomere shortening, which may contribute to the renal aging phenotype. Since these changes in culture are indicative of environmental stress, our findings indicate that renal senescence in the rat is caused at least in part by environmental stress-induced cellular changes similar to those in senescent cells *in vitro*, but that telomere attrition does not play a role.

The long telomeres that failed to shorten with age in rat kidneys are consistent with the recent realization that mouse cells in culture have long telomeres that do not shorten with cycling (11). However, this is the demonstration of this principle *in vivo*. In culture mouse cells do not use telomere shortening as a cell cycle counting mechanism, but nevertheless still reach senescence after fewer cycles than human cells (11;12;42). Thus rodent cells are much more sensitive to environmental stress than human cells *in vitro* and possibly *in vivo* (42). Mouse fibroblasts rely more on the p53 pathway to limit their proliferative capacity *in vitro*, and inactivation of p53 and/or retinoblastoma/p16<sup>INK4a</sup> are sufficient to bypass senescence (43-45). In human cells inactivation of these pathways prolongs the lifespan of the cell but does not lead to immortalization because the telomere replication counter is operative. These differences may reflect the necessity

for long-lived species to have better protection against environmental stress and oncogenesis.

My findings are compatible with a role for p16<sup>INK4a</sup> in the cell senescence phenotype *in vivo* in rat kidney. In mouse fibroblasts *in vitro*, p16<sup>INK4a</sup> is strongly associated with senescence, and may specifically reflect cumulative injury from environmental stress. In the present studies, specimens from kidney, brain, heart and spleen showed a striking increase in p16<sup>INK4a</sup> with age. Interestingly, all rats tested showed some p16<sup>INK4a</sup> expression in heart and spleen at 1 month of age, whereas no expression was found in 10 out of 11 kidneys or in brain. The increase in p16<sup>INK4a</sup> in brain was found between 1 and 9 months during the growth and development period. For kidney, however, p16<sup>INK4a</sup> increased in the growth-related and the aging-related phase.

Lipofuscin and SA- $\beta$ -GAL, which are characteristic of senescent cells, are a manifestation of age-induced cellular deterioration, and could cause in some aspects of the phenotype of aging. Lipofuscin accumulated in proximal tubules and particularly in atrophic tubules, suggesting that these segments manifest more age-related stress and that the tubules with lipofuscin are prone to atrophy. Alternatively the lipofuscin in atrophic tubules may be a reflection of atrophy, rather than a cause. Staining for SA- $\beta$ -GAL was significantly associated with lipofuscin, but more tubules displayed SA- $\beta$ -GAL than lipofuscin, suggesting that staining for SA- $\beta$ -GAL

could be an earlier or more prevalent manifestation of senescence. Lipofuscin accumulates with age in many organs, most strikingly in heart and brain. Lipofuscin is derived from oxidized proteins and lipids and forms in secondary lysosomes due their non-degradability (40). SA- $\beta$ -GAL activity has been attributed to a rise in the level of the lysosomal form of this enzyme (46;47), as a consequence of an increase in lysosomal mass in senescent cells (47;48). Lipofuscin and SA- $\beta$ -GAL may thus both be independent manifestations of impaired homeostasis of cell organelles with age, with SA- $\beta$ -GAL being an earlier or more widespread marker than lipofuscin.

While distinguishing age-related disease from aging is difficult and often becomes a semantic argument, I believe that the molecular changes described here are related to cumulative effects of environmental stress during growth, development, and aging, and not due to disease. My rats showed changes typical of aging in all rat strains, although milder than often described. Some rats have a high frequency of apparent age-related renal changes, which can vary with the environmental condition (33). However, in my 24 months rats only 4.4 % of glomeruli showed signs of sclerosis and the percentage of atrophic tubules did not exceed 3.4 %. Partial segmental sclerosis occurred in 2 % of glomeruli. I am aware that the measurement of creatinine, which is a composite of renal function and muscle mass, is not always a reliable indicator for renal function, especially in the elderly when

muscle mass is reduced. However, muscle mass remains stable in Fischer 344 rats until the age of 27 months (49). Glomerular filtration rates in Fischer 344 rats have been previously reported to be stable with age, despite some glomeruli showing spontaneous focal glomerulosclerosis (50) and (51) Fischer 344 rats do not develop hypertension (52;53). Based on the literature, our histopathological assessment and the stable creatinine levels, I believe that these old Fischer 344 rats had stable glomerular filtration rates.

The increase in kidney weight in old rats probably reflects the net balance of a complex mixture of hypertrophy, growth, fibrosis, atrophy, and apoptosis. The constant protein/DNA ratio argues against pure hypertrophy. However, the number of tubular cells per tubular cross-section did not increase with age, arguing against pure hyperplasia. Fibrosis that was three fold higher in old than in young rats, could contribute to the renal weight increase. An additional factor could be increased water content of older kidneys as reported earlier (51), although we found no overt edema on histopathology. This increase in weight occurs despite an increase in the number of apoptotic cells. Together, these findings suggest that the renal aging phenotype is heterogeneous, which is a general characteristic of aging systems.

I propose that renal aging in rats reflects the cumulative effects of environmental stress, leading to cell cycle arrest similar to mouse

fibroblasts in culture despite their long telomeres. The changes of aging are already present in rat kidneys by 9 months, and progress considerably over the next 15 months: SA- $\beta$ -GAL, lipofuscin, and p16<sup>INK4a</sup>, and the morphologic changes. My studies indicate that the tubular epithelium deteriorates as key cells needed to replace damaged cells develop organelle and other changes. At one level homeostasis is maintained: organ mass and function are preserved. Nevertheless at another level homeostasis is not capable of replacing the cells damaged by presumably oxidant related stress. Thus accumulation of senescent cells may reflect both environmental stress and limited replacement. The appearance and persistence of damaged cells then compromises homeostatic mechanisms, leading to age-related pathology. Although kidney mass and function can be maintained because of high replicative potential of the non senescent cells, the accumulation of the senescent cells reaches critical limits in some nephrons, triggering nephron shutdown by a regulatory mechanism.

### 3.5 Tables

**Table 3.1:** Kidney function and weight.

Groups	M ± SD		
	1-month	9-month	24-month
Creatinine (μmol/L)	20.4 ± 6.2	42.2 ± 10.6 <sup>a</sup>	58.0 ± 16.9
Urea (mmol/L)	7.5 ± 1.2	8.6 ± 0.9	6.6 ± 1.1
Sodium (mmol/L)	124.6 ± 9.8	142.2 ± 13.3	134.3 ± 11.2
Chloride (mmol/L)	81.2 ± 7.1	92.8 ± 8.9	92.0 ± 8.9
Kidney weight (mg)	723 ± 70	1157 ± 107 <sup>a</sup>	1403 ± 141 <sup>b</sup>
Body weight (g)	152 ± 21	409 ± 54 <sup>a</sup>	419 ± 49
Kidney/body weight ratio [10 <sup>3</sup> ]	4.9 ± 0.8	2.9 ± 0.4 <sup>a</sup>	3.4 ± 0.4 <sup>b</sup>

<sup>a</sup>1 month and 9 month old group differ P < 0.05

<sup>b</sup>9 month and 24 month old group differ P < 0.05



**Table 3.2:** Pathology of rat kidneys.

Groups	M ± SD		
	1 month N = 6	9 month N = 6	24 month N = 7
Glomeruli (# per section)	213 ± 15.6	214 ± 23.7	254 ± 20.1 <sup>b</sup>
Total sclerotic glomeruli (%)	0	0.2 ± 0.4	2.4 ± 0.9 <sup>b</sup>
Partial sclerotic glomeruli (%)	0	0.1 ± 0.2	2.0 ± 2.2 <sup>b</sup>
Glomerulitis (0-3)	0	0	0
Glomerulopathy (0-3)	0	0	0
Fusion to Bowman's capsula (%)	0	0	0.4 ± 0.8
Widened Bowman's space (%)	0	0.6 ± 0.5 <sup>a</sup>	2.6 ± 1.9
Epithelial proliferation (%)	0	0	0.1 ± 0.1
Hyaline droplets (%)	0	0	0.5 ± 0.5 <sup>b</sup>
Hyaline arteriole (%)	0	0	0.4 ± 0.4
Casts in cortex (#)	0	1.7 ± 1.4 <sup>a</sup>	14.9 ± 11.4 <sup>b</sup>
Casts in medulla <sup>c</sup>	0	0.8 ± 0.4 <sup>a</sup>	1.6 ± 0.8
Tubular atrophy <sup>d</sup>	0	0.7 ± 0.8	8.0 ± 9.0 <sup>b</sup>
Dilated tubules <sup>d</sup>	0	0.2 ± 0.4	3.7 ± 5.6 <sup>b</sup>
Mononuclear infiltrate <sup>e</sup>	0	2.2 ± 1.9 <sup>a</sup>	6.0 ± 6.0
Arteriolar hyaline thickening	0	0	0.6 ± 0.8
Vascular fibrous intimal thickening	0	0	0
Cells per tubular cross-section (#)	4.5 ± 0.3	4.1 ± 0.8	3.5 ± 0.4

<sup>a</sup>1 month and 9 month old group differ P < 0.05

<sup>b</sup>9 month and 24 month old group differ P < 0.05

<sup>c</sup>Number of cross-sections that show casts in medulla: 1 = < 50 cross-sections, 2 = 50-100 cross-sections, 3 = > 100 cross-sections

<sup>d</sup>Number of groups per kidney section that showed tubular atrophy or dilated tubules

<sup>e</sup>Number of areas that showed mononuclear infiltrate

**Table 3.3:** Lipofuscin distribution [%] in tubular epithelium of rat kidney.

Groups	1 month	M ± SD 9 month	24 month
<i>Superficial cortex</i>			
Proximal tubules	0	0.6 ± 0.8 <sup>a</sup>	5.6 ± 3.3 <sup>b</sup>
Non-proximal tubules	0	0	0.6 ± 0.5 <sup>b</sup>
Atrophic tubules (atrophic tubules [%])	- N/A	- N/A	29.3 ± 15.9 2.0
<i>Mid cortex</i>			
Proximal tubules	0	2.2 ± 1.1 <sup>a</sup>	8.7 ± 5.2
Non-proximal tubules	0	0	0.8 ± 0.8 <sup>b</sup>
Atrophic tubules (atrophic tubules [%])	- N/A	- N/A	24.3 ± 14.1 2.3
<i>Juxtamedullary cortex</i>			
Proximal tubules	0.04 ± 0.1	3.3 ± 1.5 <sup>a</sup>	10.8 ± 5.8 <sup>b</sup>
Non-proximal tubules	0	0.2 ± 0.4	0.6 ± 0.8
Atrophic tubules (atrophic tubules [%])	- N/A	- N/A	33.2 ± 13.8 3.4
<i>Medulla</i>			
Proximal tubules	0.1 ± 0.3	5.8 ± 1.9 <sup>a</sup>	13.7 ± 10.1
Non-proximal tubules	0	0.1 ± 0.3	0.8 ± 0.8
Atrophic tubules (atrophic tubules [%])	- N/A	- N/A	49.8 ± 9.0 2.3
<i>Total</i>			
Proximal tubules	0.04 ± 0.1	3.3 ± 0.7	10.0 ± 6.0 <sup>b</sup>
Non-proximal tubules	0	0.1 ± 0.1	0.7 ± 0.3 <sup>b</sup>
Atrophic tubules (atrophic tubules [%])	- N/A	- N/A	43.9 ± 11.0 1.4

<sup>a</sup>1 month and 9 month old group differ P < 0.05

<sup>b</sup>9 month and 24 month old group differ P < 0.05

**Table 3.4:** Association of lipofuscin with SA- $\beta$ -GAL staining in tubular epithelium.

Tubules with lipofuscin:	SA- $\beta$ -GAL staining positive	SA- $\beta$ -GAL staining negative	P value <sup>a</sup>
9 months old rats	73.7 %	26.3 %	< 0.001
24 months old rats	70.0 %	30.0 %	< 0.001

<sup>a</sup>2x2 table with Yates correction.

## 3.6 Figures

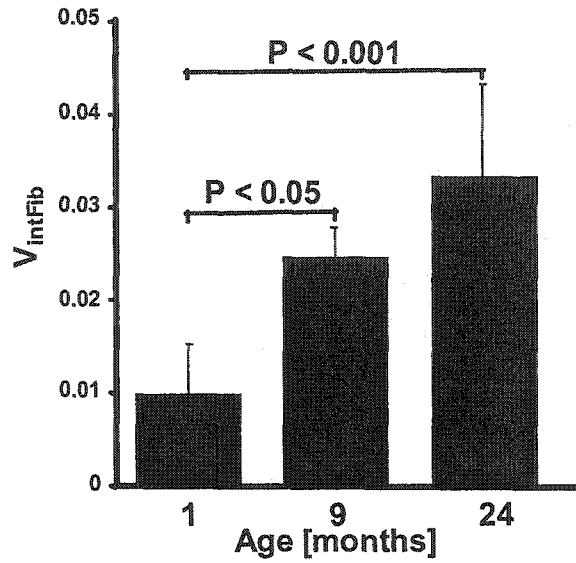


**Figure 3.1:** Fraction of cortical interstitial fibrosis in rat kidneys of three different age groups. Interstitial fibrosis increased significantly with growth, the further increase with age was not statistically significant.

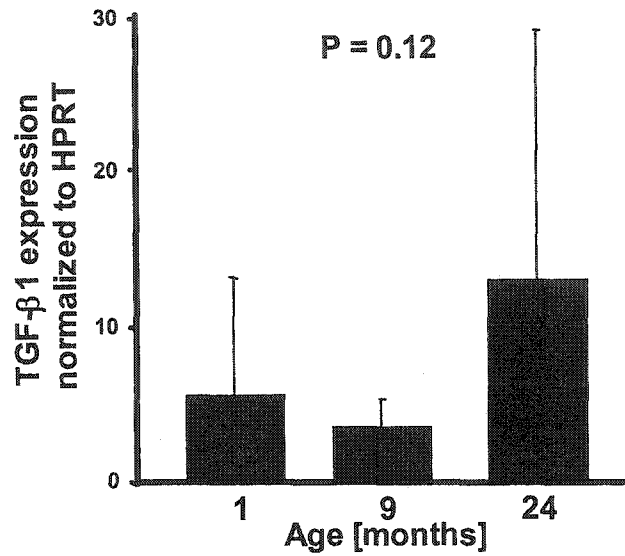


**Figure 3.2:** TGF-β1 mRNA in rat kidneys of three different age groups. TGF-β1 mRNA expression was highly variable in young and old rats. The increase with age was not statistically significant. RNA was isolated and reverse transcribed. Quantitative PCR was performed using sequence-specific primer and probe for TGF-β1 on an ABI 7700 Sequence Detection System. All values were normalized to HPRT.

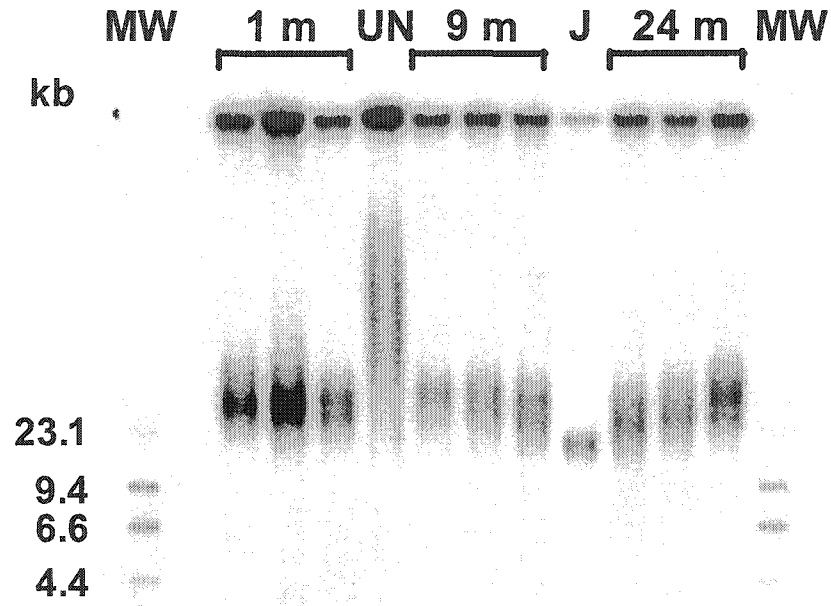


**Figure 3.3:** Representative TRF gel. High molecular weight DNA was isolated, resolved by pulse field gel electrophoresis. Hybridization with a telomere specific  $^{32}\text{P}$ -labeled oligonucleotide was performed and mean TRF length was calculated based on the signal intensity for each lane. Size (kb) is indicated. MW, molecular weight marker; J, Jurkat cell line; UN, undigested, DNA sample not digested with *Hinf*I and *Rsa* I.

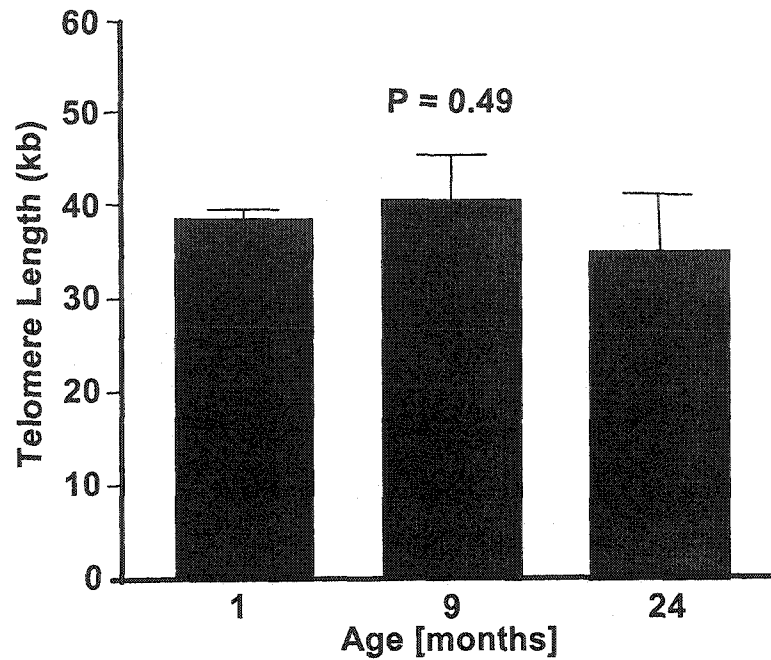


**Figure 3.4:** Mean telomere restriction fragment (TRF) length  $\pm$  SD of mean TRF length in rat kidneys of three different age groups. High molecular weight DNA was isolated, resolved by pulse field gel electrophoresis. Hybridization with a telomere specific  $^{32}\text{P}$ -labeled oligonucleotide was performed and mean TRF length was calculated based on the signal intensity (see Materials and Methods).



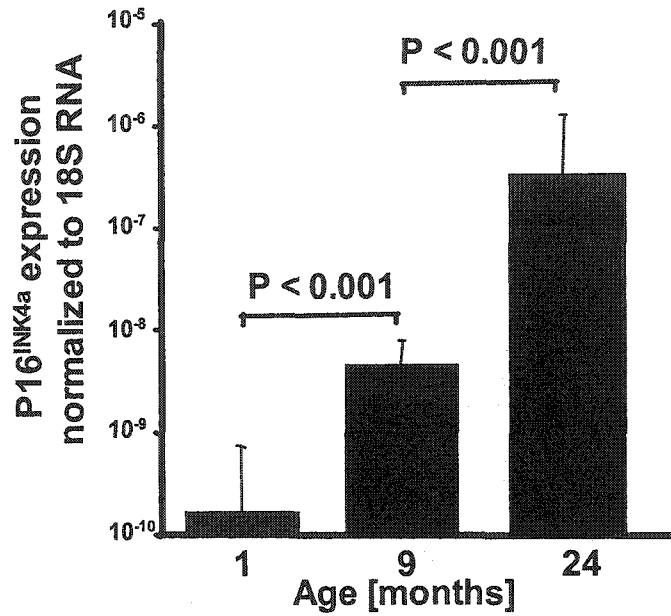


**Figure 3.5:** P16<sup>INK4a</sup> mRNA expression in rat kidneys of three different age groups. RNA was isolated and reverse transcribed. Quantitative PCR was performed using sequence-specific primer and probe for p16<sup>INK4a</sup> on an ABI 7700 Sequence Detection System. All values were normalized to 18S RNA.

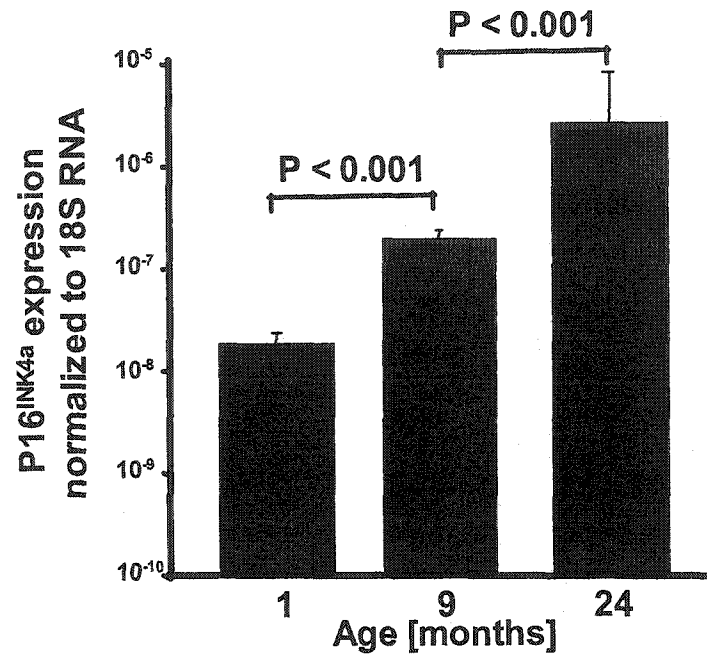


**Figure 3.6:** P16<sup>INK4a</sup> mRNA expression in rat spleens of three different age groups. RNA was isolated and reverse transcribed. Quantitative PCR was performed using sequence-specific primer and probe for p16<sup>INK4a</sup> on an ABI 7700 Sequence Detection System. All values were normalized to 18S RNA.

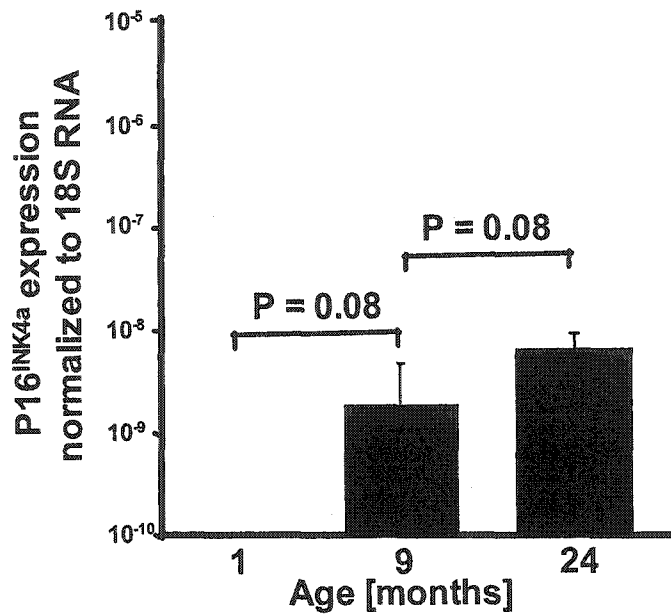


**Figure 3.7:** P16<sup>INK4a</sup> mRNA expression in rat brains of three different age groups. RNA was isolated and reverse transcribed. Quantitative PCR was performed using sequence-specific primer and probe for p16<sup>INK4a</sup> on an ABI 7700 Sequence Detection System. All values were normalized to 18S RNA.

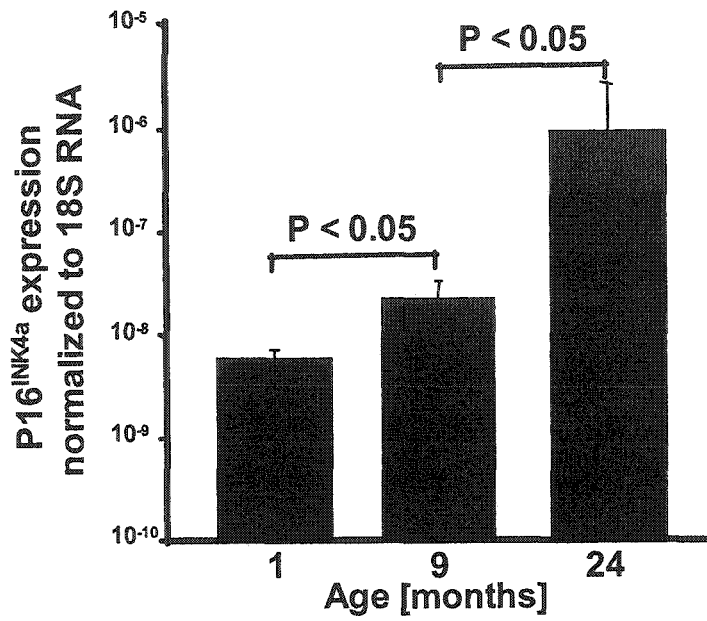


**Figure 3.8:** P16<sup>INK4a</sup> mRNA expression in rat hearts of three different age groups. RNA was isolated and reverse transcribed. Quantitative PCR was performed using sequence-specific primer and probe for p16<sup>INK4a</sup> on an ABI 7700 Sequence Detection System. All values were normalized to 18S RNA.

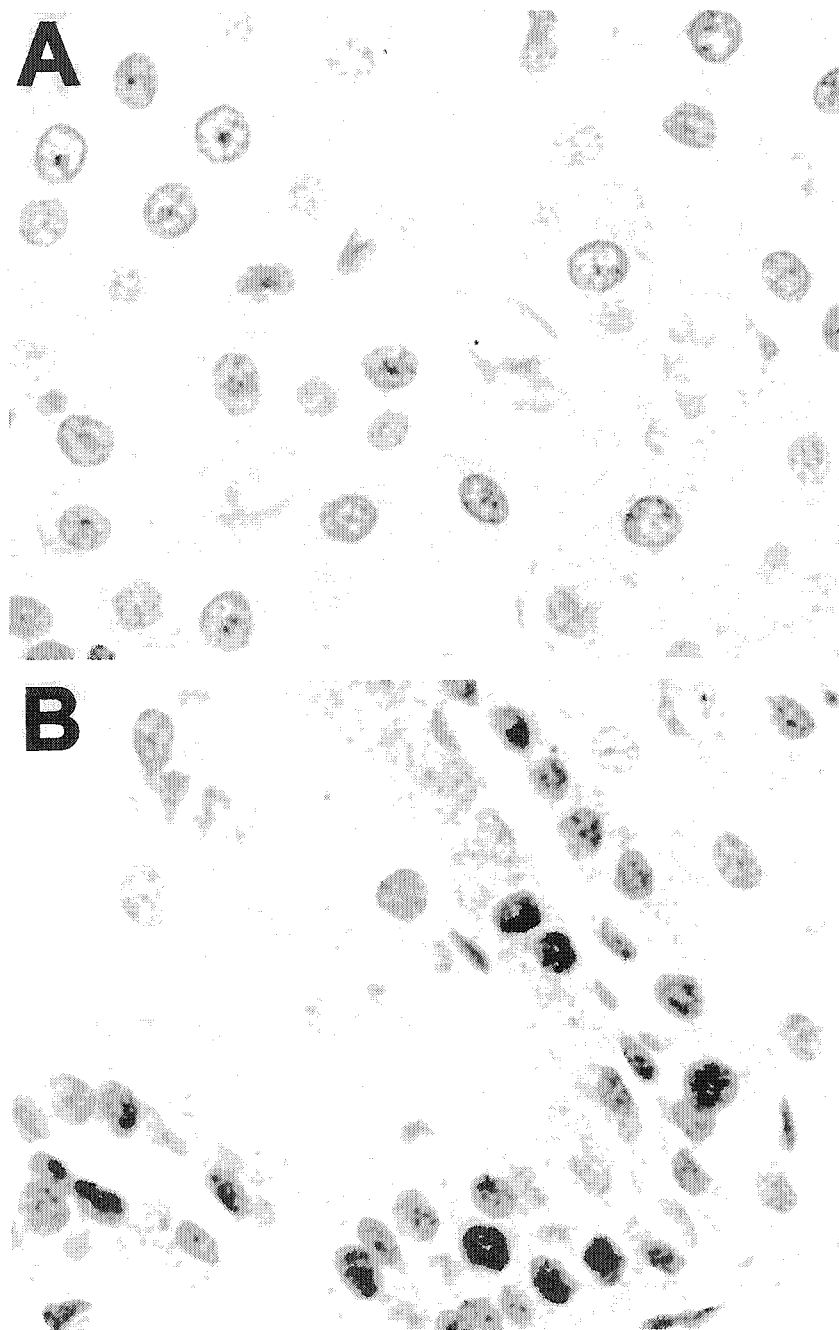


**Figure 3.9:** Representative p16<sup>INK4a</sup> staining in rat kidney tubular sections from a (A) 1 month, and (B) 24 months old rat. Immunoperoxidase staining was performed on paraffin sections with a monoclonal antibody against p16<sup>INK4a</sup> and hematoxylin counterstain. Nuclear p16<sup>INK4a</sup> staining was not or very rarely found in young, but was present in all old rat kidneys.

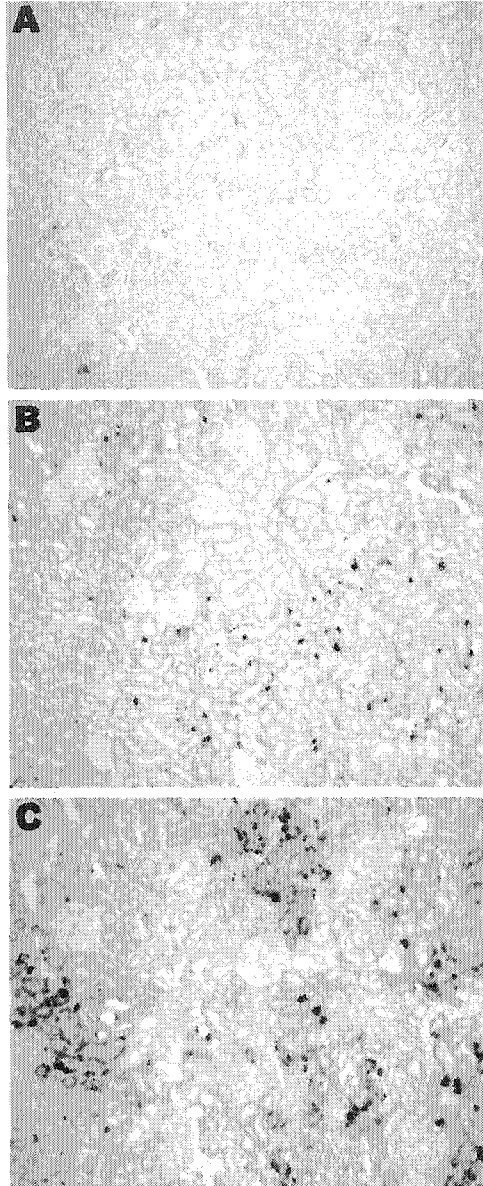


**Figure 3.10:** Representative SA- $\beta$ -GAL staining in rat kidney tissue from a (A) 1 month, (B) 9 months and (C) 24 months old rat. Frozen sections were fixed with 2% formaldehyde/0.2% glutaraldehyde and incubated for 14 hours at 37°C with SA- $\beta$ -GAL staining solution. Counterstaining was performed with eosin. SA- $\beta$ -GAL staining was only found in tubules. Glomeruli and vessels were not affected. SA- $\beta$ -GAL staining was rarely found in kidneys from 1-month old rats. Increased staining was found in 9-months old kidneys. 24-month old specimens showed a patchy pattern of intense staining.

### 3.7 References

1. Levi M and Rowe JW: Aging and the kidney. *Diseases of the Kidney*. Edited by Schrier RW and Gottschalk CW. Boston, MA, Little, Brown, and Company, 1993, pp. 2405-2432
2. Pannu N and Halloran PF: The kidney in aging. *Primer on Kidney Diseases*. Edited by Greenberg A. San Diego, CA, Academic Press, 2001, pp. 377-381
3. Epstein M: Aging and the kidney. *J Am Soc Nephrol* 1996, 7: 1106-1122
4. Lindeman RD and Goldman R: Anatomic and physiologic age changes in the kidney. *Exp Geront* 1986, 21: 379-406
5. Gourtsoyiannis N, Prassopoulos P, Cavouras D, and Pantelidis N: The thickness of the renal parenchyma decreases with age. A CT study of 360 patients. *Am J Roentgenol* 1990, 155: 541-544
6. Fliser D, Zeier M, Nowack R, and Ritz E: Renal functional reserve in healthy elderly subjects. *J Am Soc Nephrol* 1993, 3: 1371-1377
7. Nyengaard JR and Bendtsen TF: Glomerular number and size in relation to age, kidney weight, and body surface in normal man. *Anat Rec* 1992, 232: 194-201
8. Johnson FB, Sinclair DA, and Guarente L: Molecular biology of aging. *Cell* 1999, 96: 291-302
9. Finch CE and Tanzi RE: Genetics of aging. *Science* 1997, 278: 407-411
10. Hayflick L and Moorhead PS: The serial cultivation of human diploid cell strains. *Exp Cell Res* 1961, 25: 585-621
11. Wright WE and Shay JW: Telomere dynamics in cancer progression and prevention: fundamental differences in human and mouse telomere biology. *Nature Medicine* 2000, 6: 849-851
12. Blasco MA, Lee H-W, Hande MP, Samper E, Lansdorp PM, DePinho RA, and Greider CW: Telomere shortening and tumor formation by mouse cells lacking telomerase RNA. *Cell* 1997, 91: 25-34
13. Lee H-W, Blasco MA, Gottlieb GJ, Horner JWII, Greider CW, and DePinho RA: Essential role of mouse telomerase in highly proliferative organs. *Nature* 1998, 392: 569-574
14. Tang DG, Tokumoto YM, Apperly JA, Lloyd AC, and Raff MC: Lack of replicative senescence in cultured rat oligodendrocyte precursor cells. *Science* 2001, 291: 868-871

15. Mathon NF, Malcolm DS, Harrisingh MC, Cheng L, and Lloyd AC: Lack of replicative senescence in normal rodent glia. *Science* 2001, 291: 872-875
16. Serrano M, Lee H-W, Chin L, Cordon-Cardo C, Beach D, and DePinho RA: Role of the INK4a locus in tumor suppressor and cell mortality. *Cell* 1996, 85: 27-37
17. Zindy F, Quelle DE, Roussel MF, and Sherr CJ: Expression of the p16INK4a tumor suppressor versus other INK4 family members during mouse development and aging. *Oncogene* 1997, 15: 203-211
18. Sharpless NE, Bardeesy N, Lee KH, Carrasco D, Castrillon DH, Aguirre AJ, Wu EA, Horner JW, and DePinho RA: Loss of p16Ink4a with retention of p19Arf predisposes mice to tumorigenesis. *Nature* 2001, 413: 86-91
19. Krimpenfort P, Quon KC, Mooi WJ, Loonstra A, and Berns A: Loss of p16Ink4a confers susceptibility to metastatic melanoma in mice. *Nature* 2001, 413: 83-86
20. Baylis C and Corman B: The aging kidney: insights from experimental studies. *J Am Soc Nephrol* 1998, 9: 699-709
21. Corman B, Pratz J, and Poujeol P: Changes in anatomy, glomerular filtration, and solute excretion in aging rat kidney. *Am J Physiol* 1985, 248: R282-R287
22. Dodane V, Chevalier J, Bariety J, Pratz J, and Corman B: Longitudinal study of solute excretion and glomerular ultrastructure in an experimental model of aging rats free of kidney disease. *Lab Invest* 1991, 64: 377-391
23. Bich-Thuy L and Fauci AS: Recombinant interleukin-2 and gamma-interferon (IFN- $\gamma$ ) act synergistically on distinct steps of *in vitro* terminal human B cell maturation. *J Clin Invest* 1986, 77: 1173-1179
24. Mather MW: Base composition-independent hybridization in dried agarose gels: screening and recovery for cloning of genomic DNA fragments. *BioTechniques* 1988, 6: 444-447
25. Harley CB, Futcher AB, and Greider CW: Telomeres shorten during ageing of human fibroblasts. *Nature* 1990, 345: 458-460
26. Chirgwin JM, Przybyla AE, MacDonald RJ, and Rutter WJ: Isolation of biologically active ribonucleic acid from sources enriched in ribonuclease. *Biochemistry* 1979, 18: 5294-5299
27. Heid CA, Stevens J, Livak KJ, and Williams PM: Real time quantitative PCR. *Genome Res* 1996, 6: 986-994



28. Dimri GP, Lee X, Basile G, Acosta M, Scott G, Roskelley C, Medrano EE, Linskens M, Rubelj I, Pereira-Smith O, Peacocke M, and Campisi J: A biomarker that identifies senescent human cells in culture and in aging skin *in vivo*. *Proc Natl Acad Sci USA* 1995, 92: 9363-9367
29. Chkhotua A, Shapira Z, Tovar A, Shabtai E, and Yussim A: Cellular senescence: a new marker of kidney function recovery after ischemic injury in rats. *Transplant Proc* 2001, 33: 2910-2915
30. Coleman GL, Barthold W, Osbaldiston GW, Foster SJ, and Jonas AM: Pathological changes during aging in barrier-reared Fischer 344 male rats. *J Gerontol* 1977, 32: 258-278
31. Maeda H, Gleiser CA, Masoro EJ, Murata I, McMahan CA, and Yu BP: Nutritional influences on aging of Fischer 344 rats: II. Pathology. *J Gerontol* 1985, 40: 671-688
32. Yu BP, Masoro EJ, and McMahan CA: Nutritional influences on aging of Fischer 344 rats: I. physical, metabolic, and longevity characteristics. *J Gerontol* 1985, 40: 657-670
33. Masoro EJ: Mortality and growth characteristics of rat strains commonly used in aging research. *Exp Aging Res* 1980, 6: 219-233
34. Racusen LC, Solez K, Colvin RB, Bonsib SM, Castro MC, Cavallo T, Croker BP, Demetris AJ, Drachenberg CB, Fogo AB, Furness P, Gaber LW, Gibson IW, Glotz D, Goldberg JC, Grande J, Halloran PF, Hansen HE, Hartley B, Hayry PJ, Hill CM, Hoffman EO, Hunsicker LG, Lindblad AS, Marcussen N, Mihatsch MJ, Nadasdy T, Nickerson P, Olsen TS, Papadimitriou JC, Randhawa PS, Rayner DC, Roberts I, Rose S, Rush D, Salinas-Madriral L, Salomon DR, Sund S, Taskinen E, Trpkov K, and Yamaguchi Y: The Banff 97 working classification of renal allograft pathology. *Kidney Int* 1999, 55: 713-723
35. Starling JA, Maule J, Hastie ND, and Allshire RC: Extensive telomere repeat arrays in mouse are hypervariable. *Nucleic Acids Res* 1990, 18: 6881-6888
36. Melk A, Ramassar V, Helms LM, Moore R, Rayner D, Solez K, and Halloran PF: Telomere shortening in kidneys with age. *J Am Soc Nephrol* 2000, 11: 444-453
37. Bodnar AG, Ouellette M, Frolkis M, Holt SE, Chiu C-P, Morin GB, Harley CB, Shay JW, Lichtsteiner S, and Wright WE: Extension of life-span by introduction of telomerase into normal human cells. *Science* 1998, 279: 349-352
38. Sigal SH, Rajvanshi P, Gorla GR, Sokhi RP, Saxena R, Gebhard DR, Reid LM, and Gupta S: Partial hepatectomy-induced polyploidy attenuates

- hepatocyte replication and activates cell aging events. *Am J Physiol* 1999, 276: G1260-G1272
39. Ding G, Franki N, Kapasi AA, Reddy K, Gibbons N, and Singhal PC: Tubular cell senescence and expression of TGF-beta1 and p21(WAF1/CIP1) in tubulointerstitial fibrosis of aging rats. *Exp Mol Pathol* 2001, 70: 43-53
  40. Terman A and Brunk UT: Lipofuscin: mechanisms of formation and increase with age. *APMIS* 1998, 106: 265-276
  41. Palmero I, McConnell B, Parry D, Brookes S, Hara E, Bates S, Jat P, and Peters G: Accumulation of p16INK4a in mouse fibroblasts as a function of replicative senescence and not of retinoblastoma gene status. *Oncogene* 1997, 15: 495-503
  42. Sherr CJ and DePinho RA: Cellular senescence: mitotic clock or culture shock? *Cell* 2000, 102: 407-410
  43. Kamijo T, Zindy F, Roussel MF, Quelle DE, Downing JR, Ashmun RA, Grosveld G, and Sherr CJ: Tumor suppression at the mouse *INK4a* locus mediated by the alternative reading frame product p19<sup>ARF</sup>. *Cell* 1997, 91: 649-659
  44. Harvey M, Sands AT, Weiss RS, Hegi ME, Wiseman RW, Pantazis P, Giovanella BC, Tainsky MA, Bradley A, and Donehower LA: In vitro growth characteristics of embryo fibroblasts isolated from p53-deficient mice. *Oncogene* 1993, 8: 2457-2467
  45. Harvey DM and Levine AJ: p53 alteration is a common event in the spontaneous immortalization of primary BALB/c murine embryo fibroblasts. *Genes Dev* 1991, 5: 2375-2385
  46. Krishna DR, Sperker B, Fritz P, and Klotz U: Does pH 6 beta-galactosidase activity indicate cell senescence? *Mech Ageing & Dev* 1999, 109: 113-123
  47. Kurz DJ, Decary S, Hong Y, and Erusalimsky JD: Senescence-associated (beta)-galactosidase reflects an increase in lysosomal mass during replicative ageing of human endothelial cells. *J Cell Sci* 2000, 113 ( Pt 20): 3613-3622
  48. Robbins E, Levine EM, and Eagle H: Morphologic changes accompanying senescence of cultured human diploid cells. *J Exp Med* 1970, 131: 1211-1222
  49. Yu BP, Masoro EJ, Murata I, Bertrand HA, and Lynd FT: Life span study of SPF Fischer 344 male rats fed ad libitum or restricted diets: longevity, growth, lean body mass and disease. *J Gerontol* 1982, 37: 130-141

50. Van Liew JB, Davis FB, Davis PJ, Noble B, and Bernardis LL: Calorie restriction decreases microalbuminuria associated with aging in barrier-raised Fischer 344 rats. *Am J Physiol* 1992, 263: F554-F561
51. Bengel HH, Mathias RS, Perkins JH, and Alexander EA: Urinary concentrating defect in the aged rat. *Am J Physiol* 1981, 240: F147-F150
52. Kregel KC, Johnson DG, Tipton CM, and Seals DR: Cardiovascular-sympathetic adjustments to nonexertional heat stress in mature and senescent Fischer 344 rats. *J Appl Physiol* 1990, 69: 2043-2049
53. Herlihy JT and Kim S-W: Modulation of the aging cardiovascular system by dietary restriction. *Modulation of Aging Processes by Dietary Restriction*. Edited by Yu BP. Boca Raton, CRC Press, 2002, pp. 57-87

## Chapter 4

# The Strong Association of Cell Cycle Regulator p16<sup>INK4a</sup> Expression with Renal Senescence in Mouse Kidney

A version of this chapter will be submitted for publication.

Anette Melk, Oki Takeuchi, Bernhard M.W. Schmidt, Penny Turner, David Rayner, and Philip F. Halloran: The strong association of cell cycle regulator p16<sup>INK4a</sup> expression with renal aging in mouse kidney.

Portions of this publication that were contributed by co-authors are not included unless noted.

#### 4.1 Introduction

Renal aging is an area of increasing importance because of the high incidence of renal dysfunction and end stage renal disease in the elderly (1;2). The molecular basis of aging remains largely unknown, but one aspect may be changes in somatic cells over time. Limitations on somatic cell survival have been extensively studied *in vitro* in human fibroblasts and mouse embryonic fibroblasts (MEFs) (3). Hayflick observed that human fibroblasts reach a finite lifespan ("Hayflick limit") at which they stop replicating and enter a state called replicative senescence (4). Replicative senescence is due to telomeres reaching a critical length (5;6), perhaps because short telomeres are likely to be 'uncapped' and unprotected (7;8). MEFs also cease cycling, but after fewer cycles and independent of telomere length (9;10). The phenotype of MEFs that have ceased cycling is termed "stimulation and stress-induced senescent-like arrest" (STASIS) and is caused by environmental stresses ("culture shock") (11). Nevertheless murine and human fibroblasts *in vitro*, despite differences in mechanisms of reaching arrest (9;10), share many features at arrest, including altered morphology, greater heterogeneity (12;13), expression of senescence-associated  $\beta$ -galactosidase (SA- $\beta$ -GAL) (14) and accumulation of lipofuscin granules (15). Gene expression changes in senescent cells include overexpression of cyclin-dependent kinase inhibitors (p16<sup>INK4a</sup>, p21<sup>WAF1</sup>, p19<sup>ARF</sup>) (16-18), p53 (18-20), TGF- $\beta$  (21;22), and metallothioneins (MT) (23)

and decreased expression of PCNA (24) and certain heat shock proteins (Hsp 70, 90) (25;26). In addition, senescence-like changes can be stress-induced by oxidative stress (H<sub>2</sub>O<sub>2</sub>, hyperoxia) (27-29) or DNA damage (UV,  $\gamma$ -irradiation) (30).

Given these human-mouse cell differences and the role of the mouse as a model for diseases (31), it is of interest to understand aging in mouse kidney. Unlike the human kidney, which loses mass with age (32;33), murine kidney continuously grows (34). Proteinuria is present in young mice (35) and their kidneys show mesangial IgG staining but without evidence of renal disease (36). Despite sporadic cases of glomerulonephritis (37) or hydronephrosis (38), spontaneous renal disease in most laboratory mouse strains is uncommon. Kidneys of aged mice show surprisingly little pathology: they do not develop focal glomerulosclerosis like many rat strains (39) and there is no tubular atrophy, interstitial fibrosis or fibrous intimal thickening (40).

The critical question is whether the changes characteristic of senescent cells in culture occur *in vivo* in aging kidneys. I previously showed that human kidneys manifest telomere shortening in the cortex with age (chapter 2) (41). In the present experiments I evaluated senescence changes in kidneys of Balb/c mice of different ages. I studied telomere length and expression of genes associated with telomere regulatory function and the telomere capping process (7;42): Tert, the reverse

transcriptase subunit of telomerase; and TRF1 and TRF2, telomere binding proteins. I also selected candidate senescence genes previously reported to be altered in cellular senescence. I studied renal expression of these selected genes in aging compared to development and maturation and compared the change in the kidney with those in heart and brain. Candidate genes were involved in replicative senescence (p16<sup>INK4a</sup>, p19<sup>ARF</sup>, TGF- $\beta$ 1, PCNA) or stress-induced senescence (GADD45, Hsp70, HIC-5, MT1 and MT3). I also included a gene associated with an aging phenotype *in vivo* in rat liver and kidney (SMP30) (43).

## 4.2 Materials and Methods

### 4.2.1 Mice

Mouse samples were derived from 30 Balb/c mice of four age groups (newborn, n=8, 1 month, n=8, 3 months, n=6 and 18 months, n=8). All mice were derived from the University of Alberta animal colony. Mice were killed by cervical dislocation and a midline incision was performed and kidneys and heart were quickly removed. Brains were harvested last. All tissue samples were immediately snap-frozen in liquid nitrogen and stored at  $-70^{\circ}\text{C}$ . In addition, kidney tissue was fixed with paraformaldehyde for paraffin embedded sections. All experiments were performed according to the University of Alberta Animal Policy and Welfare Committee's animal care protocols.

#### 4.2.2 Reverse transcription (RT) and real-time polymerase chain reaction (PCR)

Total RNA was extracted using the RNeasy kit (QIAGEN, Santa Clarita, CA) after initial homogenization. RT was performed using random hexamer primers and Maloney murine leukemia virus (MMLV, Life Technologies, Burlington, Ontario) as previously described (44). Quantitative Real-time PCR to detect gene expression was performed on an ABIPrism SDS 7700 TaqMan (Applied Biosystems, Foster City, CA) using sequence specific primers and probe for p16<sup>INK4a</sup>, p19<sup>ARF</sup>, GADD45, PCNA, Hsp70, HIC-5, TGF- $\beta$ , SMP-30, MT1 and MT3 (table 1). I designed all the primers and probes using Primer Express software (Applied Biosystems, Foster City, CA). All samples were measured in duplicate. Relative quantification of gene expression was performed using the Relative Standard Curve method as described in the User Bulletin #2 (Applied Biosystems, Foster City, CA). Briefly, the number of PCR cycles that are needed to reach the fluorescence threshold is called threshold cycle (Ct). The Ct value for each sample is proportional to the  $\log_2$  of the initial amount of input cDNA. The calibrator used consisted of cDNA derived from different tissues and age groups. Standard curves were prepared by serial dilutions of the calibrator for both the gene of interest and the housekeeping gene HPRT. Dilutions were arbitrarily numbered 3, 1.5, 0.75, 0.375 and 0.1875. The Ct values for all samples were then assigned



an arbitrary value based on the standard curves. The arbitrary values for gene of interest and for HPRT were divided in order to normalize to HPRT. Then the mean value for the duplicates was calculated. All values are given as a gene of interest to HPRT ratio.

#### 4.2.3 Histopathology assessment

H&E and PAS staining were done using 4  $\mu\text{m}$  sections of paraffin embedded tissue. Together with a renal pathologist (David Rayner) I assessed the kidneys for morphological changes within the glomerular, tubular and interstitial compartment.

#### 4.2.4 Senescence associated (SA) $\beta$ -galactosidase ( $\beta$ -GAL) staining

Frozen sections were cut at 4  $\mu\text{m}$  and kept at  $-20^{\circ}\text{C}$  until further processed. Staining was done as previously described (chapter 3) (45). Briefly, slides were brought to RT and fixed with 2% formaldehyde/0.2% glutaraldehyde in PBS. Slides were then incubated for 14 hours at  $37^{\circ}\text{C}$  in a humidified chamber with SA- $\beta$ -GAL staining solution (2mg/ml X-gal in dimethylformamide, 40mM citric acid/sodium phosphate (dibasic), pH 6, 5mM potassium ferrocyanide, 5mM potassium ferricyanide, 150mM sodium chloride, 20mM magnesium chloride). Controls were stained for lysosomal  $\beta$ -GAL using the same SA- $\beta$ -GAL staining solution adjusted to pH 4. Following staining, slides were counterstained with eosin, dehydrated and

mounted.

Quantification of the SA- $\beta$ -GAL staining was accomplished by Image-Pro Plus Software. A set of slides without counterstain was produced and photographed. The image was opened in Image-Pro Plus and staining density for the whole section was calculated. The mean staining density of two independent experiments was taken for further calculations and statistical analysis.

#### 4.2.5 Immunohistochemistry for p16<sup>INK4a</sup>

Immunoperoxidase staining for p16<sup>INK4a</sup> was performed using 4  $\mu$ m sections of paraffin embedded tissue. Briefly, sections were deparaffinized and hydrated. The sections were immersed in 3% H<sub>2</sub>O<sub>2</sub> methanol to inactivate endogenous peroxidase. Slides were blocked with 20% normal goat serum. Tissue sections were then incubated for 1 hr at RT with the primary antibody (mouse monoclonal antibody, Clone F-12, Santa Cruz, CA) and rinsed with PBS. Following 30 minutes of incubation with the Envision monoclonal system (Dako, Ontario), sections were washed again in PBS. Visualization was performed using the DAB substrate kit (Dako, Ontario). The slides were counterstained with hematoxylin and mounted. Analysis was done by counting 5 HPF for either cortex or medulla. Percentage of positive nuclei was assessed for tubules, glomeruli and interstitium. Staining of arteries and arterioles was assessed throughout the

whole section. Each vessel was graded on a scale from 0 to 3, with 0 being no staining, 1 up to 30% stained nuclei, 2 between 30 and 60% stained nuclei and 3 more than 60% stained nuclei. The mean score was then calculated for each section.

#### 4.2.6 Terminal restriction fragments (TRF)

TRF were measured as described previously (chapter 2 and 3) (41;45). To obtain high molecular weight DNA without degradation, the tissue was disrupted by freeze grinding. DNA was then isolated by proteinase K digestion and phenol/chloroform extraction. DNA samples were digested with the restriction enzymes Hinf I and Rsa I (Boehringer Mannheim, Germany) to produce TRFs. 1.5  $\mu\text{g}$  of each digested sample was resolved on a 1.0 % agarose gel by pulse field gel electrophoresis (buffer temperature 14°C, voltage gradient 6.0 V/cm, switching interval 1-30 sec., 12h). Gel was probed directly and hybridization was done at 42° C overnight with a 5'-end-labelled  $^{32}\text{P}$ -(TTAGGG)<sub>5</sub> oligonucleotide telomere probe in a buffer containing 6x SSC, 5x Denhardt's solution, 50mM NaH<sub>2</sub>PO<sub>4</sub> (pH 7.4), 0.1 mg/ml salmon sperm DNA, 0.1 % SDS. Following stringency washes at RT in 0.2X SSC, 0.1% SDS, the autoradiography signal was digitized in a phosphoimage scanner (Fuji) using ImageGauge Software. All lanes were subdivided into intervals of 1 mm. The mean size of the TRFs was estimated using the formula  $\Sigma(\text{ODi} \times \text{Li}) / \Sigma(\text{ODi})$ , where ODi

is the density reading from interval  $i$  and  $L_i$  is the size in kbp of the interval relative to the markers (6). Mean TRF length was determined on the basis of the intensity of the signal, where the intervals averaged were higher than 1% of the total signal in that lane. (Irwindeep Sandhu did some TRF gels as part of his summer student project).

#### 4.2.7 Statistical analysis

Data analyses were performed using SPSS software. Means among four groups of mice were compared using ANOVA, and T-tests with Bonferroni correction were used for multiple pair-wise comparisons. All values are given as mean  $\pm$  standard deviation (SD).

### 4.3 Results

For the presentation of my results I designated three developmental periods. I designated “development” as the period from birth to 1 month; “Maturation” as the period from 1 to 3 months; and “Aging”: as the period from 3 to 18 months. Changes that affect the whole period will be referred to as “changes with time”.

#### 4.3.1 Morphologic changes

Representative PAS kidney sections of 1, 3 and 18 months old mice are shown in figure 4.1. The investigated kidneys showed no glomerular

disease, tubulointerstitial changes or hydronephrosis. As previously reported, the morphologic changes of aging in mouse kidneys were very mild. In the 18 months old kidneys, fibrous intimal thickening of arteries was not observed, and hyalinosis of arterioles was rare. The 18 months kidneys showed slight mesangial hyperplasia (figure 4.1 C) and occasional hyaline casts. Lipofuscin granules were rare. SA- $\beta$ -GAL staining was present in all three age groups (1, 3, 18 months). Mean staining densities were 0.169 ( $\pm$ 0.004) for 1 month, 0.194 ( $\pm$ 0.033) for 3 months and 0.221 ( $\pm$ 0.003) for 18 months. Thus SA- $\beta$ -GAL staining increased slightly over time but the increase was not significant.

Both the kidney weight and bodyweight increased continuously with age, with little change in the kidney/bodyweight ratio (table 4.2). The increases in weight were greatest during development.

#### 4.3.2 Telomere length and expression of telomere regulating genes

I measured telomere length as telomeric restriction fragments (TRF) by pulse field gel electrophoresis (figure 4.2). TRF length (kb) was  $47.3 \pm 1.2$  for 1 month,  $45.2 \pm 2.6$  for 3 months and  $44.6 \pm 1.6$  for 18 months old kidneys (figure 4.3). There was a slight but significant decrease in TRF length with time ( $p < 0.05$ ). The mean TRF length in kidneys was 45.7 kb, similar to a previous report for *M. musculus* kidneys (46) and much longer than in human kidney (about 12Kb) (41). I did not measure telomere length

in newborn mice because of the small amount of kidney tissue available.

I studied mRNA expression of the reverse transcriptase subunit of telomerase, Tert, as well as the telomere binding proteins TRF1 and TRF2. Tert (figure 4.4) and TRF1 (figure 4.5) expression were highest in newborn mice and decreased significantly during development, but persisted throughout life. TRF2 (figure 4.6) expression levels did not change significantly through life.

#### 4.3.3 P16<sup>INK4a</sup> mRNA and protein expression

P16<sup>INK4a</sup> mRNA expression (figure 4.7) was very low at birth ( $0.006 \pm 0.003$ ) and increased steadily with time (1 month:  $0.019 \pm 0.013$ , 3 months:  $0.068 \pm 0.044$ ) and in particular with aging. The highest value was in 18 months old mice ( $0.593 \pm 0.187$ ). This was almost 100-fold higher than the value in newborn and 10-fold higher than the value in 3 months old mice ( $p < 0.001$ ).

I corroborated the mRNA results by immunoperoxidase staining for p16<sup>INK4a</sup> (figures 4.8). The results are expressed as the percentage of p16<sup>INK4a</sup> positive nuclei for tubular (figures 4.9 and 4.10), glomerular (figure 4.11) and interstitial cells (figures 4.12 and 4.13) in both cortex and medulla and as a score for arteries and arterioles (figure 4.14). Kidneys from 1 month old mice showed only rare staining of single nuclei which increased modestly by 3 months. However, the major increase occurred with aging,

and was significant for nuclei in tubules in cortex and medulla as well as in arteries and arterioles. Staining of nuclei in tubular cells was seen in all segments of the nephron, including the macula densa in the 18 months old kidneys.

#### 4.3.4 Expression of p19<sup>ARF</sup> and other candidate senescence genes

I studied other candidate senescence genes and found four significant age-related expression patterns in the kidney. P19<sup>ARF</sup> showed a “U” shaped pattern (figure 4.15) with its highest relative expression in newborn mice, a sharp fall during development and a rise in aging. MT 1 (figure 4.16) also showed a “U” shaped pattern like p19<sup>ARF</sup> but the increase with aging was not significant. Changes in MT3 (figure 4.17) were reciprocal to MT1: lowest at birth, peaking at 1 month, and decreasing thereafter. The changes in Hsp70 (figure 4.18) expression over time were small: a peak at 1 month, with a significant increase during development. Three genes (TGF- $\beta$ , PCNA, HIC-5; figures 4.19-4.21) showed highest relative expression in newborn mice and significant fall with development. TGF- $\beta$  and PCNA then showed low stable expression over time, whereas HIC-5 showed significant decrease with maturation. SMP30 (figure 4.22) and GADD45 (figure 4.23) showed relatively little change over time, although SMP30 expression increased between 1 and 18 months. Thus no other candidate gene displayed the marked increase over time and particularly

with aging that was observed with p16<sup>INK4a</sup>.

#### 4.3.5 Comparison of kidney with other organs

*Differential P16<sup>INK4a</sup> mRNA expression in mouse brain and heart:* I measured p16<sup>INK4a</sup> mRNA patterns over time in brain and heart. I show the fold change versus newborn, versus the preceding group, as well as the organ to kidney ratio (table 4.3). P16<sup>INK4a</sup> mRNA expression brain and heart resembled the pattern observed in the kidney, with lowest values at birth and continuous increase in each age interval towards highest expression at 18 months. For brain and heart the major increase in p16<sup>INK4a</sup> expression occurred during development, whereas for kidney the major increase occurred in aging. When relative expression was compared, the highest overall values for the p16<sup>INK4a</sup> were seen in heart followed by brain and kidney.

*Differential gene expression of candidate genes in mouse brain and heart:* To assess relative changes in gene expression in other organs compared to kidney, I measured the expression levels for candidate genes in brain and heart (tables 4.4-4.12). The changes in gene expression in brain occurred mainly in development, and no gene showed a significant change during aging. Like brain, the changes in gene expression in heart were concentrated in development. The exceptions were p19<sup>ARF</sup>, which showed a significant increase with aging, and GADD45, which decreased.



Table 4.13 summarizes the predicted changes based on the literature and actual changes in the different organs. In conclusion, *in vivo* changes that corresponded to what had been suggested from *in vitro* studies were only seen for p16<sup>INK4a</sup> in all organs studied and for p19<sup>ARF</sup> in kidney and heart but not in brain.

#### 4.4 Discussion

I investigated whether mouse kidney aging *in vivo* shows features of cellular senescence, including morphologic changes (histology, lipofuscin), biochemical changes (SA-β-GAL), telomere shortening, and altered gene expression. Histological and biochemical changes were minor with little increase in SA-β-GAL and lipofuscin at 18 months. Similar to my previous findings in rat (chapter 3) (45), telomeres in mouse kidney were very long compared to telomeres in human kidneys (chapter 2) (41) and decreased only slightly with age. Tert and the telomere binding protein TRF1 but not TRF2 were highest in neonates but showed little change during maturation and aging. The most striking change in gene expression with development and aging was a progressive increase in expression the cell cycle regulator p16<sup>INK4a</sup>, both at the mRNA and protein level. P16<sup>INK4a</sup> was expressed in nuclei of cells in tubules, glomeruli, vessels, and interstitium. Other investigated genes tended to have their highest expression during development rather than aging, with exception of p19<sup>ARF</sup> that had high

expression in newborns and increased with age. The expression patterns for the candidate genes in kidney were also seen in brain and heart, in particular for p16<sup>INK4a</sup>. One difference was that p19<sup>ARF</sup> in brain showed highest expression in newborns and decreased, whereas in heart the highest expression of p19<sup>ARF</sup> was seen at 18 months. Thus although mouse kidney at 18 months lacked most features of senescent cells in culture, it manifested a striking increase in one characteristic of cellular senescence - a progressive increase in p16<sup>INK4a</sup> that was also seen in other organs.

The long telomeres, continued Tert expression, and lack of critical telomere shortening with aging in mouse kidneys support the conclusion that mouse cells *in vivo*, like MEFs *in vitro*, do not use telomere shortening as a replication counter (9;10). Human kidneys have shorter telomeres (about 12 kbp) and in cortex show telomere shortening through life (chapter 2) (41), probably because most human somatic tissues lack telomerase. Telomerase synthesizes telomeric DNA and is expressed in many somatic mouse tissues and cultured cells (47). The fact that mouse and rat kidneys have telomeres that remain long (chapter 3) (45) even in aging must be taken into account when comparing mouse and rat models to human diseases. Long telomeres and continued expression of telomerase may protect against the consequences of injury: mice deficient in the telomerase activity show progressive telomere shortening with increasing generations, with increased susceptibility to liver injury (48) and renal dysfunction (49).

The role of telomere function in injury and repair could be relevant to the high susceptibility of aged human kidneys to disease. One caveat is that the fact that mouse and rat lack critical telomere shortening does not guarantee that telomere capping and function is normal in aged mice. However, these species characteristics may be relevant when trying to use rodent models of disease or injury to predict the results of similar stresses in humans, especially older humans.

The striking increase in p16<sup>INK4a</sup> expression with aging in the kidney and other organs suggests that cells in mouse organs undergo cell cycle regulatory events during aging *in vivo* similar to those in MEFs in response to environmental stress. In MEFs culture induces cell cycle arrest associated with p16<sup>INK4a</sup> and p19<sup>ARF</sup> expression (9). P16<sup>INK4a</sup> and p19<sup>ARF</sup> have overlapping and complementary roles in MEF growth arrest (50), unlike human fibroblasts where p16<sup>INK4a</sup> is more important than p14<sup>ARF</sup> (the human equivalent of p19<sup>ARF</sup>) (51). The p16<sup>INK4a</sup>/retinoblastoma pathway is known to be activated by oxidative damage, DNA damage, and mitochondrial damage (16;52). P16<sup>INK4a</sup> can be thought of as an irreversible lock that is applied when somatic cells reach their limits on replication. Young cells *in vitro*, and cells in organs of young mice and rats, do not use p16<sup>INK4a</sup>. But as cells or organs age, there is a progressive increase in the number of cells expressing p16<sup>INK4a</sup> and exiting the cell cycle. *In vitro* data suggest that p16<sup>INK4a</sup> expression induces irreversible cell cycle arrest:

transfection of p16<sup>INK4a</sup> into p16<sup>INK4a</sup> negative cells induces growth arrest (53;54). Thus p16<sup>INK4a</sup> is not only an indicator but also a mediator of cell cycle arrest. The p16<sup>INK4a</sup> knockout mouse manifests an increase in cancers, especially melanoma (55;56) indicating a role for p16<sup>INK4a</sup>, like p19<sup>ARF</sup>, as a tumor suppressor. The p16<sup>INK4a</sup> knockout mouse has not been aged to assess how the absence of p16<sup>INK4a</sup> affects aging. Thus the high numbers of cells expressing p16<sup>INK4a</sup> could limit repair and even homeostasis in the aging kidney but this remains to be tested.

The remarkable changes in p16<sup>INK4a</sup> expression in mouse kidney with aging are highlighted by the lack of change in many other features of cellular senescence *in vitro*. Although selected for their proposed importance in replicative senescence and/or STASIS in fibroblast culture, no candidate gene was as strikingly associated with aging as p16<sup>INK4a</sup>. Only p19<sup>ARF</sup> showed an increase with aging but was also associated with development, with high expression in newborn mice. PCNA had high expression in development and lower but sustained basal expression through life, compatible with ongoing replication in mouse kidney. TGF- $\beta$  was highest in newborns, followed by lower but stable expression through life. The lack of increase in TGF- $\beta$  expression with aging could be relevant to the lack of interstitial fibrosis in old mice, in comparison to rat, where fibrosis and TGF- $\beta$  are increased.

The comparison between mouse and rat kidneys may provide

insights into the significance of some of these changes. The similarities are that they both show kidney weight and body weight increases, with no telomere shortening but expressing progressive increases in p16<sup>INK4a</sup>. However, mice rarely develop renal diseases and show only mild kidney pathology in aging whereas many rat strains develop renal disease (39), and rat kidneys show many morphologic and biochemical changes that are absent in mice. In my previous studies (chapter 3) (45), rat kidneys showed focal and segmental glomerulosclerosis, interstitial fibrosis and tubular atrophy. Lipofuscin and SA-β-GAL increased exponentially with age in rats, but was not prominent in mice. Thus the changes observed in rat are unlikely to be due to p16<sup>INK4a</sup> expression. The aging phenotype in a species probably reflects a number of independent events, some intrinsic to aging and some due to age related diseases, which are more specific to the species.

Despite differences between humans and mice, the mechanisms of mouse kidney aging are likely to be relevant to humans. The kidney in each species shows some features observed in senescent fibroblasts of that species: increased p16<sup>INK4a</sup> expression without telomere shortening in mouse, and increased p16<sup>INK4a</sup> expression (chapter 5) with telomere shortening in human (chapter 2) (41). This is compatible with the hypothesis that some mechanisms contributing to senescence of somatic cells *in vitro* also play a role in aging phenotypes *in vivo*. It will be important to establish

the reason for the species differences. Perhaps long lived mammals require regulatory strategies beyond those in short lived mammals such as mouse and rat e.g. superior resistance to cancer through the telomere shortening mechanism (11), and perhaps increased resistance to environmental stress. If so, studies in rodents will permit us to dissect important molecular events in aging and age-related diseases, with the caveat that additional levels of control in humans prevent any direct extrapolation to human renal aging.

## 4.5 Tables

**Table 4.1: Sequences for primers and probes used in Real-time PCR studies.**

Name	Accession Number (GenBank)		Sequence (5'→3')
p16 <sup>INK4a</sup>	L 76150	Forward primer	GGGCACTGCTGGAAGCC
		Reverse primer	AACGTTGCCCATCATCATCAC
		Probe	CCGAACTCTTTCCGGTCGTACCCCGAT
p19 <sup>ARF</sup>	L 76092	Forward primer	TCGTGAACATGTTGTTGAGGCTA
		Reverse primer	GTTGCCCATCATCATCACCTG
		Probe	CGGTGCGGCCCTCTTCTCAAGATC
GADD45	L 28177	Forward primer	ACTGTGTGCTGGTGACGAACC
		Reverse primer	ACCCACTGATCCATGTAGCGAC
		Probe	ATCACAATGGAAGGATCCTGCCTTAAGTCAA
PCNA	NM 011045	Forward primer	AGCAACTTGAATCCCAGAACA
		Reverse primer	GGTCTCGGCATATACGTGCAA
		Probe	CACCCGACGGCATCTTTATTACACAGCTG
Hsp70	NM 031165	Forward primer	CCTCATCAAGCGCAATACCAC
		Reverse primer	CCCTTTCACCTTCATACACCTGA
		Probe	CACCTACTCTGACAACCAGCCTGGTGTACTCA
TGF- $\beta$	NM 011577	Forward primer	GGCTACCATGCCAACTTCTGTCT
		Reverse primer	CCGGGTTGTGTTGGTTGTAGA
		Probe	CACACAGTACAGCAAGGTCCTTGCCCT
SMP30	U 28937	Forward primer	CGCTACTGTTTGTAGATATCCCTTCAA
		Reverse primer	AACTGACTGGGGCATCCACA
		Probe	AACTCGCTGCACTTGATTGCTGACCG
HIC-5	L 22482	Forward primer	AGCGCTTCTCCCCACGAT
		Reverse primer	GCAGCTGACGCAGCAGAA
		Probe	ACCAACCCATCCGACACAAAATGGTTACC
MT1	NM 013602	Forward primer	CACCAGCTCCTGCGCCT
		Reverse primer	CCTGGGCACATTTGGAGC
		Probe	CTGCTGCTCCTGCTG
MT3	NM 013603	Forward primer	GCACCTGCTCGGACAAATG
		Reverse primer	ACACAGTCCTTGGCACACTTCTC
		Probe	CTGCTGCTCCTGCTG
HPRT	J 00423	Forward primer	TGACACTGGTAAAACAATGCAAACCT
		Reverse primer	AACAAAGTCTGGCCTGTATCCAA
		Probe	TTCACCAGCAAGCTTGCAACCTTAACC



**Table 4.2:** Kidney weight, body weight and kidney/body weight ratio.

	Newborn N = 8	1 month N = 8	3 months N = 6	18 months N = 8
Kidney weight [mg]	16.8 ± 5.9	108.4 ± 9.5 <sup>a</sup>	133.3 ± 7.6 <sup>b</sup>	183.0 ± 11.3 <sup>c</sup>
Total body weight [g]	2.1 ± 0.3	16.2 ± 1.5 <sup>a</sup>	22.8 ± 0.7 <sup>b</sup>	27.5 ± 1.0 <sup>c</sup>
Kidney/body weight ratio [x10 <sup>-3</sup> ]	7.2 ± 1.4	6.7 ± 0.4	5.8 ± 0.2	6.7 ± 0.3

<sup>a</sup>newborn vs. 1 month old mice P < 0.05

<sup>b</sup>1 month vs. 3 month old mice P < 0.05

<sup>c</sup>3 month vs. 18 month old mice P < 0.05

**Table 4.3:** P16<sup>INK4a</sup> mRNA expression values for heart and brain in comparison to kidney.

Gene		Newborn	1 month	3 months	18 months
Brain	P16 <sup>INK4a</sup> /HPRT ratio	.005 ± .003	.127 ± .068	.136 ± .087	.578 ± .149 <sup>a</sup>
	Fold change vs. newborn	-	24.8 ↑	26.7 ↑	113.1 ↑
	Fold change vs. preceding age group	-	24.8 ↑	1.1 ↑	4.2 ↑
	Brain/kidney ratio	0.8	6.6	2.0	1.0
Heart	P16 <sup>INK4a</sup> /HPRT ratio	.009 ± .005	.481 ± .240	1.20 ± .401	5.65 ± 1.56 <sup>a</sup>
	Fold change vs. newborn	-	53.6 ↑	133.7 ↑	629.4 ↑
	Fold change vs. preceding age group	-	53.6 ↑	2.5 ↑	4.7 ↑
	Heart/kidney ratio	1.4	25.1	17.6	9.5
Kidney	P16 <sup>INK4a</sup> /HPRT ratio	.006 ± .003	.019 ± .013	.068 ± .044	.593 ± .187 <sup>a</sup>
	Fold change vs. newborn	-	3.0 ↑	10.7 ↑	93.0 ↑
	Fold change vs. preceding age group	-	3.0 ↑	3.6 ↑	8.7 ↑

<sup>a</sup>P < 0.001 when compared to newborn, 1 month and 3 month

**Table 4.4:** P19<sup>ARF</sup> mRNA expression values for heart and brain in comparison to kidney.

Gene		Newborn	1 month	3 months	18 months
Brain	P19 <sup>ARF</sup> /HPRT ratio	.48 ± .12	.14 ± .03	.09 ± .03	.22 ± .12
	Fold change vs. newborn	-	3.4 ↓	5.1 ↓	2.2 ↓
	Fold change vs. preceding age group	-	3.4 ↓	1.5 ↓	2.3 ↑
	Brain/kidney ratio	0.7	1.5	1.3	0.6
Heart	P19 <sup>ARF</sup> /HPRT ratio	.74 ± .07	.63 ± .25	.55 ± .10	1.25 ± .55
	Fold change vs. newborn	-	1.2 ↓	1.3 ↓	1.7 ↑
	Fold change vs. preceding age group	-	1.2 ↓	1.1 ↓	2.3 ↑
	Heart/kidney ratio	1.1	6.7	7.5	3.6
Kidney	P19 <sup>ARF</sup> /HPRT ratio	.67 ± .21	.09 ± .03	.07 ± .02	.35 ± .09
	Fold change vs. newborn	-	7.2 ↓	9.1 ↓	1.9 ↓
	Fold change vs. preceding age group	-	7.2 ↓	1.3 ↓	0.2 ↑

**Table 4.5:** MT1 mRNA expression values for heart and brain in comparison to kidney.

Gene		Newborn	1 month	3 months	18 months
Brain	MT1/HPRT ratio	.97 ± .08	4.38 ± 1.34	2.87 ± .61	3.83 ± 1.7
	Fold change vs. newborn	-	4.5 ↑	3.0 ↑	4.0 ↑
	Fold change vs. preceding age group	-	4.5 ↑	1.5 ↓	1.3 ↑
	Brain/kidney ratio	0.04	0.8	0.4	0.3
Heart	MT1/HPRT ratio	1.37 ± .18	3.40 ± 1.04	2.99 ± .67	3.33 ± .96
	Fold change vs. newborn	-	2.5 ↑	2.2 ↑	2.4 ↑
	Fold change vs. preceding age group	-	2.5 ↑	1.1 ↓	1.1 ↑
	Heart/kidney ratio	0.05	0.6	0.4	0.2
Kidney	MT1/HPRT ratio	25.9 ± 7.1	5.8 ± 3.0	7.3 ± 2.4	14.3 ± 4.8
	Fold change vs. newborn	-	4.5 ↓	3.6 ↓	1.8 ↓
	Fold change vs. preceding age group	-	4.5 ↓	1.3 ↑	2.0 ↑

**Table 4.6:** MT3 mRNA expression values for heart and brain in comparison to kidney.

Gene		Newborn	1 month	3 months	18 months
Brain	MT3/HPRT ratio	117 ± 12	238 ± 38	221 ± 46	216 ± 23
	Fold change vs. newborn	-	2.0 ↑	1.9 ↑	1.8 ↑
	Fold change vs. preceding age group	-	2.0 ↑	1.1 ↓	1.0 =
	Brain/kidney ratio	162	71	83	111
Heart	MT3/HPRT ratio	17.8 ± 3.2	3.6 ± 2.1	2.1 ± .7	1.9 ± .2
	Fold change vs. newborn	-	4.9 ↓	8.3 ↓	9.6 ↓
	Fold change vs. preceding age group	-	4.9 ↓	1.7 ↓	1.2 ↓
	Heart/kidney ratio	24.6	1.1	0.8	1.0
Kidney	MT3/HPRT ratio	.72 ± .17	3.36 ± .91	2.65 ± .25	1.94 ± .24
	Fold change vs. newborn	-	4.7 ↑	3.7 ↑	2.7 ↑
	Fold change vs. preceding age group	-	4.7 ↑	1.3 ↓	2.7 ↓

**Table 4.7:** Hsp70 mRNA expression values for heart and brain in comparison to kidney.

Gene		Newborn	1 month	3 months	18 months
Brain	Hsp70/HPRT ratio	1.11 ± .18	.98 ± .18	.66 ± .12	.57 ± .07
	Fold change vs. newborn	-	1.1 ↓	1.7 ↓	2.0 ↓
	Fold change vs. preceding age group	-	1.1 ↓	1.5 ↓	1.2 ↓
	Brain/kidney ratio	1.3	0.7	0.6	0.6
Heart	Hsp70/HPRT ratio	.63 ± .04	1.21 ± .13	1.34 ± .22	1.24 ± .25
	Fold change vs. newborn	-	1.9 ↑	2.1 ↑	2.0 ↑
	Fold change vs. preceding age group	-	1.9 ↑	1.1 ↑	1.1 ↓
	Heart/kidney ratio	0.7	0.9	1.2	1.3
Kidney	Hsp70/HPRT ratio	.86 ± .16	1.38 ± .44	1.16 ± .19	1.94 ± .24
	Fold change vs. newborn	-	1.6 ↑	1.3 ↑	1.2 ↑
	Fold change vs. preceding age group	-	1.6 ↑	1.2 ↓	1.2 ↓

**Table 4.8:** TGF- $\beta$  mRNA expression values for heart and brain in comparison to kidney.

Gene		Newborn	1 month	3 months	18 months
Brain	TGF- $\beta$ /HPRT ratio	.26 $\pm$ .04	.22 $\pm$ .02	.18 $\pm$ .02	.20 $\pm$ .02
	Fold change vs. newborn	-	1.2 $\downarrow$	1.5 $\downarrow$	1.3 $\downarrow$
	Fold change vs. preceding age group	-	1.2 $\downarrow$	1.2 $\downarrow$	1.1 $\uparrow$
	Brain/kidney ratio	0.1	0.2	0.2	0.2
Heart	TGF- $\beta$ /HPRT ratio	1.28 $\pm$ .09	2.29 $\pm$ .19	2.51 $\pm$ .41	2.35 $\pm$ .14
	Fold change vs. newborn	-	1.8 $\uparrow$	2.0 $\uparrow$	1.8 $\uparrow$
	Fold change vs. preceding age group	-	1.8 $\uparrow$	1.1 $\uparrow$	1.1 $\downarrow$
	Heart/kidney ratio	0.7	2.1	2.7	2.3
Kidney	TGF- $\beta$ /HPRT ratio	1.92 $\pm$ .23	1.11 $\pm$ .11	.93 $\pm$ .17	1.03 $\pm$ .13
	Fold change vs. newborn	-	1.7 $\downarrow$	2.1 $\downarrow$	1.9 $\downarrow$
	Fold change vs. preceding age group	-	1.7 $\downarrow$	1.2 $\downarrow$	1.1 $\uparrow$

**Table 4.9:** PCNA mRNA expression values for heart and brain in comparison to kidney.

Gene		Newborn	1 month	3 months	18 months
Brain	PCNA/HPRT ratio	1.89 ± .40	.70 ± .08	.66 ± .13	.69 ± .08
	Fold change vs. newborn	-	2.7 ↓	2.9 ↓	2.7 ↓
	Fold change vs. preceding age group	-	2.7 ↓	1.0 =	1.0 =
	Brain/kidney ratio	0.5	0.6	0.7	0.7
Heart	PCNA/HPRT ratio	2.80 ± .25	1.19 ± .05	1.37 ± .08	1.37 ± .08
	Fold change vs. newborn	-	2.3 ↓	2.0 ↓	2.0 ↓
	Fold change vs. preceding age group	-	2.3 ↓	1.1 ↑	1.0 =
	Heart/kidney ratio	0.8	1.0	1.4	1.4
Kidney	PCNA/HPRT ratio	3.48 ± .45	1.20 ± .13	.98 ± .09	.97 ± .06
	Fold change vs. newborn	-	2.9 ↓	3.6 ↓	3.6 ↓
	Fold change vs. preceding age group	-	2.9 ↓	1.2 ↓	1.0 =



**Table 4.10:** HIC-5 mRNA expression values for heart and brain in comparison to kidney.

Gene		Newborn	1 month	3 months	18 months
Brain	HIC-5/HPRT ratio	2.81 ± .52	1.52 ± .56	1.31 ± .56	.94 ± .31
	Fold change vs. newborn	-	1.9 ↓	2.2 ↓	3.0 ↓
	Fold change vs. preceding age group	-	1.9 ↓	1.2 ↓	1.4 ↓
	Brain/kidney ratio	0.4	0.6	0.9	0.7
Heart	HIC-5/HPRT ratio	20.5 ± 2.4	6.8 ± .4	5.4 ± .9	5.6 ± .7
	Fold change vs. newborn	-	3.0 ↓	3.8 ↓	3.7 ↓
	Fold change vs. preceding age group	-	3.0 ↓	1.3 ↑	1.0 =
	Heart/kidney ratio	3.2	2.8	3.8	4.0
Kidney	HIC-5/HPRT ratio	6.50 ± .68	2.44 ± .30	1.39 ± .37	1.42 ± .16
	Fold change vs. newborn	-	2.7 ↓	4.7 ↓	4.6 ↓
	Fold change vs. preceding age group	-	2.7 ↓	1.7 ↓	1.0 =

**Table 4.11:** SMP30 mRNA expression values for heart and brain in comparison to kidney.

Gene		Newborn	1 month	3 months	18 months
Brain	SMP30/HPRT ratio	Not detectable	Not detectable	Not detectable	Not detectable
Heart	SMP30/HPRT ratio	.19 ± .05	.10 ± .02	.12 ± .03	.13 ± .04
	Fold change vs. newborn	-	2.0 ↓	1.6 ↓	1.4 ↓
	Fold change vs. preceding age group	-	2.0 ↓	1.2 ↑	1.1 ↑
	Heart/kidney ratio	0.2	0.1	0.1	0.1
Kidney	SMP30/HPRT ratio	.90 ± .28	.90 ± .17	1.14 ± .22	1.28 ± .15
	Fold change vs. newborn	-	1.0 =	1.3 ↑	1.4 ↑
	Fold change vs. preceding age group	-	1.0 =	1.3 ↑	1.1 ↑

**Table 4.12:** GADD45 mRNA expression values for heart and brain in comparison to kidney.

Gene		Newborn	1 month	3 months	18 months
Brain	GADD45/HPRT ratio	.12 ± .03	.20 ± .07	.19 ± .04	.16 ± .05
	Fold change vs. newborn	-	1.7 ↑	1.6 ↑	1.4 ↑
	Fold change vs. preceding age group	-	1.7 ↑	1.0 =	1.2 ↓
	Brain/kidney ratio	0.1	0.2	0.2	0.2
Heart	GADD45/HPRT ratio	.09 ± .01	.52 ± .06	.58 ± .09	.43 ± .06
	Fold change vs. newborn	-	5.8 ↑	6.4 ↑	4.8 ↑
	Fold change vs. preceding age group	-	5.8 ↑	1.1 ↑	1.3 ↓
	Heart/kidney ratio	0.1	0.5	0.6	0.5
Kidney	GADD45/HPRT ratio	1.0 ± .10	1.0 ± .07	.90 ± .13	.89 ± .06
	Fold change vs. newborn	-	1.0 =	1.1 ↓	1.1 ↓
	Fold change vs. preceding age group	-	1.0 =	1.1 ↓	1.0 =

**Table 4.13:** Predicted and actual changes for the candidate senescence genes. Predicted changes are based on the literature on cultured fibroblasts and actual changes are the changes seen in kidney, brain and heart.

Gene	Predicted change for aging	Kidney	Actual changes in Brain	Heart
P19 <sup>ARF</sup>	↑	D ↓; A ↑	D ↓	A ↑
MT1	↑	D ↓	D ↑	D ↑
MT3	↑	D ↑	D ↑	D ↓
Hsp70	↓	D ↑	M ↓	D ↑
TGF-β	↑	D ↓	-	D ↑
PCNA	↓	D ↓	D ↓	D ↓
HIC-5	↑	D ↓; M ↓	D ↓	D ↓
SMP30	↓	-	D ↓	D ↓
GADD45	↑	-	n.d.	D ↑; A ↓

D, development; M, maturation; A, aging; ↑, gene expression increased significantly during the indicated period; ↓, gene expression decreased significantly during the indicated period; -, no significant change occurred; n.d., not detectable

## 4.6 Figures

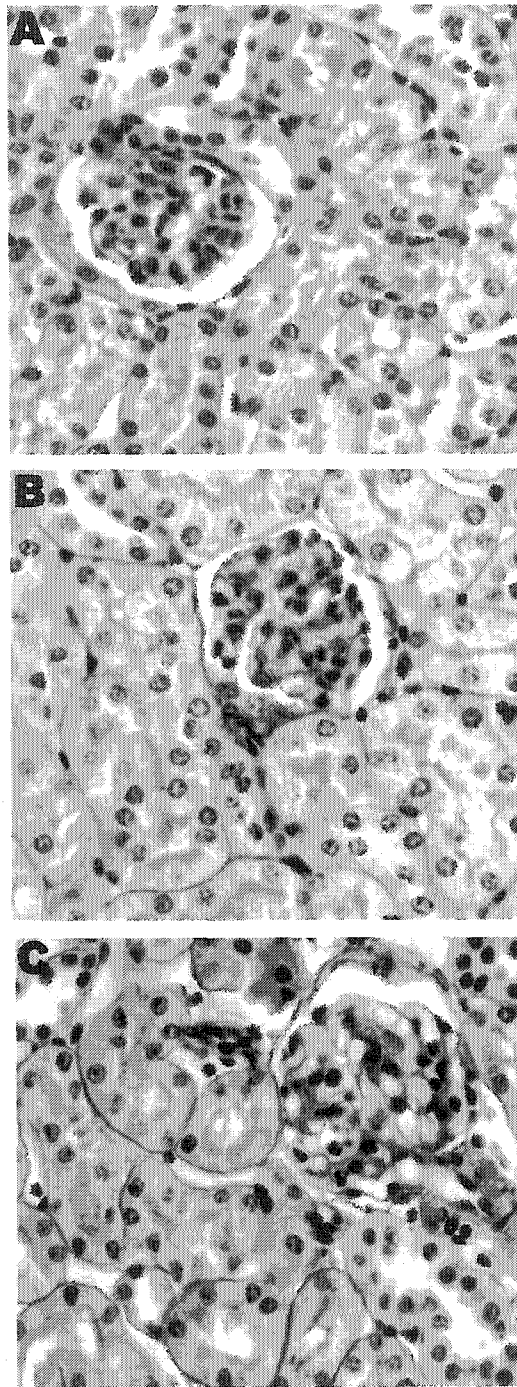


**Figure 4.1:** Representative kidney sections stained with PAS for 1 month (A), 3 months (B) and 18 months (C) old Balb/c mice. The morphological changes over time were rather mild. Glomerulosclerosis, tubular atrophy and interstitial fibrosis were not observed. 18 months kidneys showed slight mesangial hyperplasia.

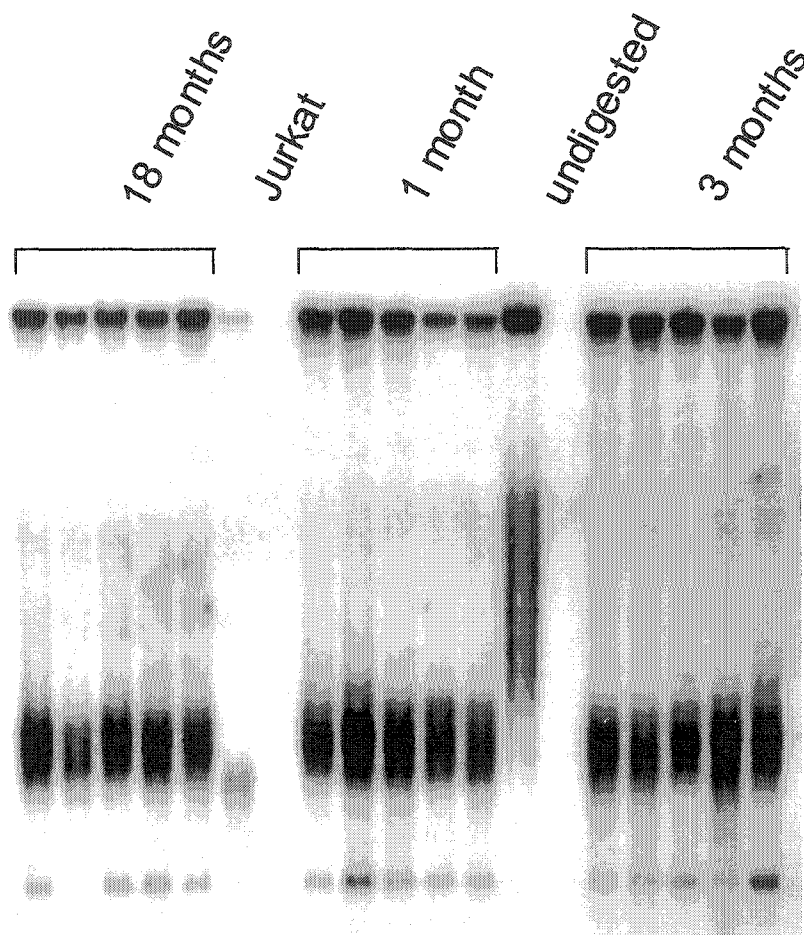


**Figure 4.2:** Representative TRF gel. High molecular weight DNA was isolated, resolved by pulse field gel electrophoresis. Hybridization with a telomere specific  $^{32}\text{P}$ -labeled oligonucleotide was performed and mean TRF length was calculated based on the signal intensity for each lane. Jurkat, Jurkat cell line; undigested, DNA sample not digested with *Hinf*I and *Rsa* I.

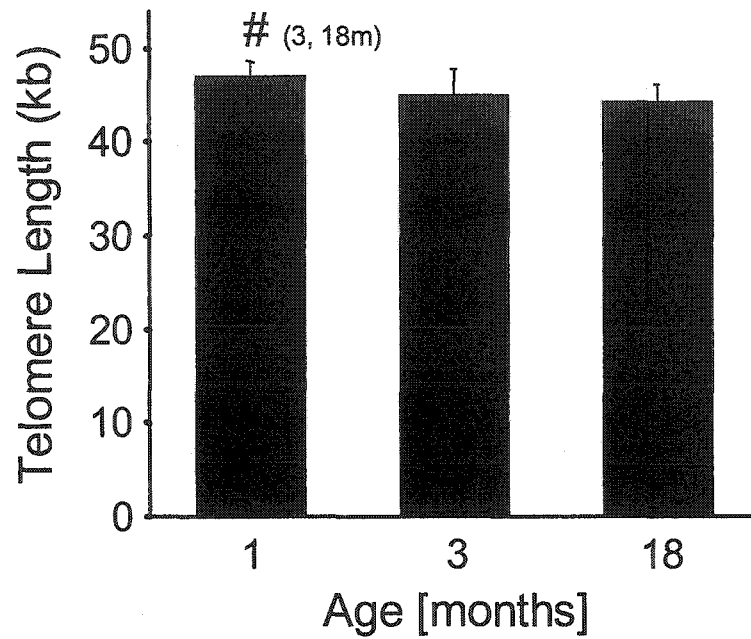


**Figure 4.3:** Mean telomere restriction fragment (TRF) length  $\pm$  SD of mean TRF length in mouse kidneys of three different age groups. High molecular weight DNA was isolated, resolved by pulse field gel electrophoresis. Hybridization with a telomere specific  $^{32}\text{P}$ -labeled oligonucleotide was performed and mean TRF length was calculated based on the signal intensity for each lane. #Significant difference ( $P < 0.05$ ) when compared to 3 or 18 months old mice, respectively.



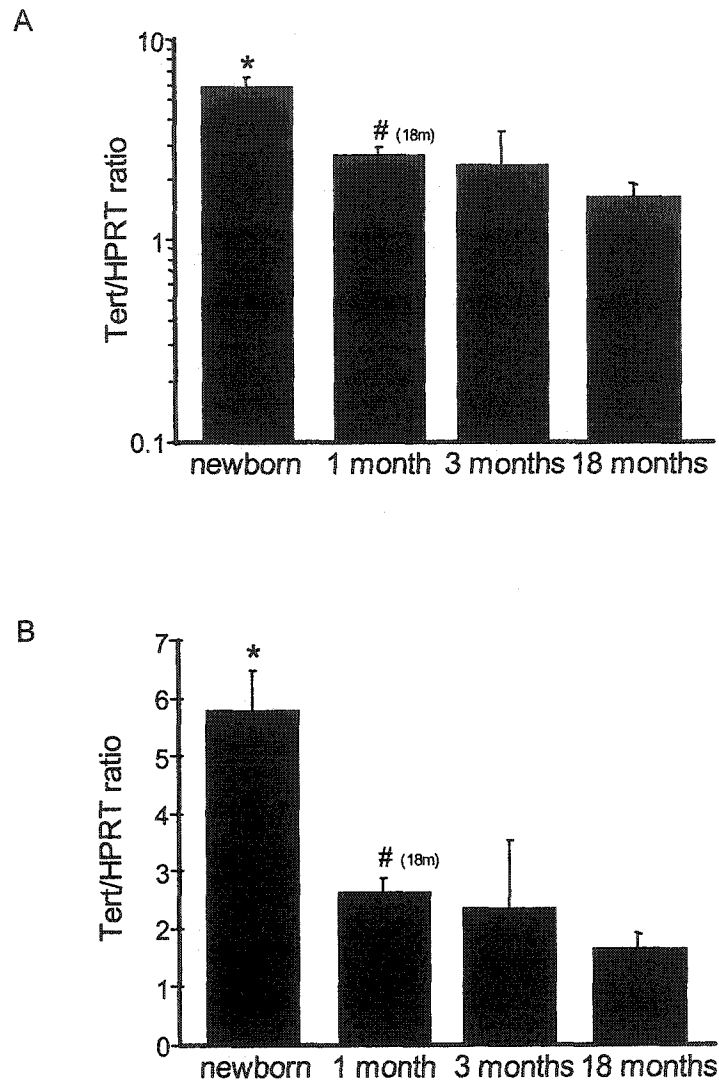


**Figure 4.4:** Tert mRNA expression in mouse kidneys of four different age groups. Values were normalized to HPRT and expressed as Tert/HPRT ratio on (A) a logarithmic scale and (B) a linear scale. RNA was isolated and reverse transcribed. Quantitative PCR was performed using sequence-specific primer and probe for p16<sup>INK4a</sup> on an ABI 7700 Sequence Detection System. \*Significant difference ( $P < 0.05$ ) compared to the other three groups and #significant difference ( $P < 0.05$ ) compared to 18 months old mice.

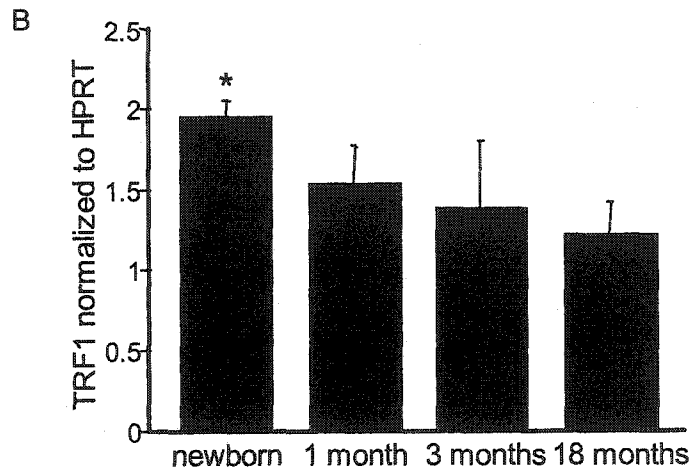
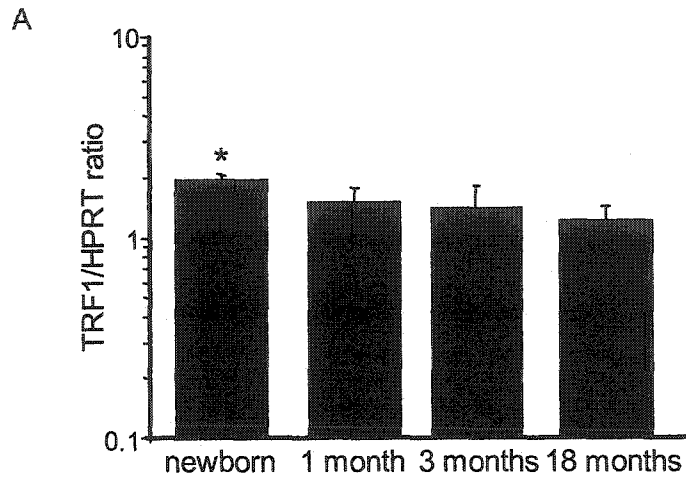


**Figure 4.5:** TRF1 mRNA expression in mouse kidneys of four different age groups. Values were normalized to HPRT and expressed as TRF1/HPRT ratio on (A) a logarithmic scale and (B) a linear scale. RNA was isolated and reverse transcribed. Quantitative PCR was performed using sequence-specific primer and probe for p16<sup>INK4a</sup> on an ABI 7700 Sequence Detection System. \*Significant difference ( $P < 0.05$ ) compared to the other three groups.

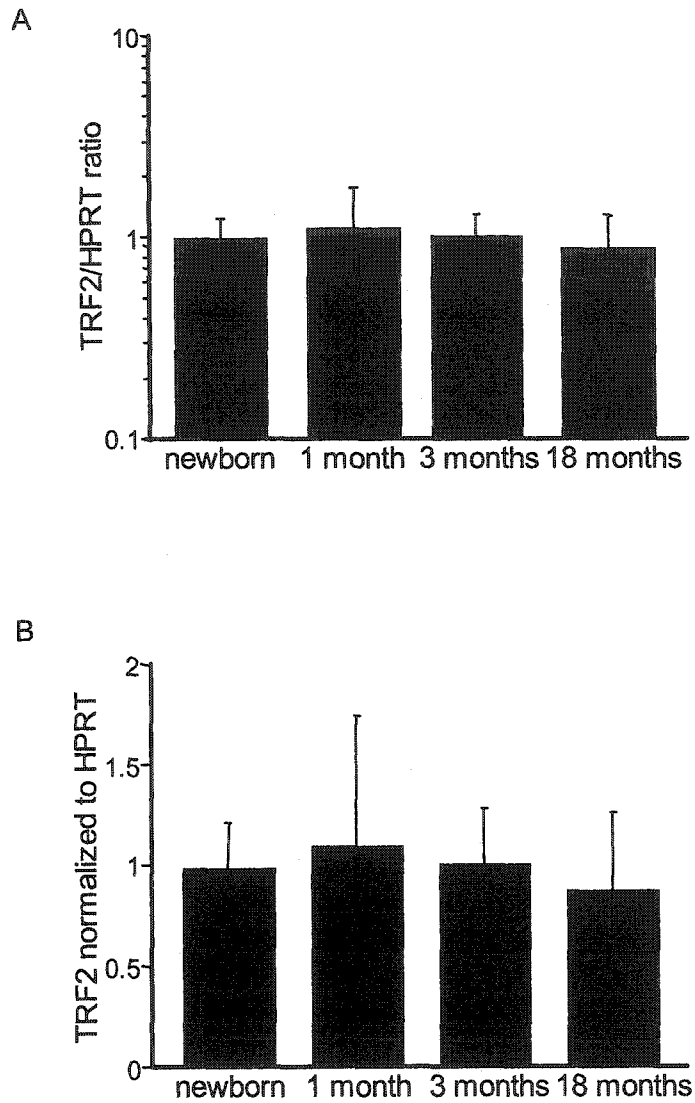


**Figure 4.6:** TRF2 mRNA expression in mouse kidneys of four different age groups. Values were normalized to HPRT and expressed as TRF2/HPRT ratio on (A) a logarithmic scale and (B) a linear scale. RNA was isolated and reverse transcribed. Quantitative PCR was performed using sequence-specific primer and probe for p16<sup>INK4a</sup> on an ABI 7700 Sequence Detection System.

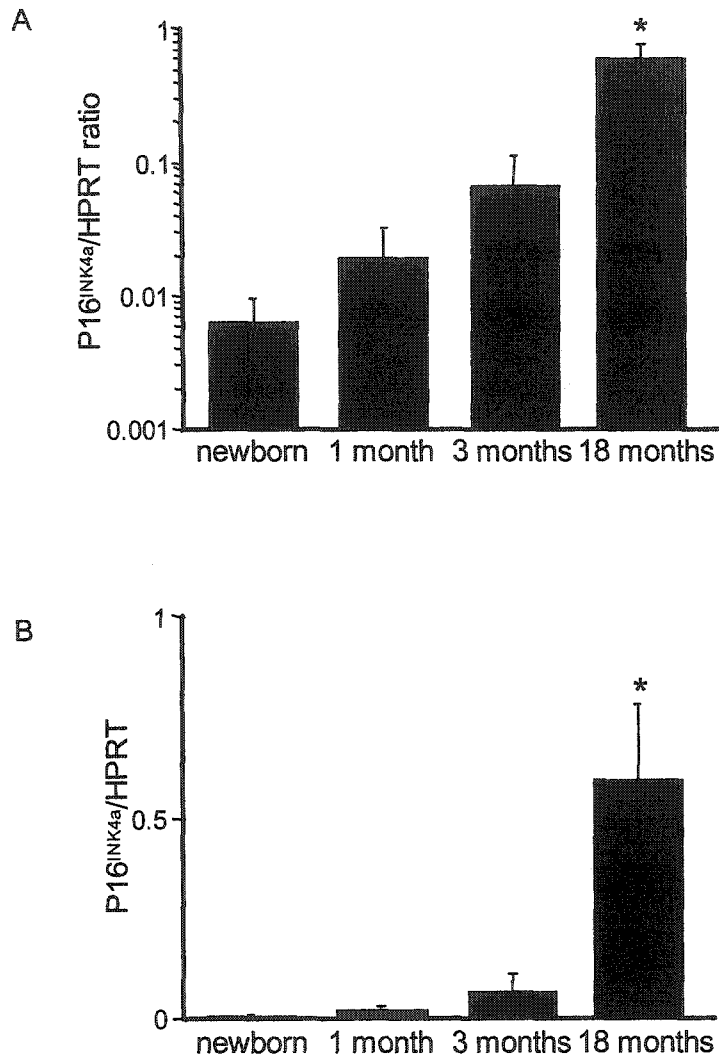


**Figure 4.7:** P16<sup>INK4a</sup> mRNA expression in mouse kidneys of four different age groups. Values were normalized to HPRT and expressed as p16<sup>INK4a</sup>/HPRT ratio on (A) a logarithmic scale and (B) a linear scale. RNA was isolated and reverse transcribed. Quantitative PCR was performed using sequence-specific primer and probe for p16<sup>INK4a</sup> on an ABI 7700 Sequence Detection System. \*Significant difference ( $P < 0.001$ ) compared to the other three groups. The differences for development and maturation were significant when tested with individual T-tests (newborn vs. 1 months:  $p = .031$ ; 1 vs. 3 months:  $p = .04$ ), but were no longer significant after correction for multiple testing.

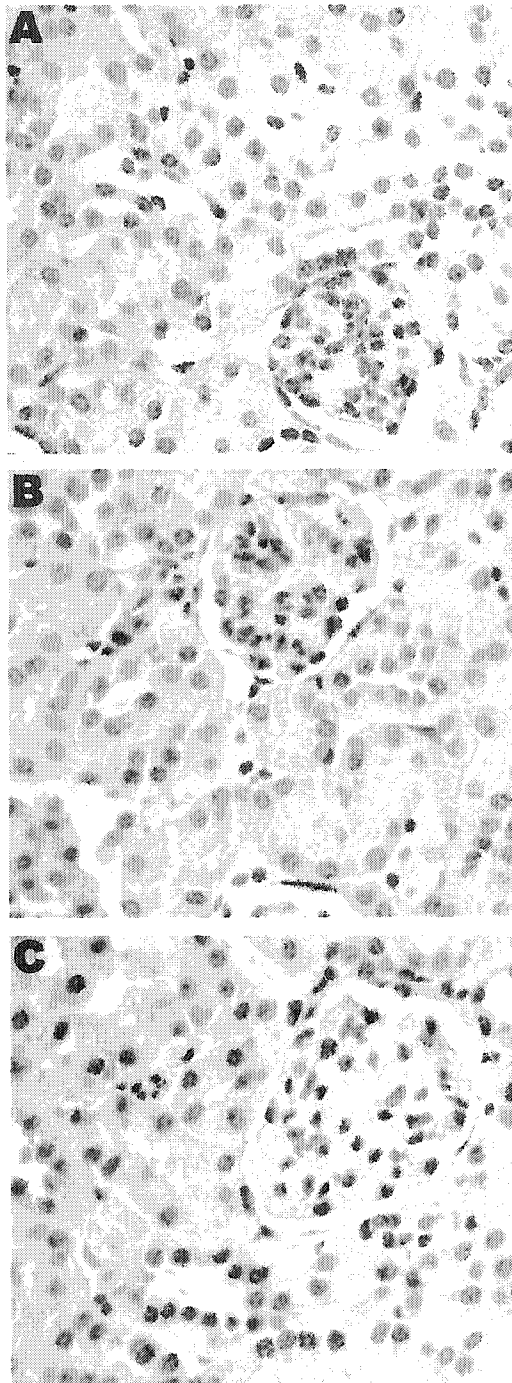


**Figure 4.8:** Representative kidney sections stained for p16<sup>INK4a</sup> and counterstained with hematoxylin for 1 month (A), 3 months (B) and 18 months (C) old Balb/c mice. Nuclear p16<sup>INK4a</sup> staining was not found in 1 month, very rarely found in 3 months, but was present in all 18 months old mouse kidneys. Staining was found mainly in tubular cells, but was also detected in glomeruli, interstitium and vasculature.

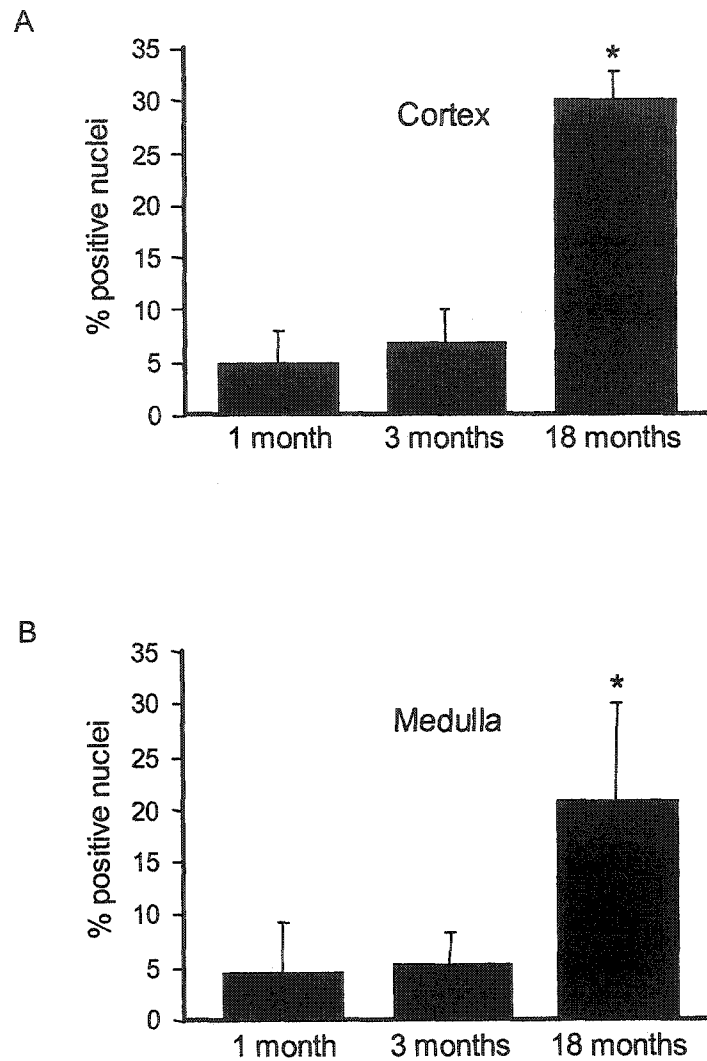


**Figure 4.9:** P16<sup>INK4a</sup> protein expression in tubular cells in mouse kidney. (A) Cortex and (B) Medulla. P16<sup>INK4a</sup> was detected by immunoperoxidase staining using a monoclonal antibody. Values are expressed as percentage of positive nuclei for tubular cells. \*Significant difference ( $P < 0.01$ ) compared to the other two groups.

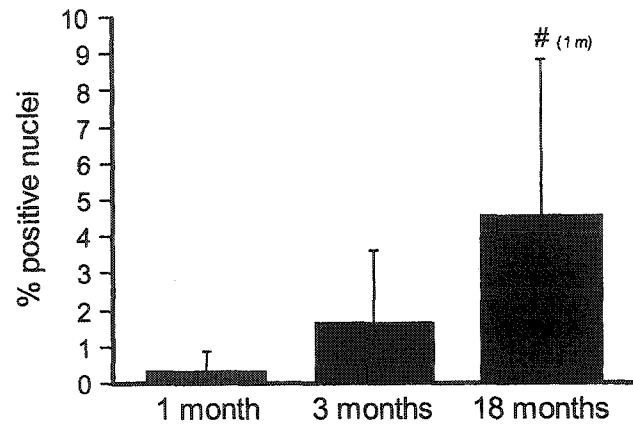


**Figure 4.10:** P16<sup>INK4a</sup> protein expression in glomeruli of mouse kidney. P16<sup>INK4a</sup> was detected by immunoperoxidase staining using a monoclonal antibody. Values are expressed as percentage of positive nuclei for glomeruli. #Significant difference ( $P < 0.05$ ) compared to 1 month old mice.

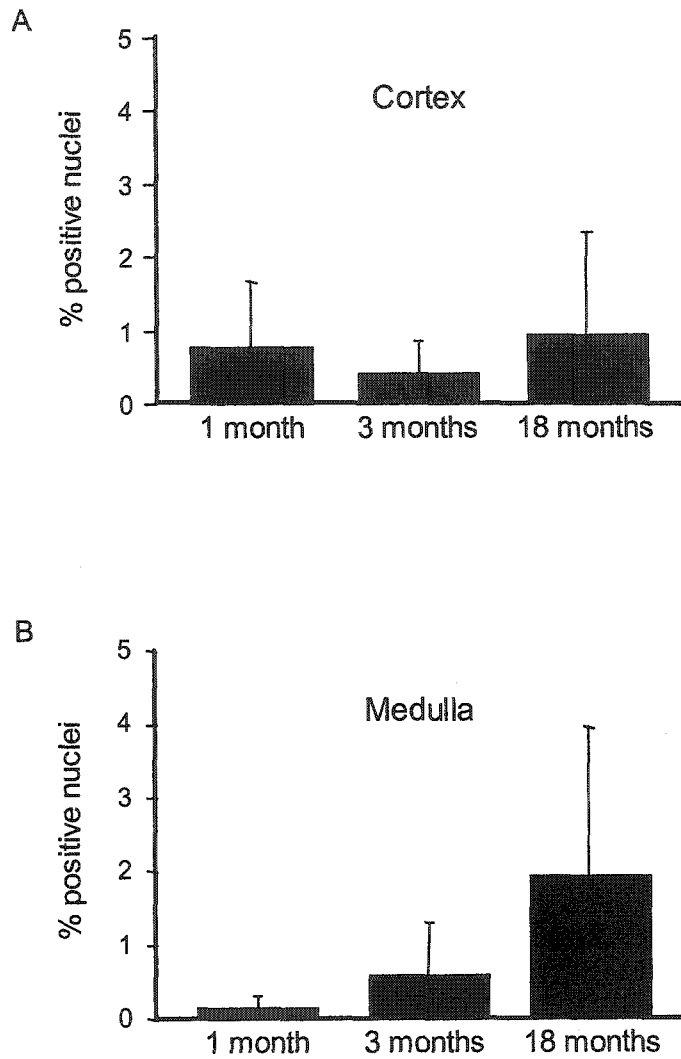


**Figure 4.11:** P16<sup>INK4a</sup> protein expression in interstitial cells of mouse kidney. (A) Cortex and (B) Medulla. P16<sup>INK4a</sup> was detected by immunoperoxidase staining using a monoclonal antibody. Values are expressed as percentage of positive nuclei for interstitial cells.



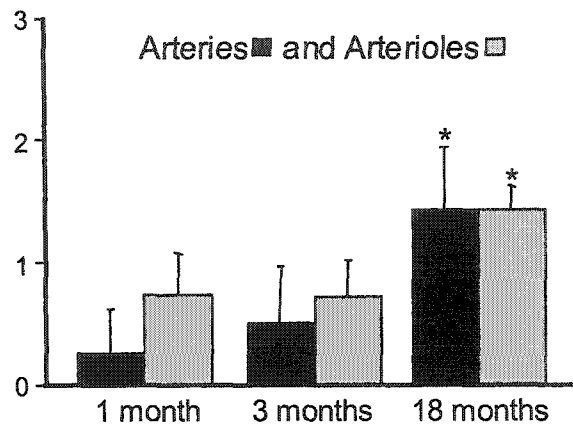


**Figure 4.12:** P16<sup>INK4a</sup> protein expression in arteries and arterioles in mouse kidney. P16<sup>INK4a</sup> was detected by immunoperoxidase staining using a monoclonal antibody. Values are expressed as a score based on the percentage of positive nuclei in arteries and arterioles. Arteries and arterioles were graded on a scale from 0 to 3 (0 = no staining of smooth muscle cells, 1 = up to 30% stained nuclei, 2 = 30-60% stained nuclei, 3 = >60% stained nuclei), the whole section was scored and a mean score was calculated. \*Significant difference ( $P < 0.01$ ) compared to the other two groups.

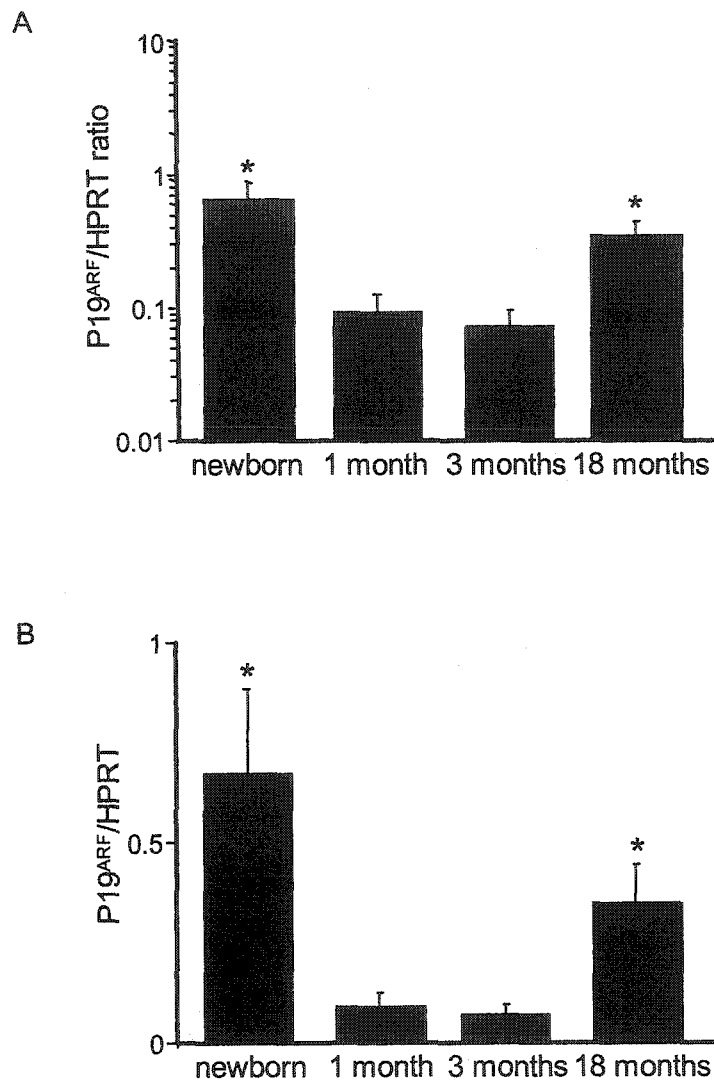


**Figure 4.13:** P19<sup>ARF</sup> mRNA expression in mouse kidneys of four different age groups. P19<sup>ARF</sup> shows a “U” shape pattern with highest values in newborns and 18 months old mice. Values were normalized to HPRT and expressed as p19<sup>ARF</sup>/HPRT ratio on (A) a logarithmic scale and (B) a linear scale. \*Significant difference (P<0.05) compared to the other three groups.

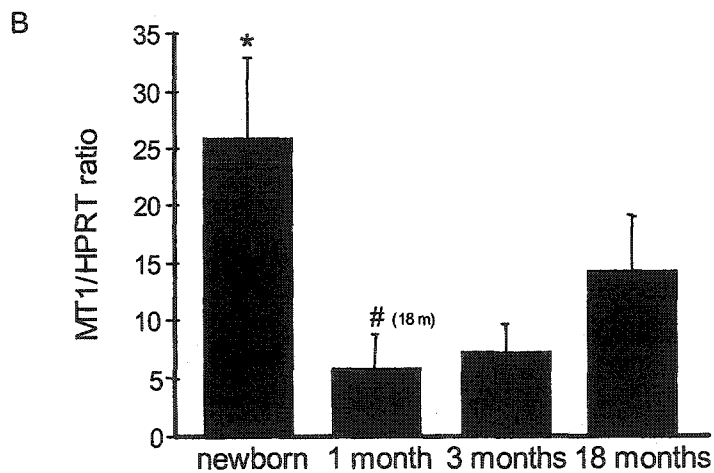
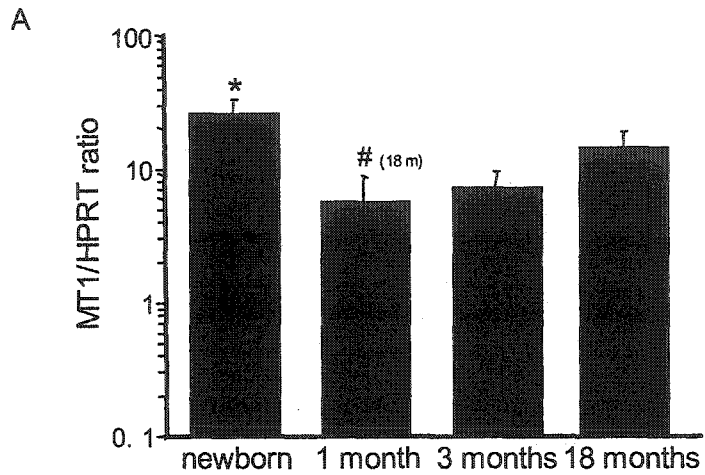


**Figure 4.14:** MT1 mRNA expression in mouse kidneys of four different age groups. MT1 shows a “U” shape pattern with highest values in newborns and 18 months old mice. Values were normalized to HPRT and expressed as MT1/HPRT ratio on (A) a logarithmic scale and (B) a linear scale. \*Significant difference ( $P < 0.05$ ) compared to the other three groups and #significant difference ( $P < 0.05$ ) compared to 18 months old mice.

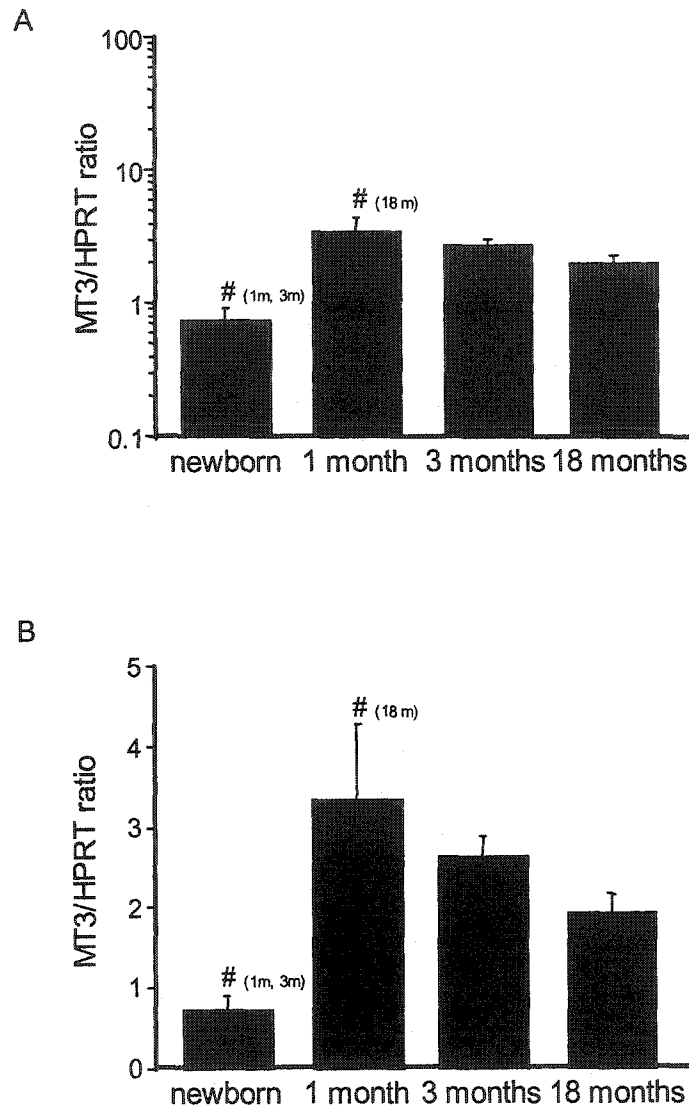


**Figure 4.15:** MT3 mRNA expression in mouse kidneys of four different age groups. MT3 shows a reciprocal “U” shape with highest expression levels at 1 months. Values were normalized to HPRT and expressed as MT3/HPRT ratio on (A) a logarithmic scale and (B) a linear scale. #Significant difference ( $P < 0.05$ ) compared to the group indicated in brackets.

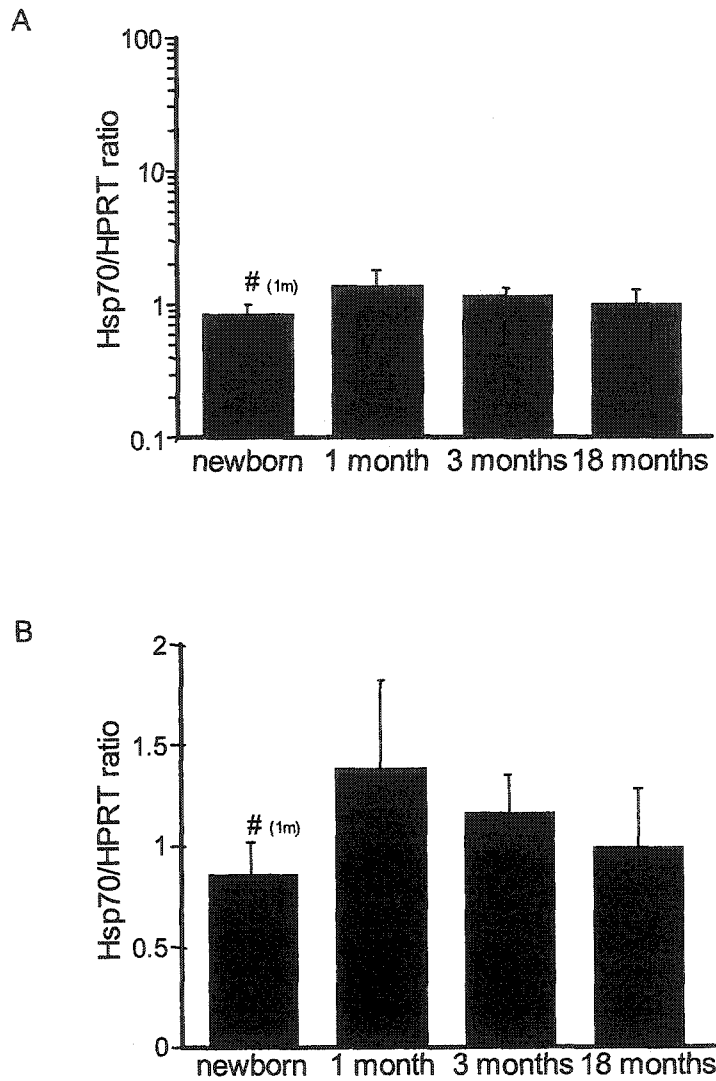


**Figure 4.16:** Hsp70 mRNA expression in mouse kidneys of four different age groups. Hsp70 shows a reciprocal “U” shape with highest expression levels at 1 months. Values were normalized to HPRT and expressed as Hsp70/HPRT ratio on (A) a logarithmic scale and (B) a linear scale. #Significant difference ( $P < 0.05$ ) compared to 1 month old mice.

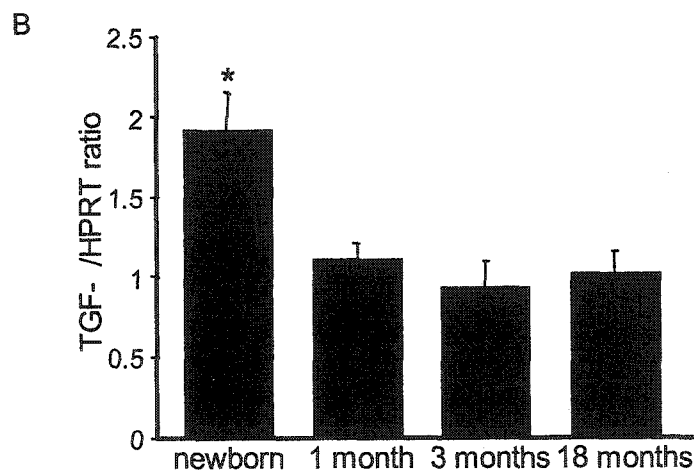
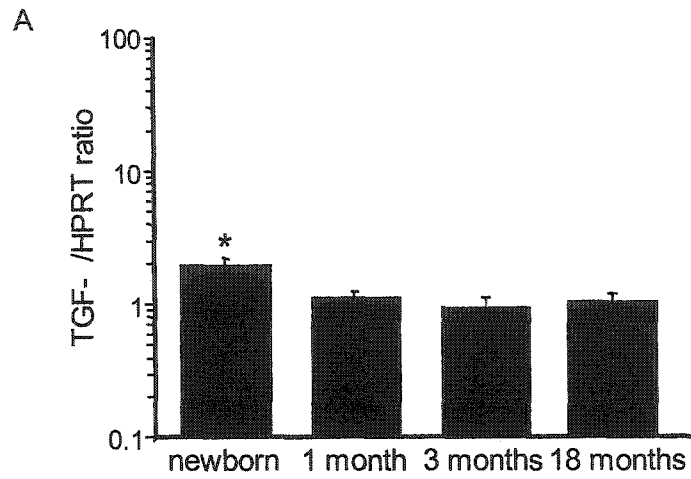


**Figure 4.17:** TGF- $\beta$  mRNA expression in mouse kidneys of four different age groups. TGF- $\beta$  decreases with age. Values were normalized to HPRT and expressed as TGF- $\beta$ /HPRT ratio on (A) a logarithmic scale and (B) a linear scale. \*Significant difference ( $P < 0.05$ ) compared to the other three groups.

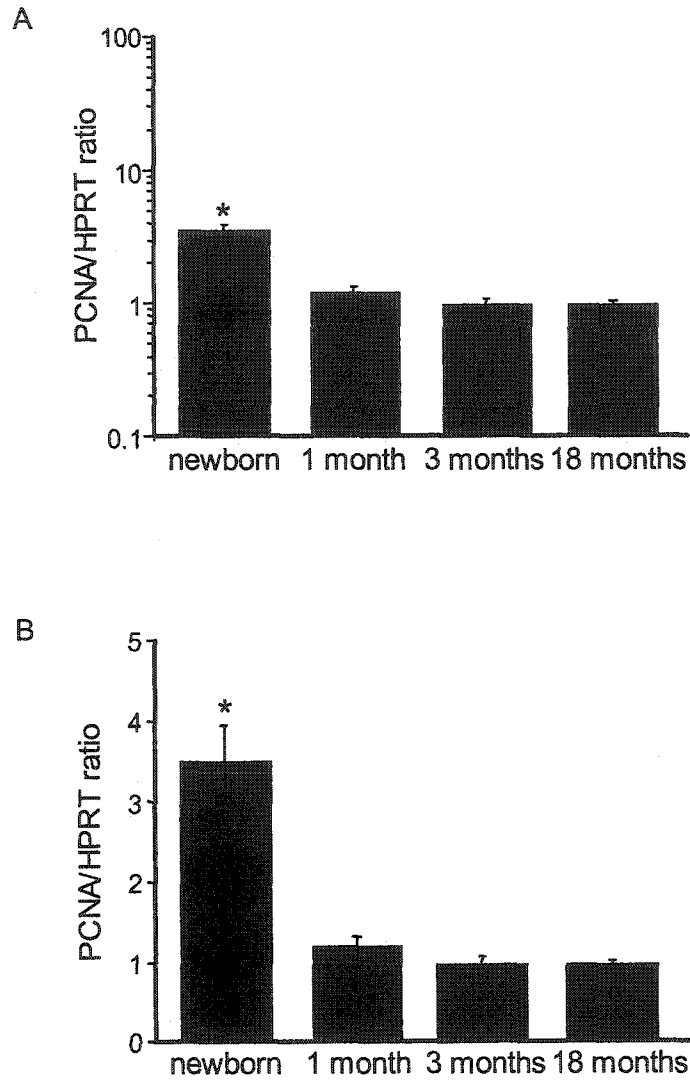


**Figure 4.18:** PCNA mRNA expression in mouse kidneys of four different age groups. PCNA decreases with age. Values were normalized to HPRT and expressed as PCNA/HPRT ratio on (A) a logarithmic scale and (B) a linear scale. \*Significant difference ( $P < 0.05$ ) compared to the other three groups.

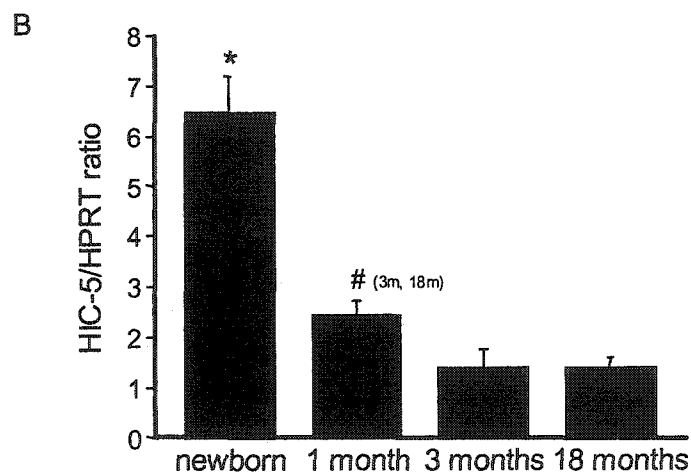
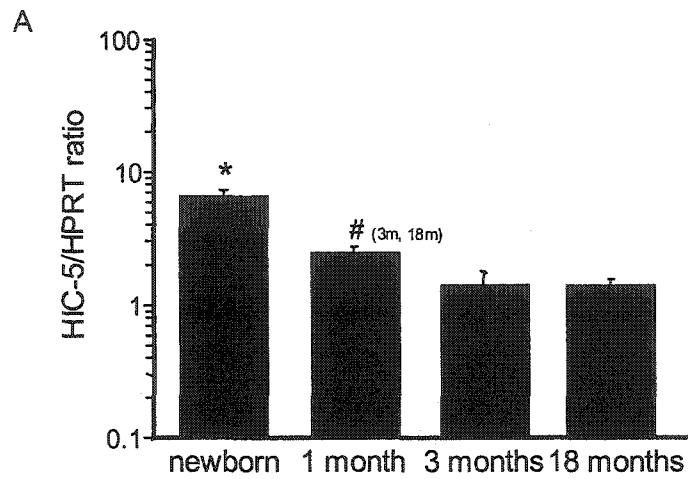


**Figure 4.19:** HIC-5 mRNA expression in mouse kidneys of four different age groups. HIC-5 decreases with age. Values were normalized to HPRT and expressed as HIC-5/HPRT ratio on (A) a logarithmic scale and (B) a linear scale. \*Significant difference ( $P < 0.05$ ) compared to the other three groups and #significant difference ( $P < 0.05$ ) compared to 3 and 18 months old mice.



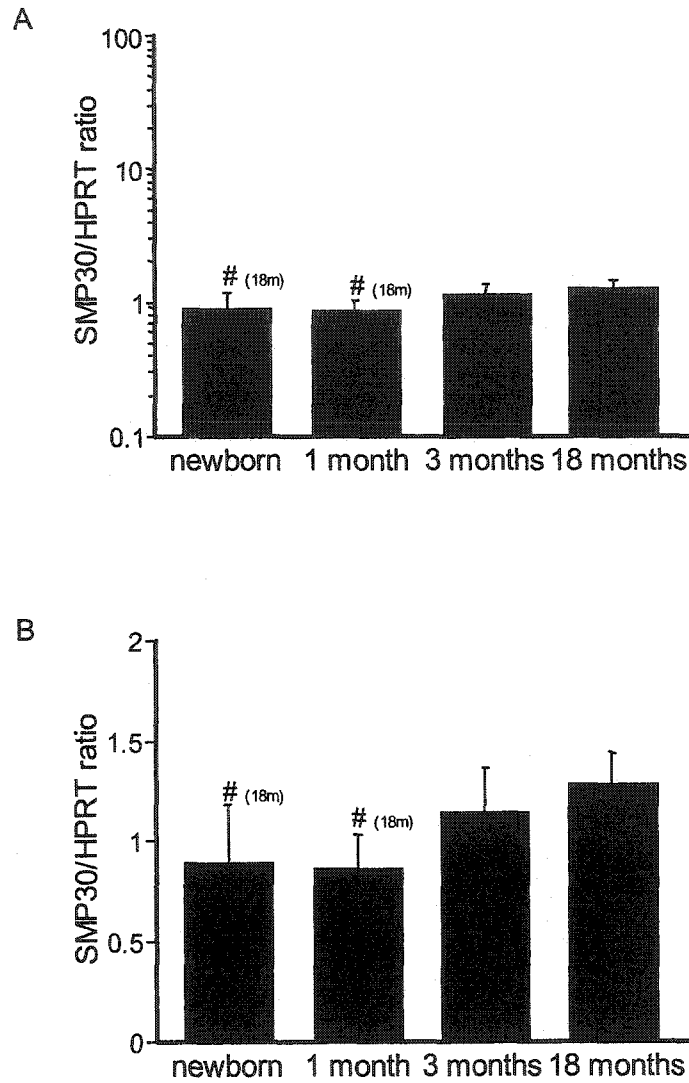


**Figure 4.20:** SMP30 mRNA expression in mouse kidneys of four different age groups. SMP30 stayed basically unchanged. Values were normalized to HPRT and expressed as SMP30/HPRT ratio on (A) a logarithmic scale and (B) a linear scale. #Significant difference ( $P < 0.05$ ) compared to the group indicated in brackets.

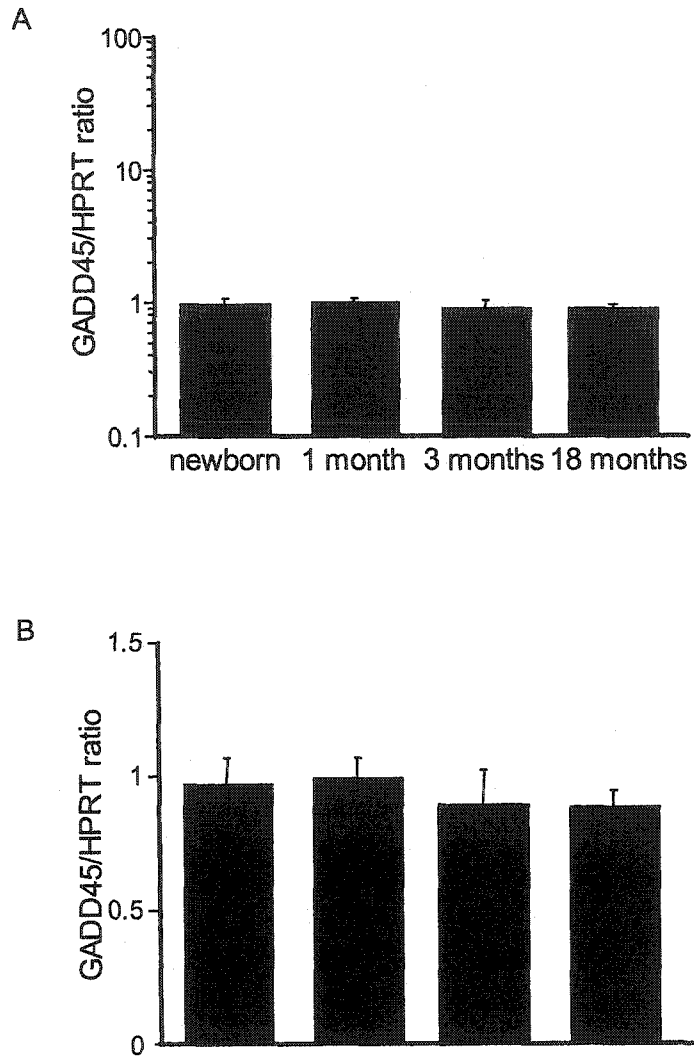


**Figure 4.21:** GADD45 mRNA expression in mouse kidneys of four different age groups. GADD45 stayed basically unchanged. Values were normalized to HPRT and expressed as GADD45/HPRT ratio on (A) a logarithmic scale and (B) a linear scale.

#### 4.7 References

1. Levi M and Rowe JW: Aging and the kidney. *Diseases of the Kidney*. Edited by Schrier RW and Gottschalk CW. Boston, MA, Little, Brown, and Company, 1993, pp. 2405-2432
2. Pannu N and Halloran PF: The kidney in aging. *Primer on Kidney Diseases*. Edited by Greenberg A. San Diego, CA, Academic Press, 2001, pp. 377-381
3. Sedivy JM: Can ends justify the means?: telomeres and the mechanisms of replicative senescence and immortalization in mammalian cells [review]. *Proc Natl Acad Sci USA* 1998, 95: 9078-9081
4. Hayflick L and Moorhead PS: The serial cultivation of human diploid cell strains. *Exp Cell Res* 1961, 25: 585-621
5. Olovnikov AM: Telomeres, telomerase, and aging: origin of the theory. *Exp Geront* 1996, 31: 443-448
6. Harley CB, Futcher AB, and Greider CW: Telomeres shorten during ageing of human fibroblasts. *Nature* 1990, 345: 458-460
7. Blackburn EH: Telomere states and cell fates. *Nature* 2000, 408: 53-56
8. Karlseder J, Smogorzewska A, and de Lange T: Senescence induced by altered telomere state, not telomere loss. *Science* 2002, 295: 2446-2449
9. Sherr CJ and DePinho RA: Cellular senescence: mitotic clock or culture shock? *Cell* 2000, 102: 407-410
10. Wright WE and Shay JW: Telomere dynamics in cancer progression and prevention: fundamental differences in human and mouse telomere biology. *Nature Medicine* 2000, 6: 849-851
11. Wright WE and Shay JW: Historical claims and current interpretations of replicative aging. *Nature Biotechnology* 2002, 20: 682-688
12. Ishino K, Kaneyama JRK, Shibamura M, and Nose K: Specific decrease in the level of Hic-5, a focal adhesion protein, during immortalization of mouse embryonic fibroblasts, and its association with focal adhesion kinase. *Journal of Cellular Biochemistry* 2000, 76: 411-419
13. Cristofalo VJ and Pignolo RJ: Replicative senescence of human fibroblast-like cells in culture. *Physiol Rev* 1993, 73: 617-638
14. Dimri GP, Lee X, Basile G, Acosta M, Scott G, Roskelley C, Medrano EE, Linskens M, Rubelj I, Pereira-Smith O, Peacocke M, and Campisi J: A

biomarker that identifies senescent human cells in culture and in aging skin *in vivo*. Proc Natl Acad Sci USA 1995, 92: 9363-9367

15. Terman A and Brunk UT: Lipofuscin: mechanisms of formation and increase with age. APMIS 1998, 106: 265-276
16. Serrano M, Lee H-W, Chin L, Cordon-Cardo C, Beach D, and DePinho RA: Role of the INK4a locus in tumor suppressor and cell mortality. Cell 1996, 85: 27-37
17. Zindy F, Quelle DE, Roussel MF, and Sherr CJ: Expression of the p16INK4a tumor suppressor versus other INK4 family members during mouse development and aging. Oncogene 1997, 15: 203-211
18. Kim H, You S, Farris J, Kong BW, Christman SA, Foster LK, and Foster DN: Expression profiles of p53-, p16(INK4a)-, and telomere-regulating genes in replicative senescent primary human, mouse, and chicken fibroblast cells. Exp Cell Res 2002, 272: 199-208
19. Harvey DM and Levine AJ: p53 alteration is a common event in the spontaneous immortalization of primary BALB/c murine embryo fibroblasts. Genes Dev 1991, 5: 2375-2385
20. Shay JW, Pereira-Smith OM, and Wright WE: A role for both RB and p53 in the regulation of human cellular senescence. Exp Cell Res 1991, 196: 33-39
21. Tremain R, Marko M, Kinnimulki V, Ueno H, Bottinger E, and Glick A: Defects in TGF beta signaling overcome senescence of mouse keratinocytes expressing v-ras(Ha). Oncogene 2000, 19: 1698-1709
22. Sorrentino V and Bandyopadhyay S: Tgf-Beta Inhibits Go/S-Phase Transition in Primary Fibroblasts - Loss of Response to the Antigrowth Effect of Tgf-Beta Is Observed After Immortalization. Oncogene 1989, 4: 569-574
23. Luce MC, Schyberg JP, and Bunn CL: Metallothionein Expression and Stress Responses in Aging Human-Diploid Fibroblasts. Exp Geront 1993, 28: 17-38
24. Chang CD, Phillips P, Lipson KE, Cristofalo VJ, and Baserga R: Senescent human fibroblasts have a post-transcriptional block in the expression of the proliferating cell nuclear antigen gene. J Biol Chem 1991, 266: 8663-8666
25. Luce MC and Cristofalo VJ: Reduction in heat shock gene expression correlates with increased thermosensitivity in senescent human fibroblasts. Exp Cell Res 1992, 202: 9-16

26. Fargnoli J, Kunisada T, Fornace AJ, Schneider EL, and Holbrook NJ: Decreased Expression of Heat-Shock Protein-70 Messenger-Rna and Protein After Heat-Treatment in Cells of Aged Rats. *Proceedings of the National Academy of Sciences of the United States of America* 1990, 87: 846-850
27. Chen Q, Fischer A, Reagan JD, Yan L-J, and Ames BN: Oxidative DNA damage and senescence of human diploid fibroblast cells. *Proc Natl Acad Sci USA* 1995, 92: 4337-4341
28. von Zglinicki T, Saretzki G, Döcke W, and Lotze C: Mild hyperoxia shortens telomeres and inhibits proliferation of fibroblasts: a model for senescence? *Exp Cell Res* 1995, 220: 186-193
29. Shibanuma M, Mochizuki E, Maniwa R, Mashimo J, Nishiya N, Imai S, Takano T, Oshimura M, and Nose K: Induction of senescence-like phenotypes by forced expression of hic-5, which encodes a novel LIM motif protein, in immortalized human fibroblasts. *Mol Cell Biol* 1997, 17: 1224-1235
30. Dileonardo A, Linke SP, Clarkin K, and Wahl GM: Dna-Damage Triggers A Prolonged P53-Dependent G(1) Arrest and Long-Term Induction of Cip1 in Normal Human Fibroblasts. *Genes & Development* 1994, 8: 2540-2551
31. Waterston RH, Lindblad-Toh K, Birney E, Rogers J, Abril JF, Agarwal P, Agarwala R, Ainscough R, Alexandersson M, An P, Antonarakis SE, Attwood J, Baertsch R, Bailey J, Barlow K, Beck S, Berry E, Birren B, Bloom T, Bork P, Botcherby M, Bray N, Brent MR, Brown DG, Brown SD, Bult C, Burton J, Butler J, Campbell RD, Carninci P, Cawley S, Chiaromonte F, Chinwalla AT, Church DM, Clamp M, Clee C, Collins FS, Cook LL, Copley RR, Coulson A, Couronne O, Cuff J, Curwen V, Cutts T, Daly M, David R, Davies J, Delehaunty KD, Deri J, Dermitzakis ET, Dewey C, Dickens NJ, Diekhans M, Dodge S, Dubchak I, Dunn DM, Eddy SR, Elnitski L, Emes RD, Eswara P, Eyraas E, Felsenfeld A, Fewell GA, Flicek P, Foley K, Frankel WN, Fulton LA, Fulton RS, Furey TS, Gage D, Gibbs RA, Glusman G, Gnerre S, Goldman N, Goodstadt L, Grafham D, Graves TA, Green ED, Gregory S, Guigo R, Guyer M, Hardison RC, Haussler D, Hayashizaki Y, Hillier LW, Hinrichs A, Hlavina W, Holzer T, Hsu F, Hua A, Hubbard T, Hunt A, Jackson I, Jaffe DB, Johnson LS, Jones M, Jones TA, Joy A, Kamal M, Karlsson EK, Karolchik D, Kasprzyk A, Kawai J, Keibler E, Kells C, Kent WJ, Kirby A, Kolbe DL, Korf I, Kucherlapati RS, Kulbokas EJ, Kulp D, Landers T, Leger JP, Leonard S, Letunic I, Levine R, Li J, Li M, Lloyd C, Lucas S, Ma B, Maglott DR, Mardis ER, Matthews L, Mauceli E, Mayer JH, McCarthy M, McCombie WR, McLaren S, McLay K, McPherson JD, Meldrim J, Meredith B, Mesirov JP, Miller W, Miner TL, Mongin E, Montgomery KT, Morgan M, Mott R, Mullikin JC, Muzny DM, Nash WE, Nelson JO, Nhan MN, Nicol R, Ning Z, Nusbaum C, O'Connor MJ, Okazaki Y, Oliver K, Larty EO, Pachter L, Parra G, Pepin KH, Peterson J, Pevzner P, Plumb R, Pohl CS, Poliakov A,

Ponce TC, Ponting CP, Potter S, Quail M, Reymond A, Roe BA, Roskin KM, Rubin EM, Rust AG, Santos R, Sapojnikov V, Schultz B, Schultz J, Schwartz MS, Schwartz S, Scott C, Seaman S, Searle S, Sharpe T, Sheridan A, Shownkeen R, Sims S, Singer JB, Slater G, Smit A, Smith DR, Spencer B, Stabenau A, Strange-Thomann NS, Sugnet C, Suyama M, Tesler G, Thompson J, Torrents D, Trevaskis E, Tromp J, Ucla C, Vidal AU, Vinson JP, Von Niederhausern AC, Wade CM, Wall M, Weber RJ, Weiss RB, Wendl MC, West AP, Wetterstrand K, Wheeler R, Whelan S, Wierzbowski J, Willey D, Williams S, Wilson RK, Winter E, Worley KC, Wyman D, Yang S, Yang SP, Zdobnov EM, Zody MC, and Lander ES: Initial sequencing and comparative analysis of the mouse genome. *Nature* 2002, 420: 520-562

32. Lindeman RD and Goldman R: Anatomic and physiologic age changes in the kidney. *Exp Geront* 1986, 21: 379-406
33. Gourtsoyiannis N, Prassopoulos P, Cavouras D, and Pantelidis N: The thickness of the renal parenchyma decreases with age. A CT study of 360 patients. *Am J Roentgenol* 1990, 155: 541-544
34. Shimkin MB, Shimkin PM, and Andervont HB: Effect of estrogens on kidney weight in mice. *J Natl Cancer Inst* 1963, 30: 135-141
35. Thung PJ: Physiological proteinuria in mice. *Acta Physiol Pharmacol* 1961, 10: 248-261
36. Halloran PF, Jephthah-Ochola J, Urmson J, and Farkas S: Systemic immunologic stimuli increase class I and II antigen expression in mouse kidney. *J Immunol* 1985, 135: 1053-1060
37. Kirschbaum, A. Spontaneous glomerulonephritis in mice. *Proceedings of the Society for Experimental Biology and Medicine* 55, 280-281. 1944.
38. Taylor DM and Fraser H: Hydronephrosis in inbred strains of mice with particular reference to the BRVR strain. *Lab Anim* 1973, 7: 229-236
39. Snell KC: Renal disease of the rat. *Pathology of laboratory rats and mice*. Edited by Cotchin E and Roe FJC. London, Blackwell Scientific Publications, 1967, pp. 105-147
40. Dunn TB: Renal disease of the mouse. *Pathology of laboratory rats and mice*. Edited by Cotchin E and Roe FJC. London, Blackwell Scientific Publications, 1967, pp. 149-179
41. Melk A, Ramassar V, Helms LM, Moore R, Rayner D, Solez K, and Halloran PF: Telomere shortening in kidneys with age. *J Am Soc Nephrol* 2000, 11: 444-453

42. Blackburn EH: Switching and signaling at the telomere. *Cell* 2001, 106: 661-673
43. Fujita T, Shirasawa T, and Maruyama N: Isolation and characterization of genomic and cDNA clones encoding mouse senescence marker protein-30 (SMP30). *Biochimica et Biophysica Acta-Gene Structure and Expression* 1996, 1308: 49-57
44. von Schnakenburg C, Strehlau J, Ehrich JH, and Melk A: Quantitative gene expression of TGF-beta1, IL-10, TNF-alpha and Fas Ligand in renal cortex and medulla. *Nephrol Dial Transplant* 2002, 17: 573-579
45. Melk A, Kittikowit W, Sandhu I, Halloran KM, Grimm P, Schmidt BMW, and Halloran PF: Cell senescence in rat kidney in vivo increases with growth and age despite lack of telomere shortening. *Kidney Int* 2003, 63: 2134-2143
46. Starling JA, Maule J, Hastie ND, and Allshire RC: Extensive telomere repeat arrays in mouse are hypervariable. *Nucleic Acids Res* 1990, 18: 6881-6888
47. Prowse KR and Greider CW: Developmental and tissue-specific regulation of mouse telomerase and telomere length. *Proc Natl Acad Sci USA* 1995, 92: 4818-4822
48. Rudolph KL, Chang S, Millard M, Schreiber-Agus N, and DePinho RA: Inhibition of experimental liver cirrhosis in mice by telomerase gene delivery. *Science* 2000, 287: 1253-1258
49. Ruiz-Torres, M. P., Perez-Rivero, G., Franco, S., Blasco, M. A., Diez-Marques, M. L., and Rodriguez-Puyol, D. Role of telomere shortening in renal function. The importance of oxidative damage. *Journal of the American Society of Nephrology* 13, 163A. 2002.
50. Carnero A, Hudson JD, Price CM, and Beach DH: p16(INK4A) and p19(ARF) act in overlapping pathways in cellular immortalization. *Nature Cell Biology* 2000, 2: 148-155
51. Wei W, Hemmer RM, and Sedivy JM: Role of p14(ARF) in replicative and induced senescence of human fibroblasts. *Mol Cell Biol* 2001, 21: 6748-6757
52. Weinberg RA: The retinoblastoma protein and cell cycle control. *Cell* 1995, 81: 323-330
53. Koh J, Enders GH, Dynlacht BD, and Harlow E: Tumour-derived p16 alleles encoding proteins defective in cell-cycle inhibition. *Nature* 1995, 375: 506-510

54. Lukas J, Parry D, Aagaard L, Mann DJ, Bartkova J, Strauss M, Peters G, and Bartek J: Retinoblastoma-protein-dependent cell-cycle inhibition by the tumour suppressor p16. *Nature* 1995, 375: 503-506
55. Sharpless NE, Bardeesy N, Lee KH, Carrasco D, Castrillon DH, Aguirre AJ, Wu EA, Horner JW, and DePinho RA: Loss of p16Ink4a with retention of p19Arf predisposes mice to tumorigenesis. *Nature* 2001, 413: 86-91
56. Krimpenfort P, Quon KC, Mooi WJ, Loonstra A, and Berns A: Loss of p16Ink4a confers susceptibility to metastatic melanoma in mice. *Nature* 2001, 413: 83-86



Chapter 5  
Expression of p16<sup>INK4a</sup> and Other Cell Cycle Regulator  
and Senescence Associated Genes  
in Aging Human Kidney

A version of this chapter has been submitted for publication.

Anette Melk, Bernhard M.W. Schmidt, Oki Takeuchi, Birgit Sawitzki, David Rayner, and Philip F. Halloran: Expression of p16<sup>INK4a</sup> and other cell cycle regulator and senescence associated genes in aging human kidney.

Portions of this publication that were contributed by co-authors are not included unless noted.

## 5.1 Introduction

Kidney aging is an important problem not only because normal aging reduces renal function but also because of the high frequency of end stage renal disease in the elderly (USRDS 2000 Annual Report). It is possible that interactions between aging and disease stresses contribute to renal failure in the elderly. Old kidneys perform badly when transplanted, and donor age represents a major correlate of transplant survival (1). The mechanisms of decline in organ function with age may be instructive about the mechanisms of decline in disease states, since stress could theoretically accelerate some aging changes. Kidney aging is also of interest as a general model for organ aging because renal function can be more readily quantitated in longitudinal studies than the changes in other organs (2).

The molecular basis of aging in organs is not known. Theories of aging include oxidative damage, genomic instability (including telomere loss), genetic programming and cell death (3). One phenomenon that may be relevant to aging is the phenotype of senescence in cultured somatic cells. Cultured mammalian somatic cells cease cycling after a finite number of population doublings and enter a state of senescence (4). The phenotype of cells in this state differs between human and rodent fibroblasts (5). Human cellular senescence is called replicative senescence and is accompanied by loss of telomeres, the DNA repeats at the ends of

chromosomes that shorten in dividing normal somatic cells because of a lack of telomerase (6). Replicative senescence in human fibroblasts is prevented by transfection with telomerase (7). In contrast, mouse and rat telomeres are relatively long and show little shortening during their life expectancy (5), and telomerase is active in almost all mouse tissues (8). I have previously shown that telomere shortening occurs in human kidneys with age (chapter 2) (9), whereas in rodent kidneys telomeres are much longer and show minimal shortening with age (chapter 3 and 4) (10). In mice and rats the cell cycle regulator p16<sup>INK4a</sup> was strongly associated with aging (chapter 3 and 4) (10), but other markers associated with cellular senescence *in vitro* were not.

In this study I focused on the expression of p16<sup>INK4a</sup> in human kidneys. I also surveyed other genes important for senescence for their relationship with age. I investigated genes for cell cycle regulation including CDK4 (11-13), p53 (14-16) and its transactivational targets p21<sup>CIP1/WAF1</sup> (17) and GADD45 (18), p14<sup>ARF</sup> (19;20), HDM2 (21), PCNA (22;23), and RAD23. I investigated genes expressed in cultured fibroblast taken from aged donors (24): MMP1, PAI1, TGFβ1, COX1 and COX2. Finally, I chose genes to reflect dysfunction of the mitochondria (LON protease) (25) or the endoplasmic reticulum (HSPA5, GADD153) (26).

## 5.2 Materials and Methods

### 5.2.1 Kidneys

Human kidney samples were derived from total nephrectomies, biopsies at time of transplantation and from autopsies. Certain samples were the same published previously (chapter 2) (27). Whenever possible cortex and medulla were collected separately. A total of 42 samples were investigated and considered 'normal' since their histology was within the limits of changes expected for age as defined by me together with a renal pathologist (David Rayner or Kim Solez). These normal kidneys were derived from autopsies (n=3), zero biopsies at time of transplantation (n=5), or nephrectomies (n=34). Nephrectomies were performed mainly because of renal malignancies (renal cell carcinoma (n=25), oncytoma (n=1) or transitional cell carcinoma (n=3), metastatic lung cancer (n=1), Wilms tumor (n=2)), but included also one case of a benign tumor (angiolioma) and discarded organs not used for transplantation (n=1). In the case of tumors, normal renal tissue remote from the tumor was chosen for analysis. Basic clinical data of these normal individuals is given in table 5.1. None of the patients had diabetes mellitus or uncontrolled arterial hypertension. Table 5.1 shows the histological grading of these normal kidney specimens. Based on the Banff classification for chronic allograft nephropathy (28), I and a blinded renal pathologist (David Rayner) assessed the amount of glomerulosclerosis, interstitial fibrosis, tubular atrophy, fibrous intimal

thickening and arteriolar hyalinosis.

All tissue samples were snap-frozen in liquid nitrogen and stored at  $-70^{\circ}\text{C}$ . In addition, tissue was embedded for frozen and paraffin sections. The study was approved by the Health Research Ethics Board of the University of Alberta, Edmonton.

### 5.2.2 Real-time RT-PCR

Total RNA was extracted from tissue samples according to a modification of the method described by Chirgwin et al. (29). Tissues were homogenized with a polytron in 4 M guanidinium isothiocyanate, and the RNA was pelleted through a 5.7M  $\text{CsCl}_2$  cushion. RNA was isolated by phenol/chloroform extraction. Concentrations were determined by absorbance at 260 nm. Transcription into cDNA was done using MMLV reverse transcriptase and random primers (Life Technologies, Burlington, Ontario). The principle of real-time quantitative PCR has been described by Heid et al. (30). cDNA was amplified in an ABI PRISM 7700 Sequence Detector (Applied Biosystems, Foster City, CA). All samples were done in duplicates and run in two separate experiments. I designed sequence specific primers and probes (table 5.2) for p16<sup>INK4a</sup>, p14<sup>ARF</sup>, LON protease, PAI1, COX1, COX2, MMP1, and HPRT using Primer Express software (Applied Biosystems, Foster City, CA). Pre-developed assay reagents (PDARs) for p53, p21<sup>CIP1/WAF1</sup>, HDM2, CDK4, PCNA, GADD45, GADD153,

RAD23, TGF- $\beta$ 1, and HSPA5 (aka GRP78) were purchased (Applied Biosystems, Foster City, CA). Quantification of gene expression was performed using the Relative Standard Curve method as described in User Bulletin #2 (Applied Biosystems, Foster City, CA). Briefly, the number of PCR cycles that are needed to reach the fluorescence threshold is called threshold cycle (Ct). The Ct value for each sample is proportional to the  $\log_2$  of the initial amount of input cDNA. The calibrator used consisted of cDNA derived from Jurkat cells and two different human kidney samples. Standard curves were prepared by serial dilutions of the calibrator for both the gene of interest and the housekeeping gene HPRT. Dilutions were arbitrarily numbered 3, 1.5, 0.75, 0.375 and 0.1875. The Ct values for all samples were then assigned an arbitrary value based on the standard curves. The arbitrary values for gene of interest and for HPRT were divided in order to normalize to HPRT. Then the mean value for the duplicates is calculated. All values are given as a gene of interest to HPRT ratio.

### 5.2.3 Senescence associated (SA) $\beta$ -galactosidase ( $\beta$ -GAL) staining

Frozen sections were cut at 4  $\mu$ m and kept at -20°C until further processed. Staining was done as described previously (chapter 3 and 4) (10). Briefly, slides were brought to RT and fixed with 2% formaldehyde/0.2% glutaraldehyde in PBS. Slides were then incubated for 14 hours at 37°C in a humidified chamber with SA- $\beta$ -GAL staining solution

(2mg/ml X-gal in dimethylformamide, 40mM citric acid/sodium phosphate (dibasic), pH 6, 5mM potassium ferrocyanide, 5mM potassium ferricyanide, 150mM sodium chloride, 20mM magnesium chloride). Controls were stained for lysosomal  $\beta$ -GAL using the same SA- $\beta$ -GAL staining solution adjusted to pH 4. Following staining, slides were counterstained with eosin, dehydrated and mounted. Quantification of the SA- $\beta$ -GAL staining was accomplished by means of a Nikon Eclipse-1000 digitizing microscope. All tubules present in 20 high power fields (HPFs; 400x bright field magnification) per specimen were counted and classified as positive or negative for SA- $\beta$ -GAL staining. Cortex and medulla were assessed separately. The presence of lipofuscin was noted as well as the numbers of glomeruli and blood vessels present in each field.

#### 5.2.4 Immunoperoxidase staining for p16<sup>INK4a</sup>

Immunoperoxidase staining for p16<sup>INK4a</sup> was performed using 2  $\mu$ m sections of paraffin embedded tissue. Briefly, sections were deparaffinized and hydrated. The sections were immersed in 3% H<sub>2</sub>O<sub>2</sub> in methanol to inactivate endogenous peroxidase. Slides were blocked with 20% normal goat serum. Tissue sections were then incubated for 1 hr at RT with the primary antibody (mouse monoclonal antibody, Clone F-12, Santa Cruz Biotechnologies, Santa Cruz, CA) and rinsed with PBS. Following 30 minutes of incubation with the Envision monoclonal system (Dako,

Mississauga, Ontario), sections were washed again in PBS. Visualization was performed using the DAB substrate kit (Dako, Mississauga, Ontario). The slides were counterstained with hematoxylin and mounted. Analysis was done by counting 10 HPFs. Percentage of positive nuclei was assessed for tubules, glomeruli and interstitium. Each vessel was graded on a scale from 0 to 3, with 0 being no staining, 1 up to 30% stained nuclei, 2 between 30 and 60% stained nuclei and 3 more than 60% stained nuclei. The mean score was then calculated for each section.

#### 5.2.5 Statistical Analysis

Data analyses were performed using SPSS. Linear regression was used to analyze the correlation between expression of candidate genes and age. Means among age groups were compared using ANOVA, and T-tests with Bonferroni correction were used for multiple pair-wise comparisons. All values are given as mean  $\pm$  standard deviation (SD).

### 5.3 Results

#### 5.3.1 P16<sup>INK4a</sup> mRNA expression in normal human kidney samples

P16<sup>INK4a</sup> expression for kidney cortex specimens increased with age as shown by linear regression analysis (figure 5.1) ( $R^2=0.47$ ;  $P<0.001$ ). The correlation with age in cortex was still significant when we studied only patients older than 30 years ( $R^2=0.36$ ,  $P<0.001$ ) and when we studied only



normotensive patients ( $R^2=0.64$ ,  $P<0.001$ ). This result was corroborated by the comparison of cortical p16<sup>INK4a</sup> expression for different age groups. For this comparison, we defined age groups as 'Young' for specimens derived from individuals between 0 and 29 years of age, 'Adult' for 30 to 49 year old individuals and 'Old' for individuals 50 years and older. Comparison of the three age groups revealed highly significant differences in cortex ( $P<0.001$ ) when 'Old' individuals were compared to either 'Adult' or 'Young' (figure 5.2).

Mean p16<sup>INK4a</sup> expression was not significantly different between cortex and medulla. However, p16<sup>INK4a</sup> expression in Young specimens was higher in medulla when compared to cortex, and p16<sup>INK4a</sup> expression in medulla did not increase significantly with age ( $R^2=0.03$ ;  $P=0.42$ ) (figure 5.1). The expression of p16<sup>INK4a</sup> mRNA was not significantly different among the three age groups in medulla (figure 5.2).

### 5.3.2 P16<sup>INK4a</sup> protein expression in normal human kidney sections

P16<sup>INK4a</sup> protein expression was observed as nuclear and cytoplasmic staining. We evaluated the extent of nuclear p16<sup>INK4a</sup> staining in the renal cortex in tubules, glomeruli, in interstitial cells, and in arteries (figure 5.3). Tubular staining occurred in all parts of the nephron, but was pronounced in distal tubules and collecting ducts. Nuclear staining was rare in proximal tubular epithelium. In glomeruli, parietal epithelium and

podocytes stained. The p16<sup>INK4a</sup> positive cells in arteries were mostly vascular smooth muscle cells and rarely endothelial cells. Nuclear p16<sup>INK4a</sup> expression increased with age in all cell types examined. The increase was more pronounced in tubular cells ( $P < 0.001$ ; figure 5.4) but also statistically significant in glomerular and interstitial cells ( $P < 0.05$ ; figure 5.5 and 5.6). Young kidneys showed staining of 7.8% ( $\pm 10.2\%$ ) of tubular nuclei, 11% ( $\pm 15.9\%$ ) of glomerular nuclei, and 2% ( $\pm 3.2\%$ ) of interstitial cell nuclei. Adult kidneys showed similar staining: 7.8% ( $\pm 8.1\%$ ) of tubular, 7.9% ( $\pm 14.3\%$ ) of glomerular and 2.2% ( $\pm 3.8\%$ ) of interstitial cell nuclei showed nuclear p16<sup>INK4a</sup> staining. In contrast, in Old kidneys p16<sup>INK4a</sup> staining was observed in 30.8% ( $\pm 18.4\%$ ) of tubular nuclei, 20.8% ( $\pm 15.6\%$ ) of glomerular nuclei, and 11.4% ( $\pm 13\%$ ) of interstitial cell nuclei. We also found a significant increase with age in arteries ( $P < 0.05$ ; figure 5.7).

In addition to the nuclear staining, we observed in some cases a fine granular cytoplasmic staining for p16<sup>INK4a</sup>. This staining was seen in 54% (13 of 24) of the Old kidneys, 18% (2 of 11) of the Adult kidneys but in none the Young kidneys ( $P < 0.005$ ,  $\chi^2$ -test). Cytoplasmic staining was mainly localized to distal tubules, including the macula densa, and occasionally to the collecting duct (figure 5.3).

### 5.3.3 Expression of candidate senescence genes in human kidney cortex

In addition to p16<sup>INK4a</sup>, I examined renal expression of a number of

genes that had been associated with cellular senescence *in vitro*. Table 5.3 shows the regression analysis for the sixteen additional genes studied and table 5.4 states gene to HPRT ratios for these genes in the three age groups. Regression analysis revealed significant changes for COX1, COX2, CDK4, MMP1 and HSPA5. However, only COX1 and COX2 showed a strong relationship between expression and aging in renal cortex (regression coefficient:  $R^2 > 0.16$ , equivalent to  $r > 0.4$ ). Comparison of the three age groups showed significant increases with age for COX1, COX2 and CDK4.

#### 5.3.4 COX1 and COX2 mRNA expression in normal human kidney

I further compared COX1 and COX2 expression in cortex versus medulla (Figures 5.8-5.11). The mean values for COX1 were significantly higher in medulla compared to cortex ( $P < 0.001$ ). In cortex, COX1 mRNA expression increased significantly with age ( $R^2 = 0.18$ ,  $P = 0.005$ ; figure 5.8) and remained significant, when only patients older than 30 years ( $R^2 = 0.13$ ,  $P < 0.05$ ) or only normotensive patients were analyzed ( $R^2 = 0.25$ ,  $P < 0.01$ ). The increase in COX1 mRNA expression in medulla with age was not significant ( $R^2 = 0.06$ ,  $P = 0.25$ ; figure 5.8). When I compared the mean values for COX1 mRNA expression in the three age groups, I confirmed that cortex of old kidneys showed higher COX1 mRNA expression than cortex of Young or Adult kidney ( $P < 0.05$ ; figure 5.9).

Unlike COX1, COX2 mRNA expression was similar in cortex and medulla. However, like COX1, COX2 mRNA increased significantly with age in cortex ( $R^2=0.19$ ,  $P<0.005$ ; figure 5.10), whereas the increase in medulla was not significant ( $R^2=0.09$ ,  $P=0.16$ ; figure 5.10). Analysis of regression in cortex including only normotensive patients was also significant ( $R^2=0.39$ ,  $P<0.001$ ). When only samples from patients older than 30 years were analyzed, the correlation with age in cortex was borderline ( $R^2=0.10$ ,  $P=0.06$ ). Comparison of mean values for COX2 mRNA expression in the three age groups revealed significant differences for the comparison of 'Old' versus 'Young' ( $P<0.05$ ; figure 5.11).

The increases in COX1 and COX2 mRNA expression have been confirmed by immunohistochemistry. This was done by Bernhard M.W. Schmidt and is therefore not presented here.

### 5.3.5 SA- $\beta$ -GAL and lipofuscin in human kidney samples

Senescent fibroblasts develop SA- $\beta$ -GAL staining and lipofuscin pigment (31;32). I performed SA- $\beta$ -GAL staining in four Young and five Old kidneys. SA- $\beta$ -GAL was present in many tubules in all specimens investigated, even very young kidneys, with higher expression in medulla. SA- $\beta$ -GAL stained tubules and collecting ducts but not glomeruli. Figure 5.12 shows that the percentage of SA- $\beta$ -GAL positive tubular cross-sections in cortex and medulla was increased in Old kidneys but the differences

were not significant.

Lipofuscin was found in none of the Young kidneys, in a third of the Adult kidneys and in all Old kidneys. Lipofuscin was found in tubular cells but not in glomeruli. It was mainly localized in the medulla in Adult kidneys, but Old kidneys developed lipofuscin in a small number of cortical tubules. Thus as expected lipofuscin increased with age. The distribution of lipofuscin and the increase in cortex in Old kidneys were similar to what I had observed in rat kidneys with age (chapter 3) (10).

I studied whether SA- $\beta$ -GAL staining was more common in tubules that have lipofuscin pigment. Lipofuscin positive tubules were more likely to be positive for SA- $\beta$ -GAL: 99 of 126 lipofuscin (79%) positive tubules were also SA- $\beta$ -GAL positive ( $P < 0.0001$ , 2x2 table).

#### 5.4 Discussion

I studied whether cells in old human kidneys show features of cellular senescence as observed in cultured somatic cells. The striking finding was that age increased the expression of the cyclin-dependent kinase inhibitor p16<sup>INK4a</sup> in renal cortex, a marker and possible mediator of the senescence phenotype in mouse and human cultured cells (33-35). The steady state mRNA levels were increased about 10 fold, associated with nuclear and cytoplasmic staining on immunohistochemistry. COX1, COX2 and, to a lesser extent, CDK4 mRNA also increased with age. Other genes

that I had selected as potential senescence or aging genes did not show a significant change with age. Lipofuscin increased in renal cells, as expected, but the increase in SA- $\beta$ -GAL was not significant. This data, taken together with my previous finding that telomere shortening occurs in renal cortex with age, suggests that some changes typical of cellular senescence *in vitro* occur in human kidney cortex with age and could contribute to the phenotype of renal aging, but others do not.

The increase in p16<sup>INK4a</sup> expression in kidney with age suggests that many cells in human kidney undergo cell cycle regulatory events during development and aging *in vivo* similar to those in senescent human fibroblasts in culture. P16<sup>INK4a</sup> was found in almost all cell types of the kidney, but mainly in tubular cells. P16<sup>INK4a</sup> expression was higher in medulla than in cortex in young kidneys. In view of my previous finding that telomeres in medulla are shorter than in cortex in young kidneys, this suggests that the replicative history of medullary cells in development, on average, is different from that of cortical cells. It is possible that these differences reflect differences in embryogenesis, such as the greater net contribution of ureteric bud to the medulla. The strong p16<sup>INK4a</sup> expression in the collecting duct, which is derived from the ureteric bud, is compatible with this possibility. Nevertheless, the fact that P16<sup>INK4a</sup> expression increases during adult life in cortex indicates that some of the increase must be due to aging.

In human fibroblasts in culture, the increase in p16<sup>INK4a</sup> can be triggered either by injury from environmental stress or by replication, suggesting that these are the forces driving p16<sup>INK4a</sup> expression in aged human kidney. One form of senescence induced by stress in human fibroblasts is Ras-induced senescence, which is at least partially triggered by oxidative stress (36). A naturally occurring p16<sup>INK4a</sup> mutation (a homozygous loss-of-function deletion designated as “Leiden”) abrogates Ras-induced senescence (37). Injury activates Ras, which in turn activates the mitogen activated protein kinase (MAPK) pathway (Ras-Raf-MEK) and its targets, transcription factors Ets1 and Ets2. Ets1 and Ets2 positively regulate the p16<sup>INK4a</sup> promoter, but are in turn inhibited by the Id family of helix-loop-helix proteins (38). In young fibroblasts, Id1 inhibition of Ets2 expression could explain the absence of p16<sup>INK4a</sup> expression, whereas in senescent fibroblasts, Id1 is downregulated (39). However, other factors such as JunB can regulate p16<sup>INK4a</sup> expression in senescent fibroblasts (40). Thus the actual mechanisms of injury-induced p16<sup>INK4a</sup> expression remain incompletely understood. Replication can also increase P16<sup>INK4a</sup> expression, but is likely to be independent from telomere shortening (41;42).

Widespread P16<sup>INK4a</sup> expression in old kidneys could have a number of consequences, both beneficial and detrimental. P16<sup>INK4a</sup> induction could include irreversible cell cycle arrest and thus could operate

as a defence against cancer but also influence the loss of renal cell mass in cortex in aging. The cell cycle arrest could influence response to injury and ability to sustain function in disease states, and thus could be relevant to the high incidence of end stage renal disease in the elderly. However, in addition to its function as cell cycle regulator, p16<sup>INK4a</sup> can affect integrin expression. In some cell lines, it increases the  $\alpha_5$  integrin chain of the  $\alpha_5\beta_1$  fibronectin receptor (43), leading to apoptosis upon loss of anchorage. It also inhibits  $\alpha_v\beta_3$  integrin receptor mediated cell spreading (44). The interactions between p16<sup>INK4a</sup> and integrins are of interest since this might be involved in the genesis of atrophic tubules.

The increases in COX1 and COX2 could be either a primary manifestation of aging or a secondary compensatory event. In microarray studies of aged fibroblasts, COX1 is increased, but COX2 is decreased (24). Whether these changes apply to renal cells remains to be evaluated, but it raises the possibility that at least COX1 could be increased as a direct consequence of age. One of the most consistent changes in human kidney with age is a rise in renal vascular resistance. Both COX1 and COX2 maintain renal perfusion by increasing renal blood flow and GFR through their metabolites prostaglandin E<sub>2</sub> and prostaglandin I<sub>2</sub> (45). Renal perfusion in old kidneys may be more dependent on vasodilator prostaglandins. The clinical observation that acute renal failure due to COX inhibition is more frequent in the elderly is compatible with this belief (46),



although comorbidities such as heart failure that compromise renal perfusion also play a role. COX2 from the macula densa is one factor triggering renin release from the juxtaglomerular apparatus (47;48). This suggests that the increase in COX2 in kidney is not a cellular feature of aging, but compensation for decreased renal blood and increased vascular resistance in older kidneys. This highlights the general problem of distinguishing the events that cause aging from the events that occur as compensatory mechanisms.

The studies of the molecular events in aging in human kidney versus rodent kidneys converge to suggest both shared (e.g. p16<sup>INK4a</sup>) and differing (e.g. telomere shortening) elements in the aging phenotype. The general observation is that the kidney in each species shows features observed in senescent fibroblasts of that species. Thus human kidneys and fibroblasts show increased p16<sup>INK4a</sup> expression, without change in p14<sup>ARF</sup>, but with telomere shortening (49), whereas mouse kidneys and fibroblasts show increased p16<sup>INK4a</sup> and to a lesser extent in p19<sup>ARF</sup> expression without telomere shortening (chapter 4). My preliminary results with human and mouse cDNA microarrays also support the finding that very few genes are strongly altered in human renal aging (50). Species differences in aging mechanisms are not surprising: long lived mammals require different regulatory strategies than those in short lived mammals such as mouse and rat. These could include superior resistance to cancer through the telomere

shortening mechanism (51), and increased resistance to environmental stress to permit long survival of post-mitotic cells. Parallel studies of *in vitro* cell behaviour and *in vivo* behaviour of cells in organs helps to understand the components of the aging phenotype in each species.

## 5.5 Tables

**Table 5.1:** Demographic data and histological grading on the 42 individuals from whom normal kidneys were derived.

	Young N = 7	Adult N = 11	Old N = 24
Mean Age $\pm$ SD (years)	5.4 $\pm$ 7.4	39.5 $\pm$ 4.8	66.7 $\pm$ 11.0
Age Range (years)	8 wks – 21 years	31 – 47 years	50 – 88 years
Gender (f/m)	1/6	6/5	12/12
Creatinine ( $\mu$ mol/L)	45.8 $\pm$ 29.9	90.8 $\pm$ 19.8 <sup>a</sup>	92.8 $\pm$ 16.9 <sup>b</sup>
Systolic Blood Pressure (mmHg)	86.3 $\pm$ 17.2	123.3 $\pm$ 18.4 <sup>a</sup>	135.8 $\pm$ 18.9 <sup>b</sup>
Diastolic Blood Pressure (mmHg)	44.3 $\pm$ 11.5	75.5 $\pm$ 9.5 <sup>a</sup>	76.7 $\pm$ 11.9 <sup>b</sup>
Proteinuria	None	None	None
History of Hypertension	1 (14%)	1 (9%)	11 (46%)
History of Diabetes mellitus	None	None	None
Glomerulosclerosis (%)	0.43 $\pm$ 0.54	2.36 $\pm$ 1.91	8.54 $\pm$ 6.57 <sup>c</sup>
Interstitial Fibrosis	0.06 $\pm$ 0.18	0.18 $\pm$ 0.40	0.88 $\pm$ 0.54 <sup>c</sup>
Tubular Atrophy	0.06 $\pm$ 0.18	0.18 $\pm$ 0.41	1.10 $\pm$ 0.36 <sup>c</sup>
Fibrous Intimal Thickening	0	0.32 $\pm$ 0.46	1.24 $\pm$ 0.80 <sup>c</sup>
Arteriolar Hyalinosis	0.13 $\pm$ 0.35	0.27 $\pm$ 0.47	1.00 $\pm$ 0.80 <sup>c</sup>

<sup>a</sup>P<0.05 for Adult vs. Young

<sup>b</sup>P<0.05 for Old vs. Young

<sup>c</sup>P<0.05 for Old vs. Adult and Old vs. Young

**Table 5.2:** Sequences for primers and probes used in Real-time PCR studies.

Name	Accession Number (GenBank)		Sequence (5'→3')
p16 <sup>INK4a</sup>	L27211	Forward primer	GTAACCATGCCCGCATAGATG
		Reverse primer	CTAAGTTTCCCGAGGTTTCTCAGA
		Probe	TCCCTCAGACATCCCCGATTGAAAGAAC
p14 <sup>ARF</sup>	U40343	Forward primer	CTGATCTCCATCGCAGGGAC
		Reverse primer	ATGTCCACGAGGTCCTGAGC
		Probe	CACCCTTGGAGCTGGCACTGCAGA
LON	U02389	Forward primer	AGAAGACCATTGCGGCCAA
		Reverse primer	GAAGGCTGCCAGGTCGTAGAA
		Probe	CATCGTCCTGCCAGCCGAGAACAA
PAI1	M16006	Forward primer	CAGCTCATCAGCCACTGGAAA
		Reverse primer	TCGGTCATTCCCAGGTTCTCT
		Probe	CGCCTCCTGGTTCTGCCCAAGTTCT
COX1	M59979	Forward primer	CTTCAATGAGTACCGCAAGAGTT
		Reverse primer	GTAGAACTCCAACGCATCAATGTCT
		Probe	CCATCTCCTTCTCTCCTACGAGCTCCTGGA
MMP1	D31815	Forward primer	TTCAAGACAGAAAGAGACAGGAGACA
		Reverse primer	GGTGACACCAGTGACTGCACAT
		Probe	TTGCCGGAGGAAAAGCAGCTCAAGAAC
HPRT	NM000194	Forward primer	GACTTTGCTTTCCTTGGTCAGG
		Reverse primer	AGTCTGGCTTATATCCAACACTTCG
		Probe	TTACCAGCAAGCTTGCGACCTTGA

**Table 5.3:** Linear regression analysis for kidney cortex.

Gene	Slope	R <sup>2</sup>	P-value
p16 <sup>INK4a</sup>	+.0160	.465	<.001
CDK4	+.0038	.131	.02
p53	+.0003	.001	.84
p21 <sup>CIP1/WAF1</sup>	+.0028	.006	.64
GADD45	+.0016	.001	.86
p14 <sup>ARF</sup>	-.0012	.026	.31
HDM2	+.0022	.030	.28
PCNA	-.0005	.012	.50
RAD23	+.0024	.015	.44
PAI1	+.0065	.002	.80
COX1	+.0030	.182	.005
COX2	+.0188	.186	.004
MMP1	-.0128	.113	.03
TGF-β1	+.0019	.023	.34
LON protease	+.0029	.010	.52
HSPA5	-.0175	.111	.03
GADD153	-.0312	.026	.31

**Table 5.4:** Expression of candidate senescence genes (M±SD) for kidney cortex in three different age groups. Numbers are gene/HPRT ratio.

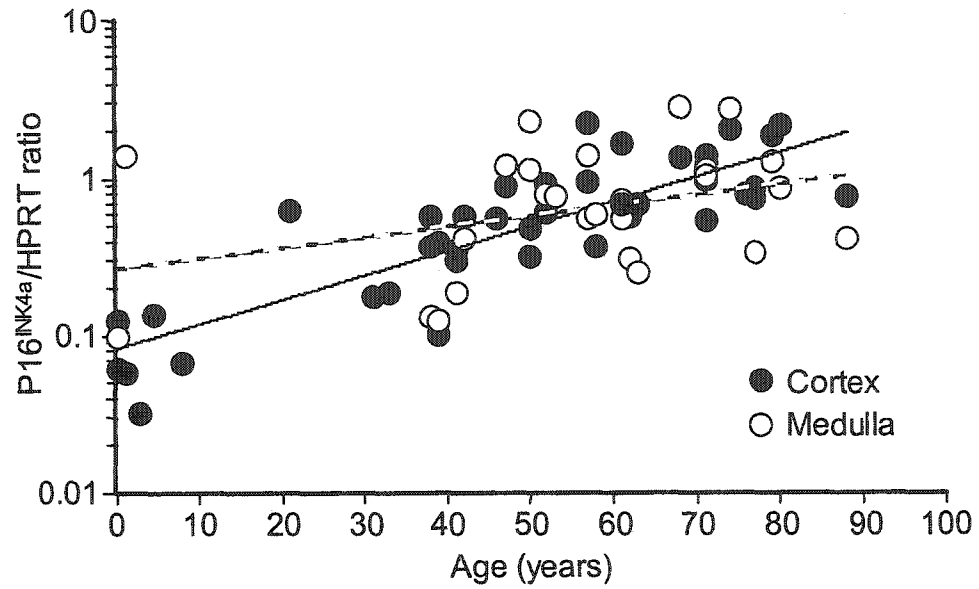
Gene	Young	Adult	Old
p16 <sup>INK4a</sup>	0.16 ± 0.21	0.41 ± 0.23	1.05 ± 0.56 <sup>a</sup>
CDK4	0.98 ± 0.36	1.08 ± 0.26	1.24 ± 0.19 <sup>b</sup>
p53	0.46 ± 0.23	0.36 ± 0.09	0.46 ± 0.21
p21 <sup>CIP1/WAF1</sup>	1.06 ± 0.83	1.14 ± 0.87	1.24 ± 1.01
GADD45	2.47 ± 1.70	3.71 ± 1.59	3.03 ± 1.15
p14 <sup>ARF</sup>	0.63 ± 0.29	0.46 ± 0.09	0.55 ± 0.17
HDM2	0.88 ± 0.35	0.77 ± 0.18	0.96 ± 0.34
PCNA	0.57 ± 0.18	0.56 ± 0.11	0.55 ± 0.07
RAD23	1.24 ± 0.42	1.22 ± 0.39	1.41 ± 0.53
PAI1	1.88 ± 1.91	4.50 ± 5.08	3.05 ± 3.86
COX1	0.14 ± 0.10	0.17 ± 0.08	0.31 ± 0.19 <sup>a</sup>
COX 2	0.82 ± 0.35	1.18 ± 0.38	1.94 ± 1.27 <sup>b</sup>
MMP1	1.51 ± 2.19	0.76 ± 0.40	0.60 ± 0.27
TGF-β1	0.62 ± 0.24	0.51 ± 0.20	0.73 ± 0.35
LON protease	1.91 ± 0.93	1.69 ± 0.43	2.00 ± 0.75
HSPA5	2.47 ± 2.96	1.21 ± 0.42	1.29 ± 0.44
GADD153	5.93 ± 3.73	6.62 ± 7.26	4.40 ± 3.46

<sup>a</sup>at least P<0.05 for Old vs. Adult and Old vs. Young

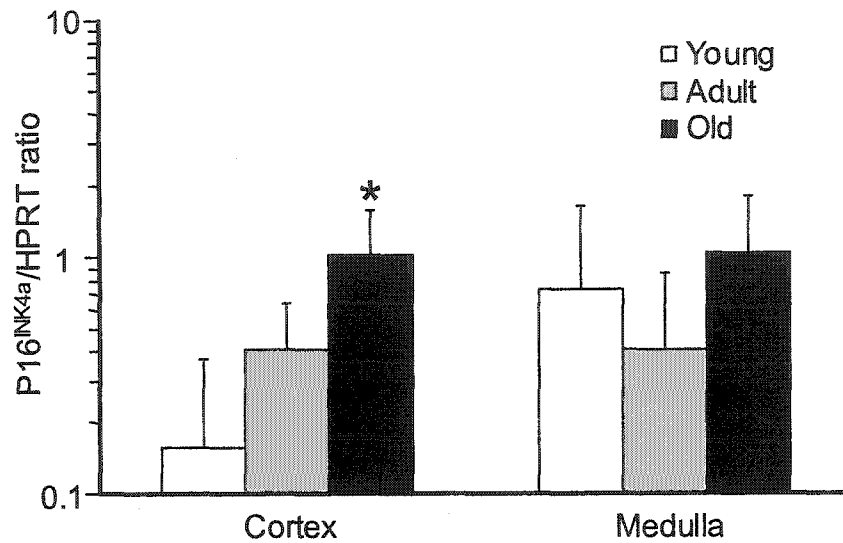
<sup>b</sup>at least P<0.05 for Old vs. Young

## 5.6 Figures



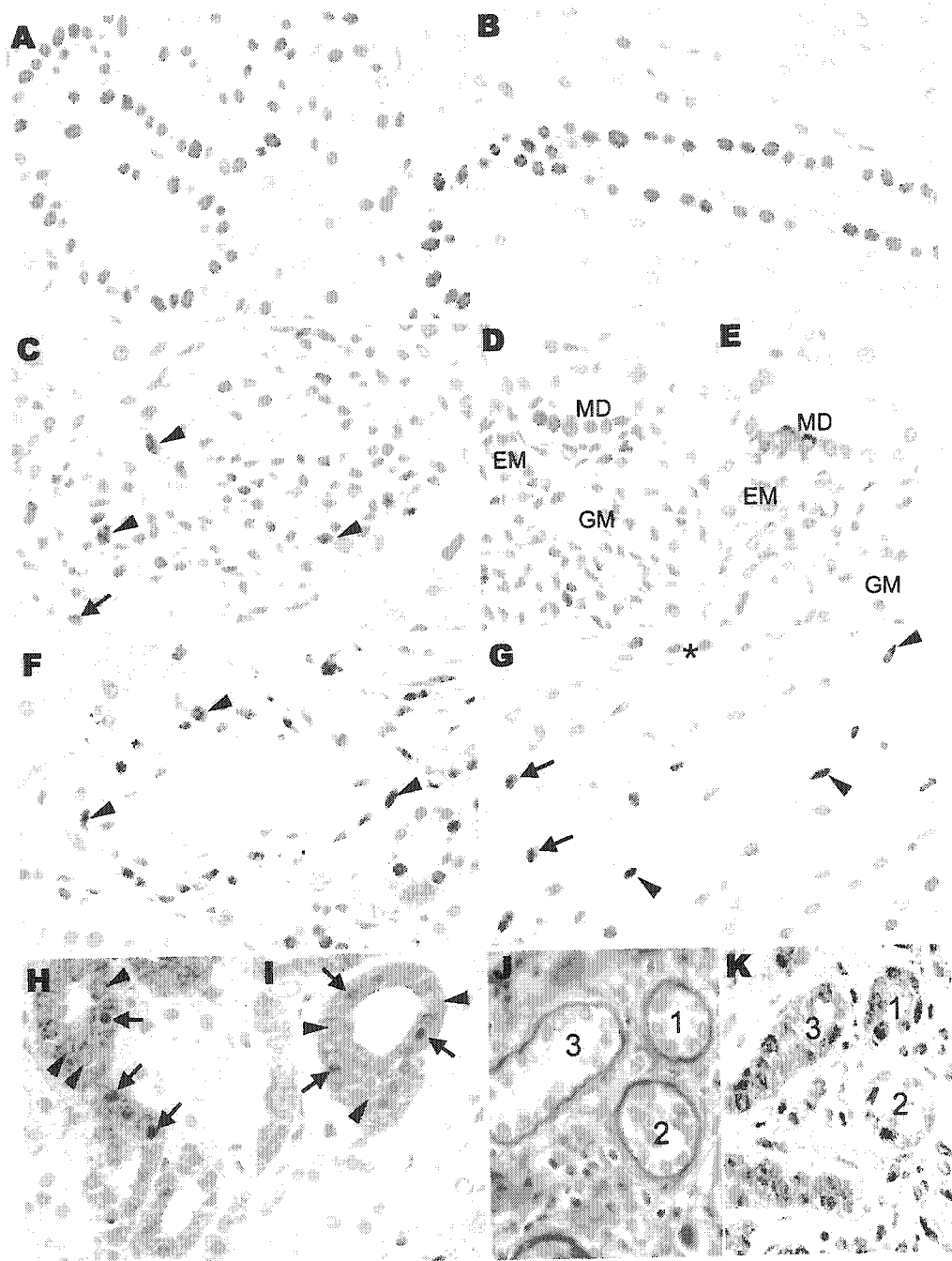


**Figure 5.1:** Regression for p16<sup>INK4a</sup> mRNA expression in renal cortex (filled circles;  $R^2=0.47$ ,  $p<0.001$ ) and renal medulla (open circles;  $R^2=0.03$ ;  $P=0.42$ ) with age. RNA was isolated and quantitative RT-PCR was performed using sequence-specific primer and probe for p16<sup>INK4a</sup> on an ABI 7700 Sequence Detection System. Values are given as p16<sup>INK4a</sup>/HPRT ratio.



**Figure 5.2:** P16<sup>INK4a</sup> mRNA expression in renal cortex and medulla. Mean ( $\pm$ SD) of p16<sup>INK4a</sup> mRNA expression in three age groups (Young, open bar; Adult, gray bar, Old, black bar) in cortex and medulla. \*P<0.001 for the comparison with Young and Adult kidneys. RNA was isolated and quantitative RT-PCR was performed using sequence-specific primer and probe for p16<sup>INK4a</sup> on an ABI 7700 Sequence Detection System. Values are given as p16<sup>INK4a</sup>/HPRT ratio.





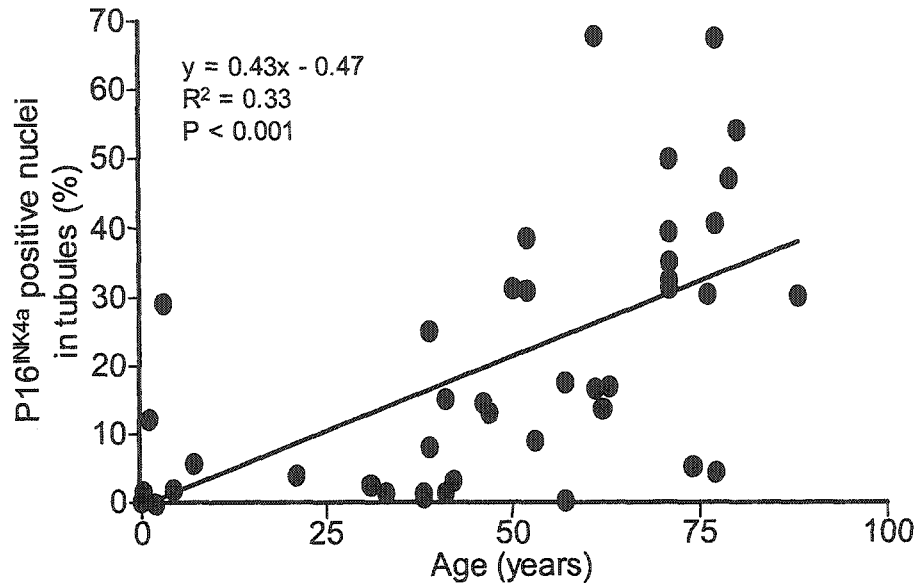


**Figure 5.4:** P16<sup>INK4a</sup> protein expression in tubular cells in renal cortex. The increase with age was highly significant (Slope,  $R^2$ , and P-values are shown), and most pronounced for tubular cells when compared to other cells. Immunoperoxidase staining for p16<sup>INK4a</sup> was assessed as percentage of positive nuclei for tubular cells in 10 HPFs.

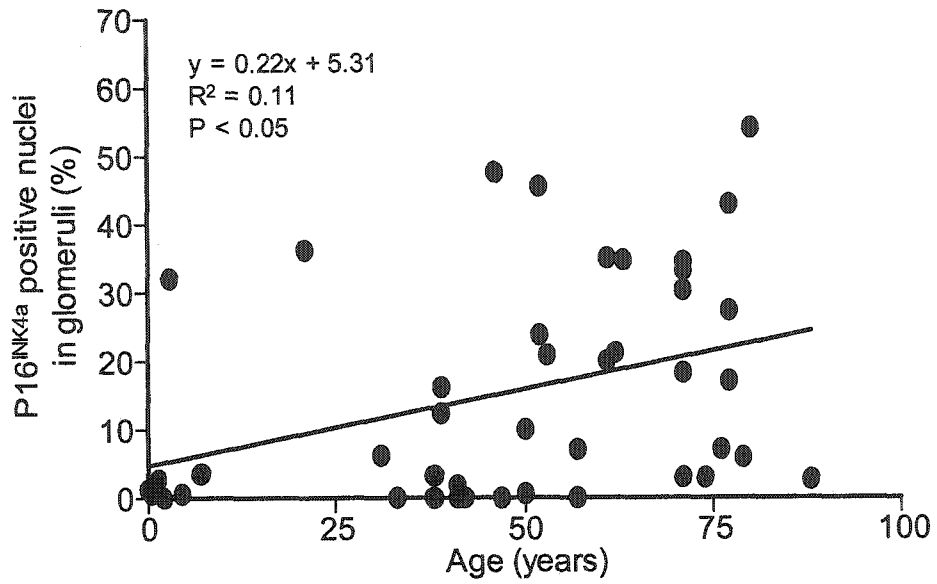


**Figure 5.5:** P16<sup>INK4a</sup> protein expression in glomeruli. The increase with age was significant (Slope, R<sup>2</sup>, and P-values are shown). Immunoperoxidase staining for p16<sup>INK4a</sup> was assessed as percentage of positive nuclei for glomerular cells in 10 HPFs.

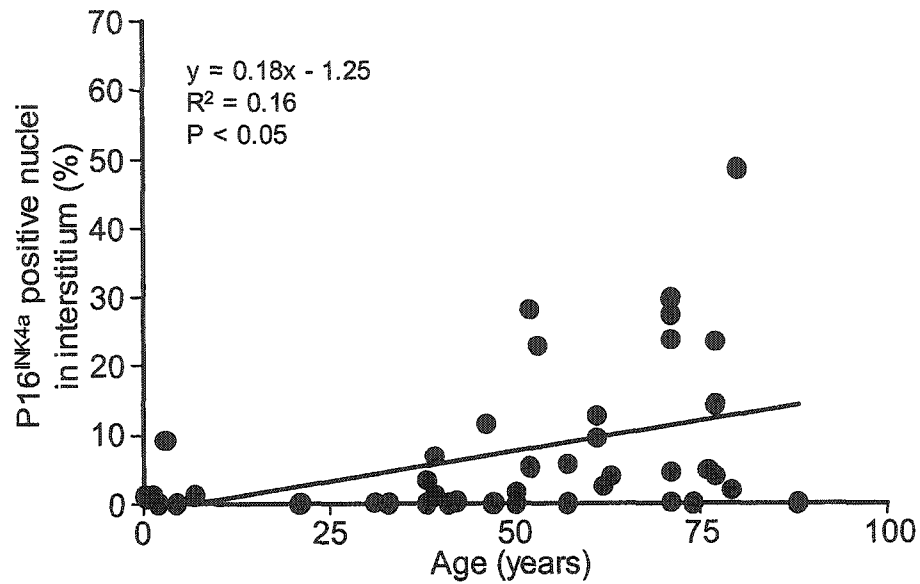


**Figure 5.6:** P16<sup>INK4a</sup> protein expression in interstitial cells in renal cortex. The increase with age was significant (Slope, R<sup>2</sup>, and P-values are shown). Immunoperoxidase staining for p16<sup>INK4a</sup> was assessed as percentage of positive nuclei for interstitial cells in 10 HPFs.





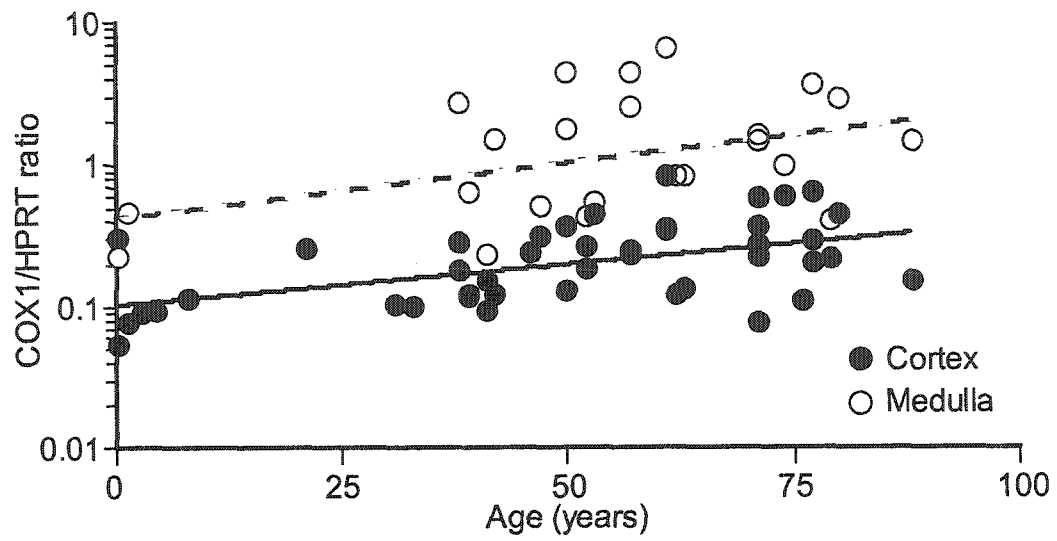


**Figure 5.8:** Regression for COX1 mRNA expression in renal cortex (filled circles;  $R^2=0.18$ ,  $p=0.005$ ) and renal medulla (open circles;  $R^2=0.06$ ,  $P=0.25$ ) with age. Values are given as COX1/HPRT ratio.

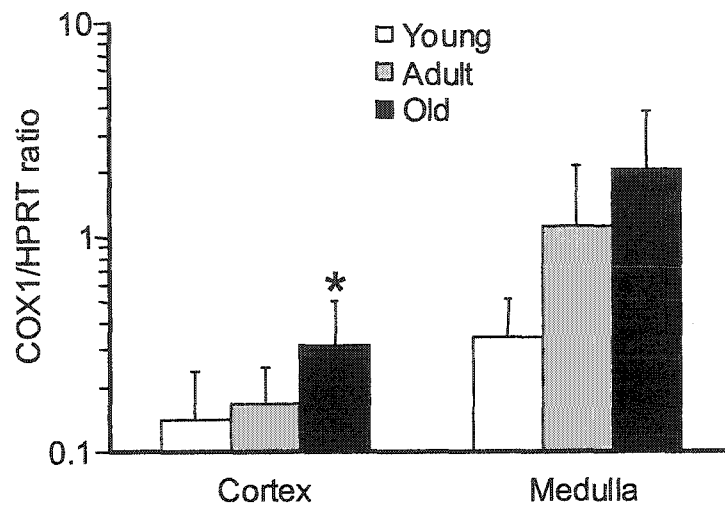


**Figure 5.9:** COX1 mRNA expression in renal cortex and medulla. Mean ( $\pm$ SD) of COX1 mRNA expression in three age groups (Young, open bar; Adult, gray bar, Old, black bar) in cortex and medulla. \* $P < 0.05$  for the comparison with Young and with Adult kidneys. Values are given as COX1/HPRT.

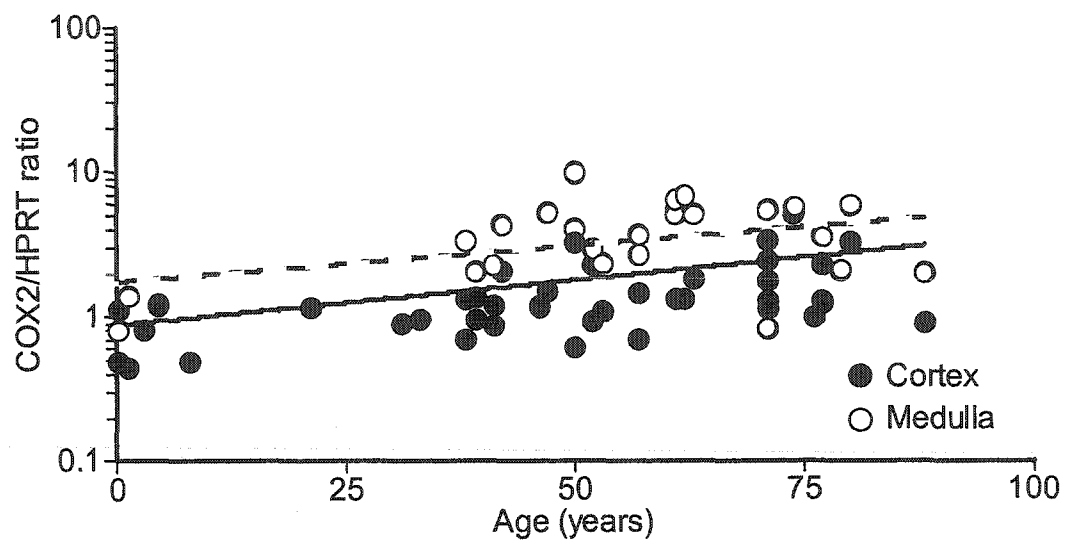


**Figure 5.10:** Regression for COX2 mRNA expression in renal cortex (filled circles;  $R^2=0.19$ ,  $p=0.004$ ) and renal medulla (open circles;  $R^2=0.09$ ,  $P=0.16$ ) with age. Values are given as COX2/HPRT ratio.

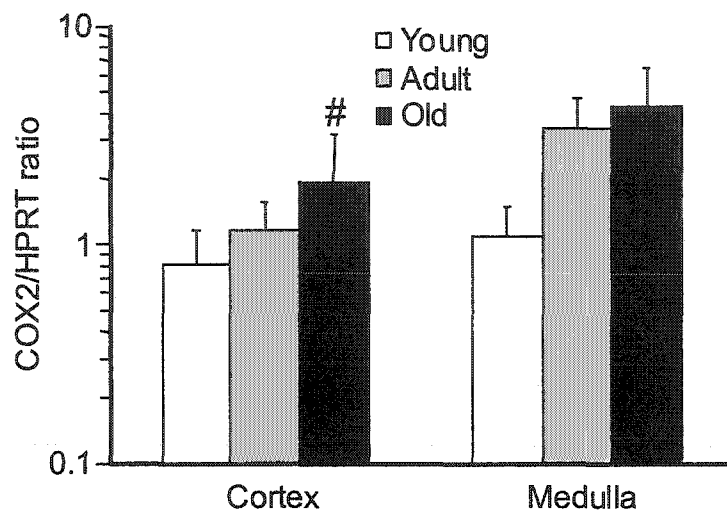


**Figure 5.11:** COX2 mRNA expression in renal cortex and medulla. Mean ( $\pm$ SD) of COX2 mRNA expression in three age groups (Young, open bar; Adult, gray bar, Old, black bar) in cortex and medulla. #P<0.05 for the comparison with Young kidneys. Values are given as COX2/HPRT ratio.

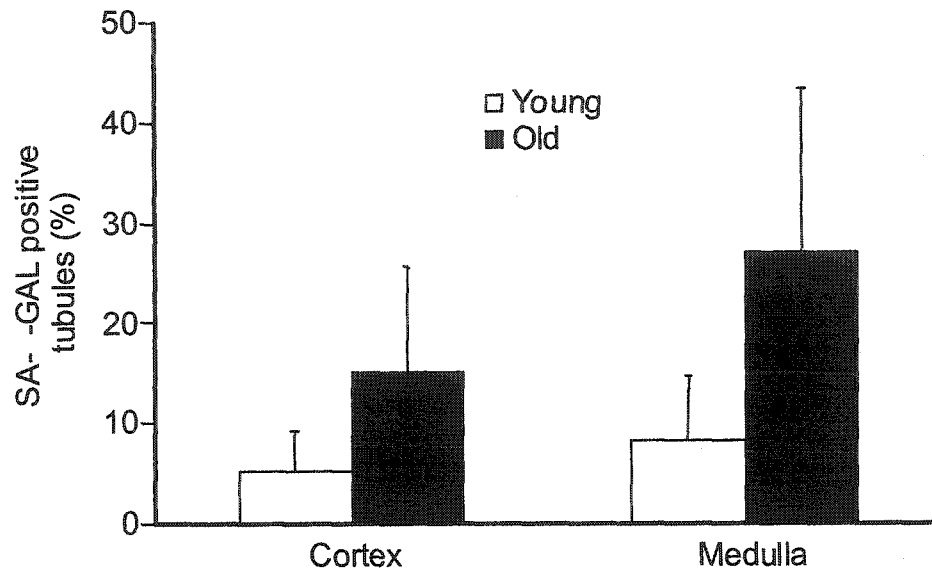


**Figure 5.12:** SA-β-GAL expression in renal cortex and medulla. SA-β-GAL was present in many tubules in all specimens investigated, but not in glomeruli. The percentage of SA-β-GAL positive tubular cross-sections in cortex and medulla was increased in Old kidneys but the differences were not significant. SA-β-GAL staining was performed using frozen sections. Percentage of SA-β-GAL positive tubules were assessed in 20 HPFs (10 HPFs for each cortex and medulla).

## 5.7 References

1. Terasaki PI, Cecka JM, and Gjertson D.W.: Impact analysis: a method for evaluating the impact of factors in clinical renal transplantation. *Clinical Transplants*. Edited by Cecka JM and Terasaki PI. Los Angeles, CA, UCLA Tissue Typing Laboratory, 1998, pp. 437-441
2. Lindeman RD, Tobin J, and Shock NW: Longitudinal studies on the rate of decline in renal function with age. *J Amer Ger Soc* 1985, 33: 278-285
3. Johnson FB, Sinclair DA, and Guarente L: Molecular biology of aging. *Cell* 1999, 96: 291-302
4. Hayflick L and Moorhead PS: The serial cultivation of human diploid cell strains. *Exp Cell Res* 1961, 25: 585-621
5. Wright WE and Shay JW: Telomere dynamics in cancer progression and prevention: fundamental differences in human and mouse telomere biology. *Nature Medicine* 2000, 6: 849-851
6. Harley CB, Futcher AB, and Greider CW: Telomeres shorten during ageing of human fibroblasts. *Nature* 1990, 345: 458-460
7. Bodnar AG, Ouellette M, Frolkis M, Holt SE, Chiu C-P, Morin GB, Harley CB, Shay JW, Lichtsteiner S, and Wright WE: Extension of life-span by introduction of telomerase into normal human cells. *Science* 1998, 279: 349-352
8. Prowse KR and Greider CW: Developmental and tissue-specific regulation of mouse telomerase and telomere length. *Proc Natl Acad Sci USA* 1995, 92: 4818-4822
9. Melk A, Ramassar V, Helms LM, Moore R, Rayner D, Solez K, and Halloran PF: Telomere shortening in kidneys with age. *J Am Soc Nephrol* 2000, 11: 444-453
10. Melk A, Kittikowit W, Sandhu I, Halloran KM, Grimm P, Schmidt BMW, and Halloran PF: Cell senescence in rat kidney in vivo increases with growth and age despite lack of telomere shortening. *Kidney Int* 2003, 63: 2134-2143
11. Ramirez RD, Herbert BS, Vaughan MB, Zou Y, Gandia K, Morales CP, Wright WE, and Shay JW: Bypass of telomere-dependent replicative senescence (M1) upon overexpression of Cdk4 in normal human epithelial cells. *Oncogene* 2003, 22: 433-444
12. Morisaki H, Ando A, Nagata Y, Pereira-Smith O, Smith JR, Ikeda K, and Nakanishi M: Complex mechanisms underlying impaired activation of

Cdk4 and Cdk2 in replicative senescence: roles of p16, p21, and cyclin D1. *Exp Cell Res* 1999, 253: 503-510

13. Serrano M, Hannon GJ, and Beach D: A new regulatory motif in cell-cycle control causing specific inhibition of cyclin D/CDK4. *Nature* 1993, 366: 704-707
14. Schmitt CA, Fridman JS, Yang M, Lee S, Baranov E, Hoffman RM, and Lowe SW: A senescence program controlled by p53 and p16INK4a contributes to the outcome of cancer therapy. *Cell* 2002, 109: 335-346
15. Serrano M, Lin AW, McCurrach ME, Beach D, and Lowe SW: Oncogenic ras provokes premature cell senescence associated with accumulation of p53 and p16(INK4a). *Cell* 1997, 88: 593-602
16. Shay JW, Pereira-Smith OM, and Wright WE: A role for both RB and p53 in the regulation of human cellular senescence. *Exp Cell Res* 1991, 196: 33-39
17. Stein GH, Drullinger LF, Soulard A, and Dulic V: Differential roles for cyclin-dependent kinase inhibitors p21 and p16 in the mechanisms of senescence and differentiation in human fibroblasts. *Mol Cell Biol* 1999, 19: 2109-2117
18. Kearsey JM, Coates PJ, Prescott AR, Warbrick E, and Hall PA: Gadd45 is a nuclear cell cycle regulated protein which interacts with p21Cip1. *Oncogene* 1995, 11: 1675-1683
19. Quelle DE, Zindy F, Ashmun RA, and Sherr CJ: Alternative reading frames of the INK4a tumor suppressor gene encode two unrelated proteins capable of inducing cell cycle arrest. *Cell* 1995, 83: 993-1000
20. Wei W, Hemmer RM, and Sedivy JM: Role of p14(ARF) in replicative and induced senescence of human fibroblasts. *Mol Cell Biol* 2001, 21: 6748-6757
21. Zhang Y, Xiong Y, and Yarbrough WG: ARF promotes MDM2 degradation and stabilizes p53: ARF-INK4a locus deletion impairs both the Rb and p53 tumor suppression pathways. *Cell* 1998, 92: 725-734
22. Chang CD, Phillips P, Lipson KE, Cristofalo VJ, and Baserga R: Senescent human fibroblasts have a post-transcriptional block in the expression of the proliferating cell nuclear antigen gene. *J Biol Chem* 1991, 266: 8663-8666
23. Nadasdy T, Laszik Z, Blick KE, Johnson LD, and Silva FG: Proliferative activity of intrinsic cell populations in the normal human kidney. *J Am Soc Nephrol* 1994, 4: 2032-2039

24. Ly DH, Lockhardt DJ, Lerner RA, and Schultz PG: Mitotic misregulation and human aging. *Science* 2000, 287: 2486-2492
25. Bota DA, Van Remmen H, and Davies KJ: Modulation of Lon protease activity and aconitase turnover during aging and oxidative stress. *FEBS Lett* 2002, 532: 103-106
26. Mengesdorf T, Althausen S, and Paschen W: Genes associated with pro-apoptotic and protective mechanisms are affected differently on exposure of neuronal cell cultures to arsenite. No indication for endoplasmic reticulum stress despite activation of grp78 and gadd153 expression. *Brain Res Mol Brain Res* 2002, 104: 227-239
27. Melk A, Ramassar V, Helms LM, Moore R, Rayner D, Solez K, and Halloran PF: Telomere shortening in kidneys with age. *J Am Soc Nephrol* 2000, 11: 444-453
28. Racusen LC, Solez K, Colvin RB, Bonsib SM, Castro MC, Cavallo T, Croker BP, Demetris AJ, Drachenberg CB, Fogo AB, Furness P, Gaber LW, Gibson IW, Glotz D, Goldberg JC, Grande J, Halloran PF, Hansen HE, Hartley B, Hayry PJ, Hill CM, Hoffman EO, Hunsicker LG, Lindblad AS, Marcussen N, Mihatsch MJ, Nadasdy T, Nickerson P, Olsen TS, Papadimitriou JC, Randhawa PS, Rayner DC, Roberts I, Rose S, Rush D, Salinas-Madrigal L, Salomon DR, Sund S, Taskinen E, Trpkov K, and Yamaguchi Y: The Banff 97 working classification of renal allograft pathology. *Kidney Int* 1999, 55: 713-723
29. Chirgwin JM, Przybyla AE, MacDonald RJ, and Rutter WJ: Isolation of biologically active ribonucleic acid from sources enriched in ribonuclease. *Biochemistry* 1979, 18: 5294-5299
30. Heid CA, Stevens J, Livak KJ, and Williams PM: Real time quantitative PCR. *Genome Res* 1996, 6: 986-994
31. Dimri GP, Lee X, Basile G, Acosta M, Scott G, Roskelley C, Medrano EE, Linskens M, Rubelj I, Pereira-Smith O, Peacocke M, and Campisi J: A biomarker that identifies senescent human cells in culture and in aging skin *in vivo*. *Proc Natl Acad Sci USA* 1995, 92: 9363-9367
32. Sitte N, Merker K, Grune T, and von Zglinicki T: Lipofuscin accumulation in proliferating fibroblasts *in vitro*: an indicator of oxidative stress. *Exp Geront* 2001, 36: 475-486
33. Alcorta DA, Xiong Y, Phelps D, Hannon G, Beach D, and Barrett JC: Involvement of the cyclin-dependent kinase inhibitor p16 (INK4a) in replicative senescence of normal human fibroblasts. *Proc Natl Acad Sci U S A* 1996, 93: 13742-13747



34. Munro J, Steeghs K, Morrison V, Ireland H, and Parkinson EK: Human fibroblast replicative senescence can occur in the absence of extensive cell division and short telomeres. *Oncogene* 2001, 20: 3541-3552
35. Palmero I, McConnell B, Parry D, Brookes S, Hara E, Bates S, Jat P, and Peters G: Accumulation of p16INK4a in mouse fibroblasts as a function of replicative senescence and not of retinoblastoma gene status. *Oncogene* 1997, 15: 495-503
36. Lee AC, Fenster BE, Ito H, Takeda K, Bae NS, Hirai T, Yu ZX, Ferrans VJ, Howard BH, and Finkel T: Ras proteins induce senescence by altering the intracellular levels of reactive oxygen species. *Journal of Biological Chemistry* 1999, 274: 7936-7940
37. Brookes S, Rowe J, Ruas M, Llanos S, Clark PA, Lomax M, James MC, Vatcheva R, Bates S, Vousden KH, Parry D, Gruis N, Smit N, Bergman W, and Peters G: INK4a-deficient human diploid fibroblasts are resistant to RAS-induced senescence. *Embo Journal* 2002, 21: 2936-2945
38. Ohtani N, Zebedee Z, Huot TJ, Stinson JA, Sugimoto M, Ohashi Y, Sharrocks AD, Peters G, and Hara E: Opposing effects of Ets and Id proteins on p16INK4a expression during cellular senescence. *Nature* 2001, 409: 1067-1070
39. Alani RM, Young AZ, and Shifflett CB: Id1 regulation of cellular senescence through transcriptional repression of p16/Ink4a. *Proc Natl Acad Sci U S A* 2001, 98: 7812-7816
40. Passegue E and Wagner EF: JunB suppresses cell proliferation by transcriptional activation of p16(INK4a) expression. *EMBO J* 2000, 19: 2969-2979
41. Munro J, Steeghs K, Morrison V, Ireland H, and Parkinson EK: Human fibroblast replicative senescence can occur in the absence of extensive cell division and short telomeres. *Oncogene* 2001, 20: 3541-3552
42. Ramirez RD, Morales CP, Herbert BS, Rohde JM, Passons C, Shay JW, and Wright WE: Putative telomere-independent mechanisms of replicative aging reflect inadequate growth conditions. *Genes & Development* 2001, 15: 398-403
43. Plath T, Detjen K, Welzel M, von Marschall Z, Murphy D, Schirner M, Wiedenmann B, and Rosewicz S: A novel function for the tumor suppressor p16(INK4a): induction of anoikis via upregulation of the alpha(5)beta(1) fibronectin receptor. *J Cell Biol* 2000, 150: 1467-1478
44. Fahraeus R and Lane DP: The p16(INK4a) tumour suppressor protein inhibits alphavbeta3 integrin-mediated cell spreading on vitronectin by

blocking PKC-dependent localization of alphavbeta3 to focal contacts. EMBO J 1999, 18: 2106-2118

45. Imig JD: Eicosanoid regulation of the renal vasculature. American Journal of Physiology-Renal Physiology 2000, 279: F965-F981
46. Perazella MA and Tray K: Selective cyclooxygenase-2 inhibitors: A pattern of nephrotoxicity similar to traditional nonsteroidal anti-inflammatory drugs. American Journal of Medicine 2001, 111: 64-67
47. Traynor TR, Smart A, Briggs JP, and Schnermann J: Inhibition of macula densa-stimulated renin secretion by pharmacological blockade of cyclooxygenase-2. American Journal of Physiology-Renal Physiology 1999, 277: F706-F710
48. Schnermann J: Cyclooxygenase-2 and macula densa control of renin secretion. Nephrology Dialysis Transplantation 2001, 16: 1735-1738
49. Melk A, Ramassar V, Helms LM, Moore R, Rayner D, Solez K, and Halloran PF: Telomere shortening in kidneys with age. J Am Soc Nephrol 2000, 11: 444-453
50. Melk, A., Halloran, P. F., and Sarwal, M. Gene expression pattern in human renal senescence using microarray technique. Am J Transplant 2[3], 383. 2002.
51. Wright WE and Shay JW: Historical claims and current interpretations of replicative aging. Nature Biotechnology 2002, 20: 682-688

## Chapter 6

# Evidence that Acute Rejection induces Epithelial Cell Senescence in Mouse Kidney

A version of this chapter will be submitted for publication.

Anette Melk, Bernhard M.W. Schmidt, Oki Takeuchi, Joan Urmson, Lin-Fu Zhu, David Rayner, and Philip F. Halloran: Evidence that acute rejection induces epithelial cell senescence in mouse kidney.

Portions of this publication that were contributed by co-authors are not included unless noted.

## 6.1 Introduction

Donor age is the major predictor of function and graft survival after kidney transplantation (1-5). This could represent the effect of senescence due to age. In addition, peri- and posttransplant stresses could accelerate senescence features. These stress-induced changes add to the already preexisting senescence changes of the kidney and might be responsible for organ failure.

In subsequent studies I have shown that features of cellular senescence *in vitro* indeed occur in normal aging in human and rodent kidneys (human: chapters 2, 5; rat: chapter 3; mouse: chapter 4) (6;7). This new finding enabled me to ask if peri- and posttransplant stresses are capable of accelerating the development of senescent changes in the kidney. Peritransplant stresses are related to brain death (8;9), preservation, cold and warm ischemia and reperfusion (10;11). A high load of peritransplant stresses leads to delayed graft function (12). The most important posttransplant stresses are immunologic and cardiovascular. Rejection episodes as well as immunosuppressive treatment itself, especially calcineurin inhibitors due to their nephrotoxicity (13), reduce renal function. Hypertension often occurs in patients after renal transplantation and if left uncontrolled has deleterious effects (14).

One could imagine two pathophysiological pathways contributing to an acceleration of senescence by stresses surrounding transplantation.

Peri- and posttransplant stresses might induce an increase in replication and could thereby lead to replicative senescence. This has been shown for bone marrow transplantation (15;16). Telomere length measured in leukocytes of donor and recipient showed significant shorter telomeres for the recipient's leukocytes. However, the stresses acting in the context of transplantation could also directly induce senescence changes without the need for replication like in "stimulation and stress-induced senescent-like arrest" (STASIS). It is thought that STASIS is caused by extrinsic stresses rather than an intrinsic program of the cell (17). STASIS is the *in vitro* phenotype that occurs in mouse embryonic fibroblasts (MEFs) in culture and is accompanied by increases in p16<sup>INK4a</sup> and p19<sup>ARF</sup> (18-21). Expression of either of those proteins will result in an irreversible cell cycle arrest (21;22).

In the study presented here I used a previously described non-life supporting vascularized renal transplantation model in mice across full MHC barriers (23) to assess the impact of the transplantation process on renal senescence. I focused on p16<sup>INK4a</sup> and p19<sup>ARF</sup> as I had established the relationship between mouse renal senescence and p16<sup>INK4a</sup> and to a much lesser extent p19<sup>ARF</sup> in my former studies (chapter 4).

## 6.2 Materials and Methods

### 6.2.1 Mice

Male CBA mice were obtained from the National Institute on Aging, Aged Rodent Colonies, at 3 (Young, N=20) or 18 months (Old, N=18) of age. C57Bl/6 (B6) mice were purchased from Jackson Laboratory (Bar Harbor, ME). All animals were maintained in a facility that is barrier maintained and specific pathogen free. The animals were transplanted within one week after arrival in our colony. All experiments were performed according to the University of Alberta Animal Policy and Welfare Committee's animal care protocols.

### 6.2.2 Renal Transplantation

Donor mice (CBA at age 3 or 18 months) were anaesthetized and the abdomen was opened through a midline incision. The right kidney was excised and preserved in cold lactate Ringer's solution. The host mice (B6 at age 2 months) were similarly anaesthetized and the right native kidney was excised. The donor kidney was anastomosed heterotopically to the inferior aorta, vena cava and bladder on the right side, without removing the host's left kidney (non-life supporting kidney transplantation). The mice were allowed to recover and were killed at day 7 or 21 following anesthesia and cervical dislocation. None of the transplanted hosts received immunosuppressive therapy. All hosts received prophylactic antibiotics to

prevent wound and urinary tract infection. Mice with technical complications or severe pyelonephritis at the time of harvesting were removed from the study. I was able to study 15 Young donors (N=7 at D7 and N=8 at D21) and 13 Old donors (N=6 at D7 and N=7 at D21). (Renal transplantation was performed by Lin-Fu Zhu).

### 6.2.3 Histopathology

Tissue sections (2  $\mu$ m) were stained with hematoxylin and eosin (H & E) or with periodic acid-Schiff (PAS), respectively. Under the supervision of a renal pathologist (David Rayner), I evaluated the histologic changes based on the Banff classification for transplant pathology (24). The acute lesions were scored from 0 to 3 based on the percentage of parenchymal involvement as described earlier. Interstitial infiltrate: I0 - representing no or trivial (<10%) interstitial inflammation; I1 - representing 10 - 25%; I2 - representing 26 - 50%; and I3 - representing more than 50% of the total parenchyma inflamed. Glomerulitis: G0 - representing no glomerulitis; G1 - representing glomerulitis in up to 25% of glomeruli; G2 - representing glomerulitis in 26 - 75% of glomeruli; and G3 - representing glomerulitis in more than 75% of glomeruli. Tubulitis: T0 - no mononuclear cells in tubules; T1 - representing foci with 1 - 4 cells per tubular cross section; T2 - representing foci with 5 - 10 cells per tubular cross section; and T3 - representing more than 10 cells per tubular cross section. Tubulitis was

assessed for non-atrophic and atrophic tubules separately. Vasculitis: V0 – no arteritis; V1 – mild-to-moderate intimal arteritis in at least one arterial cross section; V2 - severe intimal arteritis with at least 25% luminal area lost in at least one arterial cross section; V3 – transmural arteritis and/or arterial fibrinoid change and medial smooth muscle necrosis with lymphocyte infiltrate in vessel. I also recorded the extent of peritubular capillary congestion (PTC), graft necrosis, thrombosis and edema as percentage of total parenchyma involved. Assessment of chronic changes included interstitial fibrosis and tubular atrophy. These changes were scored based on the percentage of parenchymal involvement. Interstitial fibrosis: CI0 - representing interstitial fibrosis in up to 5%; CI1 - representing interstitial fibrosis in 6 - 25%; CI2 - representing interstitial fibrosis in 26 – 50%; and CI3 - representing interstitial fibrosis in more than 50% of the cross section. Tubular atrophy: CT0 - representing no tubular atrophy; CT1 - representing tubular atrophy in up to 25%; CT2 - representing tubular atrophy in 26 – 50%; and CT3 - representing tubular atrophy in more than 50% of tubules. Vascular fibrous intimal thickening and arteriolar hyaline thickening did not occur in any of the mice and were therefore not scored.

In addition, on PAS stained slides, number of nuclei per tubular cross section and tubular diameter for non-atrophic and atrophic tubules were assessed. Both assessments were done in 10 random high power fields (HPFs; 400x magnification). For the measurement of tubular diameter



pictures from randomly selected areas were taken using a Nikon Eclipse-1000 digitizing microscope. The resulting TIFF-files of these pictures (size 25.6 x 20.48 inches) were processed using Adobe Photoshop 5.0 to reduce their size (size 12.8 x 10.24 inches) making them suitable for ImageJ software (free share software, NIH, USA). The tubular diameter was measured as inches on these processed pictures.

#### 6.2.4 Antibodies

Hybridoma cell lines were obtained from ATCC (Rockville, MD). Cell lines producing monoclonal antibodies, 34-4-20S (anti H-2D), 11-5.2.1.9 (anti I-A<sup>k</sup>), 11-4.1 (anti H-2K) and 20-8-4S (anti H-2K<sup>b</sup>D<sup>b</sup>) were maintained in tissue culture in our laboratory. All other antibodies were purchased: Anti I-A<sup>b</sup> (Serotec, Raleigh, NC), anti-mouse CD45 (Cedarlane, Hornby, ON), anti-mouse CD3 (Serotec, Raleigh, NC), anti-mouse CD8 (Serotec, Raleigh, NC), anti-mouse CD4 (BD Pharmingen, Mississauga, ON), anti-p16<sup>INK4a</sup> (Santa Cruz Biotechnologies, Santa Cruz, CA).

#### 6.2.5 Immunohistochemistry

Immunohistochemistry was performed either on frozen or paraffin embedded sections.

Fresh frozen sections were fixed in acetone and then incubated with normal goat serum. Slides were then incubated with rat anti-mouse CD45,

CD3, CD4 and CD8. Control slides were treated with PBS. Next, slides were exposed to the affinity purified, goat anti-rat IgG F(ab')<sub>2</sub> fragment (ICN, Costa Mesa, CA). Slides were finally stained with 3'3 diaminobenzidine tetrahydrochloride (DAB) and hydrogen peroxide for the peroxidase reaction and counterstained with hematoxylin. Analysis was done by counting 10 random high power fields (HPFs) by a blinded observer. (Staining and counts for frozen sections were done by Joan Urmson).

Immunoperoxidase staining for p16<sup>INK4a</sup> was performed using 2 µm sections of paraffin embedded tissue. Briefly, sections were deparaffinized and hydrated. The sections were immersed in 3% H<sub>2</sub>O<sub>2</sub> methanol to inactivate endogenous peroxidase. Slides were blocked with 20% normal goat serum. Tissue sections were then incubated for 1 hr at RT with the primary antibody (mouse monoclonal antibody, Clone F-12, Santa Cruz, CA) or isotype control and rinsed with PBS. Following 30 minutes of incubation with the Envision monoclonal system (Dako, Mississauga, Ontario), sections were washed again in PBS. Visualization was performed using the DAB substrate kit (Dako, Mississauga, Ontario). The slides were counterstained with hematoxylin and mounted. Percentage of positive nuclei was assessed for tubules, glomeruli and interstitium by counting 10 random HPFs. A total of 30 mice (5 for each group) were assessed.

### 6.2.6 RNA isolation

Total RNA was extracted from tissue samples according to a modification of the method described by Chirgwin et al. (25). Tissues were homogenized with a polytron in 4 M guanidinium isothiocyanate, and the RNA was centrifuged through a 5.7 M CsCl<sub>2</sub> cushion. RNA was isolated by phenol/chloroform extraction. Concentrations were determined by absorbance at 260 nm.

### 6.2.7 Reverse transcription (RT) and real-time polymerase chain reaction (PCR)

Transcription into cDNA was done using Maloney murine leukemia virus (MMLV) reverse transcriptase and random primers (Life Technologies, Burlington, Ontario). The principle of real-time quantitative PCR has been described by Heid et al. (26). cDNA was amplified in an ABI PRISM 7700 Sequence Detector (Applied Biosystems, Foster City, CA). All samples were done in duplicates and run in two separate experiments. I designed sequence specific primers and probe (table 6.1) for IFN- $\gamma$ , perforin, granzyme B, p16<sup>INK4a</sup>, p19<sup>ARF</sup>, and hypoxanthine phosphoribosyl-transferase (HPRT) using Primer Express Software (Applied Biosystems, Foster City, CA). Relative quantification of gene expression was performed using the Relative Standard Curve method as described in the User Bulletin #2 (Applied Biosystems, Foster City, CA). Briefly, the number of PCR

cycles that are needed to reach the fluorescence threshold is called threshold cycle (Ct). The Ct value for each sample is proportional to the  $\log_2$  of the initial amount of input cDNA. The calibrator used consisted of cDNA derived from different tissues and age groups from normal and transplanted mice. Standard curves were prepared by serial dilutions of the calibrator for both the gene of interest and the housekeeping gene HPRT. Dilutions were arbitrarily numbered 3, 1.5, 0.75, 0.375 and 0.1875. The Ct values for all samples were then assigned an arbitrary value based on the standard curves. The arbitrary values for gene of interest and for HPRT were divided in order to normalize to HPRT. Then the mean value for the duplicates is calculated. All values are given as a gene of interest to HPRT ratio.

#### 6.2.8 Statistical analysis

Data analyses were performed using SPSS. For quantitative variables, means among different groups were compared using ANOVA, and T-tests with Bonferroni correction were used for multiple pair-wise comparisons. For ordinal observations, the different groups were compared using Kruskal-Wallis test, and pair-wise comparisons were performed using Mann-Whitney-U statistics. The groups used for statistical testing consisted of normal CBA mice (NCBA) at 3 months (Young; N=20) and 18 months (Old; N=18) and CBA kidneys that had been transplanted into B6 recipients

(Young CBA donors: N=7 at D7 and N=8 at D21; Old CBA donors: N=6 at D7 and N=7 at D21). All values are given as mean (M)  $\pm$  standard deviation (SD).

### 6.3 Results

To study the effect of ischemia-reperfusion and rejection for Old donor kidneys, I chose a renal transplant model. In this model transplantation is performed between two fully MHC mismatched mouse strains and without the use of immunosuppressive agents to ensure the occurrence of rejection.

#### 6.3.1 Histopathology

##### 6.3.1.1 Normal CBA mice

None of the Young NCBA mice had features consistent with aging or suggesting renal diseases (table 6.2). Four of the 18 Old NCBA showed tubular atrophy in less than 5% of the area of cortical tubules. None of the Old NCBA mice showed features consistent with renal disease. There were no significant differences in tubular diameter (table 6.3; figure 6.1) or number of nuclei per tubular cross section (table 6.3; figure 6.2). Representative pictures of tubular cross sections are shown in figure 6.3.

### 6.3.1.2 CBA mice at day 7 after renal transplantation

At day 7 both age groups developed lesions characteristic for rejecting transplants (table 6.2). There were no differences between the acute features such as tubulitis, interstitial infiltrate, glomerulitis, vasculitis, peritubular capillary congestion. Tubulitis showed a trend towards a higher score in Old mice ( $1.0 \pm 0$ , i.e. all 6 mice had a tubulitis score of 1) when compared to Young mice ( $0.6 \pm 0.5$ , i.e. 4 of 7 mice had a tubulitis score of 1). The tubulitis score in Old mice was even higher when atrophic tubules were included ( $1.2 \pm 0.4$ ), but still did not differ significantly from Young mice. Necrosis was not found in any of the Young kidney transplants and was very mild (5%) in 2 of the Old mice. Thrombosis (either arterial or venous), edema, or casts were not found in any of the two age groups. The most striking difference between Young and Old mice at day 7 was the amount of tubular basement membrane wrinkling (table 6.3; figure 6.4). Tubular basement membrane wrinkling appeared and was much more frequent in Old mice ( $60\% \pm 28\%$ ;  $P < 0.01$  when compared to Old NCBA) when compared to Young mice ( $4\% \pm 5\%$ ). The higher score for tubular atrophy in Old transplants also reflects the higher amount of basement membrane wrinkling. Old transplants showed a reduced tubular diameter ( $P < 0.01$  vs. Young D7 or Old NCBA) and lower number of nuclei per tubular cross section ( $P < 0.05$  vs. Young D7; N.S. vs. Old NCBA) (table 6.3 and figures 6.1 and 6.2). No other chronic features were found in either Old or Young

transplants.

#### 6.3.1.2 CBA mice at day 21 after renal transplantation

At day 21 both age groups showed all the acute features of rejection (table 6.2). Interstitial infiltrate, glomerulitis and peritubular capillary congestion did not change when compared to day 7. The amount of vasculitis significantly increased in both groups (Old,  $P < 0.05$ ; Young,  $P < 0.05$ ). Tubulitis increased only in Young transplants ( $P < 0.005$ ). Edema significantly increased in both groups, it was present in 4 Old ( $P < 0.05$ ) and in 5 Young transplants ( $P < 0.05$ ). Necrosis was found in 2 of the Old and in 3 of the Young mice. Casts were only found in 3 Young transplants. Arterial or venous thrombosis was not present in any of the two age groups. Old mice showed 64% ( $\pm 31\%$ ) and Young mice showed 44% ( $\pm 41\%$ ) tubular basement membrane wrinkling (comparison Old vs. Young N.S.) (table 6.3; figure 6.5). Both groups developed interstitial fibrosis (Old:  $P < 0.005$ ; Young:  $P < 0.005$  when compared to D7). The amount of tubular atrophy increased further in Old transplants ( $P < 0.05$  when compared to Old D7) and became detectable in Young transplants ( $P < 0.005$  when compared to Young D7). There was no significant difference for the amount of interstitial fibrosis or tubular atrophy between Old and Young transplants. The number of cells per tubular cross section and the tubular diameter further decreased in Old transplants (table 6.3 and figures 6.1 and 6.2). Old transplants had a

significantly fewer cells per tubular cross section ( $P < 0.005$ ) and their tubular diameter tended to be smaller ( $P = 0.06$ ), especially if they were wrinkled ( $P < 0.005$  when compared to diameter from wrinkled tubules in Young transplants).

### 6.3.2 RT-PCR for senescence-associated genes

#### 6.3.2.1 Normal CBA mice

$P16^{\text{INK4a}}$  (figure 6.6) and  $p19^{\text{ARF}}$  (figure 6.7) mRNA expression were significantly higher in kidneys from Old NCBA when compared to Young ( $p16^{\text{INK4a}}$ : 13.2 fold;  $P < 0.001$ ;  $p19^{\text{ARF}}$ : 4 fold;  $P < 0.001$ ).

#### 6.3.1.2 CBA mice at day 7 after renal transplantation

$P16^{\text{INK4a}}$  mRNA and  $p19^{\text{ARF}}$  mRNA expression increased significantly in transplants from Old mice (both  $P < 0.05$ , figures 6.6 and 6.7), whereas in Young transplants they did not. The difference for  $p16^{\text{INK4a}}$  and  $p19^{\text{ARF}}$  between Old and Young transplants was significant ( $p16^{\text{INK4a}}$ :  $P < 0.05$ ;  $p19^{\text{ARF}}$ :  $P < 0.001$ ).

#### 6.3.1.3 CBA mice at day 21 after renal transplantation

$P16^{\text{INK4a}}$  mRNA and  $p19^{\text{ARF}}$  mRNA expression further increased in transplants from Old mice ( $P16^{\text{INK4a}}$ ,  $P < 0.05$ , figure 6.6;  $p19^{\text{ARF}}$ ,  $P < 0.001$  figure 6.7; when compared to day 7). In addition,  $p16^{\text{INK4a}}$  mRNA and



p19<sup>ARF</sup> mRNA expression also increased in Young mice (P16<sup>INK4a</sup>, P<0.001, figure 6.6; p19<sup>ARF</sup>, P<0.001, figure 6.7; when compared to day 7). There was no longer a difference for p16<sup>INK4a</sup> and p19<sup>ARF</sup> mRNA expression between Old and Young transplants.

### 6.3.3 P16<sup>INK4a</sup> staining

#### 6.3.3.1 Normal CBA mice

P16<sup>INK4a</sup> staining was found in nuclei of distal tubules and collecting duct, podocytes and parietal epithelium of glomeruli, vascular smooth muscle cells and interstitial cells. The nuclear staining was assessed for tubular (figure 6.9), glomerular (figure 6.10) and interstitial cells (figure 6.11). The amount of p16<sup>INK4a</sup> staining was higher for Old NCBA in all three compartments (4.7 fold in tubules, 2.4 fold in glomeruli, 3.3 fold in interstitium when compared to Young NCBA), but the difference was only significant for tubular cells (P<0.001).

#### 6.3.3.2 CBA mice at day 7 after renal transplantation

P16<sup>INK4a</sup> staining was more difficult to assess in transplants as compared to native kidneys. The restriction was that I could not always be certain whether a nucleus belonged to a tubular cell or a podocyte and was not just an infiltrating lymphocyte. With this limitation the percentage p16<sup>INK4a</sup> positive nuclei increased in all three compartments in Old and

Young transplants but without reaching significance (figures 6.8-6.10). The percentage of p16<sup>INK4a</sup> positive nuclei in tubules in Old transplants was significantly higher when compared to Young (P=0.001).

#### 6.3.3.3 CBA mice at day 21 after renal transplantation

In tubular cells, the percentage p16<sup>INK4a</sup> positive nuclei in Old transplants stayed the same, whereas in Young transplants the percentage p16<sup>INK4a</sup> positive nuclei increased significantly (P<0.05 when compared to D7; figure 6.8). The percentage of p16<sup>INK4a</sup> positive nuclei in glomeruli or interstitium increased in both groups when compared to day 7 (glomeruli: Old, N.S.; Young, P<0.05, figure 6.9; interstitium: Old, N.S.; Young, N.S., figure 6.10). Old transplants tended towards higher expression for all three compartments but this difference was not statistically significant.

#### 6.3.4 MHC class I and II staining

##### 6.3.4.1 Normal CBA mice

Staining for class I (H-2K) and class II (I-A<sup>k</sup>) did not significantly differ between both age groups (table 6.4). In tubular cells, class I and II showed a trend towards lower levels in Old NCBA.

##### 6.3.4.2 MHC expression in CBA mice at day 7 after renal transplantation

Donor (CBA) class I and II increased in both Old and Young at day 7

after transplantation (table 6.4). The increases were observed in tubular cells (class I: Old,  $P < 0.01$ , Young, N.S.; class II: Old,  $P < 0.005$ , Young,  $P < 0.005$ ). There were no differences between Old and Young D7 transplants in donor class I and II expression. Recipient (B6) class I (H-2K<sup>b</sup>) and II (I-A<sup>b</sup>) increased for Old and Young transplants at day 7 (table 6.4). The increases were observed in interstitial cells (class I: Old,  $P < 0.001$ , Young,  $P < 0.001$ ; class II: Old,  $P < 0.001$ , Young,  $P < 0.001$ ). There were no differences between recipient class I and II expression between Old and Young D7 transplants.

#### 6.3.4.3 CBA mice at day 21 after renal transplantation

Donor (CBA) class I did not change in either Old or Young at day 21 after transplantation when compared to day 7, but was slightly higher in Old transplants when compared to Young ( $P < 0.05$ ) (table 6.4). Donor class II decreased in Old transplants when compared to day 7 ( $P < 0.05$ ). Donor class II showed a similar trend (which was not significant) for Young transplants. Recipient (B6) class I and II did not change significantly in either Old or Young transplants at day 21 (table 6.4).

### 6.3.5 Cytology and number of infiltrating lymphocytes

#### 6.3.5.1 Normal CBA mice

Infiltrating lymphocytes were very rarely found in any of the normal

mice (table 6.5).

#### 6.3.5.2 CBA mice at day 7 after renal transplantation

CD45 (total lymphocytes), CD3 (T cells), CD4 (T helper cells) and CD8 (cytotoxic T cells) positive cells increased significantly in both Old and Young transplants at day 7 (table 6.5). There were no differences in the amount of infiltrating cells between Old and Young transplants. T cells were the major contributor to the infiltrate, reflected by CD3 positive cells accounting for 80% or 79% of the CD45 positive cells.

#### 6.3.5.3 CBA mice at day 21 after renal transplantation

The number of infiltrating cells decreased for all subsets and in both Old and Young transplants at day 21 (table 6.5). Since the Banff score (table 6.2) for interstitial infiltrate did not suggest a decrease in infiltrating cells, this is probably due to a technical problem with this experiment resulting in lower sensitivity. With this limitation in mind, the results suggest that there were no differences in the amount of infiltrating cells between both groups. This interpretation is supported by the Banff score for interstitial infiltrate that was similar for both groups (table 6.2).

### 6.3.6 RT-PCR for Granzyme B, Perforin and IFN- $\gamma$

#### 6.3.6.1 Normal CBA mice

Messenger RNA expression for both cytotoxic T cell genes (granzyme B, figure 6.11; perforin, figure 6.12) and IFN- $\gamma$  (figure 6.13) were very low in both Old and Young normal CBA and did not show any significant differences between the age groups.

#### 6.3.6.2 CBA mice at day 7 after renal transplantation

Messenger RNA expression for both cytotoxic T cell genes (granzyme B, figure 6.11; perforin, figure 6.12) and IFN- $\gamma$  (figure 6.13) increased significantly in Old and Young transplants (granzyme B: Old,  $P < 0.001$ , Young,  $P < 0.001$ ; perforin: Old,  $P < 0.001$ , Young,  $P < 0.001$ ; IFN- $\gamma$ : Old,  $P < 0.001$ , Young  $P < 0.001$ ). There were no differences in expression levels between both age groups.

#### 6.3.6.3 CBA mice at day 21 after renal transplantation

Messenger RNA expression for granzyme B (figure 6.11) and IFN- $\gamma$  (figure 6.13) decreased significantly in Old and Young transplants when compared to day 7 (granzyme B: Old,  $P < 0.001$ , Young,  $P < 0.001$ ; IFN- $\gamma$ : Old,  $P < 0.005$ , Young  $P < 0.05$ ). Changes in perforin were not significant in either age group (figure 6.12). There were no differences in expression levels between both age groups.

## 6.4 Discussion

I have studied a mouse model that mimics two processes during clinical transplantation: ischemia-reperfusion injury and acute rejection. I found that transplantation induced p16<sup>INK4a</sup> and p19<sup>ARF</sup> mRNA and p16<sup>INK4a</sup> protein expression. This induction was present in Old donors already at day 7 after transplantation. Transplantation also resulted in a faster development of features of tubular atrophy in kidneys from Old donors when compared to Young donors. At day 7, Old donor kidneys had developed more tubular basement membrane wrinkling and smaller tubular diameter consistent with more tubular atrophy. Old donor kidneys lost tubular cells during the whole time course after transplantation whereas the number of tubular cells was consistent in donor kidneys from Young mice.

The increases in p16<sup>INK4a</sup> probably reflect both the response to the peri- and post transplant stresses as well as the need for increased replication. The induction of p16<sup>INK4a</sup> in Old donors at day 7 was about 7-fold higher compared to Young donors and was additive to the preexisting higher p16<sup>INK4a</sup> expression in Old normal CBA mice. The changes at day 7 reflect the damage caused by acute rejection, and possibly by ischemia-reperfusion and related stresses of the surgery itself. Since p16<sup>INK4a</sup> positive cells have irreversibly arrested and are therefore no longer capable of replication, this data suggests that 7 days after transplantation Old donor kidneys already have a significantly lower capability to withstand stresses

and to repair. Twenty-one days after transplantation, p16<sup>INK4a</sup> was increased in both Old and Young transplants consistent with the idea that ongoing acute rejection with increased need for replication will result in an exhaustion of the replicative potential also in Young donors.

Another mediator of cell cycle arrest, p19<sup>ARF</sup>, was increased after transplantation. In my former studies (chapter 4), I had shown that the association of p19<sup>ARF</sup> with senescence had been much weaker when compared to p16<sup>INK4a</sup>. This was confirmed by this data showing only a 4-fold difference for p19<sup>ARF</sup> between Old and Young NCBA (compared to a 13.2-fold difference in p16<sup>INK4a</sup>). After transplantation, the increase for p19<sup>ARF</sup> at day 7 was similar for Old and Young transplants. At day 21, the increase seen for Young transplants significantly exceeded the increase in Old transplants. Since I have not performed staining for p19<sup>ARF</sup>, I do not know how much of the increase is due to expression of p19<sup>ARF</sup> by tubular cells or infiltrating leukocytes.

The faster development of histopathological features of atrophy and cell loss reflects the lower capacity of Old donor kidneys compared to Young donor kidneys to withstand peri- and posttransplant stresses. These changes may be due to excessive cell death or shedding, or decreased cell replacement. My data is consistent with the conclusion that acute rejection has a greater impact in Old than in Young donor kidney but this was not due to differences in recipient's immune response towards the old organ or

donor's immunogenicity. This is in contrast to data from the human population that had suggested a greater impact of acute rejection due to higher immunogenicity of old donors (27). All parameters assessing the immunogenicity of the transplant as well as the activity of the recipient's immune response were indistinguishable between Old and Young transplants. In addition, gene array studies that I am currently performing support this finding on a much larger scale of investigated genes. Therefore, I conclude that Old kidneys are not more immunogenic, but the old parenchyma shows a greater susceptibility to deterioration and atrophy when rejection occurs. That suggests that the reason for the worse outcome in Old donors is intrinsic to the donor and is a combination of the underlying senescent features as well as the developing chronic features together with the loss tubular cells. This results in a decreased capability of the old donors to repair peritransplant injuries and maintain organ mass.

My study supports the hypothesis that some mechanisms of cellular senescence are active in the transplantation process and might be limiting for the survival of transplants. However, it was beyond the scope of this study to mechanistically prove the importance of p16<sup>INK4a</sup> or p19<sup>ARF</sup>. Further studies have to prove the significance of the cell cycle arrest mediated by either of these genes for the limited ability of the old donor kidney to maintain organ function if challenged. Blockade of the p16<sup>INK4a</sup> or p19<sup>ARF</sup> pathways should prevent the histological changes seen in the Old



transplanted kidneys at day 7 and in the Young at day 21. This is supported by the observation that in absence of p21<sup>CIP1/WAF1</sup>, which is a cyclin-dependent kinase inhibitor and *in vitro* senescent marker, renal ablation does not result in progressive renal failure (28).

For clinical transplantation, my data suggests that minimizing the stresses towards old donor kidneys would help to improve outcome. This is consistent with the finding that old donor kidneys can function as well as their young counterparts if they do not experience acute rejection (27).

## 6.5 Tables

**Table 6.1:** Sequences for primers and probes used in Real-time PCR studies.

Name	Accession Number (GenBank)		Sequence (5'→3')
p16 <sup>INK4a</sup>	L76150	Forward primer	GGGCACTGCTGGAAGCC
		Reverse primer	AACGTTGCCCATCATCATCAC
		Probe	CCGAACTCTTTTCGGTCGTACCCCGAT
p19 <sup>ARF</sup>	L76092	Forward primer	TCGTGAACATGTTGTTGAGGCTA
		Reverse primer	GTTGCCCATCATCATCACCTG
		Probe	CGGTGCGGCCCTCTTCTCAAGATC
Granzyme B	M22526	Forward primer	CGATCAAGGATCAGCAGCCT
		Reverse primer	CTTGCTGGGTCTTCTCCTGTTCT
		Probe	TGCTGCTCACTGTGAAGGAAGTATAATAAA TGCTCACT
Perforin	M23182	Forward primer	GAAGACCTATCAGGACCAGTACAACCTT
		Reverse primer	CAAGGTGGAGTGGAGGTTTTTG
		Probe	ACCAGGCGAAAACCTGTACATGCGACACT
IFN- $\gamma$	M28621	Forward primer	AGCAACAGCAAGGCGAAAAA
		Reverse primer	AGCTCATTGAATGCTTGCCG
		Probe	ATTGCCAAGTTTGAGGTCAACAACCCACA
HPRT	J00423	Forward primer	TGACACTGGTAAAACAATGCAAACCT
		Reverse primer	AACAAAGTCTGGCCTGTATCCAA
		Probe	TTCACCAGCAAGCTTGCAACCTTAACC

**Table 6.2:** Histopathology for kidneys from CBA mice. Data is shown for normal mice prior to transplantation (NCBA) as well as 7 days (D7) and 21 days (D21) after transplantation.

	NCBA		D7		D21	
	Young	Old	Young	Old	Young	Old
Tubulitis	0	0	0.6 ± 0.5	1.0 ± 0.0	1.7 ± 0.5	1.1 ± 0.4
Interstitial infiltrate	0	0	2.4 ± 0.5	2.8 ± 0.4	2.8 ± 0.7	2.6 ± 0.8
Glomerulitis	0	0	0.9 ± 0.4	1.0 ± 0.6	0.9 ± 0.6	1.0 ± 0.0
Vasculitis	0	0	0.6 ± 0.5	0.7 ± 0.8	1.5 ± 0.5	1.6 ± 0.5
PTC	0	0	1.4 ± 3.8	1.7 ± 2.6	7.5 ± 17.5	5.7 ± 6.7
Necrosis	0	0	0	1.7 ± 2.6	2.5 ± 3.8	1.4 ± 2.4
Thrombosis	0	0	0	0	0	0
Edema	0	0	0	0	7.5 ± 7.6	6.4 ± 6.9
Casts	0	0	0	0	3.8 ± 5.2	0
Tubular atrophy	0	0	0	1.3 ± 0.5 <sup>a</sup>	1.6 ± 0.9	2.1 ± 0.7
Interstitial fibrosis	0	0	0	0	1.0 ± 0.5	1.1 ± 0.7

PTC, peritubular capillary congestion

<sup>a</sup>P<0.05 when compared to Young D7

**Table 6.3:** Basement membrane wrinkling, tubular diameter and cell number for kidneys from CBA mice. Data is shown for normal mice prior to transplantation (NCBA) as well as 7 days (D7) and 21 days (D21) after transplantation.

	NCBA		D7		D21	
	Young	Old	Young	Old	Young	Old
TBM wrinkling (%)	0	0	3.5 ± 5.4	60.4 ± 27.9	44.2 ± 41.1	63.9 ± 31.3
Tubular diameter						
all	1.4 ± .08	1.3 ± 0.1	1.4 ± .2	1.0 ± .09	1.2 ± 0.2	0.9 ± .06
wrinkled	0	0	ND	0.9 ± .09	1.0 ± .05	0.8 ± .06
normal	1.4 ± .08	1.3 ± 0.1	1.4 ± .2	1.1 ± 0.1	1.2 ± 0.2	1.1 ± .1
Nuclei per tubular cross section (#)						
all	3.9 ± 0.9	4.1 ± 0.8	4.5 ± 0.7	3.6 ± 0.5	4.2 ± 0.2	2.6 ± 0.7
wrinkled	0	0	ND	3.3 ± 0.7	3.7 ± 0.2	1.9 ± 1.1
normal	3.9 ± 0.9	4.1 ± 0.8	4.5 ± 0.7	3.9 ± 0.3	4.9 ± 0.8	3.9 ± 2.0

TBM, tubular basement membrane; "all", diameters or nuclei for all tubules in the 10 HPFs assessed were used to calculate the mean value for either diameter or number of nuclei; "wrinkled", diameters or nuclei for tubules that appeared to be wrinkled in the 10 HPFs assessed were used to calculate the mean value for either diameter or number of nuclei; "normal", diameters or nuclei for tubules that appeared to be normal in the 10 HPFs assessed were used to calculate the mean value for either diameter or number of nuclei; ND, not done, because the amount of wrinkled tubules at day 7 for Young transplants was too small;

**Table 6.4:** Donor (CBA) and recipient (B6) MHC class I and class II expression. Data is shown for normal mice prior to transplantation (NCBA) as well as 7 days (D7) and 21 days (D21) after transplantation. Donor MHC expression was assessed in tubules and recipient MHC for interstitium.

	NCBA		D7		D21	
	Young	Old	Young	Old	Young	Old
<b>Donor MHC</b>						
Class I	.67 ± 1.4	.14 ± .36	1.9 ± 1.8	2.0 ± 1.7	0.5 ± 1.4	1.8 ± 1.5
Class II	.17 ± .38	.08 ± .27	2.9 ± 2.0	2.2 ± 1.7	0.5 ± 1.4	1.5 ± 1.6
<b>Recipient MHC</b>						
Class I	0	0	3.4 ± 1.1	3.5 ± 0.8	2.8 ± 1.0	3.5 ± 0.8
Class II	0	0	2.3 ± 0.5	2.2 ± 1.2	3.1 ± 1.1	3.7 ± 0.8

**Table 6.5:** Cytology and cell counts for infiltrating lymphocytes. Data is shown for normal mice prior to transplantation (NCBA) as well as 7 days (D7) and 21 days (D21) after transplantation.

	NCBA		D7		D21	
	Young	Old	Young	Old	Young	Old
CD45	2 ± 3	4 ± 8	148 ± 80	138 ± 86	38 ± 5	30 ± 7
CD3	1 ± 4	0 ± 1	117 ± 68	111 ± 79	44 ± 6	43 ± 10
CD4	0 ± 1	0	47 ± 38	54 ± 61	3 ± 3	4 ± 3
CD8	1 ± 2	1 ± 2	113 ± 77	88 ± 67	20 ± 6	21 ± 8

## 6.6 Figures



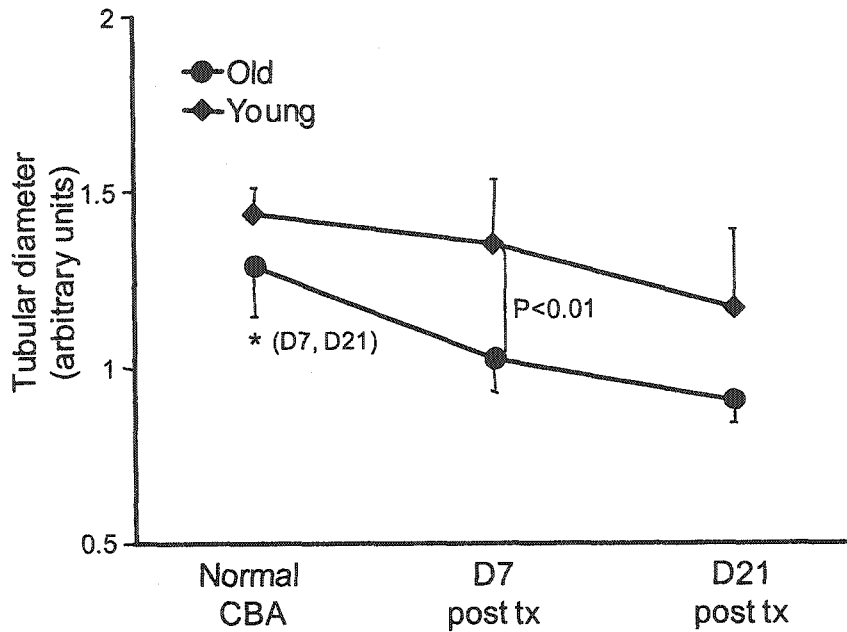


**Figure 6.1:** Tubular diameter for CBA kidneys. Normal CBA, prior to transplantation; D7, 7 days after transplantation, D21, 21 days after transplantation. Old kidneys (●), SD down; Young kidneys (◆), SD up. Significant differences are indicated.

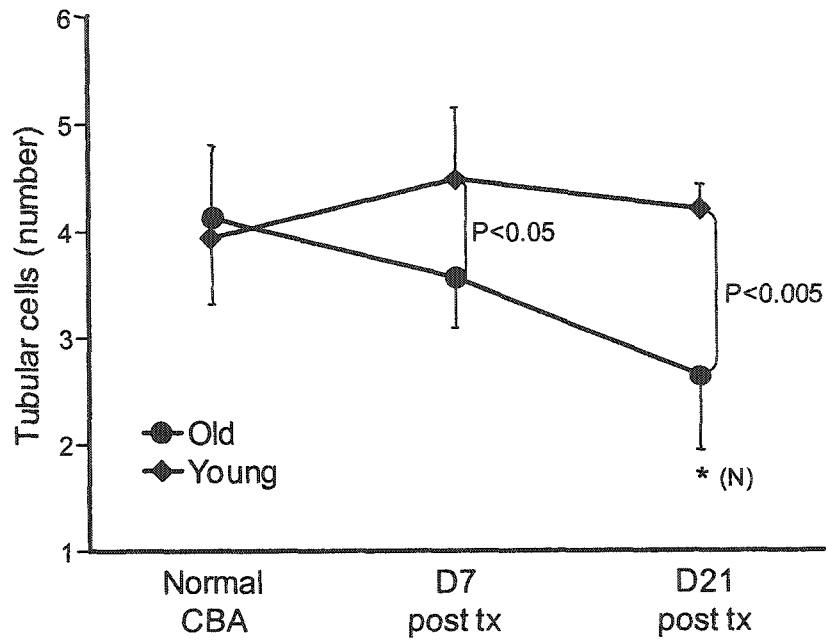
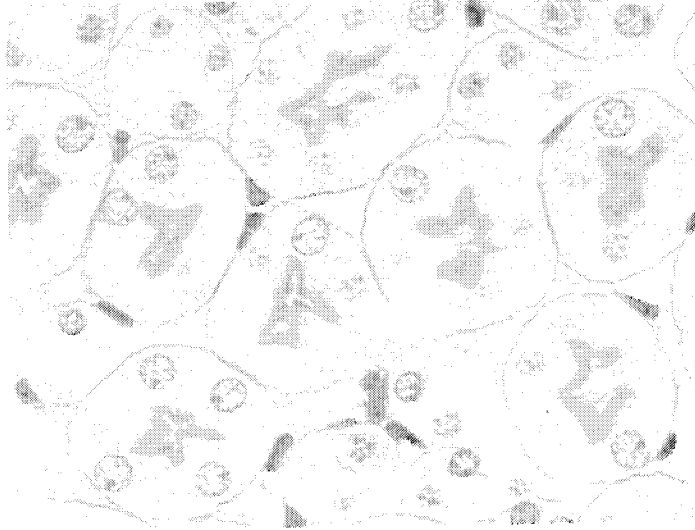


**Figure 6.2:** Number of cells per tubular cross section for CBA kidneys. Normal CBA, prior to transplantation; D7, 7 days after transplantation, D21, 21 days after transplantation. Old kidneys (●), SD down; Young kidneys (◆), SD up. Significant differences are indicated.

**A**



**B**

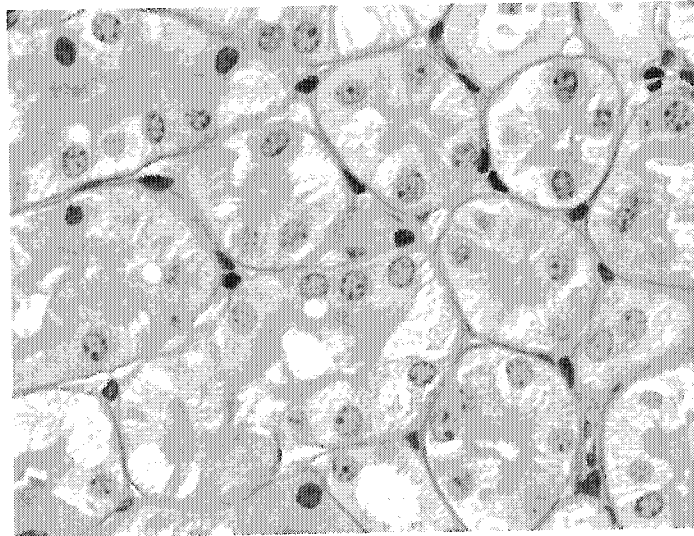
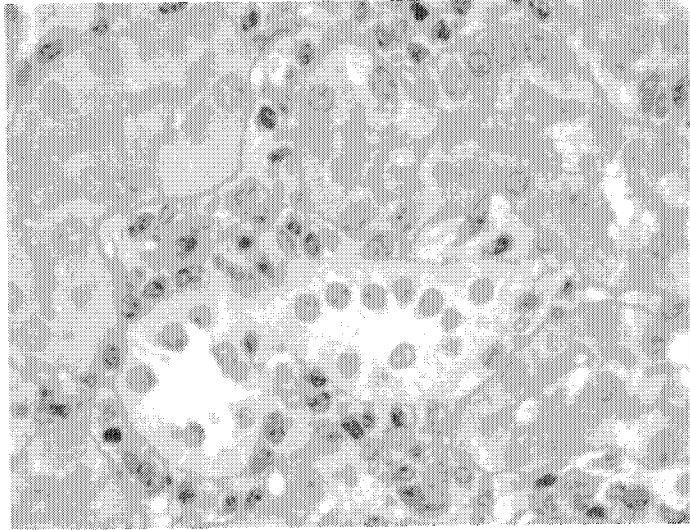


**Figure 6.3:** Tubular cross sections in normal CBA. (A) Young; (B) Old.

**A**



**B**

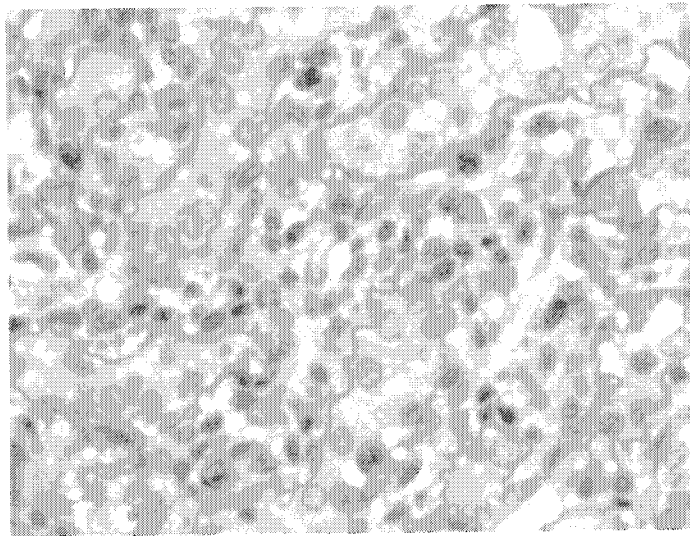
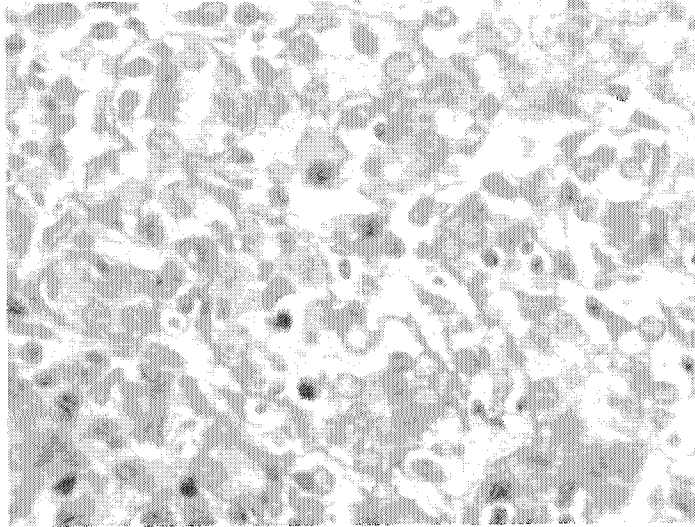


**Figure 6.4:** Tubular cross sections in CBA donors 7 days after transplantation. (A) Young; (B) Old.

A



B

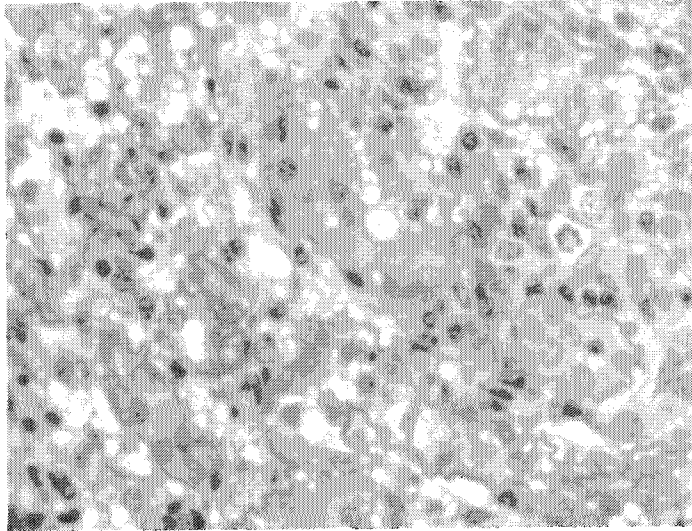


**Figure 6.5:** Tubular cross sections in CBA donors 21 days after transplantation. (A) Young; (B) Old.

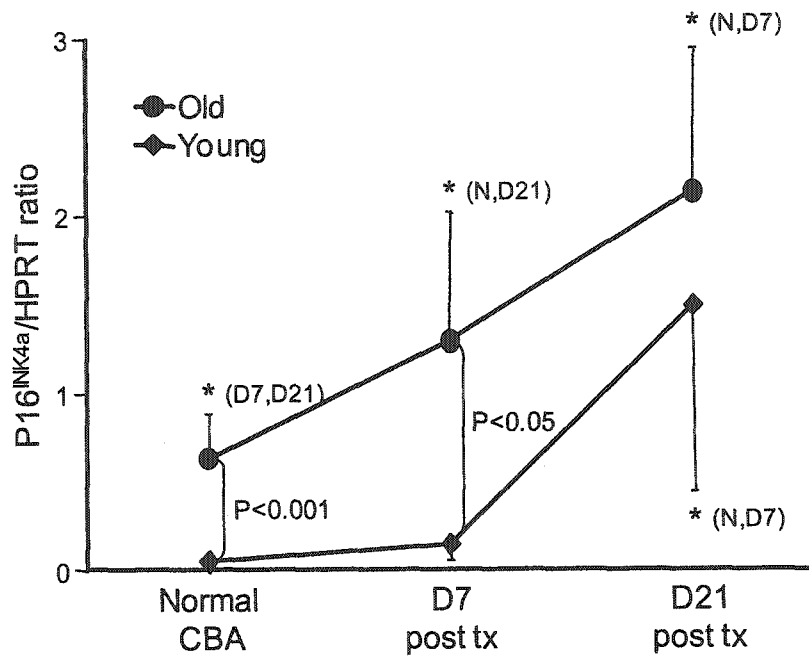


**Figure 6.6:** P16<sup>INK4a</sup> mRNA expression for CBA kidneys. Normal CBA, prior to transplantation; D7, 7 days after transplantation, D21, 21 days after transplantation. Values are given as p16<sup>INK4a</sup>/HPRT ratio. Old kidneys (●), SD up; Young kidneys (◆), SD down. Significant differences are indicated.

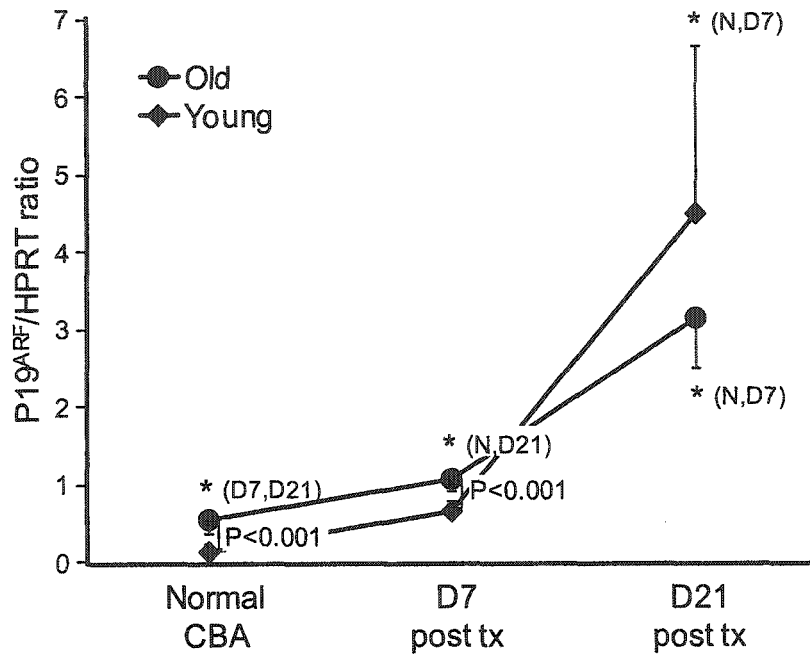


**Figure 6.7:** P19<sup>ARF</sup> mRNA expression for CBA kidneys. Normal CBA, prior to transplantation; D7, 7 days after transplantation, D21, 21 days after transplantation. Values are given as p19<sup>ARF</sup>/HPRT ratio. Old kidneys (●), SD down; Young kidneys (◆), SD up. Significant differences are indicated.

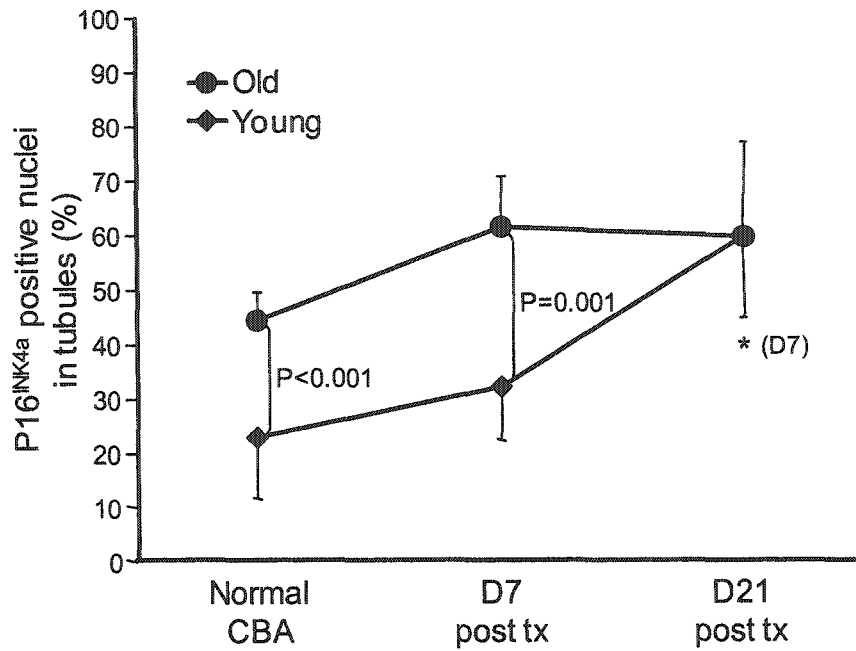


**Figure 6.8:** P16<sup>INK4a</sup> protein expression in tubular cells in renal cortex of CBA kidneys. Normal CBA, prior to transplantation; D7, 7 days after transplantation, D21, 21 days after transplantation. Old kidneys (●), SD up; Young kidneys (◆), SD down. Significant differences are indicated.



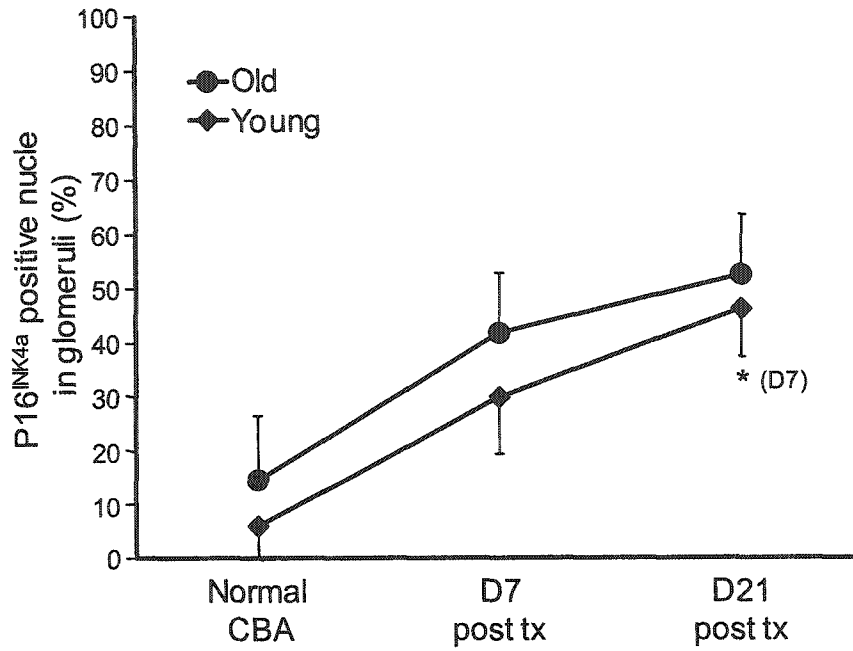


**Figure 6.9:** P16<sup>INK4a</sup> protein expression in glomeruli of CBA kidneys. Normal CBA, prior to transplantation; D7, 7 days after transplantation, D21, 21 days after transplantation. Old kidneys (●), SD up; Young kidneys (◆), SD down. Significant differences are indicated.

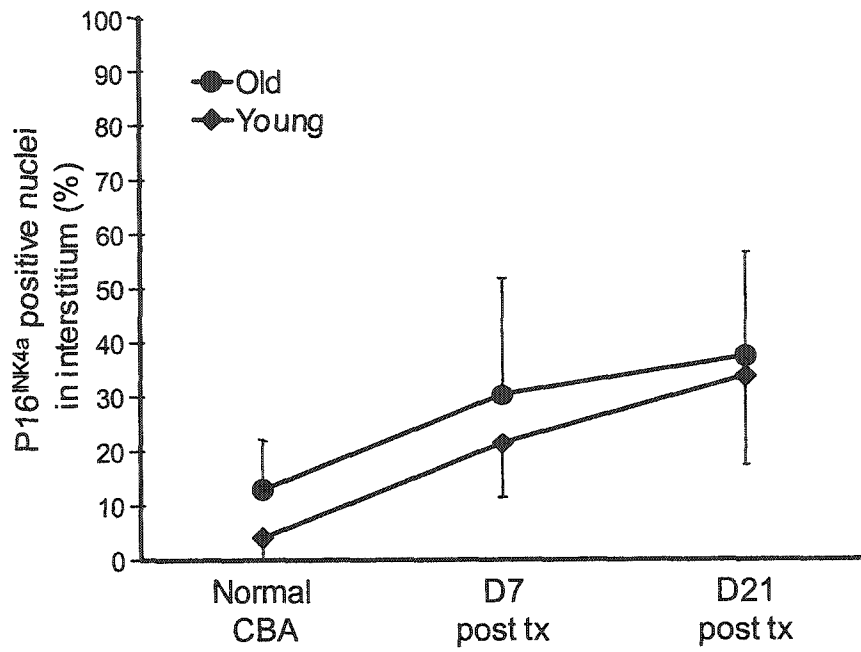


**Figure 6.10:** P16<sup>INK4a</sup> protein expression in interstitial cells in renal cortex of CBA kidneys. Normal CBA, prior to transplantation; D7, 7 days after transplantation, D21, 21 days after transplantation. Old kidneys (●), SD up; Young kidneys (◆), SD down.

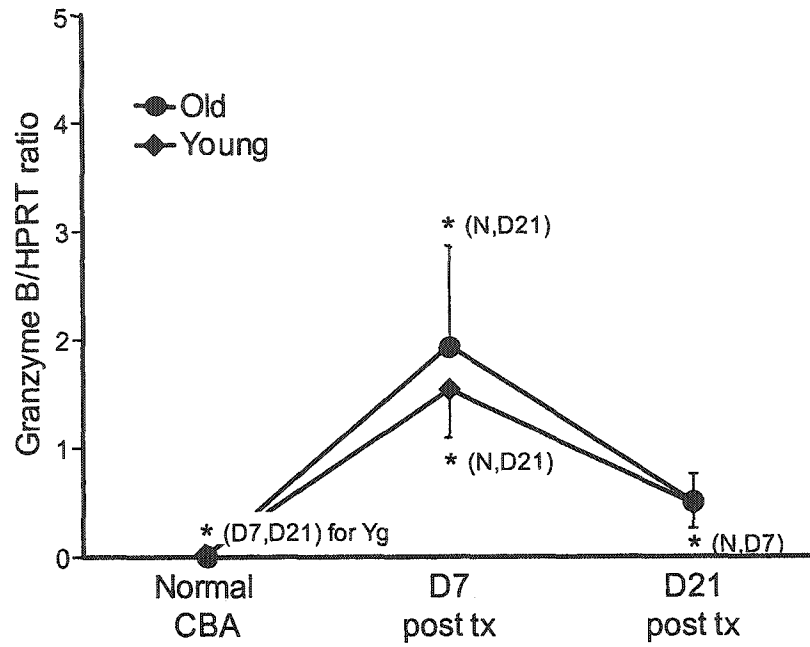


**Figure 6.11:** Granzyme B mRNA expression for CBA kidneys. Normal CBA, prior to transplantation; D7, 7 days after transplantation, D21, 21 days after transplantation; Yg, Young. Values are given as Granzyme B/HPRT ratio. Old kidneys (●), SD up; Young kidneys (◆), SD down. Significant differences are indicated.

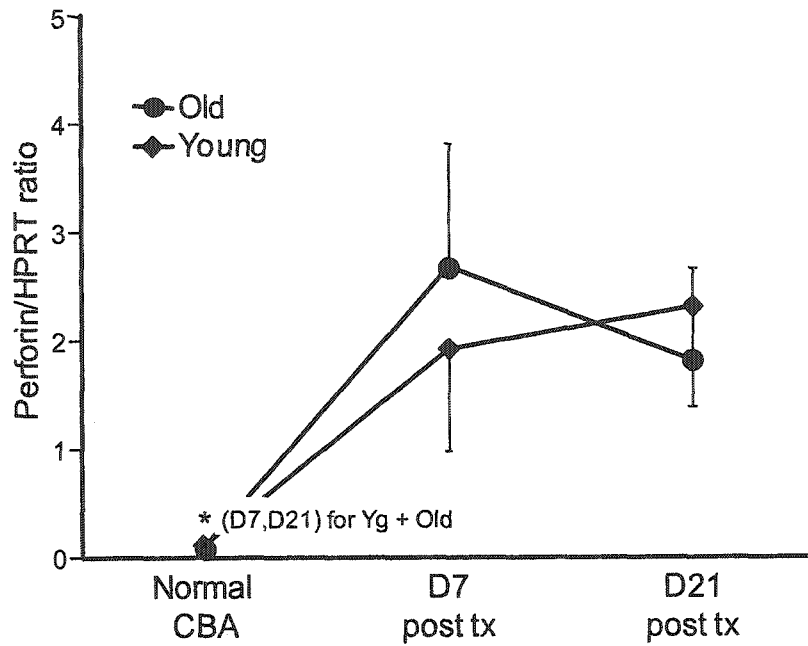


**Figure 6.12:** Perforin mRNA expression for CBA kidneys. Normal CBA, prior to transplantation; D7, 7 days after transplantation, D21, 21 days after transplantation; Yg, Young. Values are given as Granzyme B/HPRT ratio. Old kidneys (●), SD up; Young kidneys (◆), SD down. Significant differences are indicated.

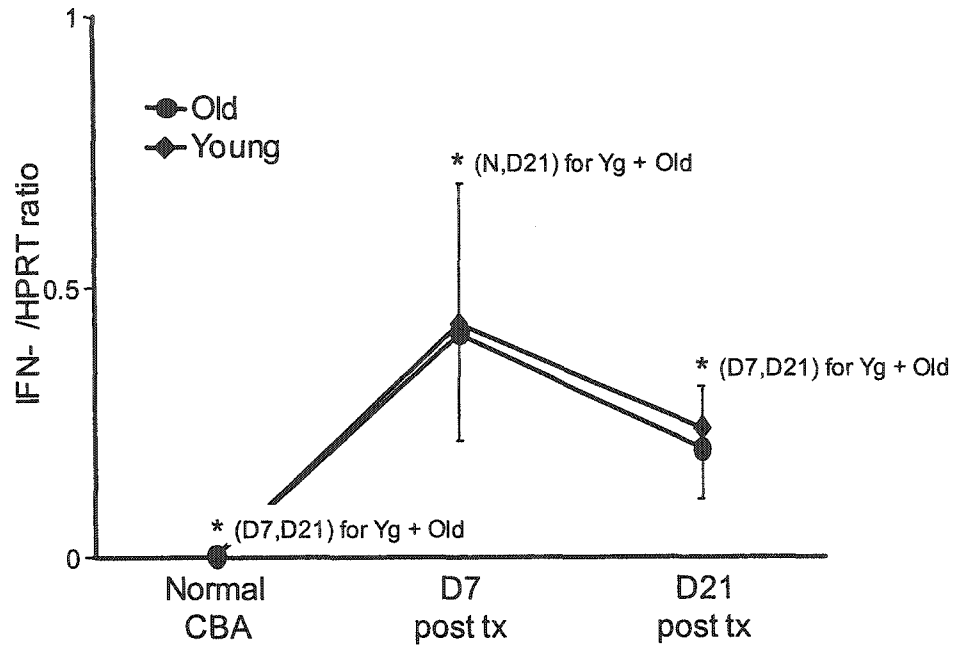


**Figure 6.13:** IFN- $\gamma$  mRNA expression for CBA kidneys. Normal CBA, prior to transplantation; D7, 7 days after transplantation, D21, 21 days after transplantation; Yg, Young. Values are given as IFN- $\gamma$ /HPRT ratio. Old kidneys ( $\bullet$ ), SD up; Young kidneys ( $\blacklozenge$ ), SD down. Significant differences are indicated.

## 6.7 References

1. Terasaki PI, Cecka JM, and Gjertson D.W.: *Impact analysis: a method for evaluating the impact of factors in clinical renal transplantation*. Clinical Transplants. Edited by Cecka JM and Terasaki PI. Los Angeles, CA, UCLA Tissue Typing Laboratory, 1998, pp. 437-441
2. Gjertson DW: *Determinants of long term survival of adult kidney transplants*. Clinical Transplants 1999. Edited by Terasaki P and Cecka JM. Los Angeles, CA, UCLA Immunogenetics Center, 2000, pp. 341-352
3. Cicciarelli J, Iwaki Y, and Mendenz R: *The influence of donor age on kidney graft survival in the 1990s*. Clinical Transplants. Edited by Cecka JM and Terasaki PI. Los Angeles, CA, UCLA Tissue Typing Laboratory, 1999, pp. 335-340
4. Prommool S, Jhangri GS, Cockfield SM, and Halloran PF: *Time dependency of factors affecting renal allograft survival*. J Am Soc Nephrol 2000, 11: 565-573
5. Toma H, Tanabe K, Tokumoto T, Shimizu T, and Shimmura H: *Time-dependent risk factors influencing the long-term outcome in living renal allografts: donor age is a crucial risk factor for long-term graft survival more than 5 years after transplantation*. Transplantation 2001, 72: 940-947
6. Melk A, Ramassar V, Helms LM, Moore R, Rayner D, Solez K, and Halloran PF: *Telomere shortening in kidneys with age*. J Am Soc Nephrol 2000, 11: 444-453
7. Melk A, Kittikowit W, Sandhu I, Halloran KM, Grimm P, Schmidt BMW, and Halloran PF: *Cell senescence in rat kidney in vivo increases with growth and age despite lack of telomere shortening*. Kidney Int 2003, 63: 2134-2143
8. Gasser M, Waaga AM, Laskowski IA, and Tilney NL: *The influence of donor brain death on short and long-term outcome of solid organ allografts*. Ann Transplant 2000, 5: 61-67
9. Cecka JM: *The UNOS scientific renal transplant registry - 2000*. Clinical Transplants. Edited by Cecka JM and Terasaki PI. Los Angeles, CA, UCLA Tissue Typing Laboratory, 2000, pp. 1-18
10. Gjertson DW: *Impact of delayed graft function and acute rejection on kidney graft survival*. Clinical Transplants. Edited by Cecka JM and Terasaki PI. Los Angeles, CA, UCLA Tissue Typing Laboratory, 2000, pp. 467-480

11. Halloran PF: Renal injury and preservation in transplantation. *Kidney Transplant Rejection*. Edited by Racusen LC and Solez K. New York, NY, Marcel Dekker, 1998, pp. 149-176
12. Halloran PF and Hunsicker LG: Delayed graft function: State of the Art, November 10-11, 2000. Summit Meeting, Scottsdale, Arizona, USA. *Am J Transplant* 2001, 1: 115-120
13. Weir MR, Ward MT, Blahut SA, Klassen DK, Cangro CB, Bartlett ST, and Fink JC: Long-term impact of discontinued or reduced calcineurin inhibitor in patients with chronic allograft nephropathy. *Kidney Int* 2001, 59: 1567-1573
14. Mange KC, Cizman B, Joffe M, and Feldman HI: Arterial hypertension and renal allograft survival. *JAMA* 2000, 283: 633-638
15. Wynn RF, Cross MA, Hatton C, Will AM, Lashford LS, Dexter TM, and Testa NG: Accelerated telomere shortening in young recipients of allogeneic bone-marrow transplants. *Lancet* 1998, 351: 178-181
16. Allsopp RC, Cheshier S, and Weissman IL: Telomere shortening accompanies increased cell cycle activity during serial transplantation of hematopoietic stem cells. *J Exp Med* 2001, 193: 917-924
17. Wright WE and Shay JW: Historical claims and current interpretations of replicative aging. *Nature Biotechnology* 2002, 20: 682-688
18. Zindy F, Quelle DE, Roussel MF, and Sherr CJ: Expression of the p16INK4a tumor suppressor versus other INK4 family members during mouse development and aging. *Oncogene* 1997, 15: 203-211
19. Palmero I, McConnell B, Parry D, Brookes S, Hara E, Bates S, Jat P, and Peters G: Accumulation of p16INK4a in mouse fibroblasts as a function of replicative senescence and not of retinoblastoma gene status. *Oncogene* 1997, 15: 495-503
20. Carnero A, Hudson JD, Price CM, and Beach DH: p16(INK4A) and p19(ARF) act in overlapping pathways in cellular immortalization. *Nature Cell Biology* 2000, 2: 148-155
21. Kamijo T, Zindy F, Roussel MF, Quelle DE, Downing JR, Ashmun RA, Grosveld G, and Sherr CJ: Tumor suppression at the mouse *INK4a* locus mediated by the alternative reading frame product p19<sup>ARF</sup>. *Cell* 1997, 91: 649-659
22. Quelle DE, Zindy F, Ashmun RA, and Sherr CJ: Alternative reading frames of the INK4a tumor suppressor gene encode two unrelated proteins capable of inducing cell cycle arrest. *Cell* 1995, 83: 993-1000

23. Afrouzian M, Ramassar V, Urmson J, Zhu LF, and Halloran PF: Transcription Factor IRF-1 in Kidney Transplants Mediates Resistance to Graft Necrosis during Rejection. *J Am Soc Nephrol* 2002, 13: 1199-1209
24. Racusen LC, Solez K, Colvin RB, Bonsib SM, Castro MC, Cavallo T, Croker BP, Demetris AJ, Drachenberg CB, Fogo AB, Furness P, Gaber LW, Gibson IW, Glotz D, Goldberg JC, Grande J, Halloran PF, Hansen HE, Hartley B, Hayry PJ, Hill CM, Hoffman EO, Hunsicker LG, Lindblad AS, Marcussen N, Mihatsch MJ, Nadasdy T, Nickerson P, Olsen TS, Papadimitriou JC, Randhawa PS, Rayner DC, Roberts I, Rose S, Rush D, Salinas-Madrigal L, Salomon DR, Sund S, Taskinen E, Trpkov K, and Yamaguchi Y: The Banff 97 working classification of renal allograft pathology. *Kidney Int* 1999, 55: 713-723
25. Chirgwin JM, Przybyla AE, MacDonald RJ, and Rutter WJ: Isolation of biologically active ribonucleic acid from sources enriched in ribonuclease. *Biochemistry* 1979, 18: 5294-5299
26. Heid CA, Stevens J, Livak KJ, and Williams PM: Real time quantitative PCR. *Genome Res* 1996, 6: 986-994
27. de Fijter JW, Mallat MJ, Doxiadis II, Ringers J, Rosendaal FR, Claas FH, and Paul LC: Increased immunogenicity and cause of graft loss of old donor kidneys. *J Am Soc Nephrol* 2001, 12: 1538-1546
28. Megyesi J, Price PM, Tamayo E, and Safirstein RL: The lack of functional  $p21^{WAF1/CIP1}$  gene ameliorates progression to chronic renal failure. *Proc Natl Acad Sci USA* 1999, 96: 10830-10835



## Chapter 7

### P16<sup>INK4a</sup> Expression Increases in Human Allograft Nephropathy Biopsies

A version of this chapter will be submitted for publication.

Anette Melk, Bernhard M.W. Schmidt, Attapong Vongwiwatana, Patricia Campbell, David Rayner, and Philip F. Halloran: Increased p16<sup>INK4a</sup> expression in chronic renal diseases.

Portions of this publication that were contributed by co-authors are not included unless noted.

## 7.1 Introduction

Our group had hypothesized that one element in the pathophysiology of allograft nephropathy (AN) could be accelerated somatic cell senescence (1). This hypothesis was based on the clinical observation that the donor is a major predictor of long-term graft survival after kidney transplantation (2-6). Further evidence in favor of this hypothesis was the histological features found in AN: tubular atrophy, interstitial fibrosis and fibrous intimal thickening (7). These lesions can also be seen in old native kidneys (8). Our hypothesis was that peri- and posttransplant stresses might lead to changes that are related to those that occur from environmental stresses in normal aging over a longer period of time (“a lifetime”). However, these changes would occur at a faster pace. They would be additional to already preexisting age-changes in older transplants and thereby have more deleterious effects in kidneys from older donors.

Peritransplant stresses are related to brain death (9;10), preservation, cold and warm ischemia and reperfusion (11;12). A high load of peritransplant stresses leads to delayed graft function (13). The most important posttransplant stresses are immunologic and cardiovascular. Rejection episodes as well as immunosuppressive treatment itself due to drug toxicity (especially calcineurin inhibitors) (14) alter renal function. Hypertension often occurs in transplant patients and correlates with decreased renal function (15). These stress-induced changes add to the

already preexisting senescence changes of the kidney and might be responsible for organ failure.

In my studies in human (chapter 2 and 5) (16) and rodent (chapter 3 and 4) (17), I have shown that aged kidneys *in vivo* show some of the mechanisms used by cultured cells that undergo senescence *in vitro*. In addition, I was able to demonstrate that certain transplant stresses (ischemia-reperfusion and rejection) lead to greater deterioration and atrophy in old mouse kidneys when compared to young mouse kidneys (chapter 6). The fact that the overall expression of senescence marker p16<sup>INK4a</sup> was always higher in old when compared to young mice suggested that this may be the reason for the limitations of the old parenchyma to withstand peritransplant injuries.

P16<sup>INK4a</sup> as effector molecule in “stimulation and stress-induced senescent-like arrest” (STASIS) (18). It might be also important in replicative senescence, as a downstream signal after critical telomere shortening or telomere dysfunction. Mouse embryonic fibroblasts (MEFs) in culture cease cycling independent of telomere length (19). This phenotype of MEFs is caused by environmental stresses (“culture shock”) (20) and the accompanied irreversible cell cycle arrest is mediated by p16<sup>INK4a</sup> (21-24;24;25).

To examine the hypothesis that AN is accompanied by accelerated senescence, I compared p16<sup>INK4a</sup> protein expression in human renal

transplant biopsies taken at the time of transplantation with a biopsy of the same kidney diagnosed with AN.

## 7.2 Material and Methods

### 7.2.1 Biopsies

Biopsies were taken at the time of transplantation after reperfusion of the kidney (implantation biopsy) and during follow up of the patients as a diagnostic tool in patients that presented with rising creatinine levels. Biopsies were fixed in 10% buffered formalin and paraffin embedded.

### 7.2.2 Immunoperoxidase staining for p16<sup>INK4a</sup>

Immunoperoxidase staining for p16<sup>INK4a</sup> was performed using 2 $\mu$ m sections of paraffin embedded tissue. Briefly, sections were deparaffinized and hydrated. The sections were immersed in 3% H<sub>2</sub>O<sub>2</sub> in methanol to inactivate endogenous peroxidase. Slides were blocked with 20% normal goat serum. Tissue sections were then incubated for 1 hr at RT with the primary antibody (mouse monoclonal antibody, Clone F-12, Santa Cruz Biotechnologies, Santa Cruz, CA) and rinsed with PBS. Following 30 minutes of incubation with the Envision monoclonal system (Dako, Mississauga, Ontario), sections were washed again in PBS. Visualization was performed using the DAB substrate kit (Dako, Mississauga, Ontario). The slides were counterstained with hematoxylin and mounted. Analysis

was done by counting 10 high power fields (HPFs). Percentage of positive nuclei was assessed for tubules, glomeruli, interstitium and arteries. Cytoplasmic staining was assessed by counting the percentage of tubular cross sections that showed p16<sup>INK4a</sup> positive staining of the cytoplasm.

### 7.2.3 Statistical analysis

Data analyses were performed using SPSS. Comparison of p16<sup>INK4a</sup> expression in the implantation biopsy and in the biopsy showing AN were compared using paired T-test. The level of significance was set at  $p < 0.05$ . All values are given as mean  $\pm$  standard deviation (SD).

## 7.3 Results

### 7.3.1 Demographic data

A total of 14 patients were included in the study. All patients had received a renal transplant for treatment of end stage renal disease between 1988 and 1998. The patients were selected from the clinical transplant data base by the following criteria: biopsy proven diagnosis of allograft nephropathy between October 1998 and June 2000, the least acute changes possible and availability of an additional paraffin embedded specimens obtained at the time of transplantation.

Ten patients were male, 4 female. Eleven patients had received cadaveric kidneys and 3 living related donation. The donor age was  $35.4 \pm$

13.4. The oldest and youngest donors were 59 and 19 years old, respectively. The patient age at time of the diagnostic biopsy was  $46.2 \pm 15.1$  years and the time elapsed since transplantation was  $4.8 \pm 3.5$  years. Serum creatinine at time of AN biopsy was  $247 \pm 90$   $\mu\text{mol/L}$ . (table 7.1)

### 7.3.2 Histology

All biopsies were graded according to the Banff classification (26). The kidneys at the time of transplantation showed few, if any pathological changes. This reflects the selection criteria of a kidney for transplantation.

The biopsies that were diagnostic for AN showed intense chronic changes. Tubular atrophy, interstitial fibrosis and vascular changes occurred to a similar extent. Transplant glomerulopathy was present in 3 of the 14 biopsies (table 7.2). In conclusion, the histological changes seen were typical for AN.

### 7.3.3. P16<sup>INK4a</sup> protein expression

P16<sup>INK4a</sup> protein expression was assessed using immunohistochemistry. P16<sup>INK4a</sup> staining was found in nuclei of distal tubules and collecting duct, podocytes and parietal epithelium of glomeruli, vascular smooth muscle cells and interstitial cells. In addition to the nuclear staining, a patchy cytoplasmic staining occurred in all parts of the nephron. The extent of this cytoplasmic staining was higher than in every normal old

kidney, which I reported previously (figure 7.1 and 7.2). Thus the changes were qualitatively similar but quantitatively greater than the changes observed in kidney with normal aging.

The nuclear staining was assessed in tubular, glomerular and interstitial cells as well as in arteries. In implantation biopsies  $16.7 \pm 14.3$  % of tubular nuclei showed p16<sup>INK4a</sup> staining, whereas AN biopsies showed  $53.3 \pm 13.5$  % ( $P < 0.001$ ; figure 7.3). The same tendency was seen in glomerular (figure 7.4) and interstitial nuclei (figure 7.5): p16<sup>INK4a</sup> positive cells increased from  $12.3 \pm 16.2$  % and  $7.7 \pm 11.3$  % to  $64.1 \pm 12.4$  and  $54.3 \pm 18.6$  %, respectively (both  $P < 0.001$ ). P16<sup>INK4a</sup> staining in vascular smooth muscle cells of arteries increased in all but one patient ( $7.0 \pm 21.4$  % to  $55.5 \pm 19.1$  %; figure 7.6).

The cytoplasmic staining was expressed as the percentage of tubular crosssections showing p16<sup>INK4a</sup> in the cytoplasm. This percentage increased in all but two patients ( $17.0 \pm 23.7$  % to  $59.5 \pm 21.9$  %; figure 7.7).

#### 7.4 Discussion

Our group had hypothesized that renal senescence could be an important pathomechanism of AN (27) and probably other renal diseases. Preexisting senescent changes might limit the ability of a transplant to cope with peri- and posttransplant stresses and these stresses might induce

accelerated senescence. In my previous studies, I have shown that changes seen in the *in vitro* phenotype of cellular senescence occur in the aging kidney in humans (chapter 2 and 5) (28) and in rodents (chapter 3 and 4) (17). Furthermore, I showed that acute rejection in a mouse model of renal transplantation induced the expression of p16<sup>INK4a</sup>, known to be an important mediator of somatic cell senescence *in vitro* (chapter 6). In the study presented here I extended my previous findings by showing that AN in humans is indeed associated with a steep increase of p16<sup>INK4a</sup> expression.

The results of this study strongly support the notion that AN could reflect accelerated aging. This is corroborated by the overlap of histopathological features of aging with those of AN. Both show tubular atrophy, interstitial fibrosis and fibrous intimal thickening. The changes in p16<sup>INK4a</sup> expression seen in AN biopsies occurred within a mean time period of less than five years whereas it would have taken decades for them to develop in normal aging. The increase in p16<sup>INK4a</sup> expression might be directly induced by peri- or posttransplant stresses or could be a downstream event of an increase replication of renal cells, which has been induced by these stresses, leading to telomere shortening and then increases in p16<sup>INK4a</sup>. Others have found increased p21<sup>CIP1/WAF1</sup> expression in human allograft nephropathy (29) and chronic liver allograft rejection (30). P21<sup>CIP1/WAF1</sup> is a marker of cellular senescence *in vitro* (31) and had



not been associated with human kidney aging in my studies (chapter 5). Since p21<sup>CIP1/WAF1</sup> is the main transactivational target of p53 (32;33), its increase could be the result of telomere shortening. Telomere shortening has been observed in a rat model of “chronic rejection” (34). Even though these results have to be seen in context with my own data showing that normal rodent cells with telomerase expression do not use the telomere mechanism in kidney aging (chapter 3 and 4) (17), they provide another piece of evidence that mechanisms also involved in cellular senescence could play a role in allograft nephropathy.

The intense cytoplasmic staining was an additional feature that I have almost never observed in normal aging. Cytoplasmic p16<sup>INK4a</sup> staining has been observed previously in certain cancer types {8182} and has been associated with more aggressive tumors (35). However, its relevance in non-malignant cells is completely unclear. I did not observe cytoplasmic staining in any of the mouse or rat kidneys, including the ones with acute rejection. This suggests that the cytoplasmic staining is a feature unique to human cells and might reflect some chronic changes. Further studies are necessary to evaluate the importance of cytoplasmic p16<sup>INK4a</sup> staining.

Future studies to prove the hypothesis that senescence is an important pathomechanism in chronic renal disease must show that the senescence mechanisms have real pathophysiological importance. One approach would be to specifically target particular senescence markers,

e.g. by studying the p16<sup>INK4a</sup> knockout mouse. Based on the current results, the acceleration of senescent changes induced by transplantation should be blunted in such animals. However, it is also possible that we will see other problems in these kidneys when they are stressed, such as tumors. It is also possible that there is redundancy in the cell cycle regulation in senescence, and that it will require multiple knockouts to obtain a phenotype. Thus p16<sup>INK4a</sup> may be a convenient marker but not sufficient or necessary in itself.

In clinical trials, one could prospectively assess human transplants to show that preexisting senescent changes are predictors of later development of AN. These studies will provide the opportunity to assess kidneys considered for transplantation more accurately. It might also enable us in the later future to target the senescence pathway pharmacologically. Both advances would improve graft survival in renal transplant patients.

## 7.5 Tables

**Table 7.1:** Demographic data for the 14 individuals from whom the biopsies were derived.

	Mean $\pm$ SD	Minimum - Maximum
Patient age (years)	46.2 $\pm$ 15.1	16.7 to 70.0
Creatinine ( $\mu$ mol/L) at AN	246.9 $\pm$ 90.3	120 to 390
Donor age (years)	35.4 $\pm$ 13.4	19.2 to 59.1
Time since transplantation (years)	4.8 $\pm$ 3.5	0.3 to 11.4
Gender (m/f)	10/4	
History of acute rejection	3/14	
Donation (CD/LD)	11/3	

An, allograft nephropathy; CD, cadaveric donation; LD, living donation

**Table 7.2:** Banff scores for the 28 biopsies. Biopsies are either prior to transplantation (Implantation Bx) or at the time the diagnosis allograft nephropathy (AN Bx) was made.

	Biopsy	Donor age	G	I	T	V	CG	CI	CT	CV	AH
#1	Implantation	40.9	0	0	0	0					0
	AN	43.6	0	1	1	0	0	2	2	2	0
#2	Implantation	29.7	0	0	0	0	0	0	0	0	1
	AN	36.7	0	1	0	0	0	3	3	3	0
#3	Implantation	26.6	0	0	0	0					2
	AN	31.1	0	2	0	0	0	2	1	1	1
#4	Implantation	21.1	0	0	0	0					
	AN	31.7	0	1	1	0	0	2	2	0	1
#5	Implantation	45.0	0	1	0	0	0	1	1	0	1
	AN	52.1	0	1	1	0	0	2	2	1	2
#6	Implantation	59.1	0	1	0	0					2
	AN	62.7	0	1	2	0	1	3	3	2	1
#7	Implantation	27.7	0	0	0	0					0
	AN	29.0	0	1	1	0	1	2	2	2	1
#8	Implantation	37.2	0	1	1	0					0
	AN	39.9	0	1	0	0	0	2	1	2	0
#9	Implantation	46.0	0	0	0	0					0
	AN	47.9	0	1	1	0	0	2	2	0	3
#10	Implantation	40.2	0	0	0	0					
	AN	45.9	0	0	1	0	1	2	2	1	2
#11	Implantation	25.1	0	0	0	0					
	AN	31.9	0	1	0	0	0	2	2	2	2
#12	Implantation	57.8	0	0	0	0					2
	AN	59.0	0	1	0	0	0	1	1	2	2
#13	Implantation	19.2	0	0	0	0					
	AN	30.6	0	1	0	0	0	2	2	3	3
#14	Implantation	19.4	0	0	0	0					1
	AN	19.7	0	1	0	0	0	1	1	2	0

G, glomerulitis; I, interstitial infiltrate; T, tubulitis; V, vasculitis; CG, allograft glomerulopathy; CI, interstitial fibrosis; CT, tubular atrophy; CV, vascular fibrous intimal thickening; AH, arteriolar hyaline thickening. These changes are based on the Banff score for renal allograft pathology (36). Changes were assessed from 0 to 3, with 0 being no changes and 3 being the most possibly changes.

## 7.6 Figures

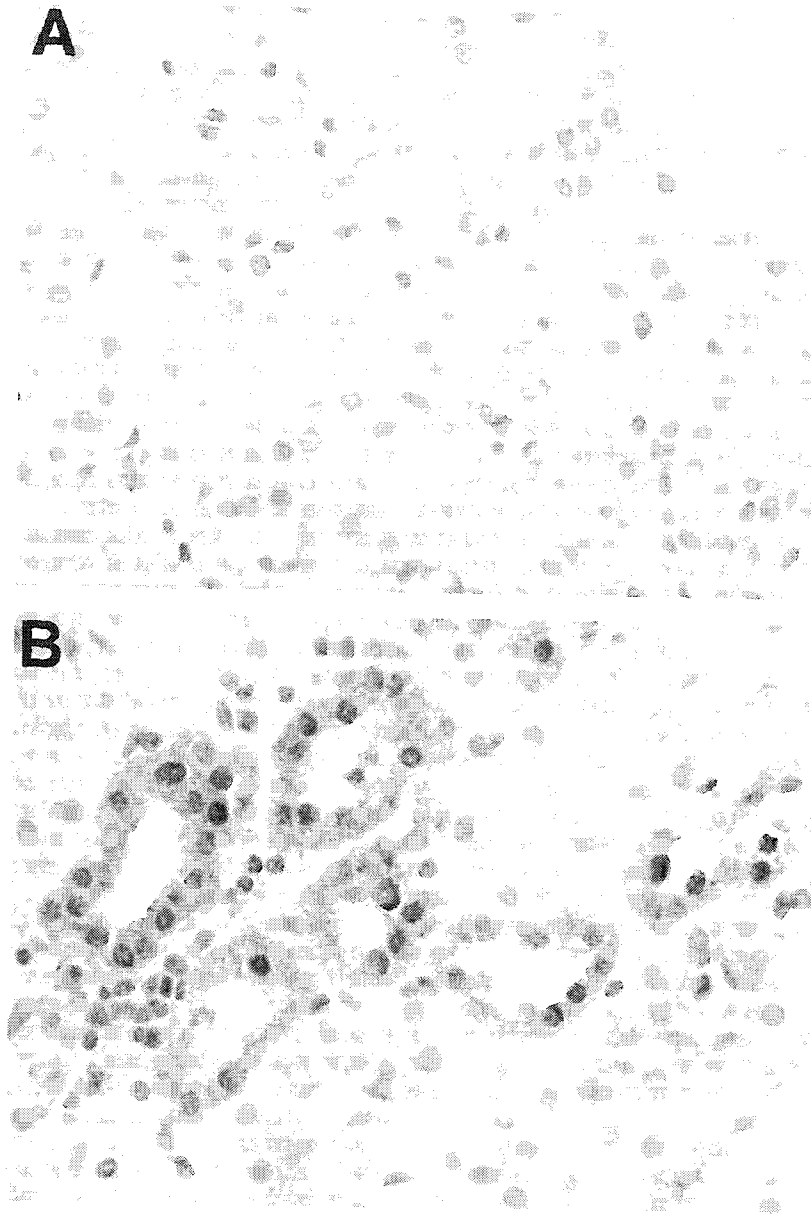


**Figure 7.1:** Kidney biopsies showing p16<sup>INK4a</sup> staining prior to and after transplantation. (A) Implantation biopsy of a 19-year old donor. (B) Biopsy diagnostic for allograft nephropathy showing increase in nuclear and cytoplasmic staining of tubules.

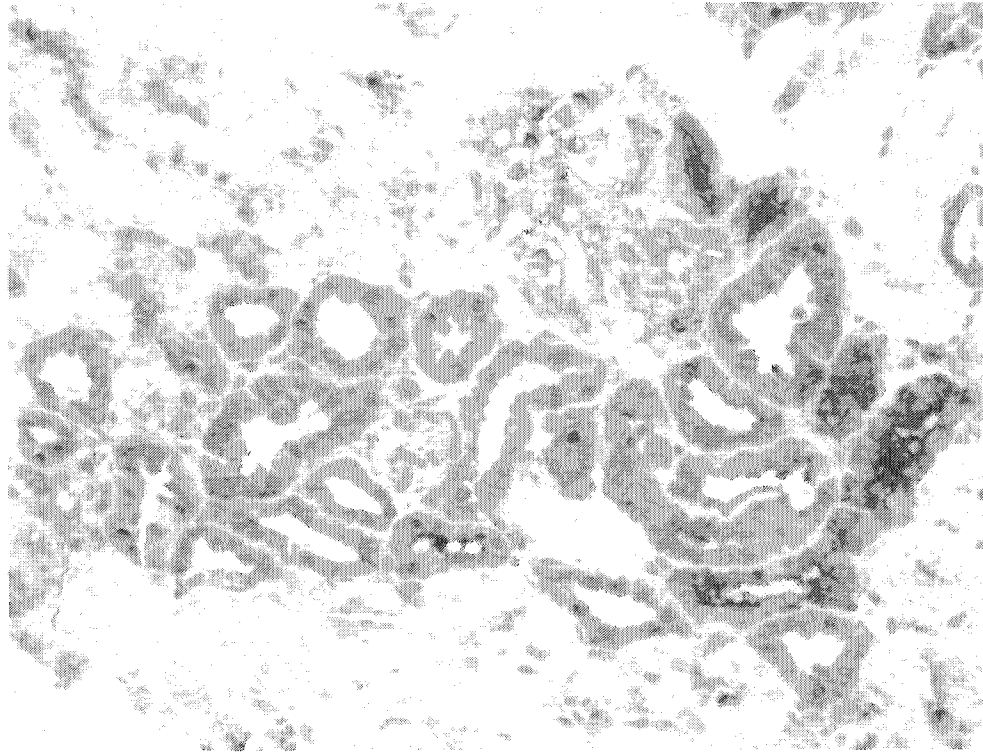


**Figure 7.2:** Kidney biopsy showing p16<sup>INK4a</sup> staining affecting one nephron. This biopsy was taken almost 3 years after transplantation and was diagnostic for allograft nephropathy. Donor age at time of transplantation had been 41 years. The staining was nuclear and cytoplasmic. The pattern suggested that a whole nephron (glomerulus and tubuli) was affected.



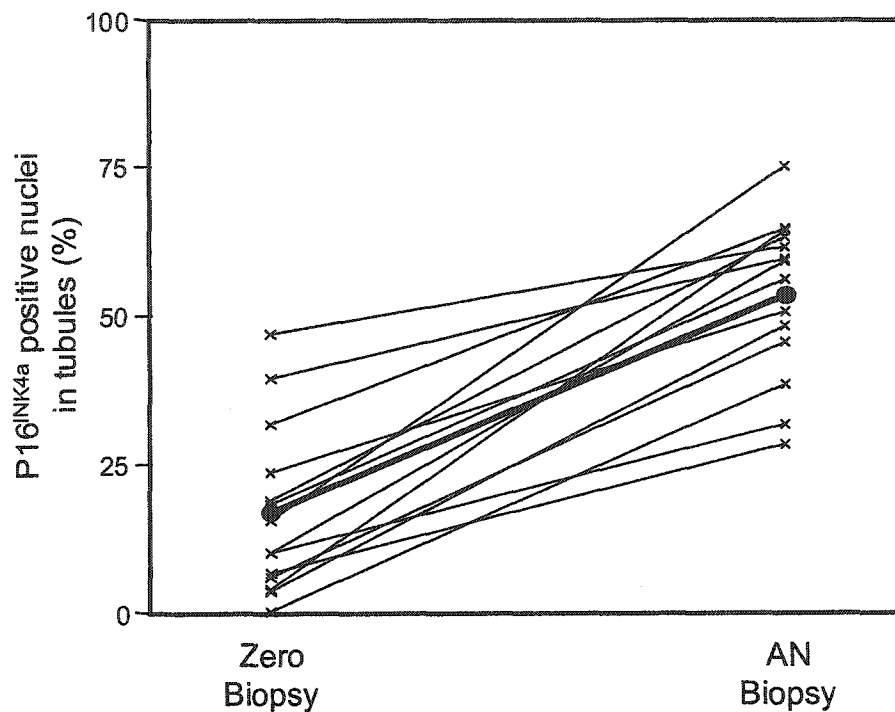


**Figure 7.3:** P16<sup>INK4a</sup> protein expression in tubular cells in 14 human kidney biopsies. Only nuclear staining was assessed. Implantation biopsy was taken at the time of transplantation and allograft nephropathy (AN) biopsy was taken at various times after transplantation (see table). Crosses (x) reflect individual values and dots (•) reflect mean value.

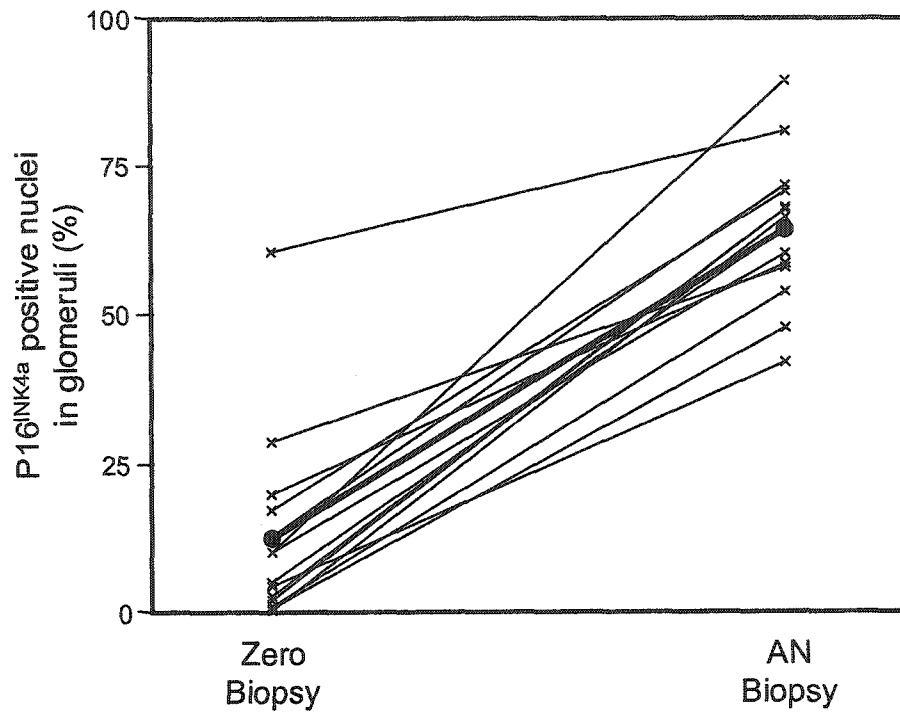


**Figure 7.4:** P16<sup>INK4a</sup> protein expression in glomeruli in 14 human kidney biopsies. Only nuclear staining was assessed. Implantation biopsy was taken at the time of transplantation and allograft nephropathy (AN) biopsy was taken at various times after transplantation (see table). Crosses (x) reflect individual values and dots (•) reflect mean value.

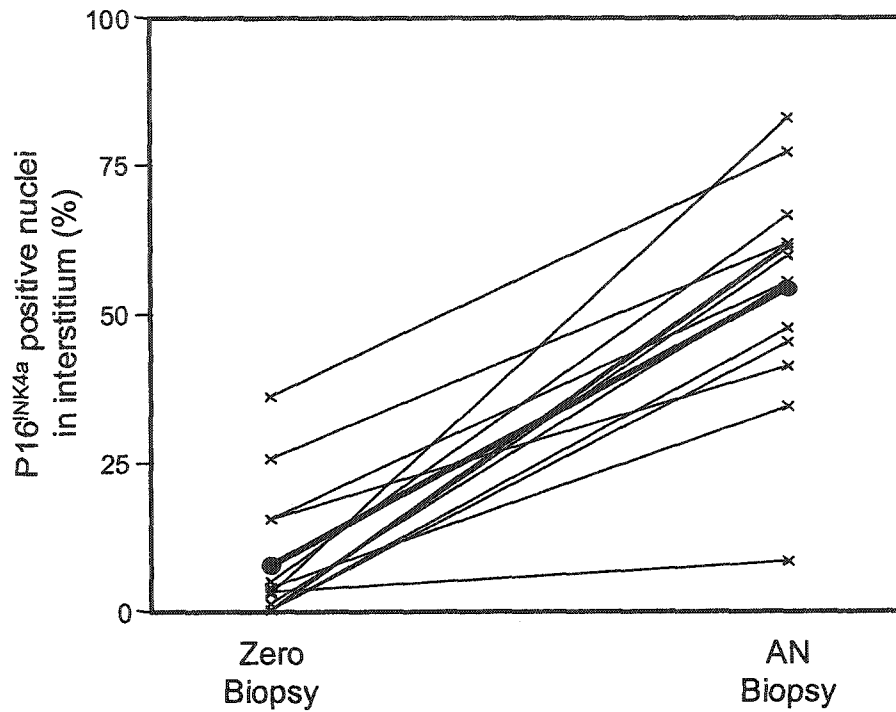


**Figure 7.5:** P16<sup>INK4a</sup> protein expression in interstitial cells in 14 human kidney biopsies. Only nuclear staining was assessed. Implantation biopsy was taken at the time of transplantation and allograft nephropathy (AN) biopsy was taken at various times after transplantation (see table). Crosses (x) reflect individual values and dots (•) reflect mean value.

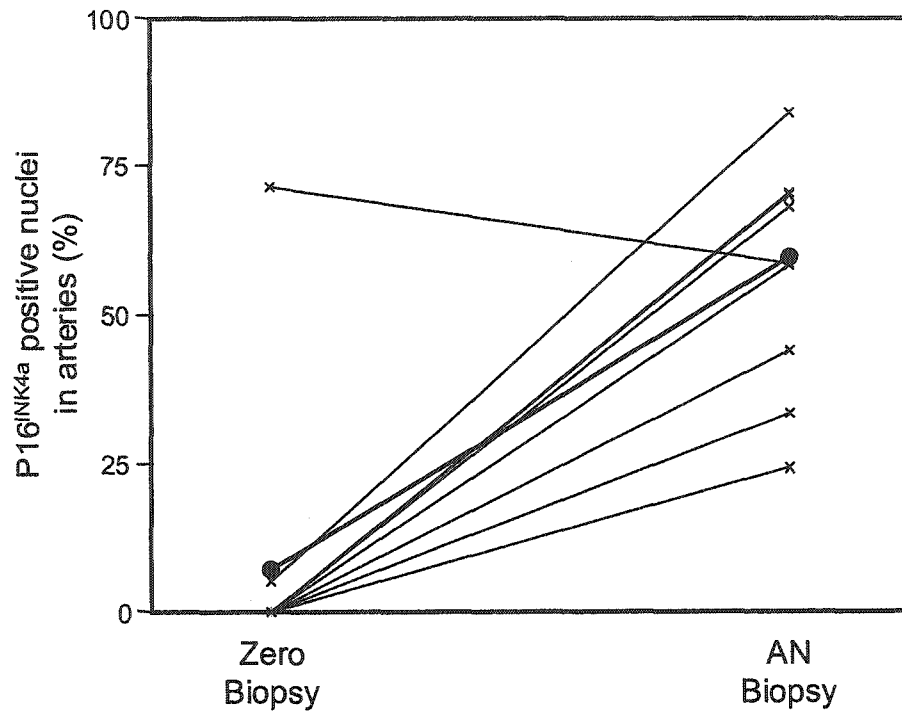


**Figure 7.6:** P16<sup>INK4a</sup> protein expression in arteries in 14 human kidney biopsies. Only nuclear staining was assessed. Implantation biopsy was taken at the time of transplantation and allograft nephropathy (AN) biopsy was taken at various times after transplantation (see table). Crosses (x) reflect individual values and dots (•) reflect mean value.

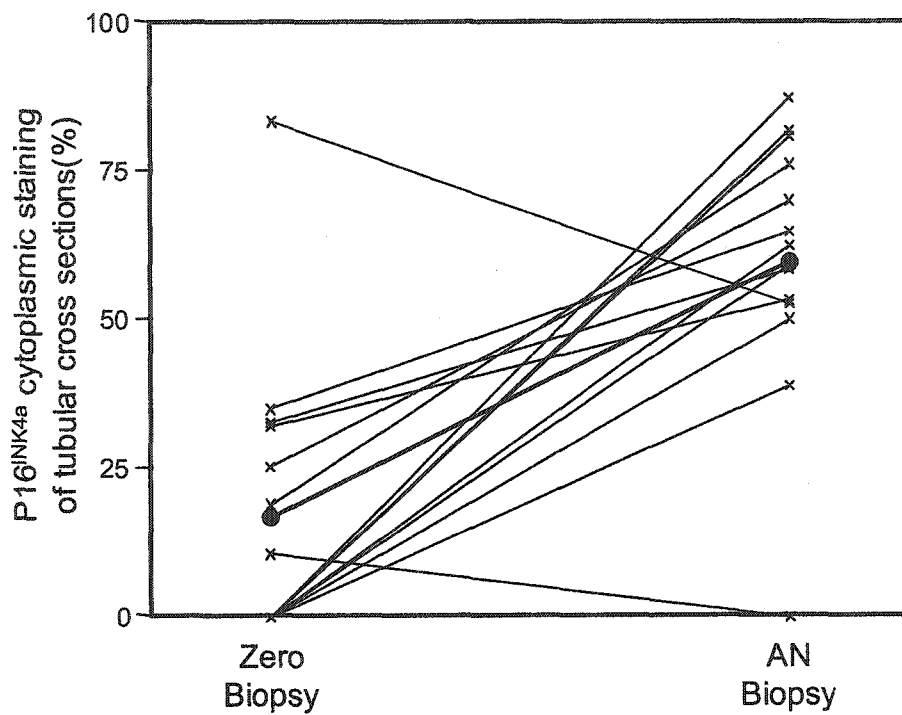


**Figure 7.7:** P16<sup>INK4a</sup> protein expression measured as cytoplasmic staining of tubular cross sections in 14 human kidney biopsies. Implantation biopsy was taken at the time of transplantation and allograft nephropathy (AN) biopsy was taken at various times after transplantation (see table). Crosses (x) reflect individual values and dots (•) reflect mean value.

## 7.7 References

1. Halloran PF, Melk A, and Barth C: Rethinking chronic allograft nephropathy: the concept of accelerated senescence. *J Am Soc Nephrol* 1999, 10: 167-181
2. Terasaki PI, Cecka JM, and Gjertson D.W.: Impact analysis: a method for evaluating the impact of factors in clinical renal transplantation. *Clinical Transplants*. Edited by Cecka JM and Terasaki PI. Los Angeles, CA, UCLA Tissue Typing Laboratory, 1998, pp. 437-441
3. Gjertson DW: Determinants of long term survival of adult kidney transplants. *Clinical Transplants 1999*. Edited by Terasaki P and Cecka JM. Los Angeles, CA, UCLA Immunogenetics Center, 2000, pp. 341-352
4. Ciciarelli J, Iwaki Y, and Mendenz R: The influence of donor age on kidney graft survival in the 1990s. *Clinical Transplants*. Edited by Cecka JM and Terasaki PI. Los Angeles, CA, UCLA Tissue Typing Laboratory, 1999, pp. 335-340
5. Prommool S, Jhangri GS, Cockfield SM, and Halloran PF: Time dependency of factors affecting renal allograft survival. *J Am Soc Nephrol* 2000, 11: 565-573
6. Toma H, Tanabe K, Tokumoto T, Shimizu T, and Shimmura H: Time-dependent risk factors influencing the long-term outcome in living renal allografts: donor age is a crucial risk factor for long-term graft survival more than 5 years after transplantation. *Transplantation* 2001, 72: 940-947
7. Kasiske BL, Kalil RSN, Lee HS, and Rao V: Histopathologic findings associated with a chronic, progressive decline in renal allograft function. *Kidney Int* 1991, 40: 514-524
8. Pannu N and Halloran PF: The kidney in aging. *Primer on Kidney Diseases*. Edited by Greenberg A. San Diego, CA, Academic Press, 2001, pp. 377-381
9. Gasser M, Waaga AM, Laskowski IA, and Tilney NL: The influence of donor brain death on short and long-term outcome of solid organ allografts. *Ann Transplant* 2000, 5: 61-67
10. Cecka JM: The UNOS scientific renal transplant registry - 2000. *Clinical Transplants*. Edited by Cecka JM and Terasaki PI. Los Angeles, CA, UCLA Tissue Typing Laboratory, 2000, pp. 1-18
11. Gjertson DW: Impact of delayed graft function and acute rejection on kidney graft survival. *Clinical Transplants*. Edited by Cecka JM and

Terasaki PI. Los Angeles, CA, UCLA Tissue Typing Laboratory, 2000, pp. 467-480

12. Halloran PF: Renal injury and preservation in transplantation. *Kidney Transplant Rejection*. Edited by Racusen LC and Solez K. New York, NY, Marcel Dekker, 1998, pp. 149-176
13. Halloran PF and Hunsicker LG: Delayed graft function: State of the Art, November 10-11, 2000. Summit Meeting, Scottsdale, Arizona, USA. *Am J Transplant* 2001, 1: 115-120
14. Weir MR, Ward MT, Blahut SA, Klassen DK, Cangro CB, Bartlett ST, and Fink JC: Long-term impact of discontinued or reduced calcineurin inhibitor in patients with chronic allograft nephropathy. *Kidney Int* 2001, 59: 1567-1573
15. Mange KC, Cizman B, Joffe M, and Feldman HI: Arterial hypertension and renal allograft survival. *JAMA* 2000, 283: 633-638
16. Melk A, Ramassar V, Helms LM, Moore R, Rayner D, Solez K, and Halloran PF: Telomere shortening in kidneys with age. *J Am Soc Nephrol* 2000, 11: 444-453
17. Melk A, Kittikowit W, Sandhu I, Halloran KM, Grimm P, Schmidt BMW, and Halloran PF: Cell senescence in rat kidney in vivo increases with growth and age despite lack of telomere shortening. *Kidney Int* 2003, 63: 2134-2143
18. Wright WE and Shay JW: Historical claims and current interpretations of replicative aging. *Nature Biotechnology* 2002, 20: 682-688
19. Wright WE and Shay JW: Telomere dynamics in cancer progression and prevention: fundamental differences in human and mouse telomere biology. *Nature Medicine* 2000, 6: 849-851
20. Sherr CJ and DePinho RA: Cellular senescence: mitotic clock or culture shock? *Cell* 2000, 102: 407-410
21. Zindy F, Quelle DE, Roussel MF, and Sherr CJ: Expression of the p16INK4a tumor suppressor versus other INK4 family members during mouse development and aging. *Oncogene* 1997, 15: 203-211
22. Palmero I, McConnell B, Parry D, Brookes S, Hara E, Bates S, Jat P, and Peters G: Accumulation of p16INK4a in mouse fibroblasts as a function of replicative senescence and not of retinoblastoma gene status. *Oncogene* 1997, 15: 495-503

23. Carnero A, Hudson JD, Price CM, and Beach DH: p16(INK4A) and p19(ARF) act in overlapping pathways in cellular immortalization. *Nature Cell Biology* 2000, 2: 148-155
24. Kamijo T, Zindy F, Roussel MF, Quelle DE, Downing JR, Ashmun RA, Grosveld G, and Sherr CJ: Tumor suppression at the mouse *INK4a* locus mediated by the alternative reading frame product p19<sup>ARF</sup>. *Cell* 1997, 91: 649-659
25. Quelle DE, Zindy F, Ashmun RA, and Sherr CJ: Alternative reading frames of the INK4a tumor suppressor gene encode two unrelated proteins capable of inducing cell cycle arrest. *Cell* 1995, 83: 993-1000
26. Racusen LC, Solez K, Colvin RB, Bonsib SM, Castro MC, Cavallo T, Croker BP, Demetris AJ, Drachenberg CB, Fogo AB, Furness P, Gaber LW, Gibson IW, Glotz D, Goldberg JC, Grande J, Halloran PF, Hansen HE, Hartley B, Hayry PJ, Hill CM, Hoffman EO, Hunsicker LG, Lindblad AS, Marcussen N, Mihatsch MJ, Nadasdy T, Nickerson P, Olsen TS, Papadimitriou JC, Randhawa PS, Rayner DC, Roberts I, Rose S, Rush D, Salinas-Madrigal L, Salomon DR, Sund S, Taskinen E, Trpkov K, and Yamaguchi Y: The Banff 97 working classification of renal allograft pathology. *Kidney Int* 1999, 55: 713-723
27. Halloran PF, Melk A, and Barth C: Rethinking chronic allograft nephropathy: the concept of accelerated senescence. *J Am Soc Nephrol* 1999, 10: 167-181
28. Melk A, Ramassar V, Helms LM, Moore R, Rayner D, Solez K, and Halloran PF: Telomere shortening in kidneys with age. *J Am Soc Nephrol* 2000, 11: 444-453
29. Chkhotua AB, Altimari A, Gabusi E, D'Errico A, Yakubovich M, Vienken J, Stefoni S, Chieco P, Yussim A, and Grigioni WF: Increased expression of P21((WAF1/CIP1)) CDKI gene in chronic allograft nephropathy correlating with the number of acute rejection episodes. *Transplant Proc* 2003, 35: 655-658
30. Lunz JG, III, Contrucci S, Ruppert K, Murase N, Fung JJ, Starzl TE, and Demetris AJ: Replicative senescence of biliary epithelial cells precedes bile duct loss in chronic liver allograft rejection: increased expression of p21(WAF1/Cip1) as a disease marker and the influence of immunosuppressive drugs. *Am J Pathol* 2001, 158: 1379-1390
31. Brown JP, Wei W, and Sedivy JM: Bypass of senescence after disruption of p21CIP1/WAF1 gene in normal diploid human fibroblasts. *Science* 1997, 277: 831-834



32. El-Deiry WS, Tokino T, Velculescu VE, Levy DB, Parsons R, Trent JM, Lin D, Mercer E, Kinzler KW, and Vogelstein B: WAF1, a potential mediator of p53 tumor suppression. *Cell* 1993, 75: 817-825
33. Deng C, Zhang P, Harper JW, Elledge SJ, and Leder P: Mice lacking p21CIP1/WAF1 undergo normal development, but are defective in G1 checkpoint control. *Cell* 1995, 82: 675-684
34. Joosten SA, Van H, V, Nolan CE, Borrias MC, Jardine AG, Shiels PG, Van Kooten C, and Paul LC: Telomere shortening and cellular senescence in a model of chronic renal allograft rejection. *Am J Pathol* 2003, 162: 1305-1312
35. Emig R, Magener A, Ehemann V, Meyer A, Stilgenbauer F, Volkmann M, Wallwiener D, and Sinn HP: Aberrant cytoplasmic expression of the p16 protein in breast cancer is associated with accelerated tumour proliferation. *Br J Cancer* 1998, 78: 1661-1668
36. Racusen LC, Solez K, Colvin RB, Bonsib SM, Castro MC, Cavallo T, Croker BP, Demetris AJ, Drachenberg CB, Fogo AB, Furness P, Gaber LW, Gibson IW, Glotz D, Goldberg JC, Grande J, Halloran PF, Hansen HE, Hartley B, Hayry PJ, Hill CM, Hoffman EO, Hunsicker LG, Lindblad AS, Marcussen N, Mihatsch MJ, Nadasdy T, Nickerson P, Olsen TS, Papadimitriou JC, Randhawa PS, Rayner DC, Roberts I, Rose S, Rush D, Salinas-Madrigal L, Salomon DR, Sund S, Taskinen E, Trpkov K, and Yamaguchi Y: The Banff 97 working classification of renal allograft pathology. *Kidney Int* 1999, 55: 713-723

## Chapter 8

### General Discussion and Conclusions

Portions of this chapter will be published.

Anette Melk: Senescence of renal cells – molecular basis and clinical implications. *Nephrology Dialysis Transplantation* 2003; in press. Used with permission of Oxford University Press.

## 8.1 Introduction

Renal senescence has many implications for nephrology, including normal aging, increased incidence in end stage renal disease (ESRD), poorer graft survival and increased cancer rates. The phenotype of renal senescence is characterized by the loss of function, cells, and nephron mass. I hypothesized that the loss of functioning cells and units in aging and diseased kidneys could follow molecular pathways that had been described for cellular senescence. The mechanism leading to cellular senescence had been studied extensively in human fibroblasts and mouse embryonic fibroblasts *in vitro*. *In vivo* studies had mainly involved leukocytes, but no studies had addressed the kidney. Because of the lack of studies showing that cellular senescence can be found in aging kidney, the first part of my studies had to establish this relationship. I therefore examined whether molecular changes and pathways involved in cellular senescence *in vitro* would occur in aged kidneys *in vivo*. I also assessed their relative contribution in different species, in particular human and rodent (mouse and rat), and their relevance to renal aging. For the second part of my studies, I focused on the importance of those senescence markers that I had found to be associated with renal senescence for disease states. I chose to investigate injuries occurring during transplantation and assessed cellular senescence for acute changes due to ischemia-reperfusion and rejection and for chronic changes in allograft

nephropathy.

## 8.2 Objectives of the thesis

The major objectives of this thesis have been:

1. The description of the molecular basis of renal senescence by defining features of *in vitro* cellular senescence in kidneys *in vivo*.
2. The documentation of possible differences in renal senescence between human and rodent kidneys *in vivo*.
3. The definition of features of cellular senescence in kidneys prior to and after transplantation.

## 8.3 Evidence for cellular senescence in kidneys *in vivo*

### 8.3.1 Telomere Shortening

Telomere shortening is the cause of replicative senescence in human fibroblasts in culture (1). I have shown that telomeres become shorter in human kidneys with age, and that the rate of loss is greater in cortex than in medulla (chapter 2) (2). I also found long telomeres, continued telomerase expression, and the lack of critical telomere shortening with aging in rat (chapter 3) and mouse kidneys (chapter 4) (3;4). Telomeres were about fourfold longer in rodent kidneys than in human kidneys. The species differences with aging support the conclusion that mouse and rat cells *in vivo*, like mouse embryonic fibroblasts *in vitro*,

do not use telomere shortening as a replication counter, but human cells do. This is illustrated in figure 8.1. The fact that mouse and rat kidneys have telomeres that remain long even in aging must be taken into account when using mouse and rat models to explain human diseases as long telomeres and continued telomerase expression may protect against the consequences of injury. Mice deficient in telomerase activity show progressive telomere loss with increased susceptibility to liver injury (5) and renal dysfunction (6). The role of telomere function in injury and repair could be relevant to the high susceptibility of aged human kidneys to disease due to a decreased capability to withstand stress.

### 8.3.2 Cellular senescence reached by other mechanisms

In addition to replication, the exposure of primary mammalian cells to certain types of stress had been shown to trigger a permanent and irreversible proliferation arrest that results in a senescence-like phenotype ("stimulation and stress-induced senescent-like arrest", STASIS) (7). It can be reached by DNA damage, oxidative stress, Ras induction, and epigenetic alterations.

The cell cycle regulators and tumor suppressors p16<sup>INK4a</sup> and p19<sup>ARF</sup> (and its human equivalent p14<sup>ARF</sup>) have been associated with this non-replication dependent growth arrest (8-10) and were of additional interest because of the differences between species. P16<sup>INK4a</sup> and p19<sup>ARF</sup>

have overlapping and complementary roles in mouse embryonic fibroblasts growth arrest *in vitro* (11) with the notion that p19<sup>ARF</sup> is more potent (12). In human fibroblasts p16<sup>INK4a</sup> but not p14<sup>ARF</sup> (13) mediates irreversible cell cycle arrest leading into senescence.

I investigated several candidate genes (e.g. p16<sup>INK4a</sup>, p14/p19<sup>ARF</sup>, p21<sup>WAF1/CIP1</sup>, heat shock proteins, TGF- $\beta$ , PAI-1, metallothioneins, GADD45) that had been reported to be altered in senescence *in vitro* and found the most striking correlation with renal aging for the cell cycle regulator p16<sup>INK4a</sup> in human (chapter 5) (14) as well as in mouse and rat kidneys (chapter 3 and 4) (3;4;15). P14<sup>ARF</sup> did not change with age in human kidney but p19<sup>ARF</sup> was highly expressed during development and aging in mouse kidney. These results suggest that human and mouse cells undergo cell cycle regulatory events during aging *in vivo* that are similar to those in culture in response to environmental stresses (figure 8.1). Young cells *in vitro*, and renal cells of young humans and rodents, do not seem to rely on p16<sup>INK4a</sup> for cell cycle arrest. But as cells or kidneys age, there is a progressive increase in the number of cells expressing p16<sup>INK4a</sup> and exiting the cell cycle. The high numbers of cells expressing p16<sup>INK4a</sup> could limit repair and even homeostasis in the aging kidney. The remarkable changes in p16<sup>INK4a</sup> are highlighted by the lack of change in many of the other genes investigated, suggesting a role for some but not all *in vitro* senescent features for *in vivo* kidney aging. This observation suggests that renal aging

has relatively little effect on transcription. This hypothesis is supported by my findings from microarray studies in human and mouse (16). Presumably this is a protective mechanism that eliminates cells with damage, thereby limiting their contribution to transcription and is part of the anticancer defense (17).

### 8.3.3 *In vivo* senescence marker

I investigated two markers of cellular senescence *in vitro* that had previously been shown to be important *in vivo* in other organs. SA- $\beta$ -GAL probably reflects an increased lysosome content of senescent cells (18;19) and lipofuscin, the well known "aging pigment", was recently suggested to be not simply an "innocent" bystander but rather a contributor to the aging process (20). My data revealed a striking association between SA- $\beta$ -GAL, lipofuscin, and aging for rat kidney. Both markers were present in tubular cells and increased with age. In rat kidney, this increase was exponential and lipofuscin showed a strong association with atrophic tubules (chapter 3). Aged human kidneys showed a similar pattern for lipofuscin, but the increase with age was less steep and the increase in SA- $\beta$ -GAL was not significant (chapter 5). Old mouse kidneys showed the least amount of lipofuscin and SA- $\beta$ -GAL when compared to the other species (chapter 4). Lipofuscin and SA- $\beta$ -GAL may both be manifestations of impaired homeostasis of cell organelles with age.

## 8.4 Evidence for cellular senescence in transplantation

A special case for possible interaction of underlying renal senescence and imposed stresses might be the poor performance of transplanted kidneys from older donors, particularly cadaveric donors (21). Our group had hypothesized that senescent cells could contribute to the diminished ability of the old donor kidney to withstand peritransplant (brain death, preservation) as well as posttransplant (rejection, hypertension) stresses, resulting in a higher incidence of allograft nephropathy and poorer graft survival (22).

### 8.4.1 Acute rejection

Transplanted kidneys from older donors perform badly compared to their younger counterparts as reflected by their poorer graft survival (23-27). They have a higher incidence of delayed graft function (DGF) (21), but even with immediate function their performance is only as good as young organs with delayed graft function (28). This suggests that stresses occurring during and after the transplantation process might add to the burden of age that the old organ already carries. Old donor kidneys that do experience acute rejection episodes do worse than young donor kidneys (29). Again, this suggests an acceleration of the senescence process by additional stresses such as rejection.

In a vascularized, fully MHC mismatched mouse transplant model



(chapter 6), I have found that acute rejection in kidneys from 18 month donors not only induced p16<sup>INK4a</sup> and p19<sup>ARF</sup> but also led to the rapid development of tubular atrophy and loss of tubular cells, despite similar host immune response and donor immunogenicity when compared to 3 month donors (30;31). At day 7 after transplantation, the increases in p16<sup>INK4a</sup> were higher in old kidneys when compared to young kidneys, whereas the increases were similar for p19<sup>ARF</sup>. At day 21, an additional increase occurred for both genes that was greater in young transplants for p19<sup>ARF</sup>. For both, p16<sup>INK4a</sup> and p19<sup>ARF</sup>, the increase after transplantation was additive to the preexisting p16<sup>INK4a</sup> and p19<sup>ARF</sup> expression in old kidneys. These results suggested that older donor age led to faster deterioration and atrophy of the parenchyma when rejection occurred. They are consistent with the idea that p16<sup>INK4a</sup> and p19<sup>ARF</sup> cause irreversible cell cycle arrest that might limit the capability of the old donor kidney to repair peritransplant injuries and maintain organ mass and function.

#### 8.4.2 Cellular senescence in allograft nephropathy

Allograft nephropathy and normal renal aging show similar features. In both cases, loss of function and loss of renal mass has been observed (32). The histological features of allograft nephropathy overlap those of aging with the occurrence of tubular atrophy, interstitial fibrosis and fibrous intimal thickening (33;34). Allograft nephropathy is strongly correlated with

donor age and posttransplant injuries such as brain death, DGF, and rejection. Based on these similarities, the importance of allograft nephropathy for long-term graft failure and my previous finding that p16<sup>INK4a</sup> expression was associated with human renal aging (chapter 5), led to the question of whether p16<sup>INK4a</sup> expression would be detectable in allograft nephropathy.

I observed a steep increase in p16<sup>INK4a</sup> in human allograft nephropathy biopsies compared to their paired biopsies at time of implantation (chapter 7). Others have found increased p21<sup>WAF1/CIP1</sup> expression in human allograft nephropathy (35) and telomere shortening in a rat model of “chronic rejection” (36). My own data and the data from the literature showed that certain features that are displayed by senescent cells in culture could be detected in allograft nephropathy *in vivo*. This suggested that peri- and posttransplant stresses are able to induce features of senescence independent of age and could be causal for the observed malfunction.

## 8.5 Summary of the findings

The major findings of this thesis have been:

1. Certain features of cellular senescence occurred in the kidney *in vivo* with age.
2. The species differences for kidneys *in vivo* resembled the

differences described for fibroblasts *in vitro*.

3. Transplantation led to the occurrence of senescence features.
4. Senescence limited the capability of older kidneys to withstand peritransplant injuries.
5. Allograft nephropathy showed increases in p16<sup>INK4a</sup>.

#### 8.6 Implications for nephrology and transplantation

In renal senescence, some cells drop out completely, some persist in damaged form (atrophic tubular cells) and others develop features that are seen in senescent cells *in vitro*. The potential importance of persisting cells with such features *in vivo* might be that they compromise the function and integrity of the tissue, since ordinarily the organized tissue rather than the individual cell accounts for function. My results are compatible with the hypothesis that some mechanisms contributing to senescence of somatic cells *in vitro* also play a role in aging phenotypes in the kidney *in vivo*. Measurements of senescence changes could emerge as better markers for function or biological age, adding to existing assessments such as histological findings and chronological age. We might find that the renal cells displaying features of senescence such as increased p16<sup>INK4a</sup> expression and shortened telomeres do not affect kidney function under normal conditions. This is supported by the clinical observation that ESRD remains uncommon in the elderly and that the majority of the elderly that do

not have other age-related diseases have normal renal function (37-39). However, based on my findings it seems likely that processes of renal senescence result in a decreased ability of the aged nephron to cope with disease stresses and that the measurement of markers such as p16<sup>INK4a</sup> or telomere length might help to explain the performance of a kidney under stress.

The pathogenesis of chronic renal failure is poorly understood. In the early sixties, Bricker showed that in failing (and aging) kidneys the functioning nephrons are intact, i.e. nephrons with partial function are eliminated. That means that a glomerulus cannot exist without its tubuli and vice versa (40). Subsequently many mechanisms have been described that are involved in the process of chronic renal failure. A considerable amount of data has been generated looking at the mechanisms regulating or generating interstitial fibrosis or glomerular sclerosis. However, up to now no mechanism has been identified that explains how nephrons are shut down as the key event in renal failure. It is possible that senescence of renal cells contributes to progression of chronic renal failure. The kidney had been considered to be an almost non-replicating, post-mitotic organ. During the last ten years it has been shown that there is replication, even in the healthy kidney (41). My studies support these findings by showing that some features of cells with replicative senescence occur in the healthy kidney with age. In addition to replicative stress, oxidative stress can cause

telomere shortening and therefore accelerate senescence. This is in agreement with my data showing factors such as p16<sup>INK4</sup> involved in the stress induced STASIS pathway are increased with aging and can be induced by stresses surrounding transplantation *in vivo*.

Based on the findings in transplanted kidneys, one could propose that induction or “acceleration” of features found in cellular senescence *in vitro* might be a common pathway for other chronic renal diseases. P16<sup>INK4a</sup> expression and/or telomere shortening could be causal in the development of tubular atrophy and interstitial fibrosis. In addition, age-related diseases might accelerate the changes contributing to the phenotype of renal senescence. The observation that telomeres are shorter in intimal cells from arteries exposed to higher blood pressure (42) would suggest an important role for hypertension. My own data on telomere length in renal arteries (not presented in this thesis) did not suggest that telomeres in arteries were shorter when compared to renal tissue from the same individual. However, since I did not study a large enough population, I cannot comment on the effect hypertension might have had on telomere length.

The hypothesis that kidney cells reach a “senescence-like” state (by showing some of the features seen in cellular senescence *in vitro*) and that this might be the critical event in chronic renal failure raises the question of which cells are required for this event. The well-known features of chronic renal failure like tubular atrophy, interstitial fibrosis and glomerular sclerosis

could be explained as reactive or reparative events triggered by senescence of such cells. Based on my studies, these key cells might be epithelial cells: the increases of senescence changes (p16<sup>INK4a</sup>, SA-β-GAL, lipofuscin) were most pronounced in tubular as compared to glomerular, interstitial or vascular cells. In addition, the finding of increased p16<sup>INK4a</sup> expression in the macula densa might - in analogy to its function as a 'nephron switch' in acute renal failure – be of particular importance (43;44). The localization of these cells makes them a very likely cell type to function as a more general 'final switch' to terminate nephron life. These cells are able to measure the functionality of the kidney by assessing the ability to retain sodium and are able to shut down the perfusion of the glomerulus. However, one could argue that senescence of the macula densa would be deleterious in order to execute this function. The cells of the macula densa are the sensors of poor performance elsewhere, possibly the sensors of senescence elsewhere, and should thereby not senesce themselves in order to mediate nephron shutdown if necessary.

## 8.7 Future work

Further studies have to focus on exploring the causal relationship between the occurrence of senescent cells and organ function and damage. The experiments have to establish that mechanisms of cellular senescence are indeed of pathophysiological relevance, that their disruption limits

normal aging and increases the ability of the kidney to withstand stresses, and that these mechanisms are important in many or even all diseases leading to chronic deterioration of renal function. If senescence turns out to have these important effects, then it will be of interest to see what cell type shuts the nephron down and how this shut down is mediated.

Based on my previous findings, the next step would be to prove that p16<sup>INK4a</sup> limits the ability of older kidneys to withstand peri- and posttransplant injuries. In order to do this, one could study transplantation in old p16<sup>INK4a</sup> knockout mice. If p16<sup>INK4a</sup> were limiting the ability to withstand transplantation stresses, then grafts from old p16<sup>INK4a</sup> knockout mice will show less organ damage and better function when compared to wildtype mice. However, one could imagine that in the absence of p16<sup>INK4a</sup>, other mechanisms of cellular senescence may become more important. The candidate gene based on my studies would be p19<sup>ARF</sup>. The p16<sup>INK4a</sup>/p19<sup>ARF</sup> double knockout could help to define these compensatory mechanisms.

In conclusion, the observation that cells with some features of senescent cells in culture can be identified in kidney and seem to be involved in certain disease states is exciting. The establishment of the pathophysiological importance of senescence mechanisms will extend our understanding of normal kidney aging and the pathogenesis of chronic renal diseases.

## 8.8 Figures



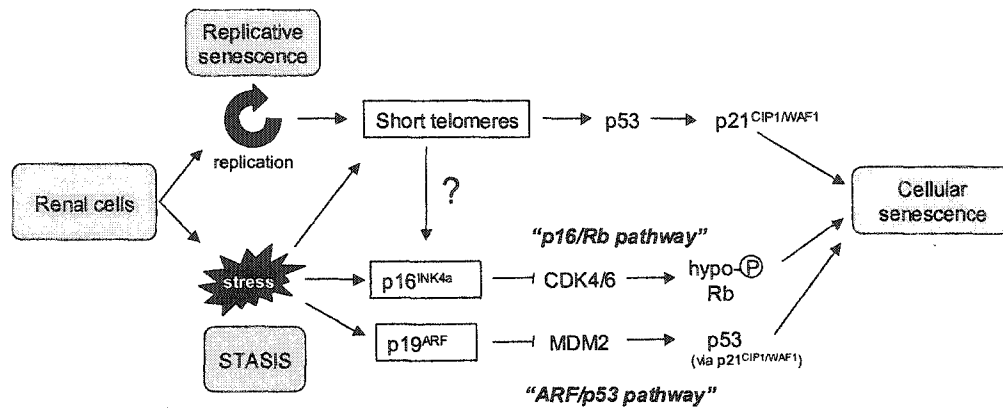


**Figure 8.1:** Cellular senescence in renal cells *in vivo*. The cartoon is based on the results of my studies and indicates the differences between the two forms of cellular senescence: “replicative senescence” and “STASIS” in the different species. In human renal cells, short, dysfunctional telomeres will trigger a DNA damage response by activation of p53 and possible p16<sup>INK4a</sup> (also p16<sup>INK4a</sup> does not seem to be essential for “replicative senescence” based on *in vitro* data). P53 leads to cell cycle arrest via its main transactivational target p21<sup>CIP1/WAF1</sup>. The increases seen in p16<sup>INK4a</sup> could be caused by environmental stresses (possibly oxidative stress) leading to the activation of the “p16/Rb pathway”. P16<sup>INK4a</sup> inhibits the activity of the cyclin-dependent kinases (CDKs) 4 and 6, thereby leading to hypophosphorylation (hypo-P) of retinoblastoma (Rb) and irreversible cell cycle arrest (STASIS). In mouse renal cells, replication in the presence of continuous telomerase expression does not result in short telomeres. Increases in p16<sup>INK4a</sup> or p19<sup>ARF</sup> result in activation of the “p16/Rb pathway” or the “ARF/p53 pathway”, respectively. P19<sup>ARF</sup> by binding to MDM2 prevents ubiquitination and degradation of p53. This results in cell cycle arrest (STASIS) mediated by p53 through p21<sup>CIP1/WAF1</sup>. Unlike in mouse embryonic fibroblasts, p16<sup>INK4a</sup> in renal cells seems to be more potent than p19<sup>ARF</sup> in regulating cell cycle arrest. The discussion whether stress can lead to telomere shortening reflecting STASIS rather than replicative senescence remains controversial. However, the data on this seems to be more substantiated for human cells.

## 8.9 References

1. Harley CB, Futcher AB, and Greider CW: Telomeres shorten during ageing of human fibroblasts. *Nature* 1990, 345: 458-460
2. Melk A, Ramassar V, Helms LM, Moore R, Rayner D, Solez K, and Halloran PF: Telomere shortening in kidneys with age. *J Am Soc Nephrol* 2000, 11: 444-453
3. Melk A, Kittikowit W, Sandhu I, Halloran KM, Grimm P, Schmidt BMW, and Halloran PF: Cell senescence in rat kidney in vivo increases with growth and age despite lack of telomere shortening. *Kidney Int* 2003, 63: 2134-2143
4. Melk, A., Rayner, D., Pehowich, E. D., Solez, K., and Halloran, P. F. Renal senescence reflects different mechanisms in human and rodent kidneys. *Journal of the American Society of Nephrology* 12, 616A-617A. 2001.
5. Rudolph KL, Chang S, Millard M, Schreiber-Agus N, and DePinho RA: Inhibition of experimental liver cirrhosis in mice by telomerase gene delivery. *Science* 2000, 287: 1253-1258
6. Ruiz-Torres, M. P., Perez-Rivero, G., Franco, S., Blasco, M. A., Diez-Marques, M. L., and Rodriguez-Puyol, D. Role of telomere shortening in renal function. The importance of oxidative damage. *Journal of the American Society of Nephrology* 13, 163A. 2002.
7. Wright WE and Shay JW: Historical claims and current interpretations of replicative aging. *Nature Biotechnology* 2002, 20: 682-688
8. Weinberg RA: The retinoblastoma protein and cell cycle control. *Cell* 1995, 81: 323-330
9. Serrano M, Lee H-W, Chin L, Cordon-Cardo C, Beach D, and DePinho RA: Role of the INK4a locus in tumor suppressor and cell mortality. *Cell* 1996, 85: 27-37
10. Ramirez RD, Morales CP, Herbert BS, Rohde JM, Passons C, Shay JW, and Wright WE: Putative telomere-independent mechanisms of replicative aging reflect inadequate growth conditions. *Genes & Development* 2001, 15: 398-403
11. Carnero A, Hudson JD, Price CM, and Beach DH: p16(INK4A) and p19(ARF) act in overlapping pathways in cellular immortalization. *Nature Cell Biology* 2000, 2: 148-155
12. Krimpenfort P, Quon KC, Mooi WJ, Loonstra A, and Berns A: Loss of p16Ink4a confers susceptibility to metastatic melanoma in mice. *Nature* 2001, 413: 83-86

13. Wei W, Hemmer RM, and Sedivy JM: Role of p14(ARF) in replicative and induced senescence of human fibroblasts. *Mol Cell Biol* 2001, 21: 6748-6757
14. Melk, A., Turner, P., Helms, L. M., Ramassar, V., Urmson, J., and Halloran, P. F. Expression of senescence regulator P16INK4a mRNA in some human kidney samples. *Journal of the American Society of Nephrology* 11, 461A. 2000.
15. Melk, A., Halloran, K., Sandhu, I., Gourishankar, S., Rayner, D., Helms, L., and Halloran, P. F. Evidence for cellular senescence in tubular epithelium of rodent and human kidneys. *Am J Transplant* 1[Suppl 1], 230. 2001.
16. Melk, A., Halloran, P. F., and Sarwal, M. Gene expression pattern in human renal senescence using microarray technique. *Am J Transplant* 2[3], 383. 2002.
17. Mathon NF and Lloyd AC: Cell senescence and cancer. *Nat Rev Cancer* 2001, 1: 203-213
18. Kurz DJ, Decary S, Hong Y, and Erusalimsky JD: Senescence-associated (beta)-galactosidase reflects an increase in lysosomal mass during replicative ageing of human endothelial cells. *J Cell Sci* 2000, 113 ( Pt 20): 3613-3622
19. Dimri GP, Lee X, Basile G, Acosta M, Scott G, Roskelley C, Medrano EE, Linskens M, Rubelj I, Pereira-Smith O, Peacocke M, and Campisi J: A biomarker that identifies senescent human cells in culture and in aging skin *in vivo*. *Proc Natl Acad Sci USA* 1995, 92: 9363-9367
20. Sitte N, Merker K, Grune T, and von Zglinicki T: Lipofuscin accumulation in proliferating fibroblasts in vitro: an indicator of oxidative stress. *Exp Geront* 2001, 36: 475-486
21. Cecka JM: The UNOS scientific renal transplant registry. *Clinical Transplants*. Edited by Cecka JM and Terasaki PI. Los Angeles, CA, UCLA Tissue Typing Laboratory, 1998, pp. 1-16
22. Halloran PF, Melk A, and Barth C: Rethinking chronic allograft nephropathy: the concept of accelerated senescence. *J Am Soc Nephrol* 1999, 10: 167-181
23. Gjertson DW: Determinants of long term survival of adult kidney transplants. *Clinical Transplants* 1999. Edited by Terasaki P and Cecka JM. Los Angeles, CA, UCLA Immunogenetics Center, 2000, pp. 341-352
24. Terasaki PI, Cecka JM, and Gjertson D.W.: Impact analysis: a method for evaluating the impact of factors in clinical renal transplantation. *Clinical*

- Transplants. Edited by Cecka JM and Terasaki PI. Los Angeles, CA, UCLA Tissue Typing Laboratory, 1998, pp. 437-441
25. Cicciarelli J, Iwaki Y, and Mendenz R: The influence of donor age on kidney graft survival in the 1990s. *Clinical Transplants*. Edited by Cecka JM and Terasaki PI. Los Angeles, CA, UCLA Tissue Typing Laboratory, 1999, pp. 335-340
  26. Terasaki PI, Gjertson DW, Cecka JM, Takemoto S, and Cho YW: Significance of the donor age effect on kidney transplants. *Clinical Transplants*. Edited by Cecka JM and Terasaki PI. Los Angeles, CA, UCLA Tissue Typing Laboratory, 1997, pp. 366-372
  27. Prommool S, Jhangri GS, Cockfield SM, and Halloran PF: Time dependency of factors affecting renal allograft survival. *J Am Soc Nephrol* 2000, 11: 565-573
  28. Boom H, Mallat MJ, de Fijter JW, Zwinderman AH, and Paul LC: Delayed graft function influences renal function, but not survival. *Kidney Int* 2000, 58: 859-866
  29. de Fijter JW, Mallat MJ, Doxiadis II, Ringers J, Rosendaal FR, Claas FH, and Paul LC: Increased immunogenicity and cause of graft loss of old donor kidneys. *J Am Soc Nephrol* 2001, 12: 1538-1546
  30. Melk, A., Schmidt, B. M. W., Takeuchi, O., Urmson, J., and Halloran, P. F. Senescence marker p16<sup>INK4a</sup> is induced in acute rejection: evidence that rejection induces epithelial cell senescence. *Am J Transplant* . 2003.
  31. Melk, A., Schmidt, B. M. W., Urmson, J., Solez, K., and Halloran, P. F. Does donor age affect immunogenicity or tissue fragility? Evidence that old kidneys develop equivalent inflammation but more tubulitis and tubular atrophy. *Am J Transplant* . 2003.
  32. Moreso F, Lopez M, Vallejos A, Giordani C, Riera L, Fulladosa X, Hueso M, Alsina J, Grinyo JM, and Seron D: Serial protocol biopsies to quantify the progression of chronic transplant nephropathy in stable renal allografts. *Am J Transplant* 2001, 1: 82-88
  33. Pannu N and Halloran PF: The kidney in aging. *Primer on Kidney Diseases*. Edited by Greenberg A. San Diego, CA, Academic Press, 2001, pp. 377-381
  34. Kasiske BL, Kalil RSN, Lee HS, and Rao V: Histopathologic findings associated with a chronic, progressive decline in renal allograft function. *Kidney Int* 1991, 40: 514-524
  35. Chkhotua AB, Altimari A, Gabusi E, D'Errico A, Yakubovich M, Vienken J, Stefoni S, Chieco P, Yussim A, and Grigioni WF: Increased expression of

P21((WAF1/CIP1)) CDKI gene in chronic allograft nephropathy correlating with the number of acute rejection episodes. *Transplant Proc* 2003, 35: 655-658

36. Joosten SA, Van H, V, Nolan CE, Borrias MC, Jardine AG, Shiels PG, Van Kooten C, and Paul LC: Telomere shortening and cellular senescence in a model of chronic renal allograft rejection. *Am J Pathol* 2003, 162: 1305-1312
37. Lindeman RD, Tobin J, and Shock NW: Longitudinal studies on the rate of decline in renal function with age. *J Amer Ger Soc* 1985, 33: 278-285
38. Fliser D, Franek E, Joest M, Block S, Mutschler E, and Ritz E: Renal function in the elderly: impact of hypertension and cardiac function. *Kidney Int* 1997, 51: 1196-1204
39. Fliser D, Zeier M, Nowack R, and Ritz E: Renal functional reserve in healthy elderly subjects. *J Am Soc Nephrol* 1993, 3: 1371-1377
40. Bricker NS, Morrin PAF, and Kime SW, Jr.: The pathologic physiology of chronic Bright's disease. An exposition of the "intact nephron hypothesis". *J Am Soc Nephrol* 1997, 8: 1470-1476
41. Nadasdy T, Laszik Z, Blick KE, Johnson LD, and Silva FG: Proliferative activity of intrinsic cell populations in the normal human kidney. *J Am Soc Nephrol* 1994, 4: 2032-2039
42. Chang E and Harley CB: Telomere length and replicative aging in human vascular tissues. *Proc Natl Acad Sci USA* 1995, 92: 11190-11194
43. Thureau K and Schnermann J: The Na concentration of the macula densa cells as a factor regulating glomerular filtration rate (micropuncture studies). 1965. *J Am Soc Nephrol* 1998, 9: 925-934
44. Schnermann J and Levine DZ: Paracrine factors in tubuloglomerular feedback: Adenosine, ATP, and Nitric Oxide. *Annu Rev Physiol* 2003, 65: 501-529

02/06/03

Dr Anette Melk

80) 407 3417

Dear Dr Melk

**NEPHROLOGY DIALYSIS TRANSPLANTATION, "Senescence of Renal Cells..." (In Press)** ✓

Thank you for your email dated 30 May 2003, requesting permission to reprint the above material. Our permission is granted without fee to reproduce the material, as you are the original author.

Use of the article is restricted to your thesis, available in *print* format only, to be used only in the *English* Language. This permission is limited to this particular use and does not allow you to use it elsewhere or in any other format other than specified above. Should your thesis be published commercially, please reapply for permission.

Please include a credit line in your publication citing full details of the Oxford University Press publication which is the source of the material and by permission of Oxford University Press or the sponsoring society if this is a society journal.

If the credit line or acknowledgement in our publication indicates that material including any illustrations/figures etc was drawn or modified from an earlier source it will be necessary for you to also clear permission with the original publisher. If this permission has not been obtained, please note that this material cannot be included in your publication/photocopies.

Please do not hesitate to contact me if I can be of any further assistance.

Yours sincerely,

✓  
**Fiona Willis**  
Head of Rights and New Business Development

For an online permissions forms visit our web site at:  
<http://www3.oup.co.uk/jnls/permissions/>

Johnson, Gwen

From:  
Sent:  
To:  
Subject: RE: Copyright permission

Dear Gwen, We will indicate in the thesis that Lippincott Williams & Wilkins is the original source and copyright owner. However, can you fax and mail us an official letter. The university will not accept an emailed permission.  
Thanks

From:  
To: .ca  
Subject: RE: Copyright permission  
Date sent: Mon, 16 Jun 2003 11:17:36 -0400

> Dear Ms. Buck,  
>  
> Permission is granted to reproduce the requested material for use in your  
> academic thesis/dissertation. Permission is granted provided a prominent  
> credit line is placed stating the original source and copyright owner  
> Lippincott Williams & Wilkins.

>  
>  
> Gwen Johnson  
> Sen. Permissions Coordinator  
> Wolters Kluwer Health  
> Medical Research

> <http://www.lww.com/resources/permissions/journals.html>  
> <<http://www.lww.com/resources/permissions/journals.html>>

> ---  
> Fro [berta.ca]  
> Sen  
> To:  
> Cc:  
> Subject: Copyright permission

Permission is granted to reproduce the requested material for use in your academic thesis/dissertation. Permission is granted provided a prominent credit line is placed stating the original source and copyright owner, © Lippincott Williams & Wilkins.

> To: Lippincott, Williams & Wilkins  
> Publisher

date: 8/12/03

> Dr. Anette Melk is requesting permission to use two articles that were  
> published in JASN in her PhD thesis to be completed at the University of  
> Alberta. The thesis will be published through the University of Alberta.  
> The articles are listed below:  
> 1. Melk, A. "Telomere Shortening in Kidneys with Age" J Am Soc Nephrol  
> 11:444-453, 2000

> 2. Melk, A. "Cell Senescence and its Implications for Nephrology, J Am Soc ✓  
> Nephrol 12: 385-393, 2001

> Please send original letter by regular mail to the mailing address below and  
> one by fax if possible.

> Thank you

> Dr. Anette Melk

Kathleen Buck  
Assistant to  
Drs. Allan Murray & Philip F. Halloran  
re



Dr Anette Melk

Canara

29th May 2003

Dear Dr Melk,

**Re: 'Melk. Kidney International Volume 63 (6) pp 2134-2143'.**

Permission is granted for you to use the material specified above in your forthcoming thesis. This is subject to the usual acknowledgements and on the understanding that nowhere in the original text do we acknowledge another source for the requested material. Non-exclusive world English Language rights granted, print and electronic.

Many thanks for your time. If you have any queries, please do not hesitate to contact me.

Yours Sincerely,

Ames  
Berlin  
Boston  
Copenhagen  
Edinburgh  
Melbourne  
Oxford  
Paris  
Tokyo  
Vienna